University of Granada
Faculty of Sciences
Department of Optics

Evaluation of the CIEDE2000(K_L:K_C:K_H) Color Difference Metrics and Development of Color Prediction Algorithms: Application to Dental Materials

PhD Thesis

Razvan Ionut Ghinea
Bachelor's Degree in Medical Physics
Master in Advanced Methods and Techniques in Physics

Granada, 2013

Universidad de Granada
Facultad de Ciencias
Departamento de Óptica

Evaluación de la fórmula de diferencia de color CIEDE2000(K_L:K_C:K_H) y desarrollo de algoritmos predictivos de color: Aplicación para materiales dentales

Tesis Doctoral

Razvan Ionut Ghinea
Licenciado en Física Médica
Máster en Métodos y Técnicas Avanzadas en Física

Granada, 2013

Editor: Editorial de la Universidad de Granada
Autor: Razvan Ionut Ghinea
D.L.: GR 357-2014
ISBN: 978-84-9028-762-0

Universidad de Granada
Facultad de Ciencias
Departamento de Óptica

Evaluation of the CIEDE2000(K_L:K_C:K_H) Color Difference Metrics and Development of Color Prediction Algorithms: Application to Dental Materials

Memoria que presenta el Licenciado en Física Médica
y Máster en Métodos y Técnicas Avanzadas en Física
Razvan Ionut Ghinea
para aspirar al título de Doctor Internacional.

Fdo.: **Razvan Ionut Ghinea**

Universidad de Granada
Facultad de Ciencias
Departamento de Óptica

Evaluation of the CIEDE2000(K_L:K_C:K_H) Color Difference Metrics and Development Of Color Prediction Algorithms: Application to Dental Materials

Las doctoras María del Mar Pérez Gómez, Catedrática de Escuela Universitaria y Ana María Yebra Rodríguez, Profesora Titular de Universidad, ambas pertenecientes al Departamento de Óptica de la Universidad de Granada.

Certifican:

Que el trabajo de investigación que recoge esta Memoria de Tesis Doctoral, titulada **"Evaluation Of The CIEDE2000(K_L:K_C:K_H) Color Difference Metrics And Development Of Color Prediction Algorithms: Application To Dental Materials"**, presentada por el Licenciado en Física Médica y Máster en Métodos y Técnicas Avanzadas en Física D. Razvan Ionut Ghinea ha sido realizada bajo nuestra dirección en el Departamento de Óptica.

Vº Bº La Directora de Tesis

Fdo. Dr. María del Mar Pérez Gómez
Catedrática de Escuela Universitaria
Departamento de Óptica
Universidad de Granada

Vº Bº La Directora de Tesis

Fdo. Dr. Ana María Yebra Rodríguez
Profesora Titular de Universidad
Departamento de Óptica
Universidad de Granada

Universidad de Granada
Facultad de Ciencias
Departamento de Óptica

Evaluation of the CIEDE2000(K_L:K_C:K_H) Color Difference Metrics and Development of Color Prediction Algorithms: Application to Dental Materials

El doctorando D. Razvan Ionut Ghinea y las directoras de la tesis, María del Mar Pérez Gómez y Ana María Yebra Rodríguez, garantizamos, al firmar esta tesis doctoral, que el trabajo ha sido realizado por el doctorando bajo la dirección de las directoras de la tesis y hasta donde nuestro conocimiento alcanza, en la realización del trabajo, se han respetado los derechos de otros autores a ser citados, cuando se han utilizado sus resultados o publicaciones.

Granada, 10.06.2013

Directoras de la Tesis:

María del Mar Pérez Gómez

Ana María Yebra Rodríguez

Doctorando:
Razvan Ionut Ghinea

Copiilor mei,

“We are like dwarfs on the shoulders of giants, so that we can see more than they, and things at a greater distance, not by virtue of any sharpness of sight on our part, or any physical distinction, but because we are carried high and raised up by their giant size.”

— Bernard De Chartres –

AGRADECIMIENTOS

Ha sido un largo recorrido y hay muchas personas que se han cruzado en mi camino y a las cuales les estoy profundamente agradecido por aportar algo a ese conjunto de eventos que, por un lado, han hecho que finalice con éxito este proyecto académico y, por el otro lado, me han convertido en la persona que soy ahora.

Esta lista solo puede empezar con la profesora María del Mar Pérez Gómez, directora de esta Tesis y responsable, en gran medida, de que yo haya llegado hasta aquí. Gracias María del Mar por introducirme en el mundo de la investigación, por enseñarme, por preocuparte continuamente por mi formación y aprendizaje, por apoyarme constantemente y creer en mí, por trabajar casi sin descanso, muchas veces de lunes a domingo, en esta línea de investigación que venimos desarrollando en los últimos anos, y, por supuesto, por abrirme las puertas de tu casa y hacerme sentir como uno más. Por todo esto, tu contribución a esta Tesis es incalculable. De todo corazón, ¡gracias!

Igualmente, quiero agradecerle a la profesora Ana María Yebra Rodríguez, directora de esta Tesis, por apoyarme de forma incondicional durante todo el periodo de desarrollo de este proyecto. Por todos tus consejos, recomendaciones, por tu disponibilidad y entrega, ¡gracias Ana!

Quiero agradecerle a la Consejería de Economía, Innovación, Ciencia y Empleo de la Junta de Andalucía por concederme, por un periodo de 4 años, una beca de Formación de Personal Docente e Investigador, que hizo posible la realización de esta Tesis Doctoral.

Quiero agradecer a los Directores del Departamento de Óptica de la Universidad de Granada, el profesor Antonio Manuel Rubiño López y la profesora Rosario González Anera, por recibirme, permitirme utilizar las instalaciones e instrumentación del Departamento y, no por último, por apoyarme y ayudarme en muchas ocasiones. Asimismo, quiero dar las gracias a los profesores, a los becarios y al personal del Departamento, por su colaboración durante estos últimos 6 años.

A la profesora Rosa Pulgar Encinas, por su colaboración, por completar este trabajo aportando valiosos conocimientos e ideas, y, en definitiva, por toda su inestimable ayuda.

Quiero agradecerle también a la profesora María Purificación Sánchez Sánchez, que me ayudó con el desarrollo de algunos de los materiales estudiados en esta Tesis. Sin su aportación, una parte de este trabajo no sería posible

Al profesor Luis Javier Herrera Maldonado, por un lado, por ser parte fundamental de esta Tesis, y por otro lado, por ser una excelente persona y un gran amigo. Sin tu dedicación, sin esas largas horas de trabajo, sin tus conocimientos, sin tus ideas, sin los debates, sin tu apoyo, no podría estar aquí. ¡Gracias Luis!

I want to thank Professor Rade Paravina for receiving me in his Laboratory at the Houston Center for Biomaterials and Biomimetics, but most importantly for helping me develop my career by making me overcome myself each day and pushing me forward to become a better scientist. Thank you for sharing your valuable knowledge and time with me. Also, I want to thank Doctor Aleksandar Aleksic, for his constant support, his unconditional help and wise advices. Thank you both for making Houston a place worth returning to.

Quiero agradecerle al profesor Ángel Ignacio Negueruela Suberviola por compartir conmigo su laboratorio y su despacho. Por enseñarme, por creer en mí, por tus palabras de apoyo y por qué eres una magnifica persona, ¡gracias Ignacio! Igualmente, gracias Conchita por recibirme en vuestra casa y por hacer de mi estancia en Zaragoza una experiencia inolvidable.

Vreau să îi mulțumesc doamnei profesoare Gabriela Iacobescu, pentru încrederea pe care a avut-o în mine la început de drum și pentru sprijinul acordat în mod continuu pe parcursul ultimilor ani.

Quiero agradecer a mis compañeros, pero sobre todo mis amigos, Oscar, Juancho y Laura, por su constante apoyo, por su amistad demostrada en múltiples ocasiones, por su ayuda, por sus aportaciones a mi desarrollo profesional y humano y por todos esos momentos geniales que hemos compartido. ¡Muchas gracias chicos! Tengo mucha suerte de teneros.

A mis compañeras de “arriba en Odontología”, Monica e Inma, por ayudarme entender mejor el mundo de la odontología, por todas sus aportaciones e inestimable ayuda y, sobre todo, por su amistad.

Vreau să îi mulțumesc Anei pentru tot ajutorul pe care mi l-a dat pe parcursul acestor ultimi ani, pentru sprijinul său, pentru că știu că pot conta pe ea și pentru prietenia extraordinară care ne leagă.

Quiero agradecer a la familia de María del Mar: Paco, Miguel, Paquillo, Paqui, Paco, Domingo, Ana Maria y a todos los demás por recibirme en sus casas, por hacerme sentir como uno más, por compartir momentos inolvidables y, sobre todo, por su generosidad y excelente carácter.

Quiero agradecer a Edi, Mariluz, Jesus, David y Mariluz por convertirse casi en nuestra segunda familia, por abrirnos la puerta de su casa y la de sus corazones. Por todos los momentos que hemos pasado juntos, ¡muchas gracias!

Vreau să îi mulțumesc familiei Ionescu, pentru încrederea acordată, pentru dragostea primită și pentru sprijinul oferit. Vreau să îi mulțumesc lui Ozzy și lui Octav, pentru tot ceea ce au făcut pentru noi, pentru complicitatea lor și pentru proiectul la care ne-am angajat împreună.

Vreau să le mulțumesc părinților mei, Octavian și Marylena, pentru că știu că ei mă vor sprijinii și mă vor iubi necondiționat, pentru că, orice s-ar intâmpla, pentru ei eu voi fi întotdeauna băiatul lor cel mic, pentru că lor le datorez educația primită și pentru că ei reprezintă oglinda în care mă uit și referința pe care o urmez. Iți mulțumesc tati! Iți mulțumesc mami! Vreau să îi mulțumesc fratelui meu Mircea, pentru că mă înțelege, mă cunoaște, mă sprijină și crede în mine și în ceea ce fac. În egală măsură, vreau să mulțumesc întregii mele familii: tata Crin, mama Speranța, Marinela, Nelu, Gabi, Dori, Vali, Flori, Berti, mama Doina, unchiul Vali, Marius, Dana, Oana, Viorel, Florin și toți ceilalți, pe care din motive de spațiu nu îi mai enumăr, vă mulțumesc pentru că întotdeauna m-ați sprijinit și m-ați ajutat să devin o persoană mai bună.

Andei, sufletul meu pereche, soția mea, prietena mea și confidentul meu. Datorită ție mă trezesc zâmbind în fiecare dimineață, mă lupt în fiecare zi ca să devin mai bun și adorm în fiecare seară cu convingerea că nimic nu este imposibil. Îți mulțumesc că exiști, că m-ai ales și că mă iubești.

CONTENTS

LIST OF FIGURES

LIST OF TABLES

CHAPTER 1

INTRODUCTION – THEORETICAL BACKGROUND

1.1. COLOR OF AN OBJECT – COLOR BASICS

It is well established that three factors are involved in the generation of a color sensation: a light source (producing the incident radiation), a sample (which modulates the incident radiation depending on its reflectance and transmittance properties) and finally an observer (or detector), which both detects the light reflected or transmitted by the sample and converts the detected signal into a response that the human brain recognizes as color (Figure 1.1). In modern applications, since the reflectance or transmittance characteristics of a sample depend on the illumination/measuring (observing) geometry, this factor is gaining more and more importance and it is worthy of being included among the main responsible of the color perception by human observers.

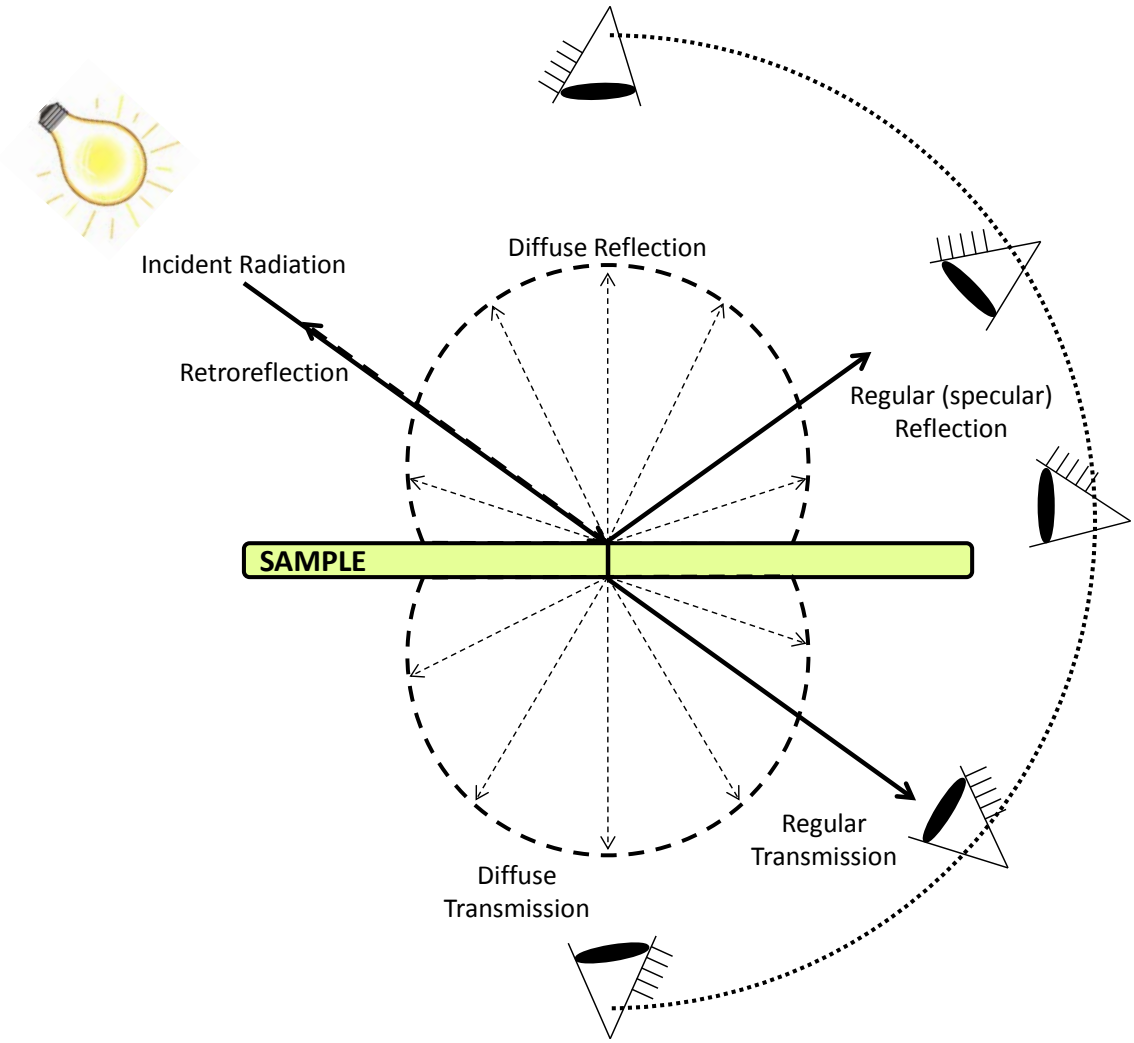

Figure 1.1: Schematical representation of the main factors that affect the perception of color.

Since all three factors presented before and shown in Figure 1.1 are required to produce color, they must also be quantified in order to produce a reliable system of color measurement. Light sources are quantified through their spectral power distribution (SPD) and standardized as illuminants, the material objects (samples) are specified by the geometric and spectral distribution of the energy they reflect or transmit and finally the human visual system is quantified through its color matching properties, that represent the first stage response (cone absorption) in the system, and are quantified as Standard Observers. Thus, colorimetry, as a combination of all these areas, draws upon techniques and results from the fields of physics, chemistry, psychophysics, physiology, and psychology (Fairchild, 2005).

The goal of most instrumental measurements is to estimate what an observer sees: the color appearance of a stimulus (Berns, 2000). However, there are many factors that have to be taken into account since they affect the color appearance of an object, including the light source spectral properties, the level of illumination, background lightness and other psychological factors.

1.1.1 LIGHT SOURCES AND ILLUMINANTS

As mentioned before, the color of a sample is the result of the interaction between the illuminant, the sample itself and the observer. In order to produce a reliable system of physical colorimetry, all three aspects must be quantified. The light sources are quantified through their spectral power distributions (SPD) and standardized as illuminants. To be able to reproduce colorimetric measurements, the SPD of the irradiating source has to be reproduced. The International Commission on Illumination (CIE) has standardized several SPDs and recommends that these should be used whenever possible when a colorimetric characterization of a material is performed.

In 1931, the CIE introduced three illuminants, called illuminant A, B, and C. They were chosen in such a form that illuminant A simulated the SPD of an average incandescent light, illuminant B simulated the SPD of direct sunlight and illuminant C simulated the SPD of average daylight. However, it turned out that illuminant B was very seldom used and was soon dropped. Illuminant C is still in use in some industries,

but in 1964, the CIE recommended a new set of daylight illuminants (CIE 1964) where the SPD was also defined in the ultraviolet (UV) part of the spectrum. One phase of daylight was selected as the most representative and is now known as CIE Standard Illuminant 65. Also, the equienergy spectrum is represented by the Illuminant E.

Currently, the CIE defines two standard illuminants: CIE Standard Illuminant A and CIE Standard Illuminant D65, and several others secondary illuminants. Physical sources that simulate the relative SPD of a CIE illuminant are called CIE sources, but it should be mentioned that often an illuminant cannot be reproduced accurately, and, in such cases, the source is defined as a simulator.

For the human visual system, the "natural" illumination is the daylight, therefore several illuminants, corresponding to different phases of the daylight, were defined. The SPD of daylight, as the sum of direct sunlight and the scattered light within the atmosphere, is variable during the day, but also depends on the season and weather conditions.

The CIE accepted a recommendation by Judd and coworkers (Judd et al., 1964) to describe phases of daylight (CIE 1967). These authors found that, although daylight is highly variable, the chromaticities of different phases of daylight fall on a curve more or less parallel to the Planckian locus on the chromaticity diagram and even their SPDs can be described using only three basic functions.

The International Commission on Illumination states that the CIE Standard Illuminant D65 is intended to represent average daylight and has a correlated color temperature of approximately 6500 K. CIE Standard Illuminant D65 should be used in all colorimetric calculations requiring representative daylight, unless there are specific reasons for using a different illuminant. Variations in the relative spectral power distribution of daylight are known to occur, particularly in the ultraviolet spectral region, as a function of season, time of day, and geographic location. However, CIE standard illuminant D65 should be used pending the availability of additional information on these variations (CIE 2004).

A spectral power distribution is a plot, or table, of a radiometric quantity as a function of wavelength. Since the overall power levels of light sources can vary over many orders of magnitude, spectral power distributions are often normalized to facilitate comparisons of color properties. The traditional approach is to normalize a spectral power distribution such that it has a value of 100 (or 1.0) at a wavelength of 560 nm (near the center of the visible spectrum). Such normalized spectral power distributions are referred to as relative spectral power distributions, and are dimensionless (Fairchild, 2005). In Figure 1.2, the relative spectral power distribution (SPD) of the CIE D65 Standard Illuminant is plotted as a function of wavelength in the 300-830nm range.

In almost all applications in dentistry, with the exception of research studies when the behavior of a material under different illuminants results of certain interest or for metameric studies, the standard illuminant of primary choice is the CIE D65 Standard Illuminant. The election of this illuminant is not arbitrary, since the teeth and, if the case, the dental restorations, are often visually judged under daylight conditions.

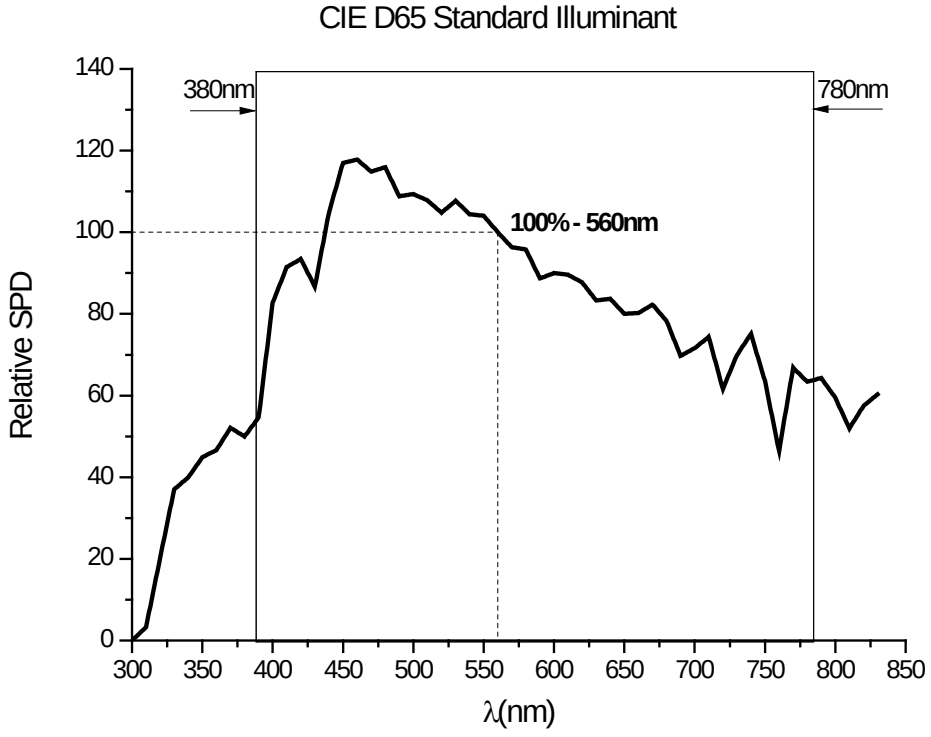

Figure 1.2:Relative spectral power distribution of the CIE Standard Illuminant D65 in the 300-830nm range.

1.1.2 SPECTRORADIOMETRY

Another main factor affecting the final color perception is the sample's reflectance and transmittance characteristics. These characteristics can be measured employing a color measuring instrument. A number of factors need to be considered when selecting a color-measuring instrument. If no spectral data is required, and all the stimuli requiring measurements are composed of the same components, then colorimeters, spectrometers or imaging systems can be used. It has to be taken into account that this type of devices are usually designed for one CIE Standard Illuminant and Observer combination (most often CIE D65 Illuminant and CIE 2° Standard Observer). However, the vast majority of measurements require spectral data, as is the case of most of the applications in dentistry. One of the main advantages in measuring complete spectral data is that it provides information about the consistency of the material and can detect potential problems of metamerism, by giving us the ability to calculate colorimetric data for the actual spectral power distribution of each source expected to illuminate the specimen.

Radiometry is the science of measuring electromagnetic radiation in terms of its power, polarization, spectral content, and other parameters relevant to a particular source or detector configuration. An instrument which measures optical radiation is called a radiometer. There are a variety of radiometric quantities that can be used to specify the properties of a sample. Of particular interest in color appearance measurements are the irradiance and, especially the radiance. Radiance differs from irradiance, since it is a measure of the power emitted from a source (or reflected from a surface), rather than incident upon a surface, per unit area per unit solid angle. Spectral radiance includes the wavelength dependency.

Radiance has the highly desirable property that, for two points p_1 and p_2, the radiance leaving p_1 in the direction of p_2 is the same as the radiance arriving at p_2 from the direction of p_1.This means that the radiance is preserved through optical systems (neglecting absorption) and is independent of distance. Thus, the human visual system responds commensurably to radiance, making it a key measurement in color appearance specification. Furthermore, radiance does not fall off with the square of

distance from the surface, since the decrease in power incident on the pupil is directly canceled by a proportional decrease in the solid angle subtended by the pupil with respect to the surface in question (Fairchild, 2005). This, together with the fact that it is a non-contact technique that can match the geometry of visual assessments, is one of the main reason why spectroradiometric measurements have recently become first choice for spectral measurements in dental color studies (Del Mar Pérez et al., 2009; Luo et al., 2009).

However, there are some important assumptions which have to be made in order to perform adequate spectroradiometric measurements, such as:

- the radiance leaving a point on a surface is due only to radiance arriving at this point (although radiance may change directions at a point on a surface, we assume that it does not skip from point to point);
- radiation leaving a surface at a given wavelength (efflux) is due to incident radiation at that wavelength (influx);
- the surface does not generate light internally, and treat sources separately.

There are many uses of radiometry in industrial applications to monitor manufacturing processes, and in scientific and technical activities that utilize the sensing of optical radiation to deduce information about a wide range of physical, chemical, and biological processes.

1.1.3 MEASURING GEOMETRIES

The interaction of radiant energy with objects is not just a simple spectral phenomenon, since the reflectance or transmittance of a sample is not just a function of wavelength, but also a function of the illumination and viewing (measuring) geometry. That is why, when evaluating the colorimetric characteristics of a material, in addition to the standard observer and the standard illuminant used, the measuring geometry must be also specified. Many materials will change their colorimetric properties depending if they are illuminated with diffuse or collimated light or if they are illuminated perpendicularly or from a given angle (Schanda, 2007). This is the reason why, if we want to be able to obtain results which can be easily compared or if we want to be able to agree on requirements and check their fulfillment, the measuring geometry has to be standardized. To fully characterize a material sample, complete bidirectional reflectance (or transmittance) distribution functions must be obtained for each possible combination of illumination angle, viewing angle, and wavelength. Measurement of such functions is extremely difficult and expensive, and produces massive quantities of data that are difficult to meaningfully utilize (Fairchild, 2005). To avoid this issue, a small number of standard illumination and viewing geometries have been established for colorimetry.

To simulate the human visual process in instrumental color stimulus measurement the use of different measuring geometries is required in order to determine the spectral (or tristimulus) reflectance or reflectance factor (or transmittance, transmittance factor) of the material sample. To be able to compare the measured results obtained by different equipments, the measuring geometries of these instruments have to comply with given standards. The CIE has tightened the standard specifications since the first recommendations were published in 1931, but there are still considerable differences between instruments of different manufacturers. Therefore, it is important that the experimenter should understand the critical parameters of an instrument. In this sense, the International Commission on Illumination has worked out a terminology that makes the definition of the measurement geometry easier. Manufacturers are urged to follow this new

terminology, as this will make the communications with their customers more efficient (CIE, 2004; Schanda, 2007).

The CIE standardized two groups of influx (incident flux) geometries for the instrumental measurement of color stimuli: diffuse and directional. Whenever a colorimetric evaluation of a sample is performed, according to the type of sample, one of these geometries has to be selected together with an efflux (outcoming flux) geometry. The CIE has defined four standard illumination and viewing geometries for reflectance measurements (CIE, 2004), which come as two pairs of optically reversible geometries (indicating first the illumination geometry and then the viewing geometry following the slash):

- Diffuse/normal (d/0°) and normal/difusse (0°/d);
- 45°/normal (45°/0°) and normal/45° (0°/45°).

1.1.3.1 Diffuse/Normal and Normal/Diffuse Geometry

In the case of diffuse influx geometry, the sample has to be irradiated from the upper hemisphere with angle independent constant radiance. The viewing/measuring angle is near to the normal at the sample surface. In the case of the reversed geometry, the normal/diffuse geometry, the sample is illuminated from an angle near to its normal and the reflected energy is collected from all angles using an integrating sphere. These two geometries are optical reversible and therefore, produce the same measurement results (assuming all other instrumental variables as constant). The measurements made are of total reflectance. One example of achieving diffuse/0 ° illuminating/viewing geometry is shown in Figure 1.3.

1.1.3.2 45°/Normal and Normal/45°

In a 45°/0° geometry, the sample is illuminated at an angle of 45° from the normal and measurements are made along the normal. In the reversed 0°/45° geometry, the sample is illuminated normal to its surface and measurements are made at a 45° angle to the normal. Again, these two geometries are optical reverses of one another and produce identical results given equality of all other instrumental variables. Use of the 45°/0° and 0°/45° measurement geometries ensures that all components of

gloss are excluded from the measurements (Fairchild, 2005). Thus these geometries are typically used in applications where it is necessary to compare the colors of materials having various levels of gloss, therefore being of high interest for the field of dentistry, since almost all dental materials present high level of gloss.

If a single collimated beam of light is used to illuminate the sample in the 45°/0° illuminating/viewing geometry, it is expected to result in insufficient amounts of light at the detector and directionally problems (Berns, 2000). Insufficient light levels are alleviated by adding a second source at the opposite azimuthal angle, a configuration known as 45°/0° illuminating/viewing geometry with two azimuthal angles. An example of achieving this geometry is shown in Figure 1.3.

Reflectance is often addressed as the ratio of reflected energy to incident energy. This definition is perfectly appropriate for measurements of total reflectance performed under one of the diffuse/0° or 0°/diffuse geometries. However, for bidirectional reflectance measurements (45°/0° and 0°/45°), the ratio of reflected energy to incident energy is exceedingly small, since only a small range of angles of the distribution of reflected energy is detected. Thus, to produce more practically useful values for any type of measurement geometry, reflectance factor measurements are made relative to a perfect reflecting diffuser (PRD).

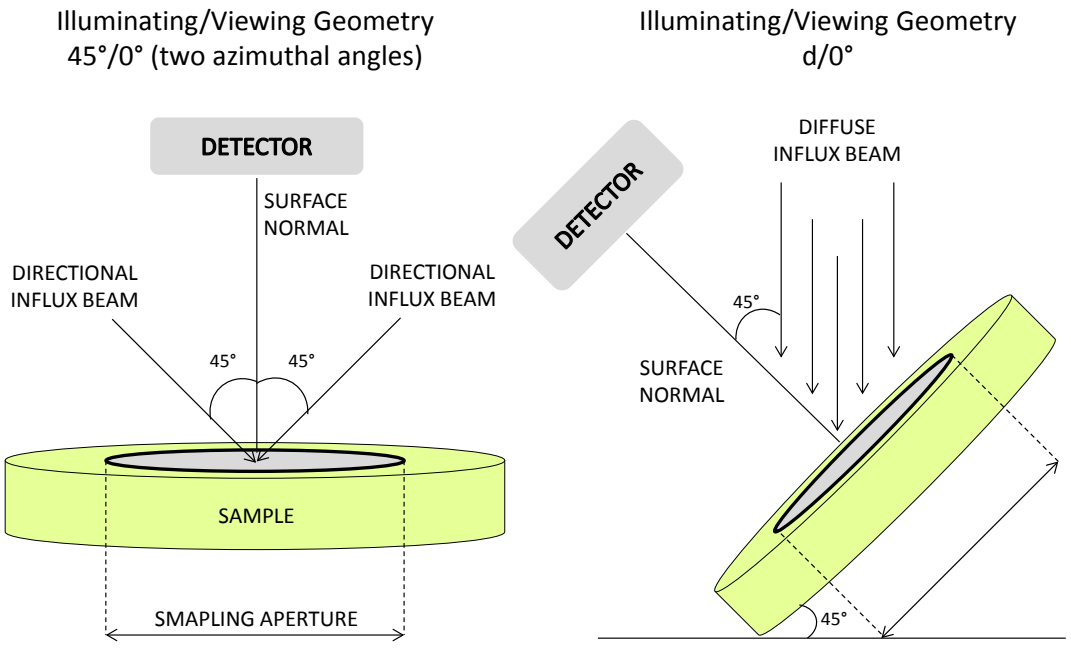

Figure 1.3: Example of a 45°/0° and a d/0° illuminating/viewing geometries.

Thus, measurements of reflectance factor are defined as the ratio of the energy reflected by the sample to the energy that would be reflected by a PRD illuminated and viewed in the identical geometry. For the bidirectional geometries, measurements of reflectance factor relative to the PRD result in a zero-to-one scale similar to that obtained for total reflectance measurements. Since PRDs are not physically available, reference standards that are calibrated relative to the theoretical aim are normally used. This type of reflectance standards are normally provided by national standardizing laboratories and/or instrument manufacturers.

1.1.4 CIE STANDARD OBSERVERS

As specified earlier, the color of an object depends on its spectral reflectance, the spectral power distribution of the light source and finally, the observer. When performing a color measurement, in order to obtain reproducible results as well as results which can be easily compared with prior studies, it is important to be able to standardize all the observation/measurement conditions.

1.1.4.1 CIE 1931 Standard colorimetric observer

The CIE 1931 Standard Colorimetric Observer is defined for a 2° foveal field of observation (the 2° field corresponds to an area of the macula lutea which has an almost constant density of photoreceptors) and a dark surround.

The CIE 1931 2° Observer was derived from the results of two experimental investigations of color matching of test stimuli with mixtures of three RGB primary stimuli, conducted by WD Wright and J Guild (Wright, 1929; Wright, 1930; Guild, 1931). The results of these studies led to the first $\bar{r}(\lambda), \bar{g}(\lambda), \bar{b}(\lambda)$ Color-Matching Functions (CMF) which characterize the CIE1931 2° Standard Observer. However, these first matching functions presented negative lobes, which referred to the fact that in some parts of the spectrum a match can be obtained only if one of the matching stimuli is added to the test stimulus.

The negative lobes present in the CMFs made calculations difficult and therefore, in 1931, the International Commission on Illumination decided to transform from the real RGB primaries to a set of imaginary primaries X Y Z, with the difference

that, in this latter case, the new CMFs that characterize the observer do not have negative lobes. Also, an equienergy stimulus was characterized by equal tristimulus values (X=Y=Z), one of the tristimulus provide photometric quantities and the volume of the tethradeon set by the new primaries should be as small as possible.

The X Y Z tristimuli values are then calculated as the integral over the visible spectrum (380nm-780nm):

$$X = k \int_{380nm}^{780nm} \phi_\lambda(\lambda)\bar{x}(\lambda)\mathrm{d}\lambda$$

$$Y = k \int_{380nm}^{780nm} \phi_\lambda(\lambda)\bar{y}(\lambda)\mathrm{d}\lambda$$

$$Z = k \int_{380nm}^{780nm} \phi_\lambda(\lambda)\bar{z}(\lambda)\mathrm{d}\lambda$$

where k is a constant; $\phi(\lambda)$ is the color stimulus function of the light seen by the observer and $\bar{x}(\lambda), \bar{y}(\lambda), \bar{z}(\lambda)$ are the CMF of the CIE1931 Standard Colorimetric Observer.

However, according to the CIE recommendations, the X Y Z tristimuli values can be calculated as numerical summation at wavelength intervals (Δλ), by applying the following equations:

$$X = k \sum_k \phi_\lambda(\lambda)\bar{x}(\lambda)\Delta\lambda$$

$$Y = k \sum_k \phi_\lambda(\lambda)\bar{y}(\lambda)\Delta\lambda$$

$$Z = k \sum_k \phi_\lambda(\lambda)\bar{z}(\lambda)\Delta\lambda$$

In the case of a non-self-luminous object, the spectral reflection of the surface is described by the spectral reflectance factor $R(\lambda)$ and the spectral transmission is described by the spectral transmittance factor $T(\lambda)$. Taking into account these

considerations, the relative color stimulus function $\phi(\lambda)$ for reflecting or transmitting objects is given by:

$$\phi(\lambda) = R(\lambda) \cdot S(\lambda) \text{ or } \phi(\lambda) = T(\lambda) \cdot S(\lambda)$$

where $R(\lambda)$ is the spectral reflectance factor; $T(\lambda)$ is the spectral transmittance factor of the object (preferably evaluated for one of the standard geometric conditions recommended by the CIE) and $S(\lambda)$ is the relative Spectral Power Distribution of the illuminant (preferably, should be one of the CIE Standard Illuminants) (Schanda 2007).

In this case, the constant k is chosen so that the tristimulus value Y=100 for objects that have $R(\lambda) = 1$ or $T(\lambda) = 1$ at all wavelengths:

$$k = \frac{100}{\sum_\lambda S(\lambda) \cdot \bar{y}(\lambda) d(\lambda)}$$

The Color-Matching Functions of the CIE1931 Standard Colorimetric Observer are given as values from 360nm to 830nm at 1nm intervals with seven significant figures (CIE 2004) (Figure 1.4). This observer should be used if the field subtended by the sample is between 1° and 4° at the eye of the observer. In technical applications, this observer is often addressed as 2° Standard Colorimetric Observer. A 2° visual field is equivalent to a diameter of about 1.74cm at a viewing distance of 50cm (Figure 1.5 top).

1.1.4.2 CIE 1964 Standard Colorimetric Observer

As specified before, the CIE1931 2° Standard Observer is recommended only for small stimuli (which subtend approximately 1° - 4° at the eye of observer). However, the description of a larger stimulus, which falls on a larger area of the macula lutea, or it is seen partially parafoveally, is required. In this sense, the International Commission on Illumination standardized a large field colorimetric system (CIE 1964), based on the visual observations conducted on a 10° visual field, which corresponds to a diameter of about 8.74cm at a viewing distance of 50cm (Figure 1.5 bottom).

The adoption of a 10° colorimetric observer was based on the works of Stiles and Burch (Stiles, 1959) and Speranskaya (Speranskaya, 1959), which used different

sets of monochromatic primaries, and the CMFs were obtained directly from the observations, and no appeal to heterochromatic brightness measurements or to any luminous efficiency function was required.

The Color-Matching Functions of the 10° system are distinguished from the 2° system by a 10 subscript. The Color-Matching Functions of the CIE1964 Standard Colorimetric Observer are given as values from 360nm to 830nm at 1nm intervals with six significant figures (CIE 2004) (Figure 1.4).

The tristimulus values are calculated similar to the case of the 2° standard observer:

$$X = k_{10} \cdot \int_{380nm}^{780nm} \phi_\lambda(\lambda)\bar{x}_{10}(\lambda)\mathrm{d}\lambda$$

$$Y = k_{10} \cdot \int_{380nm}^{780nm} \phi_\lambda(\lambda)\bar{y}_{10}(\lambda)\mathrm{d}\lambda$$

$$Z = k_{10} \cdot \int_{380nm}^{780nm} \phi_\lambda(\lambda)\bar{z}_{10}(\lambda)\mathrm{d}\lambda$$

and the k_{10} constant for non-self luminous objects is defined by the following equation:

$$k_{10} = \frac{100}{\sum_\lambda S(\lambda) \cdot \bar{y}_{10}(\lambda) d(\lambda)}$$

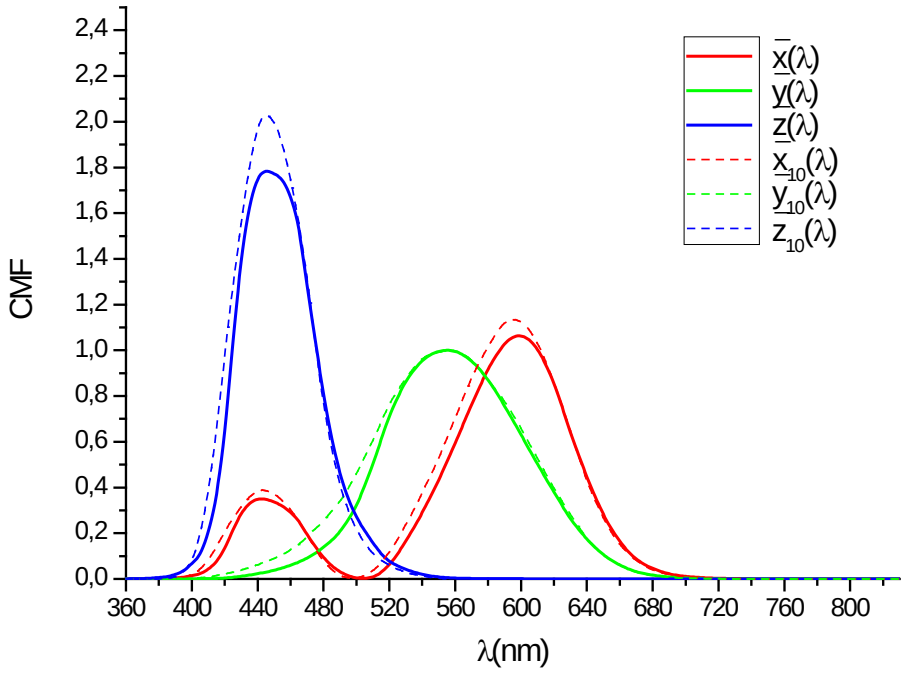

Figure 1.4: .$\bar{x}(\lambda), \bar{y}(\lambda), \bar{z}(\lambda)$Color-Matching Functions of the CIE1931 Standard Colorimetric Observer (continuous line) and the $\bar{x}_{10}(\lambda), \bar{y}_{10}(\lambda), \bar{z}_{10}(\lambda)$ Color-Matching Functions of the CIE1964 Standard Colorimetric Observer (dotted line).

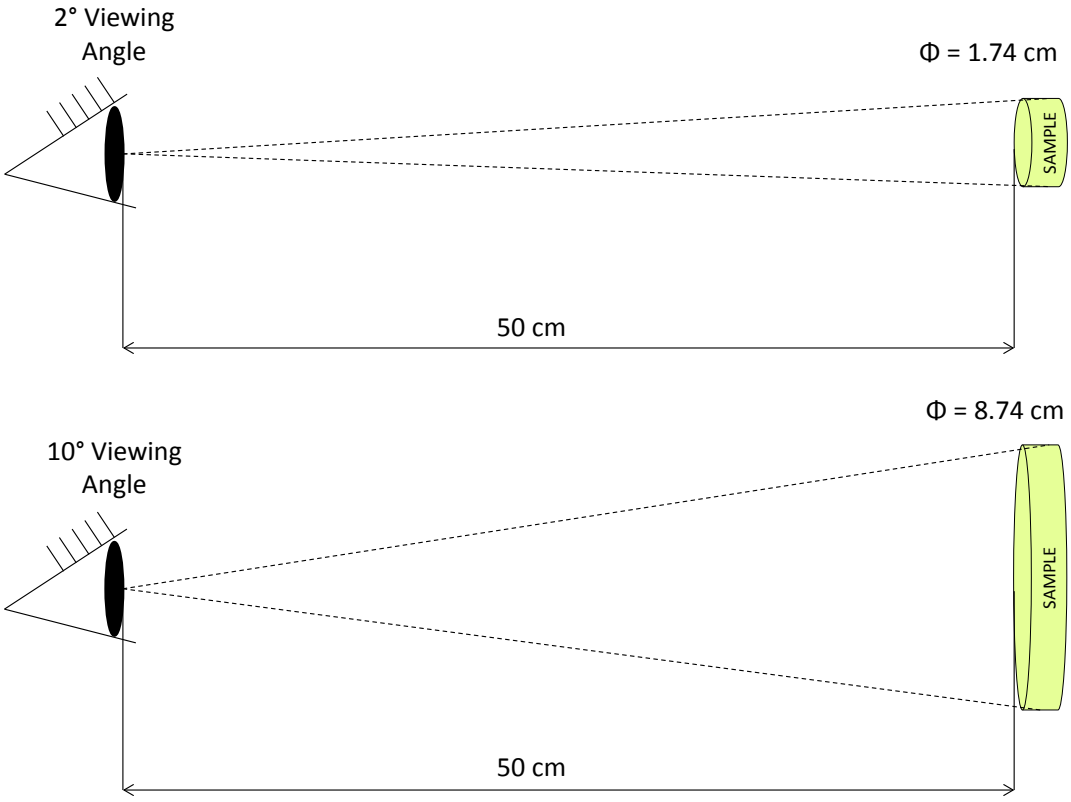

Figure 1.5: Sample size at a distance of 50cm for the CIE1931 2° Standard Observer (top) and the CIE1931 10° Standard Observer (bottom).

Apart from the recommendations regarding the field subtained by the sample, there are other factors that have to be taken into account when using the CIE 1964 Standard Colorimetric Observer. The precision of the system is higher than that of the CIE 1931 trichromatic system (Wyszecki and Stiles, 1982) since it has been determined with a higher number of observers (49 in case of Stiles and Burch and 18 in the case of Speranskaya), but the larger stimulus area rod-intrusion had to be considered as well. Also, in the case of using the 10° observer without any rod-correction the luminance levels have to be high enough. While in the case of a 2° field one can calculate with photopic adaptation down to about 10cd/m^2, this is not the case for the larger field size. In this sense, the CIE recommends the following: "The large-field color matching data as defined by the CIE 1964 standard colorimetric observer are intended to apply to matches where the luminance and the relative spectral power distributions of the matched stimuli are such that no participation of the rod receptors of the visual mechanism is to be expected. This condition of observation is important as "rod intrusion" may upset the predictions of the standard observer. For daylight, possible participation of rod vision in color matches is likely to diminish progressively above about 10 cd/m^2 and be entirely absent at about 200 cd/m^2"(CIE, 2004).

1.1.5 CIE COLOR SPACES

The color of a stimulus can be specified by a triplet of tristimulus values (X,Y,Z). In order to provide a convenient two-dimensional representation of the color, chromaticity diagrams were developed. In the transformation from tristimulus values to chromaticity coordinates, a normalization that removes luminance information is performed. This transformation is defined by:

$$x = \frac{X}{X + Y + Z}$$

$$y = \frac{Y}{X + Y + Z}$$

$$z = \frac{Z}{X + Y + Z}$$

Chromaticity coordinates attempt to represent a three-dimensional phenomenon with just two variables. To fully specify a colored stimulus, one of the tristimulus values must be reported in addition to two of the chromaticity coordinates. Usually, the Y tristimulus value is reported since it represents the luminance information. Therefore, this color space is often called the CIE Yxy space.

The CIE Yxy space is well suited to describe color stimuli. However, the practical use of colorimetry very often requires information about whether two samples will be indistinguishable by visual observation or not. MacAdam showed that the chromaticity difference that corresponds to a just noticeable color difference will be different in different areas of the xy chromaticity diagram, and also at one point in the diagram equal chromaticity differences in different directions represent visual color differences of different magnitudes (MacAdam, 1942). Many attempts were made to transform the xy diagram in such a form that the MacAdam ellipses become circles, but it has to be mentioned that still no perfect transformation is available.

Nowadays, the use of the chromaticity diagrams has become largely obsolete, and the CIE proposed CIELAB and CIELUV color spaces are the most frequently used. One of the main characteristics of these two color spaces is that they extend tristimulus colorimetry to three-dimensional spaces with dimensions that approximately correlate with the perceived lightness, chroma, and hue of a colored stimulus. This is achieved by incorporating features to account for chromatic adaptation and nonlinear visual responses. The main aim in the development of these spaces was to provide uniform practices for the measurement of color differences, something that cannot be done reliably in tristimulus or chromaticity spaces (Fairchild, 2005). The International Commission on Illumination recommended, in 1976, the use of both spaces, since there was no clear evidence to support one over the other at that time. However, over time, the CIELAB has been more largely implemented in color applications than the CIELUV color space. In the specific case of dentistry, the CIELAB color space is almost exclusively used in dental color studies or color research in the field.

*1.1.5.1 CIE 1976 (L*a*b*) color space - CIELAB*

The CIE 1976 (L*a*b*) color space, abbreviated CIELAB, is defined by the following equations (CIE 2004):

$$L^* = 116 \cdot f\left({}^{Y}/_{Y_n}\right) - 16$$

$$a^* = 500 \cdot \left[f\left({}^{X}/_{X_n}\right) - f\left({}^{Y}/_{Y_n}\right)\right]$$

$$b^* = 200 \cdot \left[f\left({}^{Y}/_{Y_n}\right) - f\left({}^{Z}/_{Z_n}\right)\right]$$

where

$$f\left({}^{X}/_{X_n}\right) = \left({}^{X}/_{X_n}\right)^{1/3} \quad if \quad \left({}^{X}/_{X_n}\right) > \left({}^{24}/_{116}\right)^3$$

$$f\left({}^{X}/_{X_n}\right) = \left({}^{841}/_{108}\right) \cdot \left({}^{X}/_{X_n}\right) + {}^{16}/_{116} \quad if \quad \left({}^{X}/_{X_n}\right) \leq \left({}^{24}/_{116}\right)^3$$

and

$$f\left({}^{Y}/_{Y_n}\right) = \left({}^{Y}/_{Y_n}\right)^{1/3} \quad if \quad \left({}^{Y}/_{Y_n}\right) > \left({}^{24}/_{116}\right)^3$$

$$f\left({}^{Y}/_{Y_n}\right) = \left({}^{841}/_{108}\right) \cdot \left({}^{Y}/_{Y_n}\right) + {}^{16}/_{116} \quad if \quad \left({}^{Y}/_{Y_n}\right) \leq \left({}^{24}/_{116}\right)^3$$

and

$$f\left({}^{Z}/_{Z_n}\right) = \left({}^{Z}/_{Z_n}\right)^{1/3} \quad if \quad \left({}^{Z}/_{Z_n}\right) > \left({}^{24}/_{116}\right)^3$$

$$f\left({}^{Z}/_{Z_n}\right) = \left({}^{841}/_{108}\right) \cdot \left({}^{Z}/_{Z_n}\right) + {}^{16}/_{116} \quad if \quad \left({}^{Z}/_{Z_n}\right) \leq \left({}^{24}/_{116}\right)^3$$

In these equations, the X, Y, and Z are the tristimulus values of the sample and the X_n, Y_n, and Z_n are the tristimulus values of the reference white. These signals are combined into three response dimensions corresponding to the light–dark, red–green, and yellow–blue responses of the opponent theory of color vision. Finally, appropriate multiplicative constants are incorporated into the equations to provide the required uniform perceptual spacing and proper relationship between the three dimensions.

The CIE L* coordinate is a correlate to perceived lightness ranging from 0.0 for black to 100.0 for a diffuse white (L* can sometimes exceed 100.0 for stimuli such as specular highlights in images). The CIE a* and CIE b* coordinates correlate approximately with red–green and yellow–blue chroma perceptions. They take on both negative and positive values. Both a*and b* have values of 0 for achromatic stimuli (white, gray, black). Their maximum values are limited by the physical properties of materials, rather than the equations themselves. The CIELAB L*, a*, and b* dimensions are combined as Cartesian coordinates to form a three-dimensional color space (Figure 1.6).

In some applications the correlates of the perceived attributes of lightness, chroma, and hue are of more practical interest. In this case, the CIELAB color space is represented using three cylindrical coordinates (Lightness - L^*; Chroma - C^*_{ab} and hue angle - h_{ab}) (Figure 1.6) . The CIE L^* coordinate is calculated as described before, while Chroma and hue angle are calculated as follows:

$$C^*_{ab} = \sqrt{\left(a^{*2} + b^{*2}\right)}$$

$$h_{ab} = arctan\left({}^{b^*}/_{a^*}\right)$$

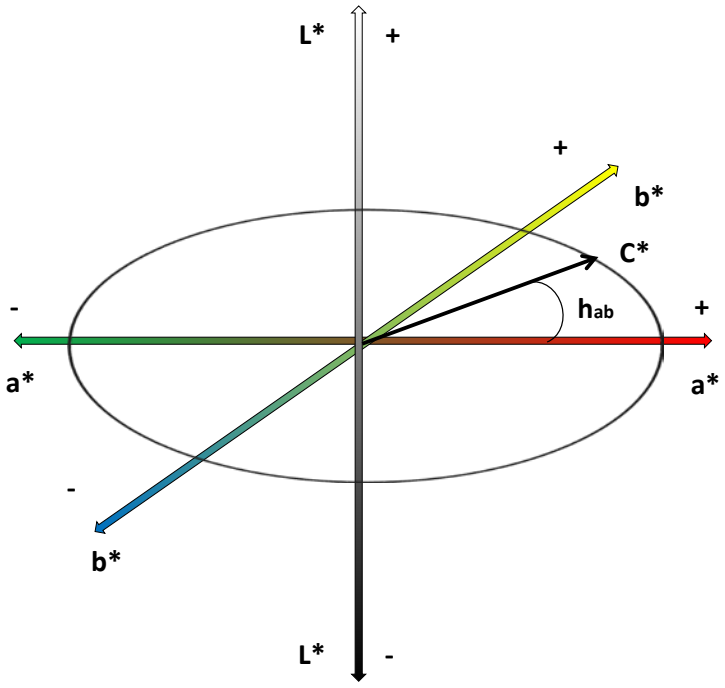

Figure 1.6: Schematic representation of the CIELAB color space.

1.1.6 COLOR DIFFERENCE EQUATIONS

In the CIELAB color space, the color difference between two object color stimuli of the same size and shape, viewed in identical white to middle-gray surroundings, by an observer photopically adapted to a field of chromaticity not too different from that of average daylight, is quantified as the Euclidean distance between the points representing them in the space. This difference is expressed in terms of the CIELAB ΔE^*_{ab}color difference formula, and calculated as:

$$\Delta E^*_{ab} = \sqrt{\Delta L^{*2} + \Delta a^{*2} + \Delta b^{*2}}$$

The CIELAB ΔE^*_{ab} color difference formula is widely adopted and it was used in multiple fields and applications. It represented a big step forward toward harmonization of color difference evaluation and also color description in the technical world.

The CIELAB color space was designed with the goal of having color differences being perceptually uniform throughout the space, but this goal was not strictly achieved. Soon after its implementation, the CIELAB ΔE^*_{ab} color difference formula was reported to present inhomogeneities (Kuehni, 1976; Mclaren, 1980). To improve the uniformity of color difference measurements, modifications of the CIELAB ΔE^*_{ab} equation have been made based upon various empirical data, but in almost all cases a poor correlation between the dataset of visual judgments and the Euclidean distances was found, hence raising the need of equation optimization (Berns, 2000).

Keeping CIELAB coordinate system as a start, several changes were applied to the components of the color difference formula by adapting weighting functions to the three component differences. The Color Measurement Committee (CMC) of the Society of Dyers and Colorists proposed a new color difference formula based on the work of Clarke and collaborators (Clarke et al., 1984), denominated CMC(l:c), which became an ISO standard for textile applications in 1995 (Schanda, 2007). Other CIELAB-based formula, called BFD(l:c), and similar in structure to the CMC(l:c) formula in most respects, was proposed in 1987 by Luo and Rigg (Luo and Rigg, 1987). Later, the CIE Technical Committee tried to find an optimization of the CIELAB color difference

formula mainly based on new experiments under well-controlled reference conditions. The resulting recommendation followed the general form of the CMC(l:c) formula, and it was called CIE94 color difference formula (ΔE_{94}^*) (CIE, 1995). In 2001, Luo and collaborators proposed a new color difference metric (Luo et al., 2001), called the CIEDE2000 color-difference, which became a CIE recommendation for color difference computation in 2004 (CIE, 2004). The CIEDE2000 formula stands as the last in a long series of developments improving the CIELAB formula, and outperforms the older CMC(l:c), BFD(l:c) and CIE94 formulas (Schanda, 2007).

The CIEDE2000 total color difference formula (Luo et al., 2001) corrects for the non-uniformity of the CIELAB color space for small color differences under reference conditions. Improvements to the calculation of total color difference for industrial color difference evaluation are made through corrections for the effects of lightness dependence, chroma dependence, hue dependence and hue-chroma interaction on perceived color difference. The scaling along the a* axis is modified to correct for a non-uniformity observed with grey colors. The resulting recommendation is as follows (CIE, 2004):

$$\Delta E_{00} = \sqrt{\left(\frac{\Delta L'}{K_L S_L}\right)^2 + \left(\frac{\Delta C'}{K_C S_C}\right)^2 + \left(\frac{\Delta H'}{K_H S_H}\right)^2 + R_T \left(\frac{\Delta C'}{K_C S_C}\right)\left(\frac{\Delta H'}{K_H S_H}\right)}$$

$$L' = L^*$$

$$a' = a^*(1 + G)$$

$$b' = b^*$$

$$G = 0.5\left(1 - \sqrt{\frac{\bar{C}_{ab}^{*\,7}}{\bar{C}_{ab}^{*\,7} + 25^7}}\right)$$

The weighting functions, S_L, S_C, S_H adjust the total color-difference for variation in perceived magnitude with variation in the location of the color-difference pair in L', a', and b' coordinates.

$$S_L = 1 + \frac{0.015(\bar{L}' - 50)^2}{\sqrt{20 + (\bar{L}' - 50)^2}}$$

$$S_C = 1 + 0.045\bar{C}'$$

$$S_H = 1 + 0.015\bar{C}'T$$

$$T = 1 - 0.17cos\left(\bar{h}' - 30\right) + 0.24cos\left(2\bar{h}'\right) + 0.32cos\left(3\bar{h}' + 6\right) - 0.20cos\left(4\bar{h}' - 63\right)$$

Visual color-difference perception data show an interaction between chroma difference and hue difference in the blue region that is observed as a tilt of the major axis of a color-difference ellipsoid from the direction of constant hue angle. To account for this effect, a rotation function is applied to weighted hue and chroma differences:

$$R_T = -sin(2\Delta\Theta)R_C$$

$$\Delta\Theta = 30\exp\left\{-\left[\left(\bar{h}' - 275\right)\Big/25\right]^2\right\}$$

$$R_C = 2\sqrt{\frac{\bar{C}'^7}{\bar{C}'^7 + 25^7}}$$

The parametric factors K_L, K_C, K_H, are correction terms for variation in experimental conditions. Under reference conditions they are all set to 1. The reference conditions are defined by the International Commission on Illumination as (CIE, 2004):

- Illumination: source simulating the spectral relative irradiance of CIE Standard Illuminant D65;
- Illuminance: 1000lx;
- Observer: normal color vision;
- Background field: uniform, neutral grey with L*=50;
- Viewing mode: object;
- Sample size: greater than 4 degrees subtended visual angle;

- Sample separation: minimum sample separation achieved by placing the sample pair in direct edge contact;
- Sample color-difference magnitude: 0 to 5 CIELAB units;
- Sample structure: homogeneous color without visually apparent pattern or non-uniformity.

1.2. COLOR OF TOOTH

From the point of view of a human observer, the appearance of a tooth is a complicated psycho-physiological process, which is influenced by different factors, such as the spectral power distribution of the illuminant, the sensitivity of the observer and the spectral characteristic of the tooth, in terms of its spectral reflectance and spectral transmittance, which are mainly determined by its absorption, reflection and transmission properties. As with any other translucent samples, when light reaches the surface of a tooth, five phenomena associated with the interaction of the radiant energy with the tooth occur: specular reflection at the tooth surface, diffuse reflectance, direct transmission through the tooth, and absorption and scattering of light within the different tooth structures (Joiner, 2004; Lee, 2007) (Figure 1.7).

It is largely accepted that the final color of a tooth is mainly determined by the scattering of the light within the internal tooth structures (van der Burgt et al., 1990). It has to be noted that the tooth presents two histologically different structures: the dentin and the enamel, which interact differently with the incident radiation. For enamel, it was found that the hydroxyapatite crystals contribute significantly to the scattering of light, while the dentine tubules are the predominant cause of scattering within this dental structure (Ten Bosch and Zijp, 1987; Zijp and ten Bosch, 1993). However, it has been reported that the tooth color is determined by the color of the dentine, since the enamel plays only a minor role in the scattering of short wavelengths (blue region) (ten Bosch and Coops, 1995).

There are several other factors that affect the overall appearance of a tooth, such as the translucency, opacity, surface gloss, surface roughness and fluorescence. Among these, the most important are the translucency and opacity, since they represent an indirect measure of the quantity and quality of light interaction with the tooth. It is well known that incisal regions of the tooth present the highest translucency (Hasegawa et al., 2000) and that the surface gloss affects the appearance and vitality of the teeth (Terry et al., 2002).

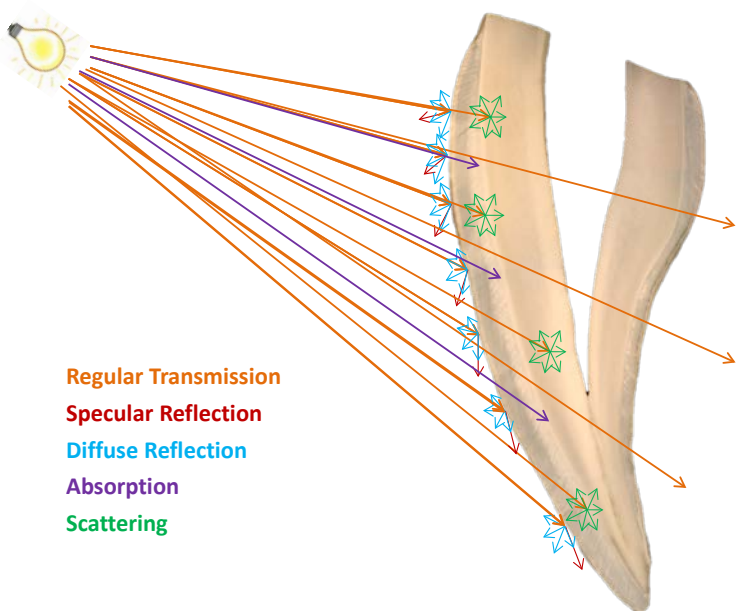

Figure 1.7: Interaction of incident radiation with the tooth: regular transmission, specular reflection, diffuse reflection, absorption and scattering.

The tooth surface morphology affects the amount and type of reflection since a rough or coarse surface allows more diffuse reflection whilst a flat smooth surface allows more specular reflection. The tooth and its internal structures are fluorescent, and this property has to be taken into account when assessing tooth color. The combination of fluorescence from dentine and enamel it is known to enhance the perceived lightness of the tooth (Joiner, 2004), but it has been reported that it does not contribute considerably to visually observed tooth color (ten Bosch and Coops, 1995).

The tooth present a longitudinal color change from the cervical to the incisal area (O'Brien et al., 1997). However, the middle area of the tooth has been described as the site that best represents the color of the tooth (Goodkind and Schwabacher 1987). This is due to the fact that the incisal site is most often translucent and is affected by its background and because the color in the cervical area is modified by the scattered light from the gingiva (Schwabacher et al., 1994).

In the dental field, the range of color and distribution of color in different regions of the tooth have been described by a large number of investigators (Joiner 2004). There are several studies which try to establish a reference chromatic space for dentistry, often addressed as the “dental color space”, within the CIELAB color space

(Rubino et al., 1994; Zhao and Zhu, 1998; Hasegawa et al., 2000; Odioso et al., 2000). The dental color space has to include the color of all natural dental structures, as well as the color of all the restorative materials designed to replace them. So far, it is established that the average values of the CIE L* a* b* C^*_{ab} and h_{ab}chromatic coordinates that more precisely define the dental color space (although it has to be taken into account that there is no large agreement yet on these coordinates, so slight variations from this coordinates are normally accepted), are: $L^* = 62 - 78$; $a^* = 1 - 6$; $b^* = 12 - 31$; $C^*_{ab} = 12 - 33$; $h_{ab} = 78 - 86$ (Baltzer, 2004). The area of the CIELAB color space bounded by the above mentioned coordinates is presented in Figure 1.8.

More recently, Gozalo-Diaz and collaborators measured the color of several craniofacial structures (central and lateral incisor and canine, attached gingiva, lips, and facial skin) of 120 subjects using a spectroradiometer and an external light source configured in 45°/0° geometry (Gozalo-Diaz et al., 2007). According to their results, the color coordinates of the central and lateral incisor and canine teeth ranged between $L^* = 38 - 89.5$, $a^* = 0.3 - 12.2$, and $b^* = 5.7 - 35.7$.

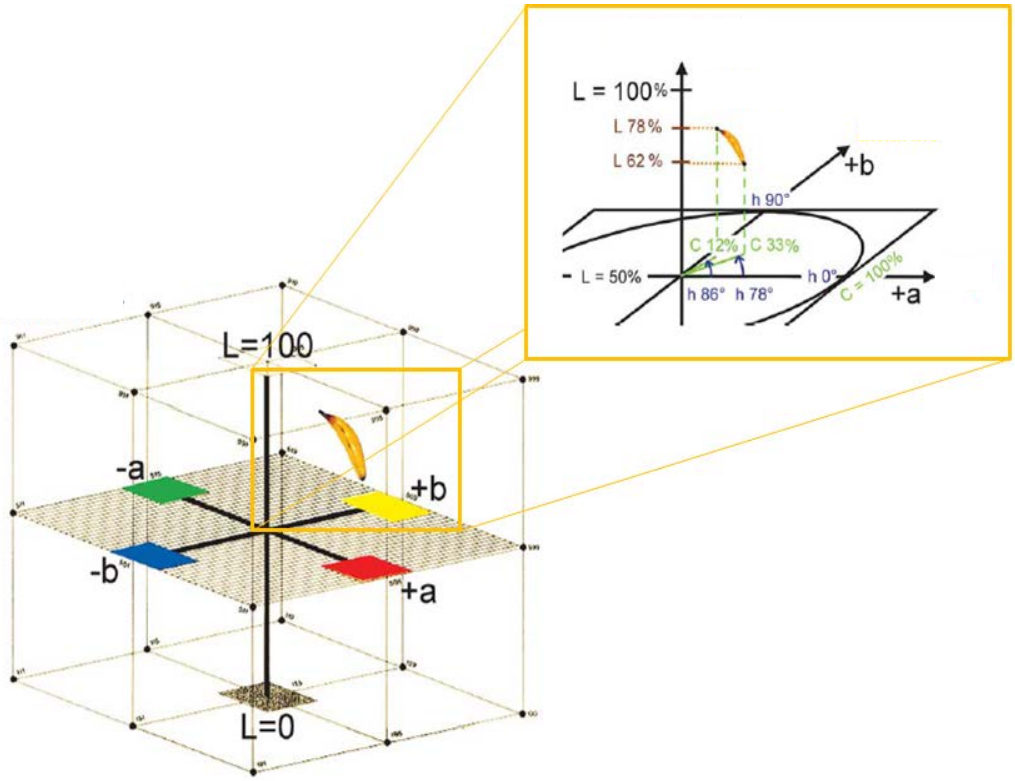

Figure 1.8: Schematic representation of the dental color space within the CIELAB color space (from (Baltzer, 2004)).

Some of the most important challenges of the application of colorimetry in the dental field (measurement of tooth color) have been recently described by Fairchild in a review paper (Fairchild, 2010). Some of them are described below:

- A tooth cannot be considered as a single uniform color stimulus, since tooth color varies spatially from the incisal to the cervical areas;
- Tooth is not opaque, as the ideal reflective stimulus, therefore, as any translucent material, its apparent color depends on the background and also the thickness of the tooth itself. The background of a translucent sample, such as the tooth, affects the values of the CIELAB coordinates. For proper color assessing and measurement, the background on which the stimulus is viewed must be uniform and medium grey. Teeth are never viewed in such controlled conditions and instead have a varied background of other teeth, the darkness of the mouth, or the redness of lips, tongues, and gums.
- Teeth have complex shape and surface geometry therefore they can present geometrical color effects. Also, although tooth can be viewed with strict control of the angle of illumination and angle of viewing, due to their complex geometries, each location on the tooth is subject to a slightly different illumination and viewing geometry and thus, theoretically, should be measured and evaluated with different geometries;
- The viewing illumination should be carefully controlled (as in a viewing booth) and ideally match the illuminant used in colorimetric computations. This is rarely accomplished even in ideal colorimetric situations. In dental applications the illumination varies across the mouth. In some cases, inter-reflections within the mouth will effectively become new, and uncontrolled illuminations, such as reflection of the gums or lips which might serve to make a very reddish effect.

It has been suggested that perceived appearance within the dental environment is too complex to be completely defined by three color parameters (Johnston and Kao, 1989). Since the perception of appearance of teeth includes many factors such as the concepts of color, translucency, gloss, etc. the simple specification of three color parameters derived from an instrument for a given illumination and observation geometry would be incomplete in solely determining the appearance of a translucent

material (Joiner, 2004). Thus, the usefulness of instrumental measurement techniques as a clinical tool has been questioned (Okubo et al., 1998). In this sense, there is a continuous effort made to develop new instrumental measurement equipment and to improve tooth color measurement methods and techniques (Chu et al., 2010). However, regardless of the instrumental technique used in the evaluation of tooth color, the final color assessments are recommended to be the visual ones (Joiner, 2004, Chu et al., 2010). In this sense, when instrumental measurements are made, the values obtained should predict what observers see. The calculated color differences should predict the visual color differences. Therefore, developing and/or improving color difference equations that predict the visual estimations performed by human observers are one of the main goals of recent research in dental colorimetry. However, it has to be taken into account that, in order for the instrumental measurements to correlate with the visual measurement, the conditions under which the samples are evaluated visually are needed to be carefully controlled (Berns, 2000).

1.3. PERCEPTIBILITY AND ACCEPTABILITY VISUAL JUDGMENTS. THRESHOLDS CALCULATIONS.

The reproduction of the coloration of materials using the eye to control the accuracy of matching is a constant challenge in color science. With the development of new optical measurement techniques and the definition of a CIE Standard Colorimetric Observer in 1931, observer judgments on color identity are increasingly replaced by the use of colorimetric devices. However, exact match of color is still a very rare event and, hence, colorimetric values of a matching pair of specimens differ to some extent. It is important to assess the correlation between the measured differences and the magnitude of the perceived color differences. Furthermore, it is of practical interest to compare the sensitivity of the human visual system in relation to the objective color measuring instrument. If the color measuring instrument is more sensitive than the human visual system, there should be an upper limit of the measured color differences which are visually equal. Such a limit is termed as a threshold of the perceived color difference (perceptibility threshold). Subthreshold color differences of matched specimens are visually identical (Schanda, 2007).

In practical (clinical) dental situations, an observer (a client or a customer) is often asked whether he accepts a color difference between two samples (it can be a tooth and the adjacent restoration), and therefore, there is a need to establish an acceptable magnitude of the color difference. It is important then to assign measured colored differences to the scales beyond threshold color differences. This can be done only with psychophysical experimentation, which means to correlate results of the observer tasks with the instrument readings. This is central to the development of color difference evaluation.

1.3.1 THRESHOLD EXPERIMENTS

Threshold experiments are designed to determine the just-perceptible change in a stimulus, sometimes referred to as a just-noticeable difference, or the difference in the stimulus considered as acceptable. Threshold techniques are used to measure the observers' sensitivity to changes in a given stimulus. Absolute thresholds are defined as the just-perceptible difference for a change from no stimulus, while

difference thresholds represent the just-perceptible difference from a particular stimulus level greater than zero. Thresholds are reported in terms of the physical units used to measure the stimulus. For example, a brightness threshold might be measured in luminance units of cd/m^2, while a color-difference thresholds is specified in units according to the color difference equation used. Sensitivity is defined as the inverse of the threshold since a low threshold implies high sensitivity (Fairchild, 2005).

Threshold techniques are useful for defining visual tolerances such as those for perceived color differences. There are several basic types of threshold experiments.

1.3.1.1 Method of adjustment

The method of adjustment is the simplest and quickest method to determine absolute and color difference thresholds. The observer controls the stimulus magnitude and adjusts it to a point that is just perceptible (absolute threshold), or just perceptibly different (perceptibility difference threshold) from a starting level. In the case of the acceptability judgments, the observer has to adjust the stimulus to a point where the difference with the reference stimulus is acceptable (acceptability difference threshold). The threshold is considered to be the average setting across a number of trials by one or more observers. A major disadvantage of this technique is that the observer is in control of the stimulus, and the result can be affected by the variability in observers' criteria and adaptation effects. It is known that if the threshold is approached from above, adaptation might result in a higher threshold than if it were approached from below. For this reason, often the method of adjustment is used to obtain a first estimate of the threshold to be used in the design of more sophisticated experiments.

1.3.1.2 Method of limits

The method of limits is slightly more complex than the method of adjustment. The experimenter presents the stimuli to the observer at predefined discrete intensity levels in either ascending or descending series. In the case of ascending series, the experimenter begins with a stimulus that is certain to be imperceptible (or acceptable in the case of acceptability judgments), and asks the observers to respond 'yes' if they

perceive it and 'no' if they do not (in the case of acceptability judgments, the observers is asked to respond 'yes' if they consider acceptable the difference with the reference stimulus and 'no' if they do not consider acceptable the difference with the reference stimulus). If they respond 'no', the experimenter increases the stimulus intensity and presents another trial. This continues until the observer responds 'yes'. In the case of a descending series, the experimenter begins with a stimulus that is clearly perceptible (or not acceptable in the case of acceptability judgments and continues until the observers respond that they cannot perceive the difference between the stimuli (or accepts the difference with the reference stimulus in the case of acceptability judgments). The average stimulus intensity at which the transition from 'no' to 'yes' in the ascending trials, or vice versa in the descending trials, is recorded as an estimate of the threshold. Ascending and descending series often yield slight but systematic differences in thresholds. Therefore, the two types of series are usually used in alternation and the results are averaged to obtain the threshold estimate and to minimize adaptation effects.

1.3.1.3 Method of constant stimuli

In the method of constant stimuli, the experimenter chooses several stimulus intensity levels which, on the basis of previous exploration, are likely to encompass the threshold value. Then each of these stimuli is presented multiple times in a quasi-random order that ensures each will occur equally often. Over the trials, the frequency with which each stimulus level is perceived is determined. From such data, a frequency-of-seeing curve, or psychometric function can be derived. The psychometric curve allows determination of the threshold and its uncertainty. By convention, the absolute threshold measured with the method of constant stimuli is defined as the value that generates "perceived" (or "acceptable") responses on 50% of the trials. Psychometric functions can be derived either for a single observer (through multiple trials) or for a population of observers. Two types of response can be obtained:

- Yes–no (or pass–fail): the observers are asked to respond 'yes' if they detect the stimulus (or stimulus change) and 'no' if they do not. The psychometric function is the percentage of 'yes' responses as a function of stimulus intensity.

A level of 50% 'yes' response is considered as the threshold level. Alternatively, this procedure can be used to measure visual tolerances above threshold by providing a reference stimulus intensity (for example a color difference anchor pair) and ask the observers to pass stimuli that fall below the intensity of the reference (for example, if they present a smaller color difference) and fail those that fall above it (for example, if they present a larger color difference). The psychometric function is represented by the percent of fail responses as a function of stimulus intensity and the 50% level is deemed to be the point of visual equality.

- Forced choice: the stimulus is presented in one of two intervals defined by either a spatial or temporal separation. The observers are asked to indicate in which of the two intervals the stimulus was presented and are forced to guess one of the two intervals if they are unsure (hence the name forced choice). The psychometric function is presented as the percentage of correct responses as a function of stimulus intensity. The function ranges from 50% correct when the observers are simply guessing to 100% correct for stimulus intensities at which they can always detect the stimulus. Thus the threshold is defined as the stimulus intensity at which the observers are correct 75% of the time and therefore, detecting the stimulus 50% of the time.

If the stimuli are well selected and the number of repetitions large enough, the method of constant stimuli provides a complete and precise view of the psychometric function. Furthermore, this method is easy to administer and, under the same conditions, yields unbiased and reliable threshold estimates.

However, when this type of threshold determination method is carried out, it has to be taken into account that the stimuli must correspond to the interval where the psychometric function increases from 0 to 1. This requires that the experimenter has to have some knowledge of this range of values before starting the experiment. Still, when there is a lot of variability between subjects, the method can still be quite inefficient as many trials are wasted over stimulus values away from the threshold.

Although the method of constant stimuli is assumed to provide the most reliable threshold estimates, it has to be taken into account that it is time-consuming and requires a patient, attentive observer because of the many trials required.

1.3.2 ANALYSIS OF THRESHOLD DATA

The performance of an observer on a psychophysical task is typically summarized by reporting one or more response thresholds—stimulus intensities required to produce a given level of performance—and by characterization of the rate at which performance improves with increasing stimulus intensity. These measures are typically derived from a psychometric function (Wichmann and Hill, 2001).

As mentioned before, the psychometric function describes the probability of an observer's response as a function of the stimulus intensity or stimulus variation. In the case of difference thresholds, the psychometric function models the probability of a positive response according to the physical quantity with which it is related (as for example color difference between two samples).

If a fixed threshold for detection exists, the psychometric function should show an abrupt transition from "not perceived" to "perceived" (or "unacceptable" to "acceptable"). However, psychometric functions seldom conform to this all-or-none rule. What we usually obtain is a sigmoid (S-shaped) curve that reflects that lower stimulus intensities are detected occasionally and higher values more often, with intensities in the intermediate region being detected on some trials but not on others.

In the context of fitting psychometric functions either a logistic function or a probit function are the most commonly employed (Berns et al., 1991; Martínez et al., 2001). Although the analytical form of these functions differ, they all have in common several properties, such as:

- they are sigmoidal (S-shaped);
- they increase monotonically from 0 to1;
- they have parameters which need to be fitted to the data analyzed.

Most theoretical psychometric functions have two parameters, α and β, that are related to the location and slope of the curve. The precise meaning of these

parameters, and their relation to the location and slope of the curve depends on the variant of the function used.

One of the most common logistic functions used for psychometric function estimation (fitting of visual data) is given by the equation:

$$f(x|\alpha,\beta) = 1/\left[1 + e^{(\alpha+\beta x)}\right]$$

while the most employed probit function (defined as the integral of the standardized normal distribution - Gaussian probability density function), is given by:

$$f(x|\alpha,\beta) = \int_{-\infty}^{\alpha+\beta x} \frac{1}{\sqrt{2\pi}} e^{-z^2} dz$$

where α is the intercept and β is the slope in both cases.

1.3.3 FUZZY LOGIC

Fitting psychometric functions is a variant of the more general problem of modeling data. Modeling data is a three step process. First, a model is chosen, and the parameters are adjusted to minimize the appropriate error metric or loss function. Second, error estimates of the parameters are derived, and third, the goodness of fit between the model and the data is assessed (Wichmann and Hill, 2001). Due to the deficiencies of the sigmoid functions, mainly derived from the shape of the function which not always properly fits the visual data, the development of new fitting techniques becomes of great interest. These techniques are able to better adjust to the observer data and to provide accurate estimates of the thresholds. Fuzzy logic is one of the best proposals that have emerged in recent years, and, due to its characteristics, is an ideal candidate to perform this task.

Fuzzy logic, or fuzzy set theory, is a machine learning technique introduced by Zadeh in 1965 (Zadeh, 1965). Since its appearance, its application in all areas has been growing due to its ability to deal with imprecise and uncertain information. Its internal operation intends to mimic the human brain in the treatment of this type of information. Its main applications are control systems and modeling of physical phenomena. In this sense, there is an important link with the neural networks, with

which it is equivalent under certain specific conditions, in this case being called neuro-fuzzy systems.

It is important to underline at this point that the basic concepts introduced here are a drastic simplification of the concepts and formulation associated with fuzzy set theory, and that the concepts and methodology explained here can be extended with introductory bibliography to fuzzy systems (Buckley, 1992; Driankov, 1996; Haykin, 2009).

We will present basic level operating of a Takagi-Sugeno-Kang (TSK) fuzzy model (Takagi and Sugeno, 1985), with numeric entry, use of T-norm product conjunction and implication, and a default set of fuzzy rules for automatic modeling of a data set. This type of models are widely used in the literature since they are relatively easy to implement, are universal approximates (any real system can be approximated as well as desired using a TSK type fuzzy system under certain basic conditions) (Castro, 1995) and they offer the possibility to obtain a model interpretable by an expert, with the ability to extract knowledge about the functioning of the underlying physical model.

1.3.3.1 Fuzzy sets and membership functions

The key concept in fuzzy logic is the fuzzy set, which is usually defined by a membership function. If X is a collection of objects generically denoted by x, a fuzzy set A in the working universe X is defined by a set of ordered pairs in the form:

$$A = \{(x, \mu_A(x))/x \in X\}$$

where $\mu_A(x)$ is the membership function of an element x to the A set. The most important feature of this function is that it can take any value within the normalized range [0,1].

The uniqueness of fuzzy logic over classical logic is that the membership of a sample x to a A set is not defined by "yes" or "no" (which can call values $\mu_A(x) = 0$, $\mu_A(x) = 1$ respectively) but considers the uncertainty that can occur when assessing the membership, as happens in countless real cases. The similarity between fuzzy logic and the probability theory is important, although they pursue different objectives.

There are numerous membership functions of fuzzy systems defined in the literature. Among these, the most well-known are the triangular functions and the Gaussian function. A Gaussian membership function has the form of a Gaussian function determined by its center and its radius, with a value of 1 in the center point and tending to zero as we move away from it, but without ever reaching it.

$$\mu(x) = e^{-\frac{(x-c)^2}{2 \bullet \sigma^2}}$$

1.3.3.2 Fuzzy rules

A fuzzy rule is a conditional statement expressed symbolically as:

IF statement_A THEN statement_B

where both statement_A and statement_B can be simple (one term) or composed (multiple terms) fuzy statements. The “IF” part is called the antecedent of the rule while the "THEN" part is called the consequent.

In the Takagi-Sugeno-Kang (TSK) model, the consequent is a numeric function of the system inputs. A TSK type fuzzy rule relates therefore the fuzzy set associated with antecedent statement with the numerical value associated with the consequent statement (not diffuse in this case).

1.3.3.3 Fuzzy inference in a rule

In order to obtain a conclusion from a given antecedent, a fuzzy inference process is normally used. For TSK systems, this process consists primarily in performing calculations between the fuzzy sets associated with the statements that compose the rules, in order to obtain a numerical conclusion. There are two fundamental mechanisms of inference: the Generalized Modus Ponens (GPM) and the Generalized Modus Tollens (GTM), although the most commonly used is the Generalized Modus Ponens, and consists of:

Premise 1: X is P'

Premise 2: IF X is P THEN Z is B

Conclusion: Z is B'

where P is a linguistic value associated with a fuzzy set, and P', B and B' are numerical values. In classical logic, a rule is triggered if and only if the premise is exactly equal to the antecedent of the rule. In fuzzy logic, on the contrary, a rule is activated as long as there is a similarity between the premise and the antecedent of the rule ($\mu_P(P') > 0$), thereby enabling different degrees of rule activation.

The value B' obtained as a conclusion after the inference process for a rule, given a value of the variable x, can be calculated as follows (using the product operator for the implication function):

$$B' = \mu_P(P') \overset{impliccation}{\tilde{\bullet}} B = \alpha_1 \bullet B$$

where α_1 symbolizes the degree of similarity between the value P of the antecedent of the rule and the P' measured value (value of the membership function for $\mu_P(x)$ for $x = P'$).

Generalizing the formulation of the fuzzy logic theory, the value B' obtained as a conclusion after the inference process for a rule, given the values of the variables x and y, can be calculated as follows (using the product operator for the implication function and the conjunction of the premises):

$$B' = \left(\mu_P(P') \overset{conjunction}{\tilde{\bullet}} \mu_Q(Q') \right) \overset{implication}{\tilde{\bullet}} B = \alpha_1 \bullet \alpha_2 \bullet B = \alpha_{rule} \bullet B$$

where α_1 represents the degree of similarity between the value P of the antecedent of the rule and the mean P' value (value of the membership function for $\mu_P(x)$ for $x = P'$); α_2 represents the degree of similarity between the value Q of the antecedent of the rule and the mean Q' value (value of the membership function $\mu_Q(y)$ for $y = Q'$) and α_{rule} the total activity of the rule.

1.3.3.4 Fuzzy Inference in a system of rules

Finally, if instead of having a single rule we have a system of rules, we must resort to a last operation in the process of inference, called aggregation operator, so that we can, from a given fuzzy input, obtain the output inferred by a set of fuzzy rules. This operator is usually a weighted average for TSK systems. So, if we have a set of rules, which can represent generically as:

$$IF\ x_1\ is\ \mu_1^k(x_1)\ AND\ \ldots\ AND\ x_n\ IS\ \mu_n^k(x_n)\ THEN\ Z\ is\ B_k$$

where $\mu_i^k(x_i)$ is the membership function of the rule k for the input variable x_i, n is the number of input variables, and B_k the constant value of the consequent of the rule k. The value B' of the output variable Z for a system of rules defined as described above, can be calculated as:

$$B' = \frac{\underbrace{\sum_{k=1}^{nrules}}_{aggregation} \alpha_k \underbrace{\bullet}_{implication} B_k}{\underbrace{\sum_{k=1}^{nrules}}_{aggregation} \alpha_k}$$

where α_k is the degree to which the input vector activates the rule k, B_k is the value given by the consequent of the rule k and α_k are calculated as a function of the exact numerical values of input $\vec{x} = \{x_1, \ldots, x_n\}$, $\vec{x}' = \{x_1', \ldots, x_n'\}$:

$$\alpha_k \equiv \underbrace{\prod_{i=1}^{n}}_{conjunction} \alpha_{i,k} = \underbrace{\prod_{i=1}^{n}}_{conjunction} \mu_i^k(x_i')$$

From the above equations, the numerical output of our system for a non-fuzzy generic input vector is given by:

$$\widetilde{F}(\vec{x}) = \frac{\sum_{k=1}^{nrules} B_k \cdot \prod_{i=1}^{n} \mu_i^k(x_i)}{\sum_{k=1}^{nrules} \prod_{i=1}^{n} \mu_i^k(x_i)}$$

1.3.3.5 Optimizing a rule-based fuzzy system for data modeling

The optimization of a fuzzy set to model a system with given input and output data, involves the following steps:

- calculation of the optimal consequent of the rules (values in the rules);
- adjustment of the parameters of the membership functions according to the antecedents (adjustment of centers and radius of the Gaussian membership functions);
- cross-validation of the fitting in order to determine the optimal number of rules and avoid overfitting.

There are a number of methodologies described for fuzzy systems learning. Among these, we can distinguish mainly between two types: automatic techniques (Pomares et al., 2002) and techniques based on genetic algorithms and genetic fuzzy systems (Cordon et al., 2001). Genetic algorithms are highly effective at finding solutions, yet have the problem of computational cost, which for complex fuzzy systems can be excessive. Normally, for TSK Fuzzy applications, the consequent of the rules are optimized given a set of fuzzy sets and partitioning of the input space given (Rojas et al., 2000; Pomares et al.,2002).

1.3.3.6 Optimizing a fuzzy system from a set of rules with fixed antecedents

The optimization of a linear or nonlinear model typically attempts to minimize the mean square error given by

$$J = \frac{\sum_{m \in D} \left(\widetilde{F}\left(\vec{x}^m\right) - y^m \right)^2}{\# D}$$

where D is the set of input and output data indexed by the index m $\left\{\vec{x}^m, y^m\right\}$, and # D is its size. Since the output function of TSK type fuzzy system is linear with respect to all parameters of the consequent, the minimization of the error function leads to the creation of a system of equations which can be solved mathematically with the Singular Value Decomposition (SVD) method (Golub, 2012). In addition to calculating the optimal values, the SVD method provides a ranking of the most relevant coefficients, allowing the exclusion of values with low weight which, in some cases, lead to redundancy and unmanageable solutions (could eliminate unnecessary rules).

Furthermore, the minimization of J given in the above equation with respect to the B_k consequents is performed by equating the derivative of this function with respect to corresponding parameters to 0. Thus, for each B_k :

$$\frac{\partial J}{\partial B^k} = \frac{2}{\#D}\sum_{m\in D}\left(y^m - \frac{\sum_{j=1}^{nrules}\mu^j\left(\vec{x}^m\right)\bullet B^j}{\sum_{j=1}^{nrules}\mu^j\left(\vec{x}^m\right)}\right)\frac{\mu^k\left(\vec{x}^m\right)}{\sum_{j=1}^{nrules}\mu^j\left(\vec{x}^m\right)}$$

which equaling to 0 leads to a system of equations (one for each B_k coefficient) of the form (which is resolved by SVD):

$$\sum_{j=1}^{nrules}\sum_{m\in D}\frac{\mu^k\left(\vec{x}^m\right)\mu^j\left(\vec{x}^m\right)\bullet B^j}{\sum_{j=1}^{nrules}\mu^j\left(\vec{x}^m\right)} = \sum_{m\in D}\frac{y^m\mu^k\left(\vec{x}^m\right)}{\sum_{j=1}^{nrules}\mu^j\left(\vec{x}^m\right)}$$

As already mentioned, the solution of this system of equations would provide the optimal consequents for the set of rules, which optimizes the fit (lower value of mean square error J) of a given set of input/output D.

1.3.4 COLOR DIFFERENCE THRESHOLDS IN DENTISTRY

The need to establish chromatic discrimination thresholds in dentistry emerged as a need to respond to the increasing esthetic demands of modern dental restorations.

The study of Kuehni and Marcus (Kuehni and Marcus, 1979) is one of the main references in assessing acceptability and perceptibility thresholds for small color differences. In this study, no significant differences were found between perceptibility and acceptability judgments, and a level of ΔE^*_{ab}=1 was determined as both acceptable and perceptible color difference for 50% of the observers. However, it has to be mentioned that perceptibility is strictly a visual judgment, whereas the acceptability considers the intended application. In 1989, Seghi and collaborators evaluated the perceptibility thresholds for translucent dental porcelains according to the visual judgments performed by a panel of 27 observers, all of whom were dental professionals (Seghi et al., 1989). They concluded that sample pairs producing a measured color-difference value of greater than 2 ΔE^*_{ab} units were correctly judged by the observer group 100% of the time, incorrect judgments were made infrequently by the observers when the measured color differences fell within the 1 to 2 ΔE^*_{ab} unit range and observer misses became much more frequent when the measured values of the sample pairs were less than one unit. They also suggested the need of establishing acceptable color difference, which, although were not assessed in their work, are expected to be two or three times greater than the detectable limits. In their paper on color stability of dental composite resin materials for crown and bridge veneers, Ruyter and collaborators stated that, color differences with corresponding ΔE^*_{ab} values lower than approximately 3.3 units are considered as acceptable (Ruyter et al., 1987). Later, Ragain and Johnston specifically studied the color acceptance of direct dental restorative materials by a panel of human observers which contained dental auxiliaries, dentist, dental material scientists and dental patients (Ragain and Johnston, 2000). According to their results, the 50:50% acceptability threshold was set as ΔE^*_{ab}=2.72 units.

Douglas and Brewer studied the acceptability and perceptibility of color differences in metal ceramic crowns using a panel of twenty prosthodontists with an

average of 14 years experience and considering the a* and b* axes of the CIELAB color space as independent (Douglas and Brewer, 1998). They concluded that the 50:50% thresholds for perceptibility judgments (mean value ΔE^*_{ab}=0.4 units) were considerably lower than 50:50% thresholds for acceptability judgments (mean value ΔE^*_{ab}=1.7 units). Furthermore, they established that for samples differing in values of the a* axis, the threshold value was ΔE^*_{ab}=1.1 units, while for samples differing in values of the b* axis, the threshold value was ΔE^*_{ab}=2.1 units. However, one of the main flaws of this study is the use of linear fitting between the visual data (observer answers) and the instrumentally measured color differences.

More recently, Douglas and collaborators determined the tolerance of dentists for perceptibility and acceptability of shade mismatch, using a test denture that was fabricated to allow 10 maxillary left central incisors of varying shade mismatch with the right central incisor to be interchanged within the denture base (Douglas et al., 2007). According to their results, the acceptability and perceptibility color tolerances at the 50:50% level were significantly different, as their 95% confidence limits did not overlapped. The predicted color difference at which 50% of the dentist observers could perceive a color difference (50:50% perceptibility) was ΔE^*_{ab}=2.6 units, while the color difference at which 50% of the subjects would remake the restoration due to color mismatch (clinically unacceptable color match) was established as ΔE^*_{ab}=5.5 units.

Sim and collaborators studied the color perception among different dental personnel by having them select a Vita Lumin shade tab that best matched each of a series of shade tabs (Sim et al., 2001). According to their results, the mean differences between test and matching tabs in the L*, a*, and b* directions of CIELAB space considered as perceptible were 4.5, 0.69, and 2.4, respectively. It should be mentioned that these estimates of threshold were not based on independent tests along each color axis, but represented the outcome of subjects attempting to select a match among preset color shade tabs that varied in all three dimensions of color space.

Lindsey and Wee studied the perceptibility and acceptability of CIELAB color differences in computer-simulated teeth (Lindsey and Wee, 2007). They analyzed the color differences in each of the three principal axes of CIELAB color space (L*, a*, and

b*) according to the visual judgments performed by a panel consisting of twelve dental professionals (four from each of the following groups: dentists, dental auxiliaries, and fixed prosthodontic technicians) and four dental patients. According to their results, 50% match or acceptance points averaged 1.0 unit in the L* and a* directions, and 2.6 units in the b* direction. No differences between thresholds for acceptability versus perceptibility were found.

In summary, although there exists a sizeable literature on the perceptibility and/or acceptability of dental color differences, this literature is diverse both in methodologies employed as well as in the results obtained in the study of tooth color differences. Furthermore, to the best of our knowledge, there are no studies on perceptibility and acceptability judgments in dentistry using the CIEDE2000 color difference formula.

1.4. DENTAL RESTORATIVE MATERIALS - DENTAL RESIN COMPOSITES

The application of materials science to medicine, the so-called "biomaterials science" is a subject of growing interest since the beginning of the 21st century. Over the last forty years, numerous artificial materials (metals, ceramics and polymers) have been used for a wide range of applications, such as orthopedics (hips, knees, fingers), craniofacial reconstruction, cardiovascular surgery (heart valves, stents, vascular implants), ophthalmic surgery, dentistry, etc.

The main goal of dentistry is to maintain or improve the quality of life of the dental patient. This goal can be accomplished in many ways, as by preventing disease, relieving pain, improving mastication efficiency, enhancing speech or improving the appearance of the dental structures (Anusavice et al. 2013). Since many of these objectives require the alteration or even the replacement of a tooth structure, one of the main challenges for centuries have been the development and selection of biocompatible, long-lasting, direct-filling tooth restoratives and indirectly processed prosthetic materials that can withstand the conditions of the oral environment.

A wide variety of materials have been used as tooth crown and root replacements, including animal teeth, bone, human teeth, ivory, seashells, ceramics, and metals. However, the four main groups of materials used in dentistry today are metals, ceramics, polymers, and composites. Despite recent improvements in the physical properties of dental materials, none of these can be used as a permanent restoration. Dentists, material scientists, physicist and chemists are working together in order to find the ideal dental restorative material, which, among many other properties, has to: be biocompatible; display a permanent bond to the tooth, structure or bone; display physical properties similar to those of tooth enamel, dentin or other dental tissues which will replace; be capable of initiating tissue repair or regeneration of missing or damaged tissues; and finally but not least, and especially in esthetic dentistry, have the ability to match the natural appearance of the natural tooth structure which will finally replace (Anusavice et al., 2013).

Within the large field of dental materials, the sub-class of restorative dental materials consist of all synthetic components that can be used to repair or replace

tooth structure, including primers, bonding agents, liners, cement bases, amalgams, resin-based composites, compomers, hybrid ionomers, cast metals, metal-ceramics, ceramics, and denture polymers.

Restorative materials may be used for temporary, short-term purposes (such as temporary cements and temporary crown and bridge resins), or for long-term applications (dentin bonding agents, inlays, onlays, crowns, removable dentures, fixed dentures, and orthodontic appliances). These materials can also be designed as controlled-delivery devices for release of therapeutic or diagnostic agents. Restorative materials may further be classified as direct restorative materials or indirect restorative materials, depending on whether they are used intraorally (to fabricate restorations or prosthetic devices directly on the teeth or tissues) or extraorally (the materials are formed indirectly on casts or other replicas of the teeth and other tissues).

1.4.1 DENTAL RESIN COMPOSITES

In dentistry, the term resin composite generally refers to a reinforced polymer system used for restoring hard tissues, for example, enamel and dentin. The proper materials science term is *polymer matrix composite* or for those composites with filler particles often used as direct-placed restorative composites, *particulate-reinforced polymer matrix composite*.

Dental resin composites are used to replace missing tooth structure and modify tooth color and contour, thus enhancing esthetics. An important number of commercial resin composites are available for various applications. Traditionally some have been optimized for esthetics and others were designed for higher stress bearing areas. More recently, nanocomposites, which are optimized for both excellent esthetics and high mechanical properties for stress bearing areas have become available (Craig and Powers, 2002).

Resin-based composites were first developed in the early 1960s and provided materials with higher mechanical properties than acrylics and silicates, lower thermal coefficient of expansion, lower dimensional change on setting, and higher resistance to

wear, thereby improving clinical performance. Early composites were chemically activated and the next generation were photo-activated composites, initiated with ultraviolet (UV) wavelengths. These were later replaced by composites activated in the visible wavelengths. Continued improvements in composite technology have resulted in modern materials with excellent durability, wear-resistance, and esthetics that mimic the natural teeth. In particular, the incorporation of nanotechnology in controlling the filler architecture has made dramatic improvements in these materials. Moreover, the development of bonding agents for bonding composites to tooth structure has also improved the longevity and performance of composite restorations.

1.4.2 DENTAL RESIN COMPOSITES: CHEMICAL COMPOSITION

Chemistry of a biomaterial is of critical importance since it provides information regarding the composition of the materials, the nature of its surface behavior, its potential for degradation in vivo and so on, and all of these aspects impinge on the durability and useful service life of the material. On the other hand, there is a growing understanding of biology at the molecular level - the level at which biology shades into chemistry –so a complete understanding of the chemistry of a biomaterial will also provide comprehensive explanation of the biological interactions between the synthetic material and the natural structure.

A dental resin composite is composed of four major components: organic polymer matrix, inorganic filler particles, coupling agent, and the initiator-accelerator system as well as other components in small quantities: inhibitors, fluorescent agents, pigments, etc.

1.4.2.1 Resin Matrix

The vast majority of monomers used as organic resin matrix are dimethacrylate compounds. Two monomers that have been commonly used are 2,2-bis[4(2-hydroxy-3-methacryloxy-propyloxy)-phenyl] propane (Bis-GMA) and urethane dimethacrylate (UDMA). Both contain reactive carbon double bonds at each end that can undergo addition polymerization initiated by free-radical initiators. The use of aromatic groups

provides a good match of refractive index with the radiopaque glasses and thus provides better overall optical properties of the composites.

A difficulty with Bis-GMA is that it is very viscous at room temperature, as a result of the presence of OH groups in the molecule (Braden and Davy, 1986), and this makes handling and incorporation of fillers difficult. Consequently, it is usually diluted with lower viscosity monomers which present low molecular weight with difunctional carbon double bonds, for example triethylene-glycol-dimethacrylate (TEGDMA). Although the use of diluents reduces considerably the viscosity, one of the disadvantages of adding diluent is that it tends to increase the contraction on polymerization. This effectively limits the amount of diluent that can be added to a practical formulation for clinical use (Nicholson, 2002). However, adding lower viscosity monomers to Bis-GMA is the only way of achieving a clinical consistency when the resin mixture is compounded with the filler (Craig and Powers, 2002). The problem of polymerization contraction is an inherent feature of polymer-based restorative systems. However, it can be significantly reduced, if not overcome completely, by the inclusion of fillers in the material. Nowadays, modern dental resin composites use a mixture of Bis-GMA, TEGDMA and UDMA monomers. The chemical structure of these three compounds is shown in Figure 1.9.

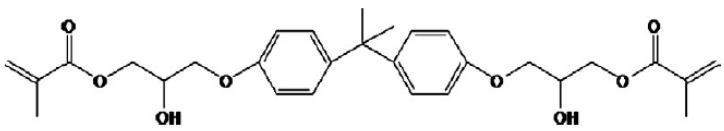

Structure of Bis-GMA.

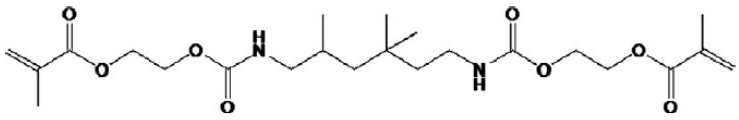

Structure of UDMA.

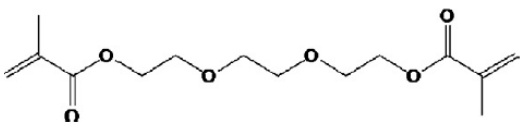

Structure of TEGDMA.

Figure 1.9: Chemical structure of 2,2-bis[4(2-hydroxy-3-methacryloxy-propyloxy)-phenyl] propane (Bis-GMA), urethane dimethacrylate (UDMA) and triethylene glycol dimethacrylate (TEGDMA).

The degree of conversion of Bis-GMA monomer under clinical conditions has been shown to be approximately 55% for a chemically cured system (Gebelein et al., 1981) and about 48% for a UV cured system (Braden, 1997). Use of diluent can increase it to more than 70%. This increase in conversion leads to improvements in the stability of the cured resin and to an increase in the degree of crosslinking, which in turn brings about an increase in modulus, due to reduced mobility of polymer chains (Nicholson, 2002).

1.4.2.2 Fillers

Fillers represent a major portion by volume or weight of the composite. The addition of fillers, confer to the dental composite many desirable properties. The function of the filler is to reinforce the resin matrix, provide the appropriate degree of translucency, control the volume shrinkage of the composite during polymerization and reduce water uptake and coefficient of thermal expansion. They also improve mechanical properties of the material, such as compressive strength, tensile strength, Young's modulus and abrasion resistance (Nicholson, 2002).

Fillers have been traditionally obtained by grinding minerals such as quartz, glasses, or sol-gel derived ceramics. Most glasses contain heavy-metal oxides such as barium or zinc so that they provide radiopacity for visualization when exposed to x-rays. Also, fillers based on silicas or silicates of various types, can be blended into the monomer phase to produce the composite system (Lutz and Phillips, 1983).

Colloidal silica particles (0.04 μm size range) may be prepared by pyrolytic processes in which $SiCl_4$ is burned in an atmosphere of oxygen and hydrogen. Alternatively, they can be prepared from colloidal SiO_2 or by reacting colloidal sodium silicate with HCl. The resulting fine dust-like particles of silica are spheroidal in shape, and are referred to as microfiller. Their very small size means there is a severe limitation on the amount that can be incorporated into the monomer blend without producing an excessively viscous paste (Nicholson, 2002). However, it is worth mentioning that it is advantageous to have a distribution of filler diameters so that smaller particles fit into the spaces between larger particles and provide more efficient packing (Craig and Powers, 2002).

Normally, the classification of the dental composites is made accordingly to the particle size, shape, and the particle-size distribution of the filler. In this sense, it can be distinguished between:

- Macrofills: contain large spherical or irregular shaped particles of average filler diameter of 20 to 30μm. The resultant composites are opaque and have low resistance to wear;
- Hybrid: hybrid composites present two types of fillers that are blended together: fine particles of 2-4μm average particle size and 5% to 15% of microfine particles, usually silica, of 0.04-0.2μm particle size;
- Microhybrid: in microhybrid composites, the fine particles of a lower average particle size (0.04-1μm) are blended with microfine silica. The distribution of filler particles provides efficient packing so that high filler loading is possible while maintaining good handling of the composite for clinical placement. Microhybrid composites may contain 60% to 70% filler by volume, which, depending on the density of the filler, translates into 77% to 84% by weight in the composite;
- Nanocomposites: within the nanocomposite class it can be distinguished between: Nanofills - contain only nanometer sized particles (1-100nm) throughout the resin matrix, and Nanohybrids - consist of mixture of large particles (0.4-5μm) and nanometer sized particles (1-100nm).

1.4.2.3 Coupling Agent

For a composite to have successful clinical performance, a good bond must be formed between the inorganic filler particles and the organic resin matrix. Also, if properly bound to the matrix, fillers provide mechanical reinforcement. This enables the stress to be transferred from the lower modulus polymeric phase to the higher modulus filler (Lutz and Phillips, 1983). This is achieved through the use of compounds called coupling agents, the most common of which are organic silicon compounds, called silane coupling agents. The most extensively used coupling agent in dental resin composite formulation is y-methacryl-oxy-propyl-tri-methoxysilane (Nicholson, 2002). This substance is deposited onto the surface of the filler using a 0.025-2% aqueous

solution considered to be sufficient to create a monolayer. Adhesion is achieved by the siloxane bond between the silanol groups of the hydrolysed silane and the equivalent functional groups on the surface of the filler. It is not only adhesion of filler to matrix that is enhanced by the presence of these coupling agents but hydrolytic degradation of the interface has also been shown to be reduced when these silanes are present (Soderholm, 1981).

Therefore, the coupling agent plays an important role in the composite formulation, since it forms an interfacial bridge that strongly binds the filler to the resin matrix, it enhances the mechanical properties of the composite and minimizes the plucking of the fillers from the matrix during clinical wear. As mentioned, the resulting interfacial phase provides a medium for stress distribution between adjacent particles and the polymer matrix and also provides a hydrophobic environment that minimizes water absorption of the composite (Craig and Powers, 2002).

1.4.2.4 Initiators and Accelerators

The curing of composites is triggered either by light or a chemical reaction, with the first one being actually more common. Light activation is accomplished with blue light at a peak wavelength of about 465 nm, which is absorbed usually by a photo-sensitizer added to the monomer mixture during the manufacturing process in amounts varying from 0.1% to 1.0%. The initiator used in dental resin composites is camphorquinone – CQ – (bornanedione,1,7,7-trimethylbicyclo[2.2l.] heptane-2,3-dione), typically in association with amines (Gruber, 1992). In methacrylate composites, free radicals are generated upon activation. The setting is initiated by the use of a special dental curing lamp that emits radiation with 465nm wavelength and with a light intensity of at least 500 W/m^2 (Watts et al., 1984). However, care is needed with these materials, as they will undergo some sluggish polymerization under normal clinical illumination conditions (Dionysopoulos and Watts, 1990).

The reaction is accelerated by the presence of an organic amine. Various amines have been used, both aromatic and aliphatic. The amine and the camphorquinone are stable in the presence of the oligomer at room temperature, as long as the composite is not exposed to light. When camphorquinone is irradiated in

the presence of hydrogen donors, such as the amine accelerators used in dental composites, there is an initial abstraction of hydrogen by the excited camphorquinone molecule, CQ*. The radicals thus formed from the hydrogen donors can initiate the required polymerization with the Bis-GMA and other monomers. A typical accelerator is ethyl 4-dimethylaminobenzoate (Nicholson, 2002).

Although camphorquinone is the most common used photo-sensitizer, other photo-initiators are casually used to accommodate special esthetic considerations. It is well known that camphorquinone adds as light yellow tint to the uncured composite paste. Although the color bleaches during cure of the dental composite, sometimes clinicians find shade matching difficult due to the color shift. Some composites, such as core and provisional products, are dual cured. These formulations contain initiators and accelerators that allow light activation followed by self-curing or self-curing alone (Craig and Powers, 2002).

In clinical use, care has to be taken over depth of cure with light-activated composites. Light is attenuated as it passes through the composite, which means that there is less light to activate polymerization deep within the material. This means that the upper layer cures better than the lower layers (Sustercic et al., 1997) and in the extreme, the very bottom may not cure at all. In addition, the color of the restoration affects the depth of cure, since darker shades attenuate light more than lighter shades. To overcome these problems, the technique of incremental build-up of restorations is used, each increment being 2 mm or less, to ensure there is adequate light-penetration even at the bottom of the layer (Nicholson, 2002).

1.4.2.5 Pigments

To produce the desired esthetic effects of a restoration the incorporation of colored pigments in nonmetallic materials such as resin composites, denture acrylics, silicone maxillofacial materials, and dental ceramics it is often required. The perceived color results from the absorption of specific wavelengths of light by the pigments and the reflection of other wavelengths. Inorganic pigments are often preferred to organic dyes because the pigments are more permanent and durable in their color qualities. When colors are combined with the proper translucency, restorative materials can be

made to closely match the surrounding tooth structure or soft tissue. To match the color of the tooth, various shades of yellow, red and occasionally even some blue or green pigments are added and blended into the white base material (Craig and Powers, 2002; Anusavice et al. 2013).

Inorganic oxides are usually added in small amounts to provide shades that match the majority of tooth shades. The most common pigments are oxides of iron. A UV absorber may also be added to minimize color changes caused by oxidation.

1.4.2.6 Fluorescence

Sound human teeth emit fluorescent light when excited by ultraviolet radiation (365 nm), the fluorescence being polychromatic with the greatest intensity in the blue region (450 nm) of the spectrum. Therefore, in order to mimic the natural appearance of the tooth structure, the use of fluorescing agents in the formulations of the anterior restorative materials and dental porcelains is recommended.

Fluorescent agents are added to enhance the optical vitality of the composite and mimic the appearance of natural teeth. These are dyes or pigments that absorb light in the ultraviolet and violet region (usually 340-370 nm) of the electromagnetic spectrum, and re-emit light in the blue region (typically 420-470 nm). These additives are often used to enhance the appearance of color causing a perceived “whitening” effect, making materials look less yellow by increasing the overall amount of blue light reflected.

Resin composites have been successfully used in a variety of clinical situations and they show reasonable longevity. These include direct filling materials, but also prosthodontic applications, such as bonding of crowns and bridges, luting and so-called core build-up - the reinforcement of the core part of a tooth, prior to the replacement of a metal or ceramic crown (Nicholson, 2002).

CHAPTER 2

MOTIVATION AND OBJECTIVES

MOTIVACIÓN Y OBJETIVOS

This PhD Thesis is intended to contribute to the progress of knowledge in the field of esthetic dentistry and development of dental materials as well as its application in both clinical practice and industry.

Nowadays, the development of dental materials which are able to successfully replace the dental tissues and also mimic the surrounding dental structure is of great clinical and social interest, and it represents a research field which concentrates the efforts of an important part of the scientific community. In this context, a better understanding of the colorimetric characteristics of these materials is a research area of particular relevance.

In dentistry, being able to properly measure and specify the color, following the latest implemented and most rigorous criteria and standards, is, beyond any doubt, very useful, but its utility would be considerably higher if the measurements and the visual perception of patients were strongly correlated.

The CIELAB color space and its associated ΔE^*_{ab} total color difference have been widely used in research and applications in the dental field. However, the lack of uniformity of CIELAB had led to the development of new color difference formulas, being the CIEDE2000(K_L:K_C:K_H) formula the currently recommended by the International Commission on Illumination (CIE). It becomes therefore necessary to evaluate the adequacy of this new metric in the dental field, particularly for applications involving the use of dental materials and in color research in dentistry.

Moreover, and within a wider framework, a deeper and more complex understanding of the colorimetric characteristics of the dental materials requires the knowledge of how the structure and chemical components of the material influence these characteristics. In particular, in the case of the dental resin composites, the type and quantity of pigment used in the chemical formulation of the resin composite is a determining factor. Therefore, the development of mathematical algorithms that are able to establish or even predict the final chromatic coordinates or reflectance spectra of these materials represents an important advance with direct applications in clinical practice and industry.

Therefore, in this PhD Thesis we established the following objectives:

Main Objective

To evaluate the adequacy of the application of the CIEDE2000(K_L:K_C:K_H) color difference metric in dentistry and the development of mathematical algorithms able to predict the final color of dental materials.

Specific Objectives

1. To determine the (50:50%) perceptibility and acceptability thresholds for dental materials using the new CIEDE2000 color difference formula and TSK Fuzzy Approximations as fitting procedure.

2. To evaluate the differences in visual sensitivity by calculating the (50:50%) CIEDE2000(K_L:K_C:K_H) acceptability thresholds for variations in lightness, chroma, and hue in the dental color space.

3. To evaluate the suitability of the use of CIEDE2000(2:1:1) color difference formula versus CIEDE2000(1:1:1) formula in dentistry by calculating the (50:50%) acceptability thresholds and new evaluation techniques: TSK TaSe Fuzzy Approximation and the statistical performance factors PF/3 and STRESS.

4. To develop algorithmic models that allow the prediction of the color and reflectance spectrum of experimental dental resin composites based on the quantities and types of pigments used in its formulation and to evaluate these models by means of the values of the chromatic discrimination thresholds.

5. To develop algorithmic models that allow the determination of the quantity and type of pigments used in the formulation of the experimental dental resin composites based on their final chromaticity coordinates and spectral reflectance values.

According to these objectives, from this point, this PhD thesis is structured in 4 Chapters, describing the State of the Art, the Materials and Methodology used and the corresponding Results and relevant Discussion, each one designed in order to accomplish the proposed objectives (Chapters 3-6). Chapter 7 shows the final conclusions of our study. All the references are provided in Chapter 8, whereas Chapter 9 enumerates the published papers related with the work presented in this PhD Thesis.

Con la presente Tesis Doctoral se pretende contribuir al avance del conocimiento en el campo de la estética dental y en el desarrollo de materiales dentales asi como de su aplicación tanto en la práctica clinica como en el ambito industrial.

En la actualidad, el desarrollo de materiales dentales capaces de sustituir con éxito los tejidos dentales y que se mimetizan con la estructura dental que las rodea es una realidad que despierta gran interés clínico y social, y en la que concentra sus esfuerzos una parte importante de la comunidad científica. En este contexto, profundizar en el estudio de las características colorimétricas de estos tipos de materiales es una línea de investigación de especial relevancia.

En odontología, la posibilidad de medir y especificar el color siguiendo los criterios y estándares más rigurosos y de recién implementación es, sin duda, de gran utilidad, pero esta utilidad sería considerablemente mayor siempre que dicha medida y la percepción visual de los pacientes estuvieran fuertemente correlacionadas.

El espacio de color CIELAB y su diferencia de color asociada ΔE^*_{ab} han sido, hasta la actualidad, ampliamente empleados en investigación y aplicaciones dentales. No obstante, la falta de uniformidad de CIELAB ha dado lugar al desarrollo de nuevas fórmulas de diferencia de color, siendo la fórmula CIEDE2000(K_L:K_C:K_H) la actualmente recomendada por la Commission Internationale de l'Éclairage (CIE). Se hace por tanto necesario evaluar la adecuación de esta nueva métrica en el ámbito dental, en concreto para aplicaciones que implican el uso de materiales dentales y para la investigación relacionada con el color en odontología.

Por otra parte, y dentro de un marco general, profundizar en el conocimiento de las características colorimétricas de los materiales dentales requiere conocer la influencia de su estructura así como de sus componentes químicos sobre éstas. En concreto, para las resinas dentales de composite, el tipo y cantidad de pigmento empleado en su formulación es un factor determinante. Por ello, el desarrollo de algoritmos matemáticos que permitan establecer, e incluso predecir, las coordenadas cromáticas finales o los espectros de reflectancia de dichos materiales, supone un importante avance con aplicación directa en clínica e industria.

Por todo ello, en la presente Tesis Doctoral nos planteamos los siguientes objetivos:

Objetivo General

Evaluar la adecuación de la aplicación de la fórmula de diferencia de color CIEDE2000(K_L:K_C:K_H) en el ámbito de la odontología y desarrollar algoritmos matemáticos capaces de predecir el color final de los materiales dentales.

Objetivos específicos

1. Determinar los umbrales de perceptibilidad y aceptabilidad (50:50%) para materiales dentales empleando la nueva fórmula de diferencia de color CIEDE2000 y métodos de ajustes basados en aproximaciones TSK Fuzzy.

2. Evaluar las diferencias en sensibilidad visual mediante el cálculo de los umbrales de aceptabilidad CIEDE2000(K_L:K_C:K_H) (50:50%) para variaciones en luminosidad, croma y tono en el espacio cromático dental.

3. Evaluar la idoneidad del uso de la formula CIEDE2000(2:1:1) en odontología frente a la formulaCIEDE2000(1:1:1), mediante el cálculo de los umbrales de aceptabilidad (50:50%) y nuevas técnicas de evaluación: Aproximación TSK TaSe Fuzzy y los factores estadísticos de rendimiento PF/3 y STRESS.

4. Desarrollar modelos algorítmicos que permitan predecir el color y el espectro de reflectancia de resinas de composite experimentales a partir de las cantidades y tipos de pigmentos utilizados para su formulación. Evaluar estos modelos a partir de los valores de los umbrales de discriminación cromática.

5. Desarrollar modelos algorítmicos que permitan determinar la cantidad y tipo de pigmentos utilizados en la formulación de resinas de composite experimentales a partir de sus coordenadas cromáticas finales o de los valores de la reflectancia espectral.

De acuerdo con el planteamiento de estos objetivos, la presente Tesis Doctoral se estructura a continuación en 4 capítulos, cada uno describiendo los antecedentes, los materiales y la metodología utilizados, así como los resultados obtenidos y su correspondiente discusión, con el fin de cumplir con los objetivos propuestos (Capítulos 3-6). El Capítulo 7 presenta las conclusiones finales de nuestro estudio. Todas las referencias se proporcionan en el Capítulo 8, mientras que el Capítulo 9 enumera las publicaciones científicas relacionadas con el trabajo presentado en esta Tesis.

CHAPTER 3

PERCEPTIBILITY AND ACCEPTABILITY COLOR DIFFERENCE THRESHOLDS IN DENTISTRY

3.1 STATE OF THE ART

The correlation between the perceived and instrumentally measured color is an issue of great practical interest in colorimetry. The ability to measure color and rigorously specify it is, beyond any doubt, very useful, but this utility would be even greater if the experimental measurement and the perception of normal color vision observers were strongly correlated. A particular aspect of this problem is represented by the correlation between the perceived color differences (ΔV) and the instrumentally measured color differences (ΔE). Therefore, the color difference formulas (ΔE) are expected to be able to provide a quantitative representation of the perceived color difference (ΔV) between a pair of colored samples under a given set of experimental conditions.

In dentistry, the color difference formulas have been used extensively, covering a wide range of applications, such as the quantification of color change caused by processing dental materials (Rosenstiel et al., 1989; Rosenstiel et al., 1989), the study of coverage errors of available dental shade guides (O'Brien et al., 1991; Bayindir et al., 2007), the study of the performance assessment of colorimetric devices on dental porcelains (Seghi et al., 1989), the color accuracy and precision of digital cameras for use in dentistry (Wee et al., 2006), studies of color perceptibility or acceptability by human observers (Ragain and Johnston, 2000; Wee et al., 2007) or the study of the translucency parameter in oral applications (Johnston et al., 1995).

In almost all of the color dental studies, the color coordinates of the studied samples as well as the associated color differences are quantified using the CIELAB color space and the associated ΔE^*_{ab}, respectively. However, there is still an important gap between the perceived and computed color differences when using the CIELAB formula, and in past years, there have been several new color differences formulas developed with the aim of minimizing (improving) these differences: the CMC (l:c) color difference formula (Clarke et al., 1984), the CIE94 color difference formula (CIE, 1995) and the most recent CIEDE2000 color difference formula (CIE, 2001; Luo et al., 2001; CIE, 2004). Nowadays, the International Commission on Illumination

recommends the use of the CIEDE2000 color difference formula, whenever in the past the CIE94 or CMC formulas were used (CIE, 2004).

What distinguishes the CIEDE2000 formula from other color difference formulas is the use of the concepts of chroma and hue, reinforcing the importance of the conceptual developments of Munsell, but most importantly the introduction of a rotation term that accounts for the interaction between chroma and hue differences. In dentistry, there are several studies available which are performing comparisons between the CIELAB and the CIEDE2000 formulas (Lee, 2005; Del Mar Pérez et al., 2007). Although recent reports have shown that there are strong correlations between the values obtained using the two color difference formulas (Kim et al. 2005; Lee, 2005; Paravina et al., 2005), the majority of the reported correlations showed only that the values obtained from these formulas were proportional, but not that the two color difference formulas could be used interchangeably in dental research.

One of the applications of the color difference formulas is the calculus of either perceptible or acceptable thresholds. As presented in Chapter 1 of this Phd Thesis, just perceptible color difference refers to the smallest color difference that can be detected by an average human observer with normal color vision. A color difference that can be noticed by 50% of a representative panel of observers corresponds to the so-called 50:50% perceptibility threshold. Analogously, the difference in color that is considered as acceptable by 50% of the observers corresponds to the 50:50% acceptability threshold. To determine the level of perceptibility or acceptability, the responses of the panel of observers are plotted as a function of the instrumental color differences (psychometric function), consequently fitted either with an S-Shaped function or with a logistic regression analysis and finally the 50% levels calculated (Ragain and Johnston, 2000; Martínez et al., 2001; Wee et al., 2007). Nevertheless, there are new fitting procedures available, such as the Fuzzy Approximation with a complementary Takagi-Sugeno-Kang (TSK) model (Takagi and Sugeno, 1985), which are based on the fuzzy logic and were already used successfully in dental research (Herrera et al., 2010) and might be able to improve the quality of the fit of the visual judgments with respect to the instrumental color measurements. Also, the new color difference formulas are expected to provide better correlation between the visual judgments by

human observers and instrumental color differences. An improved correlation might lead to a more suitable color difference formula for samples in the dental color space and a more accurate clinical interpretation of the color differences in dentistry.

Perceptibility and acceptability color difference thresholds have been extensively studied in dentistry (Ruyter et al., 1987; Seghi et al., 1989; Ragain and Johnston, 2000; Wee et al., 2007). However, these mentioned studies predominantly use the oldest CIELAB color difference formula, while the number of studies that used the newest CIEDE2000 color difference formulas is very limited. Another important aspect to consider when evaluating these studies is the fact that they used diverse methodology and the results obtained are very hard to compare.

The main objective of this Chapter is to establish, using the CIEDE2000 color difference formula and TSK Fuzzy fitting procedures, a 50:50% perceptibility and acceptability thresholds for dentistry. The null hypothesis tested was that there was no difference between the perceptibility and acceptability thresholds for dental ceramics.

3.2 MATERIALS AND METHODS

3.2.1 SAMPLE FABRICATION

For the development of the present study, a total of 15 ceramic discs were fabricated using mixtures of Vita Omega 900, Vitapan 3D-Master opaque powders and pink, white and mauve color opaque powders (VITA Zahnfabrik, Germany), as previously described in a published study (Wee et al., 2007). All samples were disc shaped with 14mm diameter and 3 mm thick (Figure 3.1).

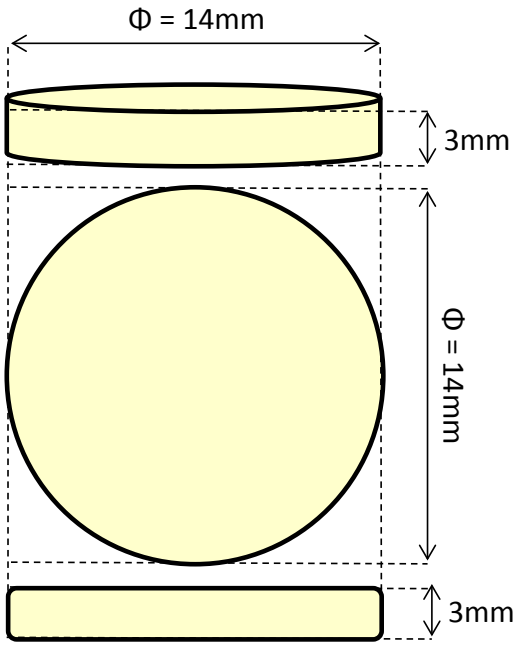

Figure 3.1: Schematic representation of the manufactured ceramic discs.

3.2.2 REFLECTANCE MEASUREMENTS AND COLOR CALCULATIONS

A non-contact SpectraScan PR-704 spectroradiometer (Photo Research, USA) was used to measure the reflectance spectra of all ceramic discs. This type of device has been used previously in dental research (Del Mar Pérez et al., 2009; Luo et al., 2009) due to its versatility and ability to measure color in a way that perfectly matches the geometry of a visual assessment (Figure 3.2).

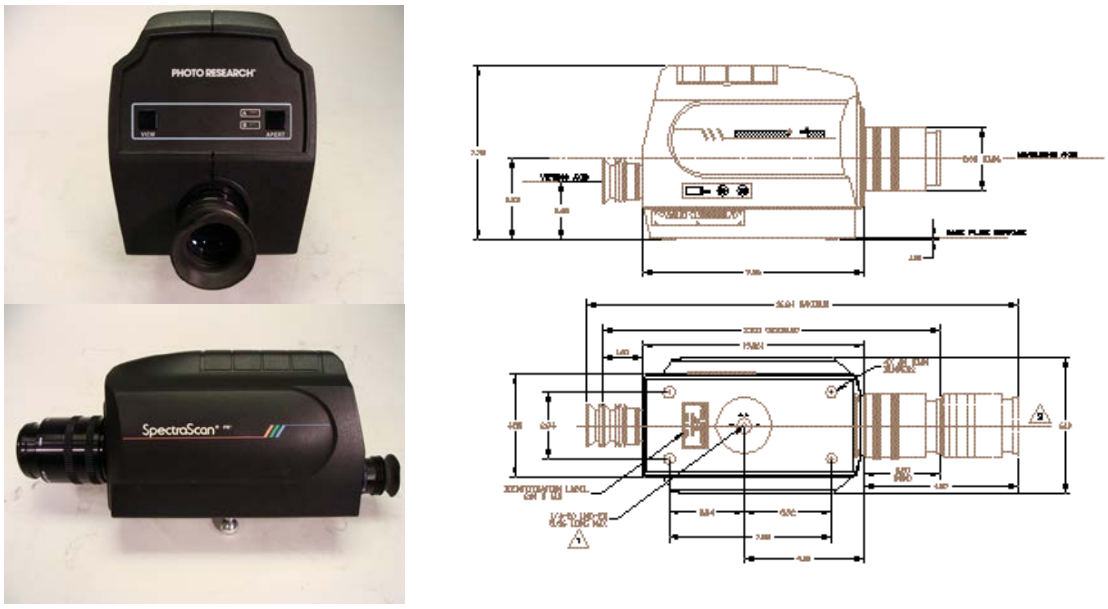

Figure 3.2: Photoresearch SpectraScan PR-704 spectroradiometer used for reflectance measurements.

The SpectraScan PR-704 is a parallel acquisition (fast-scan) spectroradiometer with a fixed polychromator (diffraction grating) which disperses the majority of the visible spectrum (380nm-780nm) onto a thermoelectrically cooled 256 silicon photodiode array detector. Each of the 256 detectors measures a specific wavelength which allows the measurement of the entire spectrum simultaneously. The photodiode array is scanned electronically in a very short time. By thermoelectrically cooling the detector, changing the exposure time and digitally integrating repeated scans, the sensitivity and dynamic range is optimized for the sample being measured.

The ceramic discs were positioned 40cm away from the spectroradiometer, over a 45° tilted base and in the center of a VeriVide CAC60 viewing cabinet (VeriVide Ltd., United Kingdom). To provide consistent measuring conditions, all samples were illuminated with a light source simulating the spectral relative irradiance of the CIE D65 standard illuminant. The corresponding illuminating/measuring geometry obtained corresponded to diffuse/0° (Figure 3.3). The CIE 1931 2° Colorimetric Standard Observer was used to calculate color coordinates of each sample. Since teeth are translucent and the oral cavity is dark, a Munsell black background (L*=2.8, a*=0.7, b*=1.9) was used for all measurements performed in this study. In order to avoid specular reflection from the glossy surface, and similar to another study (Luo et al., 2009), a triangular stand was built to hold the samples.

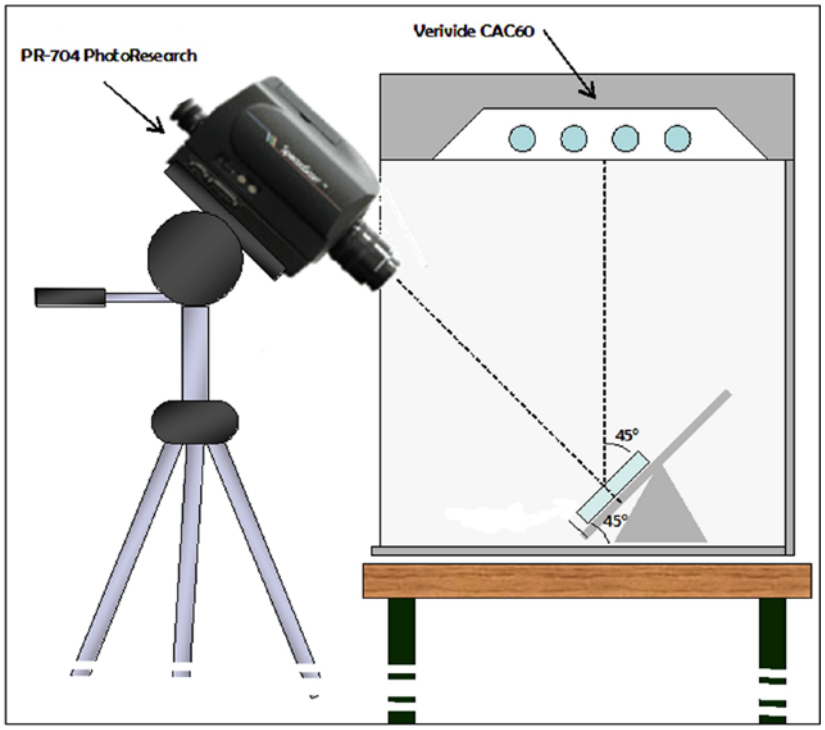

Figure 3.3: Schematic representation of the experimental set-up used for reflectance measurements.

The range of the color coordinates of the ceramic discs were L*=53.95 – 76.05, a*=0.33 – 9.94 and b*=4.59 – 29.75, all within the color range of central and lateral incisor (Gozalo-Diaz et al., 2007).

The CIELAB color difference (ΔE^*_{ab}) was computed as:

$$\Delta E^*_{ab} = [(\Delta L^*)^2 + (\Delta a^*)^2 + (\Delta b^*)^2]^{1/2}$$

where ΔL^*, Δa^* and Δb^* are the differences between the two samples forming the pair in lightness, green-red coordinate and blue-yellow coordinate, respectively.

The CIEDE2000 color difference (ΔE_{00}) was calculated as:

$$\Delta E_{00} = \sqrt{\left(\frac{\Delta L'}{K_L S_L}\right)^2 + \left(\frac{\Delta C'}{K_C S_C}\right)^2 + \left(\frac{\Delta H'}{K_H S_S}\right)^2 + R_T\left(\frac{\Delta C'}{K_C S_C}\right)\left(\frac{\Delta H'}{K_H S_H}\right)}$$

where $\Delta L'$, $\Delta C'$ and $\Delta H'$ are the differences between the two samples forming the pair in lightness, chroma and hue, and R_T is the rotation function which accounts for the interaction between chroma and hue differences in the blue region. The weighting functions S_L, S_C and S_H adjust the total color difference for variation in the location of the color difference pair in L', $a'$and b' coordinates and the parametric factors K_L, K_C

and K_H are correction terms for experimental conditions. For calculations made in this study, all the parametric factors were set to 1. All the discontinuities due to mean hue computation and hue-difference computation pointed out and characterized by Sharma and collaborators (Sharma et al., 2005) were taken into account when the calculations with the CIEDE2000 color difference formula were performed.

The 15 ceramic discs were combined to create a total of 105 disc pairs, with CIELAB color differences ranging from 0.3 to 13.17 units while the CIEDE2000 color differences ranged from 0.10 to 9.91 units. The distribution of the color differences among the 105 sample disc pairs is shown in Figure 3.4, for calculations made with the CIELAB formula (Figure 3.4 top) and with the CIEDE2000 color difference formula (Figure 3.4 bottom).

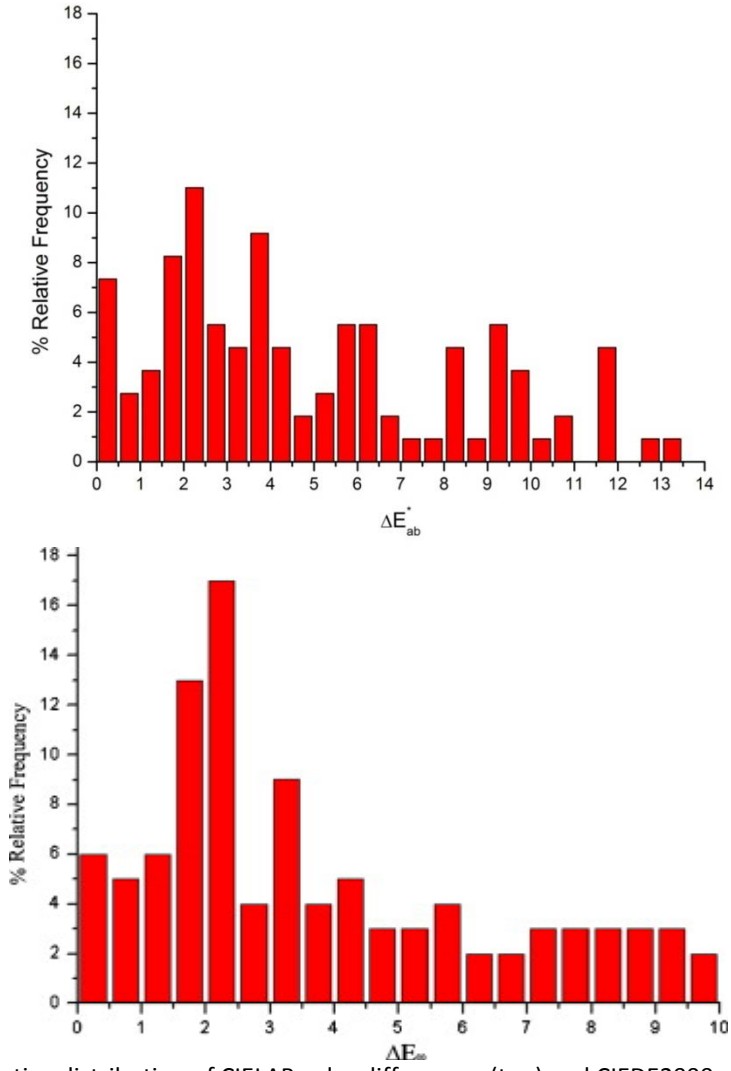

Figure 3.4: Relative distribution of CIELAB color differences (top) and CIEDE2000 color differences (bottom) among pairs of ceramic discs.

3.2.3 PSYCHOPHYSICAL EXPERIMENTS

3.2.3.1 Observers

In order to perform the visual evaluation (judgments) of the 105 ceramic pairs, a panel of 13 observers was recruited (7 females and 6 males aged between 20 and 48 years). In order to be included in the panel, all the observers had to pass a normal color vision test (Ishihara Color Vision Test, Kamehara Trading, Japan) and also all had previous experience in color discrimination experiments.

3.2.3.2 Visual judgments

For visual judgments (comparisons), the sample pair was situated in the middle of the viewing cabinet and illuminated with a source simulating the relative spectral distribution of the CIE D65 Standard Illuminant. The observers were situated approximately 40cm away from the ceramic discs pair, which was the same distance used for instrumental color measurements. All the experiments were conducted in complete darkness and, prior to the beginning of the visual experiment, the observers were allowed two minutes for adaptation to darkness. Each observer was instructed to focus his attention in the central area of the sample and, by judging only the color of the samples, answer the corresponding question:

- Acceptability Threshold: “Would you accept the color difference between the two ceramic discs under clinical conditions?”
- Perceptibility Threshold: “Can you detect a color difference between the two ceramic discs?”

Each observer performed 105 acceptability judgments and 105 perceptibility judgments. The acceptability and perceptibility judgments were performed independently in separate sessions. The responses for each pair of ceramic discs and each observer were annotated and consequently processed.

3.2.3.3 Fitting Procedures

For the evaluation of both acceptability and perceptibility thresholds, two different fitting procedures were used: an S-Shaped curve and a TSK Fuzzy Approximation.

Independently of the fitting procedure used, from the resultant fitting curves obtained, the 95% Upper Confidence Limit (UCL) and the 95% Lower Confidence Limit (LCL) were estimated. The 50:50% threshold levels (50% of positive answers and 50% of negative answers) were calculated for both perceptibility and acceptability as the value of the color difference for which an observer has a 50% probability of making a dichotomous judgment.

1. **S-Shaped curve**: the correlation between the visually perceived and the instrumentally measured color differences was evaluated using a procedure described in previous studies (Strocka et al., 1983, Martínez et al., 2001). For each pair of samples, the percentage of unacceptable (%unacceptable) or imperceptible (%imperceptible) answers were plotted against the instrumentally measured CIELAB and CIEDE2000 color differences. An S-Shaped curve given by:

$$y = A/\left[1 + e^{(B+Cx)}\right]$$

was fitted to the point cloud using an iterative algorithm of successive approximations to the function and its derivatives until maximizing the value of R (Matlab 7.1 Optimization Toolbox, Mathworks, USA).

2. **TSK Fuzzy Approximation:** the main advantage of the TSK Fuzzy Approximation is that it is generally a method to approximate the unknown function that generates the set of observed data. This approach is used to obtain a smooth curve without a pre-designed shape that likewise fits experimental data. In this study, a TSK Fuzzy Approximation with Gaussian membership functions and constant consequents was used to perform the approximation of unacceptable (%unacceptable) or imperceptible (%imperceptible) answers against the instrumentally measured CIELAB and CIEDE2000 color differences (Matlab 7.1 Optimization Toolbox, Mathworks, USA).

3.2.3.4 Acceptability thresholds in the L', C' and H' directions ($\Delta L'$, $\Delta C'$ and $\Delta H'$)

Complementary to this work, a preliminary study of acceptability thresholds for lightness, chroma and hue differences has been performed. To calculate the acceptability threshold for lightness ($\Delta L'$), only the sample pairs which presented

absolute differences in chroma ($\Delta C'$) and hue ($\Delta H'$) smaller than 0.5 units (15 pairs) were selected from the initial 105 ceramic disc pairs. Therefore, it can be considered that the color difference among the samples forming these pairs is originated basically from the lightness differences. The values of $\Delta L'$ among the selected 15 sample pairs ranged from 0.12 to 3.11 units.

Similarly, to evaluate the chroma acceptability threshold ($\Delta C'$), only 18 pairs which presented absolute differences in lightness ($\Delta L'$) and hue ($\Delta H'$) smaller than 0.5 units were selected from the initial 105 ceramic disc pairs. The values of $\Delta C'$ among the selected 18 sample pairs ranged from 0.15 to 7.44 units.

For the evaluation of the hue acceptability threshold ($\Delta H'$), only pairs with lightness ($\Delta L'$) and chroma ($\Delta C'$) absolute differences below 0.5 units were used (16 pairs). The values of $\Delta H'$ among the 16 sample pairs ranged from 0.13 to 4.07 units.

3.3 RESULTS AND DISCUSSION

In Figure 3.5 are plotted the percentages of unacceptable answers (% unacceptable) by the observers against the calculated CIEDE2000 color difference with S-Shaped fitting curve (Figure 3.5 a) and TSK Fuzzy Approximation fit (Figure 3.5 b), as well as their corresponding 95% Upper Confidence Limit and Lower Confidence Limit. In Figure 3.6 are represented the percentages of unacceptable (% unacceptable) answers by the observers against the calculated CIELAB color difference with their corresponding S-Shaped fitting curve (Figure 3.6 a) and TSK Fuzzy Approximation fit (Figure 3.6 b).

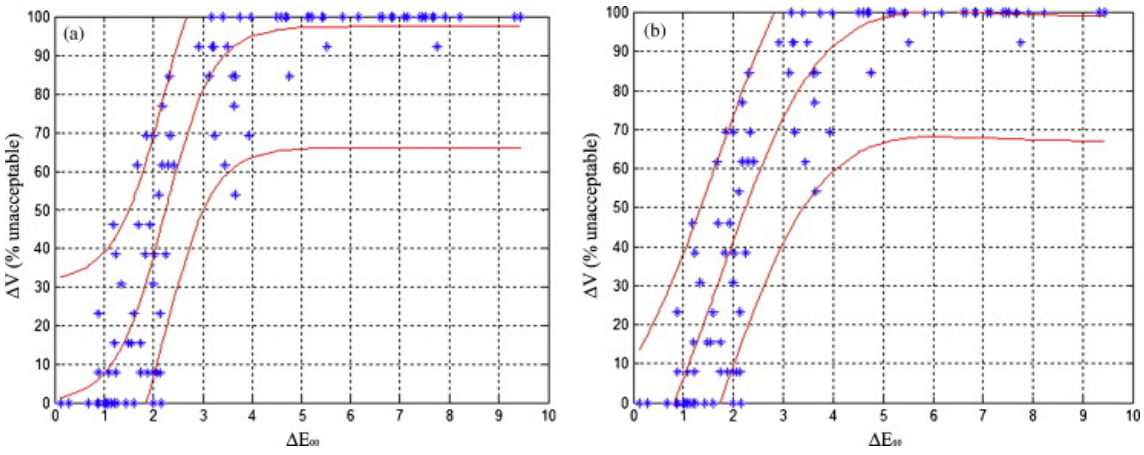

Figure 3.5: Unacceptable percentages versus color differences (ΔE_{00}) between pairs of ceramic discs: (a) fitted S-shape curve y = A/[1 + exp(B + Cx)] (b) TSK Fuzzy Approximation with 4 equally distributed rules along the x-axis and constant consequents.

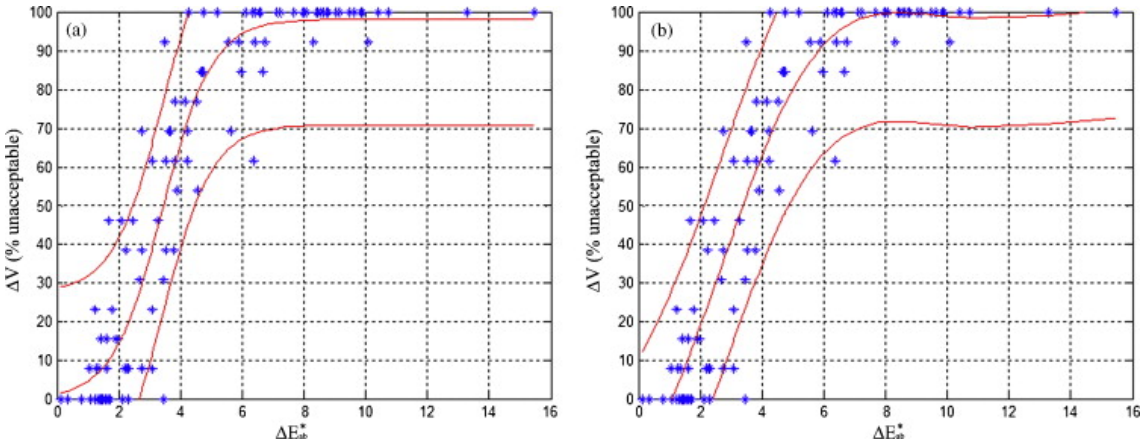

Figure 3.6: Unacceptable percentages versus color differences (ΔE^*_{ab}) between pairs of ceramic discs: (a) fitted S-shape curve y = A/[1 + exp(B + Cx)] (b) TSK Fuzzy Approximation with 4 equally distributed rules along the x-axis and constant consequents.

For the 50:50% acceptability thresholds, the optimal parameters which describe the S-Shaped fitting curve, the optimal number of rules for the TSK Fuzzy Approximation and the values of R^2 of the fit for the two different color difference formulas, are presented in Table 3.1.

When using the S-Shaped fitting curve as adjustment method, the CIEDE2000 color difference corresponding to 50% acceptability was ΔE_{00}=2.25 (95% confidence interval 1.52-3.03) while the corresponding value obtained with the TSK Fuzzy Approximation was ΔE_{00}=2.23 (95% confidence interval 1.55-3.00). The values of the 50:50% acceptability thresholds as calculated with the two different fitting procedures are very similar, but the TSK Fuzzy Approximation presented a slightly better adjustment (R^2=0.89) than the S-Shaped Curve (R^2=0.88) (Table 3.1). In a recent study, Wee and collaborators obtained lower values for the CIEDE2000 acceptability threshold (Wee et al., 2007), but there are numerous important differences between their study and the current one, including the range of color differences and the different experimental conditions, such as surround, use of a shutter, etc. All these differences might have caused the discrepancy between their reported values and the ones found in this study.

For the CIELAB color difference formula, the color difference corresponding to 50% acceptability was ΔE^*_{ab}=3.46 (95% confidence interval 2.48-4.48). When using the TSK Fuzzy Approximation, the corresponding value was ΔE^*_{ab}=3.48 (95% confidence interval 2.49-4.44), with better adjustment obtained for the fuzzy fitting procedure (0.86 compared with 0.85).

50:50% Acceptability Thresholds						
	S-Shaped Curve				TSK Fuzzy	
	A	B	C	R^2	Rules	R^2
ΔE_{00}	97.40	4.53	-2.03	0.88	4	0.89
ΔE^*_{ab}	98.12	4.29	-1.25	0.85	4	0.86

Table 3.1: Optimal parameters of the S-Shaped fitting curve, optimal numbers of rules of the TSK Fuzzy Approximation and R^2 values for the ΔE_{00} and ΔE^*_{ab} 50:50% acceptability threshold.

In Figure 3.7 are plotted the percentages of imperceptible answers (% imperceptible) by the observers against the calculated CIEDE2000 color difference with S-Shaped fitting curve (Figure 3.7 a) and TSK Fuzzy Approximation fit (Figure 3.7 b), as well as their corresponding 95% Upper Confidence Limit and Lower Confidence Limit. In Figure 3.8 are represented the percentages of imperceptible (% imperceptible) answers by the observers against the calculated CIELAB color difference with their corresponding S-Shaped fitting curve (Figure 3.8 a) and TSK Fuzzy Approximation fit (Figure 3.8 b).

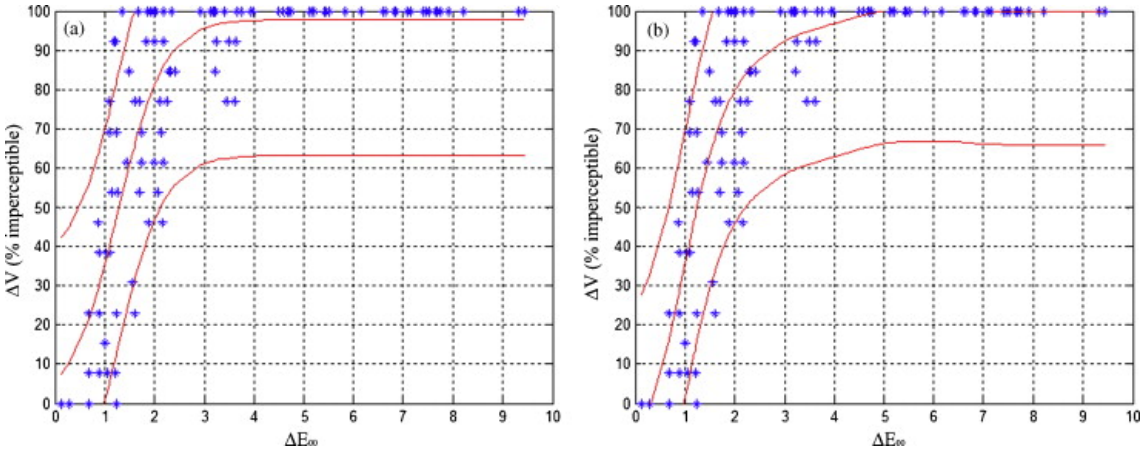

Figure 3.7: Imperceptible percentages versus color differences (ΔE_{00}) between pairs of ceramic discs: (a) fitted S-shape curve y = A/[1 + exp(B + Cx)] (b) TSK Fuzzy Approximation with 5 equally distributed rules along the x-axis and constant consequents.

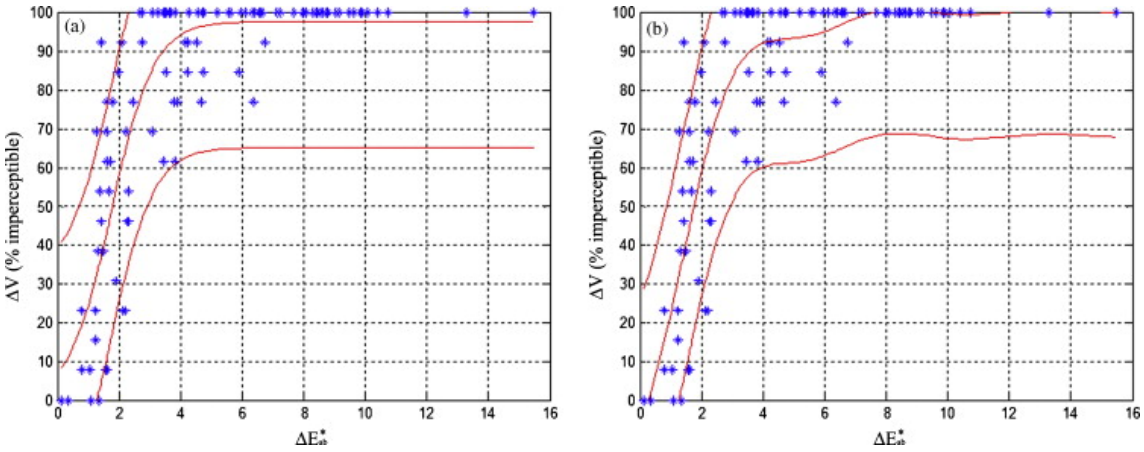

Figure 3.8: Imperceptible percentages versus color differences (ΔE^*_{ab}) between pairs of ceramic discs: (a) fitted S-shape curve y = A/[1 + exp(B + Cx)] (b) TSK Fuzzy Approximation with 5 equally distributed rules along the x-axis and constant consequents.

50:50% Perceptibility Thresholds						
	S-Shaped Curve				TSK Fuzzy	
	A	B	C	R^2	Rules	R^2
ΔE_{00}	97.91	2.75	-2.16	0.74	5	0.75
ΔE^*_{ab}	97.56	2.59	-1.47	0.70	5	0.71

Table 3.2: Optimal parameters of the S-Shaped fitting curve, optimal numbers of rules of the TSK Fuzzy Approximation and R^2 values for the ΔE_{00} and ΔE^*_{ab} 50:50% perceptibility threshold.

For the 50:50% perceptibility thresholds, the optimal parameters which describe the S-Shaped fitting curve, the optimal number of rules for the TSK Fuzzy Approximation and the values of R^2 of the fit for the two different color difference formulas, are presented in Table 3.2.

The ΔE_{00} values corresponding to the 50:50% perceptibility threshold were ΔE_{00}=1.30 units (95% confidence interval 0.50-2.13) when the S-Shaped function was used as fitting method and ΔE_{00}=1.25 units (95% confidence interval 0.69-2.22) when the TSK Fuzzy approximation was used as fitting method. When computing with the ΔE^*_{ab} color difference formula, the 50:50% perceptibility threshold values found were ΔE^*_{ab}=1.80 units (95% confidence interval 0.74-2.92) when the S-Shaped function was used as fitting method and ΔE^*_{ab}=1.74 units (95% confidence interval 0.94-2.94) when the TSK Fuzzy approximation was used as fitting method.

As the case of the acceptability thresholds, the ΔE_{00} corresponding to 50:50% perceptibility thresholds were similar when the S-Shaped adjustment curve or the TSK Fuzzy Approximation were used, with better fit obtained in all cases with the latter method (Table 3.2). Furthermore, the values obtained in the present study for the CIEDE2000 acceptability and perceptibility thresholds equal to a ratio of approximately 70% of the values obtained when the CIELAB color difference formula was used to calculate the thresholds. This behavior was already pointed out by other authors (Paravina et al., 2005; Del Mar Pérez et al., 2007), which found linear relationships between ΔE_{00} and ΔE^*_{ab}, with ΔE_{00} values corresponding to approximately 70-80% of the ΔE^*_{ab} values. It should be pointed out that, although this behavior was found to be valid for a specific region of the color space (the dental color space), it is not necessarily valid for the entire color space. In a recent work (Del Mar Pérez et al.,

2007), the variation between the CIELAB ΔE^*_{ab} and the CIEDE2000 ΔE_{00} color differences for dental resin composites was studied, and it was found that, although there is a significant correlation between the values obtained with the two formulas, due to the important contribution of the weighting functions for lightness, chroma and hue, the use of the ΔE_{00} color difference formula is recommended. Future studies should be carried out in order to clearly establish a relationship between the two formulae for all the regions of the color space.

The values of the CIEDE2000 50:50% acceptability and perceptibility thresholds obtained with the method which provided the best fit (in this case the TSK Fuzzy Approximation) were ΔE_{00}=2.23 and ΔE_{00}=1.25, respectively. When computed with the CIELAB total color difference formula, the 50:50% acceptability and perceptibility thresholds obtained with the best fit method (TSK Fuzzy Approximation) were ΔE^*_{ab}=3.48 and ΔE^*_{ab}=1.74, respectively. As a summary, Table 3.3 shows the values of the acceptability and perceptibility thresholds, as well as the corresponding 95% Upper and Lower Confidence Limits, as calculated with the two color difference formulae.

The null hypothesis was rejected for both color difference formulas and both fitting procedures. If we assume the 50:50% values as normal distribution with variance estimated according to the confidence intervals of the respective curves, the acceptability and perceptibility thresholds were statistically different, as confirmed by a t-test ($p<0.001$ in all cases).

50:50% Threshold		**S-Shaped Curve**		**TSK Fuzzy**	
		Value	**95% CI**	**Value**	**95% CI**
Acceptability	ΔE_{00}	**2.25**	1.52-3.03	**2.23**	1.55-3.00
	ΔE^*_{ab}	**3.46**	2.48-4.48	**3.48**	2.49-4.44
Perceptibility	ΔE_{00}	**1.30**	0.50-2.13	**1.25**	0.69-2.22
	ΔE^*_{ab}	**1.80**	0.74-2.92	**1.74**	0.94-2-94

Table 3.3: ΔE_{00}andΔE^*_{ab} 50:50% Acceptability and Perceptibility thresholds with corresponding 95% Confidence Intervals, as obtained with the two different fitting procedures.

In our study, the 50:50% perceptibility thresholds were lower than the corresponding 50:50% acceptability thresholds, independently of the color difference formula or the fitting procedure used to compute it. In a recent work, Lindsey and Wee, using computer simulated teeth and a panel of 12 dental professionals and 4 dental patients, reported that the acceptability and perceptibility thresholds are nearly identical (Lindsey and Wee, 2007).

In other study, which used 60 ceramic fused to metal crowns as samples and a panel of 20 prosthodontists with an average of 14 years of practice as observers, it was found that the ΔE^*_{ab} acceptability threshold was significantly higher than the perceptibility threshold (Douglas and Brewer, 1998). However, in this study the comparison between the two types of thresholds was not performed independently, since only subjects who previously identified the color difference between the two samples as perceptible were allowed to judge whether the difference was acceptable or not. This procedure forces the values of the thresholds to be clearly different. In our study, the sensorial experiments were performed independently, so the results could not be affected by the experimental method used in the visual judgments.

One of the objectives of the present study was to compare the performance of the two different color difference formulas by means of adjustment to visual judgments performed by observers. It is largely accepted that the use of an adequate color difference formula is important to obtain a better correlation of perceptibility and acceptability to instrumental color difference values. An improved correlation is expected to provide a more accurate clinical interpretation of color differences which can eventually result in research targeted at improving the color replication process in dentistry. According to our results, the CIEDE2000 color difference formula provided higher degree of fit when compared with the CIELAB formula, both for perceptibility and acceptability judgments. The adjustment for the hue importance introduced in the computation of the ΔE_{00} formula, leads to significantly improved performance of the formula against visual data when compared to CIELAB. There are other factors involved in the calculations of the CIEDE2000 color difference formula which are not so largely studied, like the weighting functions or the parametric factors, which, if improved, may result in an even better fit with the visual judgments. The use of an

efficient research design to determine the optimum adjustment functions for color of human teeth is also beneficial. The use of a valid and applicable formula will improve the modeling of tooth colored aesthetic materials and, ultimately, patient satisfaction.

In addition to the standard usual fitting procedure (such as the S-Shaped curve), in this study we used a novel Fuzzy Approximation of the %imperceptible and %unacceptable answers by observers, using a Takagi-Sugeno-Kang (TSK) Fuzzy model (Takagi and Sugeno, 1985; Herrera et al., 2010) with Gaussian membership functions and constant consequents. Emerged as an alternative method to traditional statistics inference, data fuzzy modeling represents a flexible and effective method to model an unknown function from a set of observed data relative to that function or phenomenon (Rojas et al., 2000). This technique is receiving more and more attention in explaining and predicting clinical results in medical sciences (Mahfouf et al., 2001) and it is being currently used in colorimetric studies in dentistry (Herrera et al., 2010).

In a one dimensional problem, as the case of determining the 50:50% acceptability and perceptibility thresholds, the optimization of a TSK Fuzzy Approximation resides in the determination of the optimal number of rules, the position of their respective centers and the calculation of the optimal consequents (Pomares, 2004). In the present work, the rule centers were considered to be equally distributed along the input space and the rule consequents were optimally obtained using their derivatives with respect to the model output in the minimization of the value of R (Least Square Error approach) (Herrera et al., 2005). In each case, the number of rules was selected using a 10-fold cross-validation procedure. The number of rules for which the model provided the lowest cross-validation error was chosen to perform the approximation of data.

Apart from the direct evaluation based on the value of the goodness of fit (R^2), the performance and generalization capabilities of both fitting procedures were additionally assessed using a combined repeated 10-fold cross-validation (10 times 10-fold cross-validation using different random re-orderings) and a t-test statistical analysis. The t-test confirmed that the TSK Fuzzy Approximation outperformed the S-Shaped fitting curve. In general, we can claim that the real shape of the curve

representing the relationship between the instrumental color differences and the response of the human-eye is unknown. The TSK Fuzzy Approximation enable soft and accurate approximations, without limiting the expected shape of the objective function by not modeling a predefine function shape, allowing the adaptation to unknown shapes on the available data, opposite to what occurs with the S-Shaped functions.

According to the results of this study, the TSK Fuzzy Approximation led to a slightly better accuracy in the approximation of the curves, than the S-Shaped function, being therefore a reliable alternative for this problem and a recommendable methodology for approximating color data in dentistry in future studies.

In addition to the study of the total color difference acceptability and perceptibility thresholds for dental ceramics, a pilot study on the acceptability thresholds for lightness ($\Delta L'$), chroma ($\Delta C'$) and hue ($\Delta H'$) differences was carried out. This study was not conducted as an independent study, since for the estimation of these thresholds we used, from the available samples pairs, the ones that fulfilled specific characteristics, as well as their corresponding answers. To calculate the acceptability threshold for lightness ($\Delta L'$) only 15 sample pairs which presented absolute differences in chroma ($\Delta C'$) and hue ($\Delta H'$) smaller than 0.5 units were used, to evaluate the chroma acceptability threshold ($\Delta C'$) only 18 pairs which presented absolute differences in lightness ($\Delta L'$) and hue ($\Delta H'$) smaller than 0.5 units were employed while for the chroma acceptability threshold ($\Delta C'$) only 18 pairs which presented absolute differences in lightness ($\Delta L'$) and hue ($\Delta H'$) smaller than 0.5 units were selected.

As noted, the numbers of pairs used to calculate the thresholds for lightness, chroma and hue differences are considerably lower than the one used for total color difference acceptability thresholds, but nevertheless are similar to the number of sample pairs used in reported literature (Wee, Lindsey et al. 2007).

50:50% Acceptability Thresholds						
	S-Shaped Curve				TSK Fuzzy	
	A	B	C	R^2	Rules	R^2
$\Delta L'$	758.44	5.13	-0.95	0.92	3	0.93
$\Delta C'$	93.69	3.32	-1.10	0.96	3	0.96
$\Delta H'$	68.90	3.11	-1.26	0.95	3	0.96

Table 3.4: Optimal parameters of the S-Shaped fitting curve, optimal numbers of rules of the TSK Fuzzy Approximation and R^2 values for the.$\Delta L'$,$\Delta C'$, and $\Delta H'$50:50% Acceptability thresholds.

In Table 3.4 are presented the optimal parameters which describe the S-Shaped fitting curve, the optimal number of rules for the TSK Fuzzy Approximation and the values of R^2 of the fit for the three data sets of 50:50% acceptability thresholds. As it can be seen, the TSK Fuzzy Approximation provided a better fit than the S-Shaped curve in all cases, with R^2 values equal or higher for all three studied color differences.

The values of the 50:50% acceptability thresholds for $\Delta L'$, $\Delta C'$ and $\Delta H'$ as obtained with the two different fitting procedures are presented in Table 3.5. The results of our study revealed slight differences in tolerance for thresholds in lightness, chroma and hue, especially for the latter two ($\Delta L'$=2.71, $\Delta C'$=3.25 and $\Delta H'$=3.33 when fitted with the S-Shaped Curve and $\Delta L'$=2.44, $\Delta C'$=3.15 and $\Delta H'$=3.24 when fitted with the TSK Fuzzy Approximation).

It is well documented in the available literature that in the Euclidean metric of CIELAB, there is an increase of the tolerance when the color difference is due essentially to the difference in chroma or hue, or when the difference in chroma is very large (Melgosa et al., 1995). In CIELAB-based color difference formulas, such as the CIEDE2000 formula, the tolerance of chroma difference is corrected with a specific weighting function (S_C). Several authors have proven that chroma correction is sufficient to eliminate tolerance difference in lightness, chroma and hue, and that the hue correction, although it is significant, is less important than the chroma correction itself (Huertas, 2004).

50:50% Threshold		S-Shaped Curve	TSK Fuzzy Approximation
Acceptability	$\Delta L'$	**2.71**	**2.44**
	$\Delta C'$	**3.25**	**3.15**
	$\Delta H'$	**3.33**	**3.24**

Table 3.5: $\Delta L'$,$\Delta C'$, and $\Delta H'$50:50% Acceptability thresholds as obtained with the two different fitting procedures.

The slight difference between the tolerance in lightness compared to tolerances in chroma and hue could be due to the specific weighting fucntions defined for lightness in the CIEDE2000 color difference formula computation, or to the fact that the parametric factor K_L should have a different value. In addition, the rotation function (R_T) introduced in ΔE_{00} to weight the interaction between the chroma and hue differences in the blue region, was found to be close to zero for the dental color space, which implies that this term might have not influenced the values of the ΔE_{00}. It becomes therefore necessary to further study this issue, and future studies focused on the development of a new term that includes the interaction between lightness and chroma and hue differences could better explain the results.

The calculated 50:50% acceptability threshold for $\Delta L'$, $\Delta C'$ and $\Delta H'$ were higher than the total 50:50% acceptability thresholds recorded. This result could be justified by the weighting functions (S_L, S_C and S_H). In our study, the tolerances in lightness, chroma and hue were calculated from the differences between the values of lightness, chroma and hue of each sample of the pair, according to:

$$\Delta L' = L'_2 - L'_1$$

$$\Delta C' = C'_2 - C'_1$$

$$\Delta H' = 2 \cdot \sqrt{C'_1 C'_2} sin\left(\frac{\Delta h'}{2}\right)$$

while when calculating with the ΔE_{00} total color difference formula, the differences in lightness, chroma and hue are weighted by their corresponding functions, which are always greater than unity. Therefore, for proper comparison between the acceptability

threshold and tolerances for each of the directions, the influence of the weighting functions on the values of the total color difference should be considered.

In summary, the TSK Fuzzy Approximation led to a slightly better accuracy than the traditional S-shaped function in the color threshold calculation procedure. The CIEDE2000 color difference formula provided a better fit than CIELAB formula in the evaluation of color difference thresholds for dental ceramics, which recommends its use in dental research and in-vivo instrumental color analysis. We also found a statistically significant difference between perceptibility and acceptability thresholds in dentistry.

CHAPTER 4

ACCEPTABILITY THRESHOLDS FOR LIGHTNESS, CHROMA AND HUE DIFFERENCES IN DENTISTRY

4.1 STATE OF THE ART

There is an important variety of instruments used for color measurements in dentistry, such as spectrophotometers, colorimeters and more recently, spectroradiometers. In terms of color matching, shade verification (quality control), communication and reproduction of color in dentistry, the use of these instruments can help overcoming some shortcomings of the visual method by bringing accuracy and also reducing the chair side time. Each of these instruments has its pros and cons, like the colorimeters for example, which although showed good measurement repeatability, are exposed to systematic errors caused by edge-loss effects related with sample surface. Or, for example, spectrophotometers which precisely measure color from reflectance or transmittance data, but they are difficult to use for in vivo tooth color evaluation (Chu et al., 2010). In this sense, the recent incorporation of spectroradiometers for color measurements in dental research provided accurate and highly repeatable non-contact measurements (Ghinea et al., 2010).

The development of the CIELAB color space, and the associated color difference formulas, have helped overcome some of the main problems of color measurements in dentistry. Several authors, studying perceptibility and acceptability color difference thresholds, have pointed out that there is a variance in sensitivity with respect to lightness (L*), green-red coordinate (a*) and blue-yellow coordinate (b*) of the CIELAB color space. In their study using computer-simulated teeth, Lindsey and Wee found that, for observers with a certain level of performance, the acceptability thresholds based on 50% hit rates were 1.00 units in the L* and a* directions and 2.6 in the b* direction (Lindsey and Wee, 2007). Douglas and Brewer in their study of perceptibility and acceptability for shade differences in metal ceramic crowns, reported acceptability levels of 1.1 for the a* axis and 2.1 for the b* axis (Douglas and Brewer, 1998). They were not able to provide lightness acceptability thresholds or perceptibility thresholds for all axes of the CIELAB color space due to poor correlations between instrumental and visual assessments.

The experimental conditions of measurement do not affect the dependence of direction of the CIELAB color differences on color sensitivity. This issue is due to the

fact that the formulas currently employed to convert CIE1931 colorimetric values into CIE L*a*b* coordinates do not adequately capture the perceived color differences (Wyszecki and Stiles, 1982). More advanced color difference formulas were recently introduced in order to improve the correlation between the instrumental and visual color differences, through the implementation of various corrections of the original CIELAB color difference formula ΔE^*_{ab}(CIE, 2004).

Generally, it is assumed that CIELAB is a uniform color space. However, it has been proven that variations in different axis of the color space are not perceived equally. In a study of the performance of several CIELAB-based color difference formulas against wide data sets, it has been shown the need of using weighting functions in order to improve the prediction of the perceived color difference (Melgosa, 1999). Furthermore, in the same study, it has been concluded that the influence of specific parametric factors, such as those affecting the optimal weighting factors for lightness differences, should be further investigated. In this sense, there are several color difference formulas, such as CMC(l:c), CIE94(K_L:K_C:K_H) and CIEDE2000(K_L:K_C:K_H), which employ such weightings factors to adjust the inaccuracies.

The CIEDE2000 color-difference formula incorporates several corrections to improve its capacity to adjust to visual judgments: specific corrections for non-uniformity of the CIELAB color space (the so-called weighting functions: S_L, S_C and S_H), a rotation term that accounts for the interaction between chroma and hue differences in the blue region (R_T) and a modification of the a* coordinate, which mainly affects color with low chroma. For applications in the field of dentistry, this correction is very important, since most of the dental materials present low values of chroma. Also, it incorporates three parametric factors (K_L:K_C:K_H) which account for the influence of the experimental conditions in the color difference evaluation (Luo et al., 2001). The parametric factor ratio was proposed as a way to control changes in the magnitude of tolerance judgments and as a way to adjust for scaling of acceptability rather than perceptibility (Berns, 1996). There are several authors which assume that the texture of the sample only affects lightness tolerances but not chroma or hue tolerances (Steen and Dupont, 2002; Choo and Kim, 2003), therefore proposing the use of K_L=2 instead of the standard value of K_L=1 (Mangine et al., 2005). Regarding the rotation

term (R_T), it was found that its value is close to zero for sample inside the dental color space (Del Mar Pérez et al., 2007).

In the previous Chapter of this PhD Thesis, we reported that the CIEDE2000 color difference formula provided better fit than the CIELAB color difference formula when evaluating visual judgments by a panel of observers, therefore providing better indicators of human perceptibility and acceptability of color differences between tooth colors. It is expected that, an improvement of the weighting functions and/or the parametric factors used to compute the CIEDE2000 color difference formula, will result in an even better fit with the visual judgments.

The preliminary study proposed at the end of the previous Chapter, as it has been pointed out, was a pilot study, which was not designed especially for calculating the lightness ($\Delta \mathrm{L}'$), chroma ($\Delta C'$) and hue ($\Delta \mathrm{H}'$) thresholds. Furthermore, the number of sample pairs used was not the most adequate for a proper evaluation of the thresholds. Therefore, at this point, and since no more extra information is available on CIEDE2000 acceptability thresholds for lightness ($\Delta \mathrm{L}'$), chroma ($\Delta C'$) and hue ($\Delta \mathrm{H}'$) differences for dental materials, we propose a more complete and thorough study for the evaluation of the variability of the visual sensitivity for lightness, chroma and hue. The knowledge of these thresholds can lead to a valid and applicable formula to improve the modeling of tooth colored aesthetic materials, and, ultimately, patient satisfaction.

Two null hypotheses were tested: 1) There is no difference between CIEDE2000 50:50% acceptability thresholds for lightness, chroma and hue; and 2) There is no difference in performance between CIEDE2000(1:1:1) and CIEDE2000(2:1:1) total color difference formulas in evaluation of color differences of dental ceramics.

4.2 MATERIALS AND METHODS

4.2.1 SAMPLE FABRICATION

For the development of the current study a total number of 58 ceramic discs samples were fabricated using mixtures of Vita Omega 900, Vitapan 3D-Master opaque powders and pink, white and mauve color opaque powders (Vita Zahnfabrick, Germany), as described in previous studies (Wee et al., 2007; Ghinea et al., 2010). All samples were 14mm in diameter and 3mm in thickness. The surface to be observed of each sample underwent a sequential polishing procedure up to 800 grit using silica paper (Struers A/S Ballerup, Denmark).

The color coordinates of the ceramic samples were ranged between L'=56.09-75.30, C'=5.60-28.89 and h'=62.16-85.00, all within the color range of central and lateral incisor from a published study (Gozalo-Diaz et al., 2007). The 58 ceramic discs were combined to create a total of 1653 disc pairs, with CIEDE2000(1:1:1) color differences ranging from 0.10 to 10.02 units.

4.2.1.1 Subsets of sample pairs

In order to perform the visual judgments for the three types of acceptability thresholds, the sample pairs were divided into three subsets of sample pairs, as follows:

- **Lightness subset** (only pairs of sample where the total color difference is mainly due to changes in lightness): 40 pairs of samples that met $|\Delta L'/\Delta E_{00}| \geq 0.9$ ($\Delta L'$ ranging from 0.32 to 8.03);
- **Chroma subset** (only pairs of sample where the total color difference is mainly due to changes in chroma): 40 pairs of samples that met $|\Delta C'/\Delta E_{00}| \geq 0.9$ ($\Delta C'$ ranging from 0.99 to 7.89);
- **Hue subset** (only pairs of sample where the total color difference is mainly due to changes in hue): 31 pairs of samples that met $|\Delta H'/\Delta E_{00}| \geq 0.9$ ($\Delta H'$ ranging from 0.17 to 3.36).

The distribution of the values of $\Delta L'$, $\Delta C'$ and $\Delta H'$among the three subsets of sample pairs is shown in Figure 4.1. The range of the hue variation is significantly smaller than the variation of lightness and chroma, since the samples are intended to mimic the color of the human natural teeth (Gozalo-Diaz, Lindsey et al. 2007), therefore having only slight variations in hue. The total number of sample pairs used to perform this study was 111.

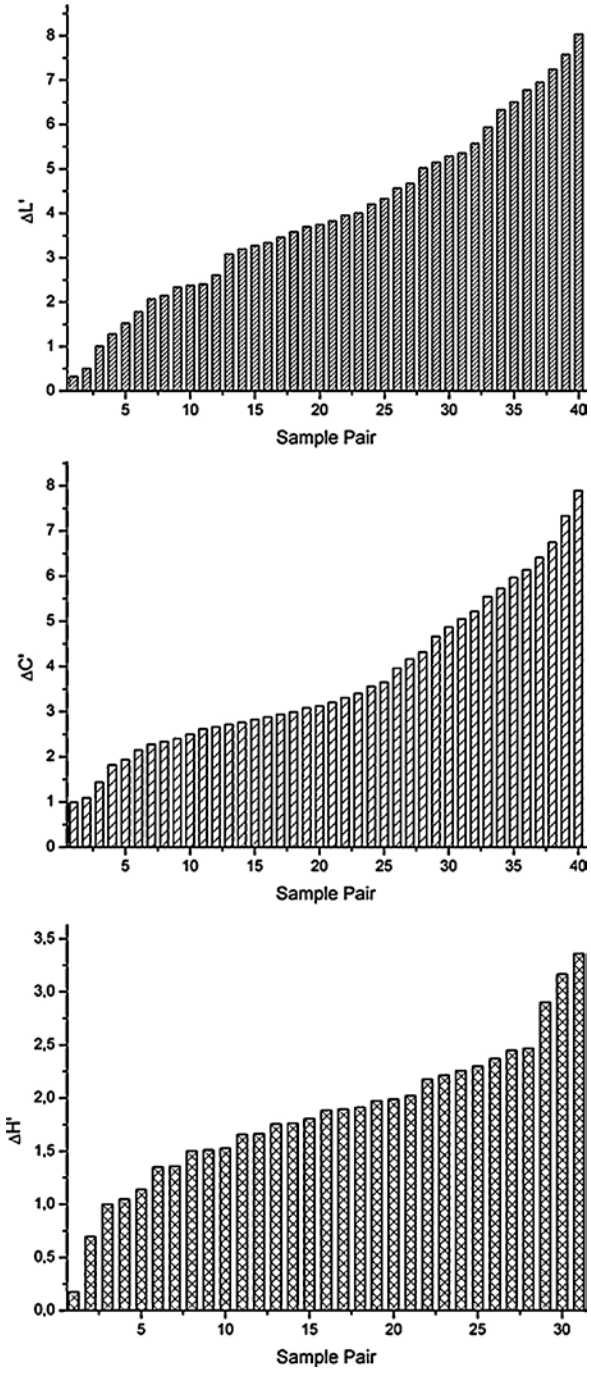

Figure 4.1: Distribution of the lightness ($\Delta L'$),chroma ($\Delta C'$) and hue ($\Delta H'$) differences among the three subsets of sample pairs.

4.2.2 COLOR MEASUREMENTS

The reflectance spectra of all the ceramic discs were measured using a non-contact SpectraScan PR-704 spectroradiometer (Photo Research, USA). As stated in Chapter 3, this device has the ability to measure the color of a sample in a way that matches the geometry of a visual assessment, and it has been used in several dental color studies so far (Del Mar Pérez et al., 2009; Luo et al.; 2009, Ghinea et al., 2010).

For reflectance measurements, the ceramic samples were placed on a 45° tilted base and in the center of a viewing booth (CAC60, Verivide Ltd., UK). The viewing cabinet has several light sources available to provide consistent illuminating/viewing conditions. For this experiment, a light source simulating the spectral relative irradiance of the CIE D65 standard illuminant was used. The spectroradiometer was positioned at 40cm away from the samples so that the measuring angle was 0°. The illuminating/measuring geometry corresponded to diffuse/0°, as recommended by the International Commission on Illumination (CIE, 2004) (Figure 4.2 a). To calculate the color coordinates of each sample, the matching functions of the CIE1931 2° Standard Observer were used.

Since the oral cavity is dark and the teeth are translucent, a Munsell black background was used for reflectance measurements in this study (L*=2.8, a*=0.7, b*=1.9). A triangular stand was built to fold the samples in order to avoid the specular reflection from the glossy surface (Luo et al., 2009, Ghinea et al., 2010).

The total color difference between the two samples forming the sample pair was calculated according to the CIEDE2000 (ΔE_{00}) color difference formula, as follows:

$$\Delta \mathrm{E}_{00} = \sqrt{\left(\frac{\Delta L'}{K_L S_L}\right)^2 + \left(\frac{\Delta C'}{K_C S_C}\right)^2 + \left(\frac{\Delta \mathrm{H}'}{K_H S_S}\right)^2 + R_T \left(\frac{\Delta C'}{K_C S_C}\right)\left(\frac{\Delta \mathrm{H}'}{K_H S_H}\right)}$$

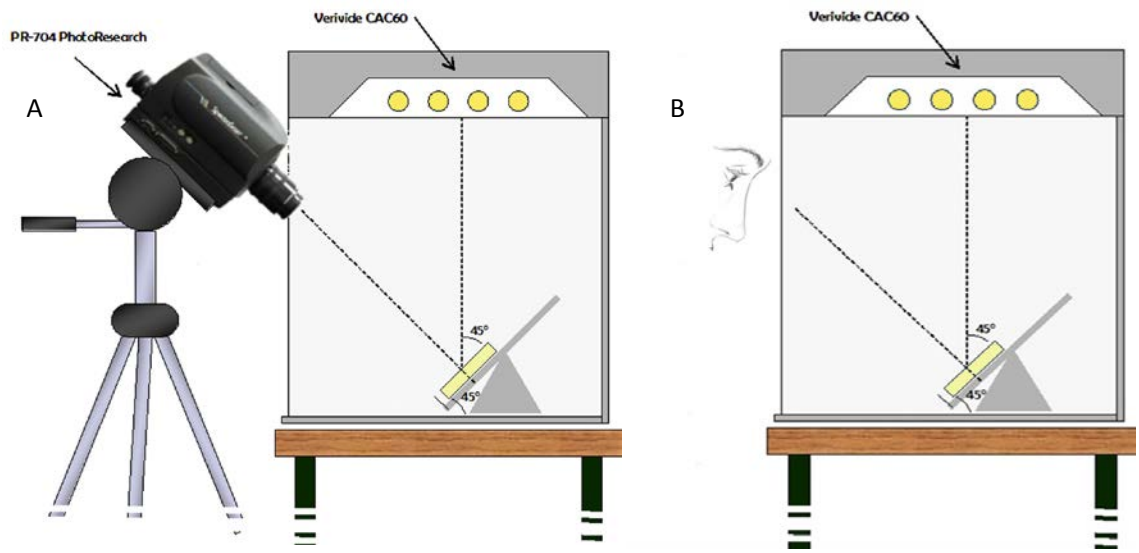

Figure 4.2:Schematical representation of the experimental set-up used for (a) reflectance measurements with the PR-704 spectrorradiometer and (b) visual judgments by the panel of observers.

For the development of this study, the CIEDE2000 lightness (ΔE_L), chroma (ΔE_C) and hue (ΔE_H) color differences were defined as follows (Nayatani, 2005):

$$\Delta E_L = \frac{\Delta L'}{(K_L \cdot S_L)}$$

$$\Delta E_C = \frac{\Delta C'}{(K_C \cdot S_C)}$$

$$\Delta E_H = \frac{\Delta H'}{(K_H \cdot S_H)}$$

where $\Delta L'$, $\Delta C'$ and $\Delta H'$ are metric differences between the corresponding values of the two samples forming the sample pair, computed on the basis of uniform color space used in CIEDE2000, and $K_L \cdot S_L$, $K_C \cdot S_C$ and $K_H \cdot S_H$ are empirical terms used for weighting the metric differences to the CIEDE2000 differences for each coordinate. When calculating the CIEDE2000 color difference formula, all the discontinuities due to mean hue computation and hue-difference, as pointed out and characterized by Sharma et al., were taken into account (Sharma et al., 2005). For calculating the CIEDE2000(1:1:1) total color difference formula, the parametric factors were set to 1 (K_L=1, K_C=1 and K_H=1), while for calculating the CIEDE2000(2:1:1) total color difference formula, the parametric factors were set to K_L=2, K_C=1 and K_H=1.

4.2.3 PSYCHOPHYSICAL EXPERIMENT

In order to perform the visual judgments of the three subsets of sample pairs (lightness, chroma and hue), a panel of 30 non-dental professional observers was recruited. The panel was formed by 12 female and 18 male observers, with age ranging from 19 to 55 years. All the observers had previous experience in color discrimination experiments and, before performing the visual judgments, were screened for normal color vision using the Ishihara charts (Ishihara Color Vision Test, Kamehara Tradig Inc., Japan).

The observers were placed at a distance of approximately 40cm away from the sample pair to be judged (the same distance used for instrumental color measurements), with their head fixed on a chin rest and inclined 45°, achieving this way a illumination/observation geometry of diffuse/0° (Figure 4.2 b). Each observer was instructed to focus his attention on the center of the ceramic discs forming the pair of samples, and, judging exclusively the color of the samples, to answer the following question:

"Would you rate the color difference between the two discs as acceptable?"

The responses of each observer and for each of the pairs of ceramic discs (ΔV – visual color difference) were recorded and consequently processed as described in the previous Chapter of this PhD Thesis.

4.2.3.1 Fitting procedure

The fitting method chosen to approximate observers answers to the instrumentally measured color differences was the method that, according to the results presented in Chapter 3, provided the better fit with visual judgments, i.e. a Takagi-Sugeno-Kang (TSK) Fuzzy Approximation model with Gaussian membership functions and constant consequents (Matlab 7.1 Fuzzy Logic Toolbox, MathWork Inc., USA) (Takagi and Sugeno, 1985; Ghinea et al., 2010; Herrera et al., 2010). The rule centers of the TSK model were equally distributed along the input space and the rule consequents were optimally obtained using their derivatives with respect to the model output when the minimization of R was achieved (Least Squares LSE approach)

(Herrera et al., 2010). The number of rules for each approximation was determined using a 10-fold cross-validation procedure, which means that the number of rules for which the model provided the lowest cross-validation error was chosen to perform the approximation using all data.

For each TSK Fuzzy Approximation performed, the 95% Confidence intervals (95% CI), in terms of 95% Lower Confidence Limit (95% LCL) and 95% Upper Confidence Limit (95% UCL) were estimated and, from the fitting curve, the value of the total color difference corresponding to 50% positive and 50% negative answers (50:50% acceptability threshold) was calculated.

50:50% acceptability thresholds were calculated for all of the following set of samples: lightness subset ($\Delta L'$), chroma subset ($\Delta C'$), hue subset ($\Delta H'$), CIEDE2000 lightness subset (ΔE_L), CIEDE2000 chroma subset (ΔE_C), CIEDE2000 hue subset (ΔE_H), CIEDE2000(1:1:1) and CIEDE2000(2:1:1).

4.2.3.2 Statistical analysis

The 50:50% acceptability threshold values were considered as normal distributions with variance estimated according to the confidence intervals (95% CI) of the respective fitting curves. A t-test was used to evaluate the difference amongst the lightness, chroma and hue thresholds, both for the metric differences $\Delta L'$, $\Delta C'$ and $\Delta H'$ as well as for the CIEDE2000 lightness (ΔE_L), chroma (ΔE_C) and hue (ΔE_H) color differences (SPSS 15, SPSS, USA).

The performance of the CIEDE2000(1:1:1) and CIEDE2000(2:1:1) total color differences against the answers of the panel of observers (ΔV) was tested using the PF/3 Performance Factor (Guan and Luo, 1999). One of the main advantages of this parameter is that allows the statistical comparison of two data sets by means of combining three measures of fit: the gamma factor γ, CV and V_{AB} (Huertas et al., 2006):

$$PF/3 = \frac{100 \cdot \left[(\gamma - 1) + V_{AB} + \frac{CV}{100} \right]}{3}$$

A perfect agreement between the instrumentally measured color differences and the perceived color difference by the panel of observers it is indicated by a value of the performance factor PF/3 of zero, while higher values correspond to worse agreement. There is no mathematical limitation for the PF/3 values, so they can be greater than 100%.

4.3 RESULTS AND DISCUSSION

Many industries have already established color tolerances, such as the textile industry, the car industry or the money printing, and there is a rising interest to establish these types of tolerances for dentistry. With recent advances, this task can be satisfactorily fulfilled, since there are new methods and techniques available which will help to perform more accurate studies. Practical application of technology that quantifies color and color differences in dentistry requires that color difference formulas provide a quantitative representation of the visual color difference, by maintaining a strong direct relationship with this latter one. The latest total color difference formula proposed by the International Commission on Illumination, the CIEDE2000 color difference formula (ΔE_{00}) (CIE, 2004), started to be increasingly used in dental research and other dental applications (Wee et al., 2007; Johnston, 2009; Ghinea et al., 2010).

Data fuzzy modeling represents a flexible and effective method to model an unknown function from a set of observed data relative to that function or phenomenon (Takagi and Sugeno, 1985, Herrera et al., 2010). The 50:50% acceptability thresholds for lightness, chroma and hue and the CIEDE2000(1:1:1) and CIEDE2000(2:1:1) 50:50% acceptability thresholds were calculated using TSK Fuzzy Approximation. As pointed out in the previous Chapter of this PhD Thesis, when compared with a traditional S-Shaped fitting function, the TSK Fuzzy Approximation enabled soft and accurate approximations, without limiting the expected shape of the objective function, providing in all cases better fit to the visual data than the S-shaped function, being a reliable alternative for the color threshold calculation procedure.

The acceptability of color differences between the natural teeth and the adjacent restoration can be interpreted, both in a clinical or laboratory situation, by means of an acceptability threshold value. The TSK Fuzzy Approximation fitted curves of the percentages of acceptance (%acceptance) against the instrumentally measured lightness difference ($\Delta \mathrm{L}'$) and CIEDE2000 lightness difference (ΔE_L), together with their corresponding 95% confidence intervals, are plotted in Figure 4.3. For $\Delta \mathrm{L}'$, the 50:50% acceptability threshold was established at a level of $\Delta \mathrm{L}'$=2.92 units, with 95% CI: 1.22-

4.96 and R^2=0.76. For CIEDE2000 lightness difference, the level of 50:50% acceptability threshold was 2.86, with 95% LCL=1.20 and 95% UCL=4.84 units and a value of R^2=0.75..

In Figure 4.4 are shown the TSK Fuzzy Approximation fitted curves of % acceptance against the instrumentally measured chroma difference ($\Delta C'$) (Figure 4.4 a) and CIEDE2000 lightness difference (ΔE_C) (Figure 4.4 b), together with their corresponding 95% confidence intervals. From the fitted curve of acceptable percentages against the chroma difference $\Delta C'$, the 50:50% acceptability threshold was $\Delta C'$=2.52 units (1.31-4.19 95% CI; R^2=0.71) while from the fitted curve against the CIEDE2000 chroma difference, the level of 50:50% acceptability threshold was ΔE_C=1.34, with 95% LCL=0.22 and 95% UCL=2.96 and R^2=0.56.

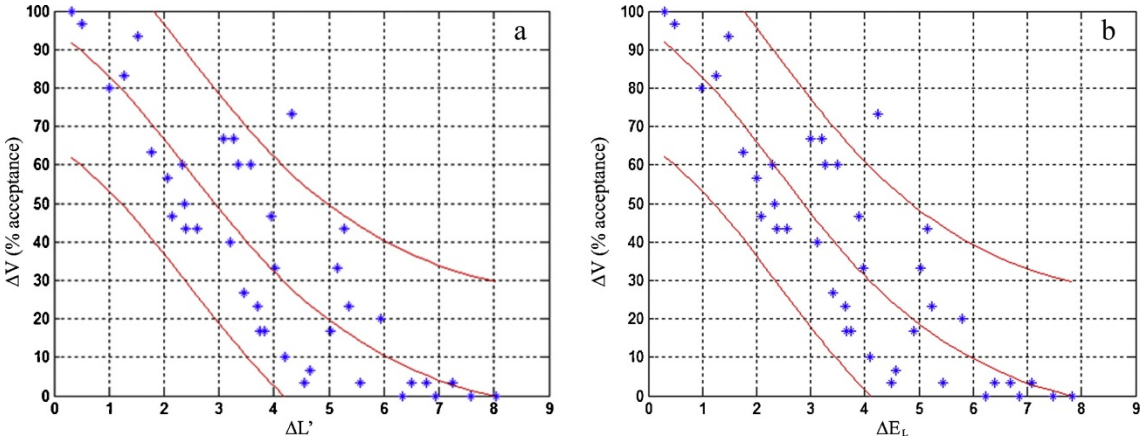

Figure 4.3: TSK Fuzzy Approximation fitted curve and 95% LCL and UCL for visual acceptability in percentages versus (a) $\Delta L'$ of pairs of ceramic discs; (b) ΔE_L of pairs of ceramic discs.

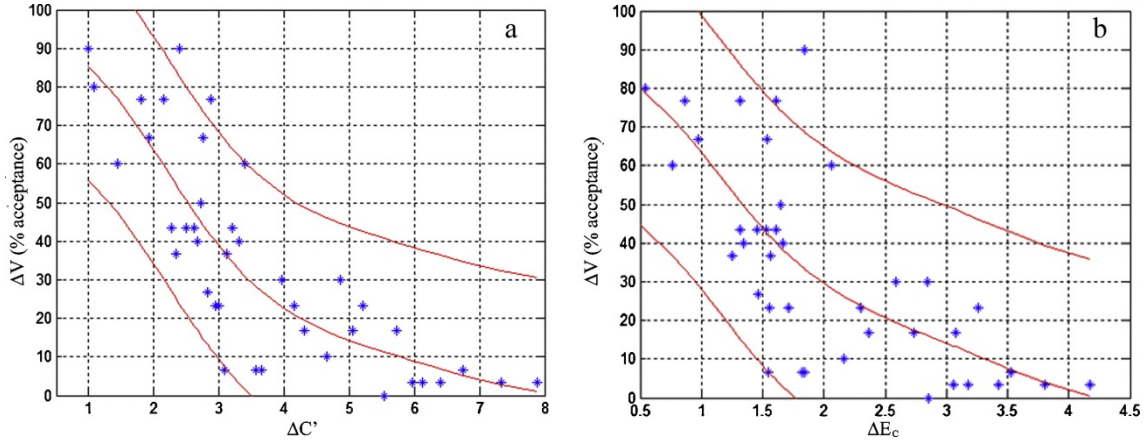

Figure 4.4: TSK Fuzzy Approximation fitted curve and 95% LCL and UCL for visual acceptability in percentages versus (a) $\Delta C'$ of pairs of ceramic discs; (b) ΔE_C of pairs of ceramic discs.

In Figure 4.5 are plotted the TSK Fuzzy Approximation fitted curves against %acceptable visual answers (ΔV) against both the hue metric difference ($\Delta H'$) (Figure 4.5 a) and the CIEDE2000 hue difference (ΔE_H) (Figure 4.5 b), together with their corresponding 95% confidence interval. The corresponding levels of 50:50% acceptability thresholds, as calculated from the fitted curves, were $\Delta H'$=1.90 (95% CI: 1.63 – 2.15; R^2=0.88) and ΔE_H=1.65 (95% CI: 1.10 – 1.87; R^2=0.82).

The statistical t-test confirmed that there were significant differences between the 50:50% acceptability threshold values when calculating with the metric differences in lightness $\Delta L'$, chroma $\Delta C'$ and hue $\Delta H'$, with p <0.001 in all cases. However, when the threshold values were calculated with the CIEDE2000 lightness (ΔE_L), chroma (ΔE_C) and hue (ΔE_H) differences, the statistical analysis confirmed significant differences between ΔE_L and ΔE_C and between ΔE_L and ΔE_H (p<0.001), but no differences were found when comparing ΔE_C and ΔE_H (p=0.1). When considering K_L=2, K_C=1, and K_H=1, the values of the corresponding 50:50% acceptability thresholds were ΔE_L=1.43, ΔE_C=1.34 and ΔE_H=1.65, with no statistically significant differences between threshold values of lightness and chroma or between lightness and hue (p>0.1). The lack of statistically significant differences is an indicator of the fact that the corrections introduced in the computation of color difference compensate, to some extent, the lack of uniformity of the CIELAB color space.

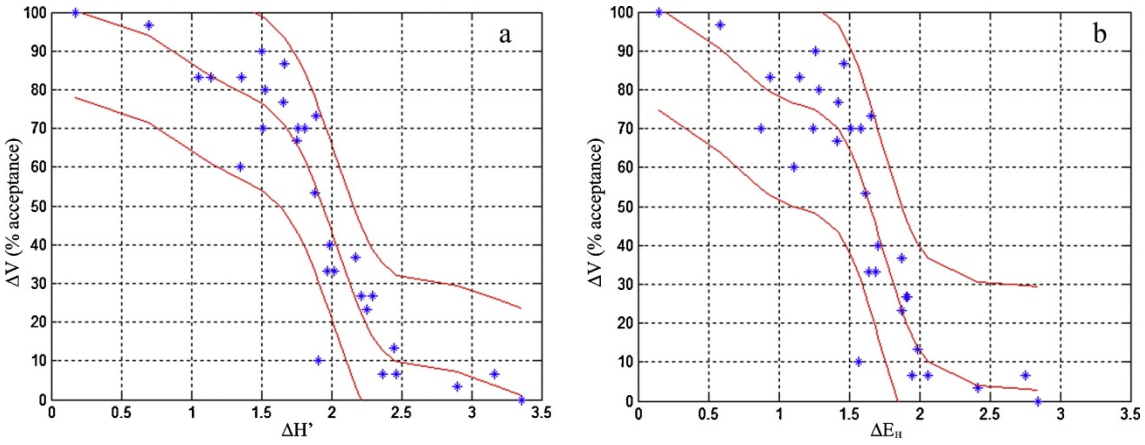

Figure 4.5: TSK Fuzzy Approximation fitted curve and 95% LCL and UCL for visual acceptability in percentages versus (a) $\Delta H'$ of pairs of ceramic discs; (b) ΔE_H of pairs of ceramic discs.

	50:50% Acceptability Threshold			
	Value	**95% LCL**	**95% UCL**	**R^2**
$\Delta \mathbf{L}'$	2.92	1.22	4.96	0.76
$\Delta \boldsymbol{E_L}$	2.86	1.20	4.84	075
$\Delta \mathbf{C}'$	2.52	1.31	4.19	0.71
$\Delta \boldsymbol{E_C}$	1.34	0.22	2.96	0.56
$\Delta \mathbf{H}'$	1.90	1.63	2.15	0.88
$\Delta \boldsymbol{E_H}$	1.65	1.10	1.8	0.82

Table 4.1: CIEDE2000 50:50% acceptability threshold values and 95% CI for lightness, chroma and hue.

It can be stated that the first null hypothesis of this study was rejected. According to the results, there are differences in sensitivity for change in lightness, chroma and hue in the dental color space, and the t-test confirmed that these differences were statistically significant in almost all cases for lightness $\Delta \mathrm{L}'$, chroma $\Delta C'$ and hue $\Delta \mathrm{H}'$ thresholds. These findings are in agreement with previous studies (Douglas and Brewer, 1998; Lindsey and Wee, 2007), which also reported differences in sensitivity among different directions of the CIELAB color space, although they used the ΔE^*_{ab}formula. The values of all the CIEDE2000 50:50% acceptability thresholds for lightness, chroma and hue, as well as their corresponding 95% confidence intervals and the values of R^2, are contained in Table 4.1.

Figure 4.6 displays the dependence of the observer's answers on the color coordinates of the samples forming the sample pair. The percentages of visual acceptability against $\Delta \mathrm{L}'$ and the average value of lightness of each judged pair of samples is presented in Figure 4.6 a; the visual acceptability percentages of chroma against $\Delta \mathrm{C}'$ and average CIEDE2000 chroma is shown in Figure 4.6 b, whilst the visual acceptability percentages of hue against $\Delta \mathrm{H}'$ and averageCIEDE2000 hue angle for each judged pair of samples is illustrated in Figure 4.6 c.

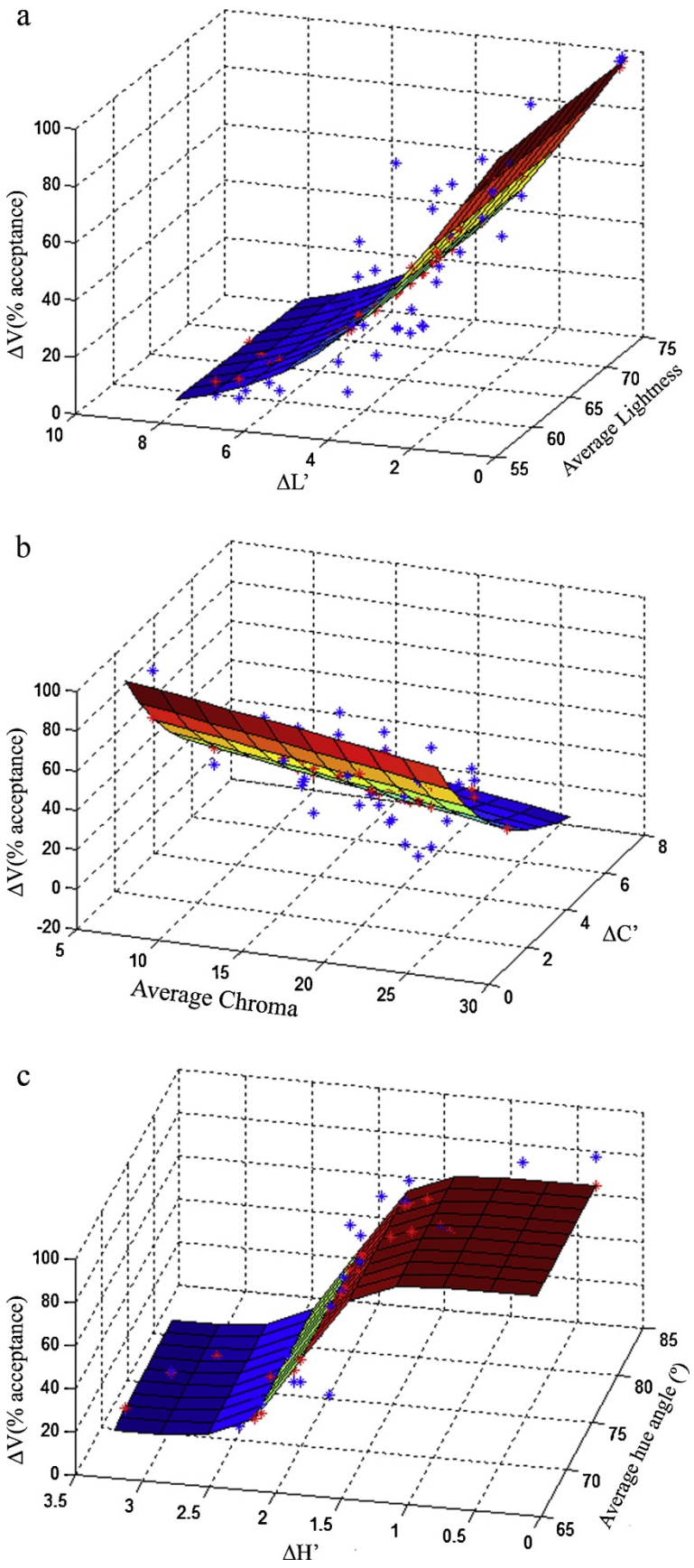

Figure 4.6: Acceptance percentages against: (a) lightness differences and average lightness of pairs of ceramic discs; (b) chroma differences and average chroma of pairs of ceramic discs; (c) hue differences and average hue angle of pairs of ceramic discs..

The L* scale was reported to give too large ΔL^* values for lightness differences both for dark (low L* values) and for light (high L* values) samples (Chou et al., 2001). In CIEDE2000, the lightness is corrected with a specific weighting function (S_L). Melgosa and collaborators studied the relative significance of the correction terms within the CIEDE2000 color difference formula and determined that the lightness correction is not statistically significant for color pairs having mainly lightness difference (Melgosa et al., 2004). In our study no dependence between the $\Delta L'$ and L' was found, suggesting that this correction may not be significant for the dental color space.

On the other hand, if the color difference is mainly due to differences in chroma or hue, or when the difference in chroma is very large, in the Euclidean metric of the CIELAB color space, an increase of the tolerance is experimented (Melgosa et al., 1995). According to our results, there is no dependence between $\Delta H'$and H', but there was a slight dependence between $\Delta C'$ and C'. The dependence between the increase in chroma ($\Delta C'$) and the chroma value (C') was already pointed out in the development of the CMC color difference formula (Clarke et al., 1984), which introduces a correction of the chroma difference by means of a weighting functions which depends on the chroma value, in the sense that an increase of the C' value would result in a lower value of the difference. However, in order to clarify this issue, further studies, with new experimental data, are required.

The three parametric factors (K_L, K_C and K_H) introduced in CIEDE2000 are set to 1 for so-called reference conditions (CIE, 2004). Among several others, one of those reference conditions implies the use of homogeneous samples. It has been proven that the surface structure of the sample (texture) has an effect on the perceived color differences (Montag and Berns, 2000; Xin et al., 2005). Generally, it has been assumed that texture only affects lightness tolerance but does not affect chroma or hue tolerances (Griffin and Sepehri, 2002; Choo and Kim, 2003; Mangine et al., 2005). We obtained higher values for CIEDE2000 acceptability thresholds for lightness compared to chroma or hue thresholds, which, as mentioned above, might be due to surface texture of the sample

According to our results, there were differences in sensitivities between CIEDE2000 lightness, chroma and hue difference: ΔE_L= 2.86, ΔE_C=1.34 and ΔE_H=1.65, and the statistical analysis confirmed the differences between lightness and chroma and between lightness and hue. However, there were no statistically significant differences between chroma and hue. These differences between ΔE_L and ΔE_C or ΔE_H could be due to the fact that the parametric factor of lightness (K_L) should have a different value than parametric factors of chroma (K_C) or hue (K_H). In this study, the CIEDE2000 ΔE_L, ΔE_C and ΔE_H were specifically calculated to establish the influence of the weighting functions, thus providing a basis to justify considering the use of K_L = 2 instead of K_L = 1.

In Figure 4.7 are illustrated the TSK Fuzzy Approximation fitted curves and their corresponding 95% Confidence Intervals of the percentage of acceptance (%acceptance) against the instrumentally measured total color differences as calculated with the CIEDE2000(1:1:1) (Figure 4.7 a) and CIEDE2000(2:1:1) formulas (Figure 4.7 b). The 50:50% acceptability thresholds were determined as ΔE_{00}=1.87 (R^2=0.62: optimal number of rules 3) for the CIEDE2000(1:1:1) color difference formula and ΔE_{00}=1.78 (R^2=0.68; optimal number of rules 4) for the CIEDE2000(2:1:1) color difference formula.

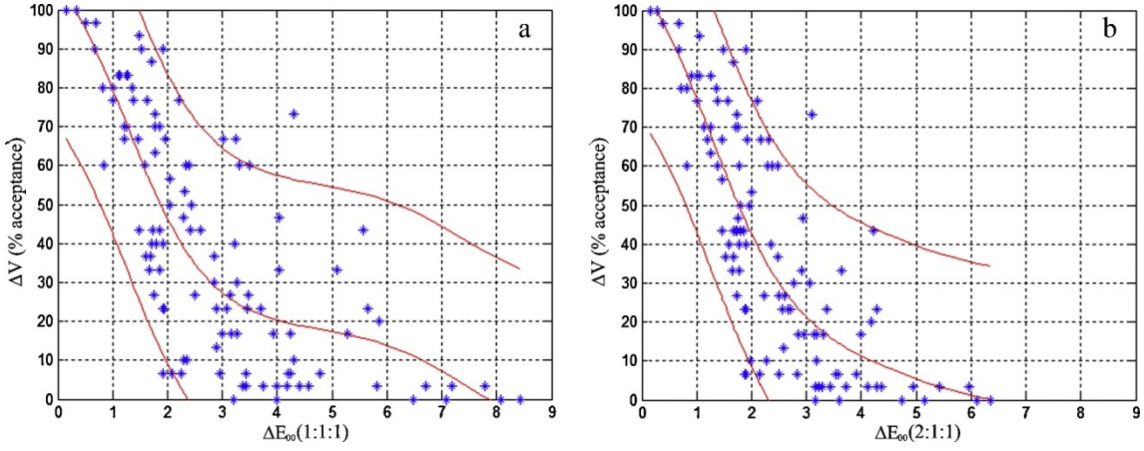

Figure 4.7: TSK Fuzzy Approximation fitted curve and 95% LCL and UCL for visual acceptability in percentages versus CIEDE2000(1:1:1) (a) and CIEDE2000(2:1:1) (b) total color difference of pairs of ceramic discs.

Table 4.2 shows the values of γ, CV, V_{AB} and PF/3 for both the CIEDE2000(1:1:1) and the CIEDE2000(2:1:1) total color difference formulas. In the case of the CIEDE2000(2:1:1) color difference formula we obtained the lowest values of gamma factor, CV and V_{AB}, indicating a better adjustment of this formula to the visual judgments performed by the panel of observers.

The values of the PF/3 factor have been used as an indicator for the performance of color-difference formulas in comparison with visual results. In our study we obtained lower PF/3 values for CIEDE2000(2:1:1) color difference formula when compared with the CIEDE2000(1:1:1) color difference formula. Moreover, although the values of the 50:50% acceptability thresholds as calculated with the CIEDE2000(1:1:1) and CIEDE2000(2:1:1) were similar, the CIEDE2000(2:1:1) TSK Fuzzy Approximation exhibited slightly better fit, in terms of R^2-value.

The second null hypothesis was also rejected. According to the obtained results, the CIEDE2000(2:1:1) color difference formula performed better than CIEDE2000(1:1:1) in evaluation of acceptability thresholds of dental ceramics.

When considering K_L=2, the 50:50% acceptability threshold value for the CIEDE2000 lightness drops to a value of ΔE_L=1.43, and the statistical t-test confirmed that there were no significant differences between the threshold values for lightness and chroma (p>0.1) or for lightness and hue (p>0.1). Therefore, taking into account all the above mentioned, the results of this study suggest considering the use of K_L=2 instead of K_L=1 when evaluating CIEDE2000 lightness differences in dentistry.

Color Difference Formula	Performance Factors			
	γ	CV	V_{AB}	PF/3
CIEDE2000(1:1:1)	2.98	88.98	1.33	139.86
CIEDE2000(2:1:1)	2.87	83.03	1.27	132.31

Table 4.2: Fit parameters and performance factors for the CIEDE2000(1:1:1) and CIEDE (2:1:1) color-difference formulas against visual judgments for the whole set of samples.

It should be mentioned that the parametric factors K_L, K_C and K_H proposed in this study correspond exclusively to color differences in lightness, chroma, or hue, which means that the parametric factor have been computed independently. Generally, a color difference includes simultaneously lightness, chroma and hue differences; thus the three factors must be combined, and possible interactions should be investigated. Nevertheless, further research is needed to test the performance of this color difference formula and its adequacy to accurately predict the perceived color difference in dentistry. In particular, to expand the number of colors and types of materials used (dental resin composites, in vivo teeth, etc.) and comparatively analyze data, thereby evaluating the degree of disagreement between observers and calculated color differences would be of great interest.

Within the limitations of this study, we found statistically significant differences between CIEDE2000 50:50% acceptability thresholds for lightness, chroma and hue differences. Also, the CIEDE2000 formula performed better using K_L, K_C and K_H parametric factors set to 2:1:1 rather than 1:1:1, which recommends its usage in dental research and in vivo instrumental color analysis.

CHAPTER 5

TESTING THE PERFORMANCE OF CIEDE2000(1:1:1) AND CIEDE2000(2:1:1) COLOR DIFFERENCE FORMULAS FOR APPLICATIONS IN DENTISTRY

5.1 STATE OF THE ART

As stated in the previous chapters, the main purpose of a color difference formula is to provide a quantitative representation (ΔE) of the perceived color difference (ΔV) between a pair of colored samples under a given set of experimental conditions. Therefore, it can be stated that the color difference formulas should be designed for bridging the gap between the visual perception and the instrumental measurements. Until now, in the majority of the dental color studies, the color and color difference between two samples have been quantified using the CIELAB color space and the associated ΔE^*_{ab} color difference formula (Johnston, 2009). However, as proven in Chapter 4 of this PhD Thesis, the sensitivity of the human visual system is not equal for all the directions of the color space, and therefore, the assumption of uniformity of CIELAB cannot stand longer. This is the reason why, the most recently introduced color difference formulas, all incorporate weighting factors which adjust the possible inaccuracies when computing the total color differences.

The CIEDE2000(K_L:K_C:K_H) total color difference formula, incorporates specific corrections for non-uniformity of CIELAB color space (the so-called weighting functions: S_L, S_C, S_H), a rotation term (R_T) that accounts for the interaction between chroma and hue differences in the blue region and a modification of the a* coordinate of CIELAB, which mainly affects colors with low chroma (neutral colors), and parameters accounting for the influence of illuminating and vision conditions on color difference evaluation (the so-called parametric factors: K_L, K_C, K_H) (Luo et al., 2001). The parametric factor ratio was proposed as a way to control changes in the magnitude of tolerance judgments and as a way to adjust for scaling of acceptability rather than perceptibility (Berns, 1996).

The recent advances experimented in the area of fuzzy logic, have led to their extensive implementation in the design of control systems in very different areas, such as industry and medicine (Mahfouf et al., 2001). In the field of dentistry, the fuzzy systems were used to model color change phenomena after bleaching, obtaining interpretable solutions which can highly improve the understandability of the obtained models by the experts (Herrera et al., 2010).

In previous chapters of this PhD Thesis it has been shown that, on one hand, the Fuzzy systems proved to be a reliable alternative to the traditional S-Shaped function for data fitting (providing a better fit to visual judgments) and, on the other hand, that it can successfully be used to approximate data obtained from a psychophysical experiment involving a panel of observers to obtain values of acceptability thresholds for dentistry. In Chapter 4 of this PhD thesis, the use of K_L=2 instead of K_L=1 when evaluating the CIEDE2000(K_L:K_C:K_H) color difference in dentistry was suggested (CIEDE2000(2:1:1)), but since it was a pilot study, based on the values of the acceptability thresholds for lightness chroma and hue, it has been stated that further research is needed to properly test the performance of this color difference formula and its adequacy to accurately predict the perceived color difference in dentistry.

In the present study the CIEDE2000(1:1:1) and CIEDE2000(2:1:1) total color difference formulas were used to evaluate the 50:50% acceptability thresholds in dentistry. The performance of the two color difference formula was evaluated by means of the PF/3 (Guan and Luo, 1999) and STRESS (García et al., 2007) performance parameters. The approximation of the acceptable percentage curves and the threshold estimation was realized using a Taylor Series (TaSe) based TSK Fuzzy system (Herrera et al., 2005).

The two null hypotheses tested were: 1) there is no difference between the acceptability threshold as computed with the CIEDE2000(1:1:1) or the CIEDE2000(2:1:1) total color difference formulas; 2) there is no difference in the performance of CIEDE2000(1:1:1) and CIEDE2000(2:1:1) total color difference formulas, in terms of PF/3 and STRESS parameters.

5.2 MATERIALS AND METHODS

5.2.1 SAMPLES

For the development of this study, 58 tabs from two tooth shade guides were used (3D MASTER with Bleach, VITA Zahnfabrik, Germany) (Figure 5.1). From all possible combinations of pairs of tabs, only 55 sample pairs, with CIEDE2000(1:1:1) - ΔE_{00}- ranging from 0.12 to 8.2 units, were selected for the visual judgments.

Figure 5.1: VITA Toothguide 3D-MASTER with 3 Bleach Shades.

5.2.2 COLOR MEASUREMENTS

The reflectance spectrum of all samples was measured using a non-contact spectroradiometer (SpectraScan PR-704, PhotoResearch, USA), with its corresponding software (SpectraView, PhotoResearch, USA) and a reflection standard (OPST3-C, Optopolymer, Germany). The spectroradiometer is top choice for this type of measurements since, aside of not requiring contact with the samples, it is able to match the geometry of a visual assessment, and it is gaining more and more ground in color and appearance research in dentistry (Del Mar Pérez et al., 2009; Luo et al., 2009; Ghinea et al., 2010).

The samples were situated over a 45° tilted support in the center of a standardized viewing cabinet (CAC60, VeriVide Ltd., UK) and illuminated with a light

source simulating the spectral relative irradiance of the CIE D65 standard illuminant. The distance between the spectroradiometer and the samples was fixed at 40 cm and the geometry of illuminating/measuring corresponded to diffuse/0° (CIE 2004). To calculate the colorimetric coordinates of each sample, the CIE 1931 2° Standard Colorimetric Observer was used.

As specified in previous chapters, the CIEDE2000 color difference (ΔE_{00}) was calculated as:

$$\Delta E_{00} = \left[\left(\frac{\Delta L'}{K_L S_L} \right)^2 + \left(\frac{\Delta C'}{K_C S_C} \right)^2 + \left(\frac{\Delta H'}{K_H S_H} \right)^2 + R_T \left(\frac{\Delta C'}{K_C S_C} \right) \left(\frac{\Delta H'}{K_H S_H} \right) \right]^{12}$$

where ΔL', ΔC', ΔH' are metric differences between the corresponding values of the samples, computed on the basis of uniform color space used in CIEDE2000, and $K_L \cdot S_L$, $K_C \cdot S_C$ and $K_H \cdot S_H$ are empirical terms used for correcting, (weighting) the metric differences to the CIEDE2000 differences for each coordinate. For this study, the parametric factors were set to K_L=1, K_H=1 and K_C=1 for CIEDE2000 (1:1:1) and K_L=2, K_H=1 and K_C=1 for CIEDE2000 (2:1:1)

5.2.3 PSYCHOPHYSICAL EXPERIMENT

For the visual evaluation of the 55 pairs of dental samples, a panel of 28 non-dental professional observers was recruited. The panel was formed by 13 female and 15 male observers, with age ranging from 21 to 58 years. All observers were screened for normal color vision using pseudo-isochromatic plates (Ishihara Color Vision Test, Kamehara Trading Inc., Japan) and all had previous experience in color discrimination experiments.

For visual assessments, the samples were situated inside the viewing booth and illuminated with a CIE D65 daylight simulator. The observers were positioned at 40cm away, with their head placed on a chin rest and inclined at 45°, in order to replicate the illuminating/evaluating geometry used for instrumental color measurements. Each observer was instructed to focus his attention on the center of the sample and answer the following question:

"Would you consider the color difference between the two dental samples as clinically acceptable?"

The responses of each observer for each pair of samples were processed as follows:

$$\%Acceptance = \frac{S_i}{N_i}$$

and observational data were converted to visual differences (ΔV) - or visual data - using the following function:

$$\Delta V = 5 + \log_e\left(\frac{S_i + 0{,}5}{N_i - S_i + 0{,}5}\right)$$

where S_i= number of observers who found the match acceptable and N_i = total number of observers (Mangine et al., 2005)

5.2.3.1 Fitting Procedure

The fitting of the instrumental color difference (ΔE_{00}) to visual data (%Acceptance and ΔV) was performed using a Taylor Series based TSK Fuzzy system (TaSe model) (Matlab Fuzzy Logic Toolbox, MathWork Inc., USA) (Herrera et al., 2005). The rule consequents were selected to be linear in order to improve the flexibility of the model, without falling into over-fitting. The TaSe model is characterized by a special type of membership function (OLMF basis) (Bikdash, 1999), and consequents in a polynomial centered form around the rule centers. This is the reason why the rule consequents functions coincide with the global model output (its Taylor series) at the rule centers. This property provides a more direct interpretability of the fuzzy rules than traditional TSK fuzzy models (Bikdash, 1999; Herrera et al., 2005; Herrera et al., 2011). The TaSe models took the rule centers equally distributed along the input space, and the rule consequents were optimally obtained using their derivatives with respect to the model output in the minimization of the value of R (Least Squares LSE approach) (Rojas et al., 2000). The selected number of rules in each case was 3, selected using a 10-fold cross-validation procedure; the number of rules for which the

model provided a lowest cross-validation error was chosen to perform the approximation using all data.

The 95% confidence intervals (CI, 95% Lower Confidence Limit – LCL and the 95% Upper Confidence Limit – UCL) were estimated for the data approximations, supposing a normal distribution of the error along the curves. The level of acceptability was calculated as the corresponding Computed Color Difference value of the 50:50% (50% of positive answers and 50% negative answers) point for the %Acceptance data sets and as the corresponding Computed Color Difference value of the ΔV=5 for the Visual Difference data sets.

5.2.3.2 Performance Test

The performance of CIEDE2000(1:1:1) and CIEDE2000(2:1:1) total color difference formulas against visual results, was tested using the performance factor PF/3 proposed by Guan and collaborators (Guan and Luo, 1999) and the Standardized Residual Sum of Squares (STRESS) (García et al., 2007). The PF/3 parameter allows a statistical comparison of two data sets by means of combining three measures of fit: gamma factor γ, CV and V_{AB} (Huertas et al., 2006).

The computation of PF/3 is given as:

$$PF/3 = \frac{100 \cdot \left[(\gamma - 1) + V_{AB} + \frac{CV}{100} \right]}{3}$$

where:

$$\log_{10}(\gamma) = \sqrt{\frac{1}{N}\sum_{i=1}^{N}\left[\log_{10}\left(\frac{\Delta E_i}{\Delta V_i}\right) - \overline{\log_{10}\left(\frac{\Delta E_i}{\Delta V_i}\right)} \right]^2}$$

$$V_{AB} = \sqrt{\frac{1}{N}\sum_{i=1}^{N}\frac{(\Delta E_i - F\Delta\Delta_i)^2}{\Delta E_i F \Delta\Delta_i}}$$

$$F = \sqrt{\frac{\sum_{i=1}^{N}\frac{\Delta E_i}{\Delta V_i}}{\sum_{i=1}^{N}\frac{\Delta V_i}{\Delta E_i}}}$$

$$CV = 100\sqrt{\frac{1}{N}\sum_{i=1}^{N}\frac{\left(\Delta E_i - f\Delta\Delta_i\right)^2}{\overline{\Delta E}^2}}$$

A PF/3 value of zero indicates perfect agreement between computed and perceived color differences; higher values indicating worse agreement. From the mathematical point of view, there is no maximum limit for PF/3 values (for example, they can be greater than 100%).

The computation of STRESS is given as:

$$STRESS = \sqrt{\left(\frac{\sum_{i=1}^{N}\left(\Delta E_i - F_1\Delta V_i\right)^2}{\sum_{i=1}^{N}F_{1^2}\Delta V_{i^2}}\right)}$$

$$F_1 = \frac{\sum_{i=1}^{N}\Delta E_{i^2}}{\sum_{i=1}^{N}\Delta E_i\,\Delta V_i}$$

5.3 RESULTS AND DISCUSSION

In this chapter, for approximating the observer's answers to the instrumentally measured CIEDE2000(1:1:1) and CIEDE2000(2:1:1) total color differences and obtaining the acceptable fitting curves, a modification of the Tagaki-Sugeno-Kang fuzzy model – the TaSe model – was used. For the determination of the 50:50% Acceptability threshold and the ΔV=5 Acceptability threshold, the TaSe model (Herrera et al., 2005) used OLMF membership functions (Bikdash, 1999) and linear consequents. One of the main advantages of the TaSe model is that it is able to provide more interpretable rules than traditional TSK models, as they directly explain the output of the model within rule parameters, as the rule consequents precisely provide the model output value and behavior around the respective rule centers.

In Figure 5.2 are plotted the values of the computed total color difference CIEDE2000(1:1:1) against the %Acceptance (Figure 5.2 a) and visual differences ΔV (Figure 5.2 b) with their corresponding TSK Fuzzy Approximation fitting curve and 95% Confidence Intervals. The corresponding Acceptability thresholds values found were ΔE_{00}=1,83 units (CI:0,84 – 4.00; r^2=0,75) at a level of 50:50% of Acceptance and ΔE_{00}=1,89 units (CI:0,61 – 3,62; r^2=0,75) for ΔV=5 (Table 5.1).

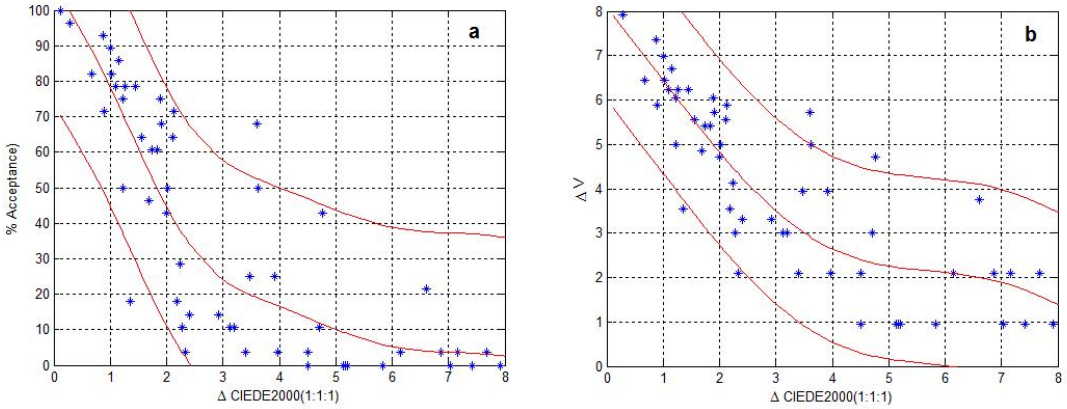

Figure 5.2: (a) %Acceptance and (b) Visual Differences (ΔV) vs CIEDE(1:1:1) color difference values for each sample pair with corresponding TaSe Fuzzy Approximation fitting curves and 95% Confidence Intervals.

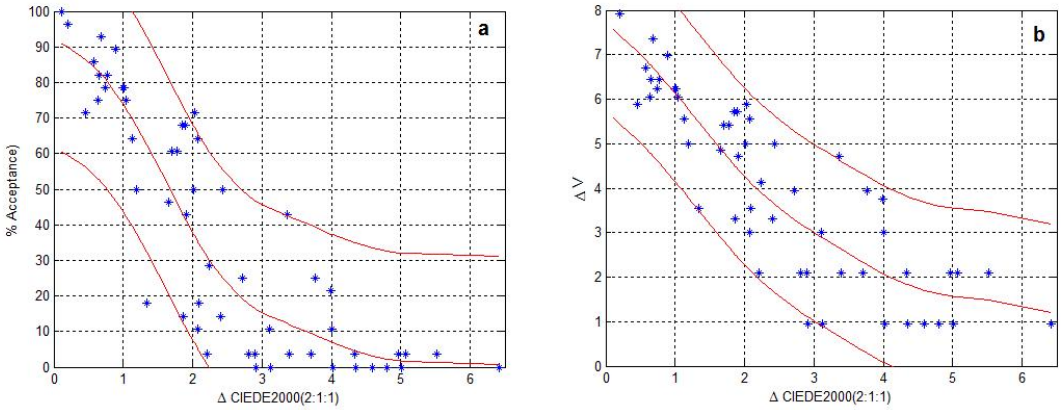

Figure 5.3: (a) %Acceptance and (b) Visual Differences (ΔV) vs CIEDE(2:1:1) color difference values for each sample pair with corresponding TaSe Fuzzy Approximation fitting curves and 95% Confidence Intervals.

The values of the computed total color difference CIEDE2000(2:1:1) against the % Acceptance (Figure 5.3 a) and visual differences ΔV (Figure 5.3 b) with their corresponding TSK Fuzzy Approximation fitting curve and 95% Confidence Intervals are presented in Figure 5.3. From the fitting curves, the calculated values of the Acceptability thresholds are ΔE_{00}=1,67 units (CI:0,76 – 2,68; r^2=0,80) for 50:50% Acceptance and ΔE_{00}=1,59 units (CI:0,51 – 2,99; r^2=0,78) for ΔV=5, respectively (Table 5.1).

The first null hypothesis of this work has been rejected, since we found difference between the acceptability thresholds when calculated with the CIEDE2000(1:1:1) and CIEDE2000(2:1:1) total color difference formulas.

In a one dimensional approximation problem, the optimization of a TSK Fuzzy model requires the determination of the number of rules, the position of their respective centers and the calculation of the optimal consequents (Pomares, 2004).

ΔE_{00}	Acceptability Threshold					
	50:50% Acceptance			ΔV=5		
	Value	95% CI	R^2	Value	95% CI	R^2
CIEDE(1:1:1)	1.83	0.84-4.00	0.75	1.89	0.61-3.62	0.75
CIEDE(2:1:1)	1.67	0.76-2.68	0.80	1.59	0.51-2.99	0.78

Table 5.1: Values of the Acceptability thresholds as calculated from fitting curves of CIEDE2000(1:1:1) and CIEDE2000(2:1:1) color difference formulas.

In this study, the rule centers were considered equally distributed along the input space, and the rule consequents were optimally obtained using their derivatives with respect to the model output in the minimization of the value of R (Least Squares LSE approach) (Herrera et al., 2005). The number of rules in each case was selected using a 10-fold cross-validation procedure which means that the number of rules for which the model provided a lowest cross-validation error was chosen to perform the approximation using all data.

As an example, in Figure 5.4 are presented the details of the TaSe approximation model for the computed color difference CIEDE2000(1:1:1) against the %Acceptance. The black dots on the x axis represent the three rule centers that characterize this model, and the black lines represent the linear models of the respective rule consequents. As it can be seen, the consequents represent the Taylor series of the model output around each rule center. These results facilitates the interpretability of the obtained rules, as they explain the value of the acceptability curves at the rule centers, as well as its trend on that point (first derivative).

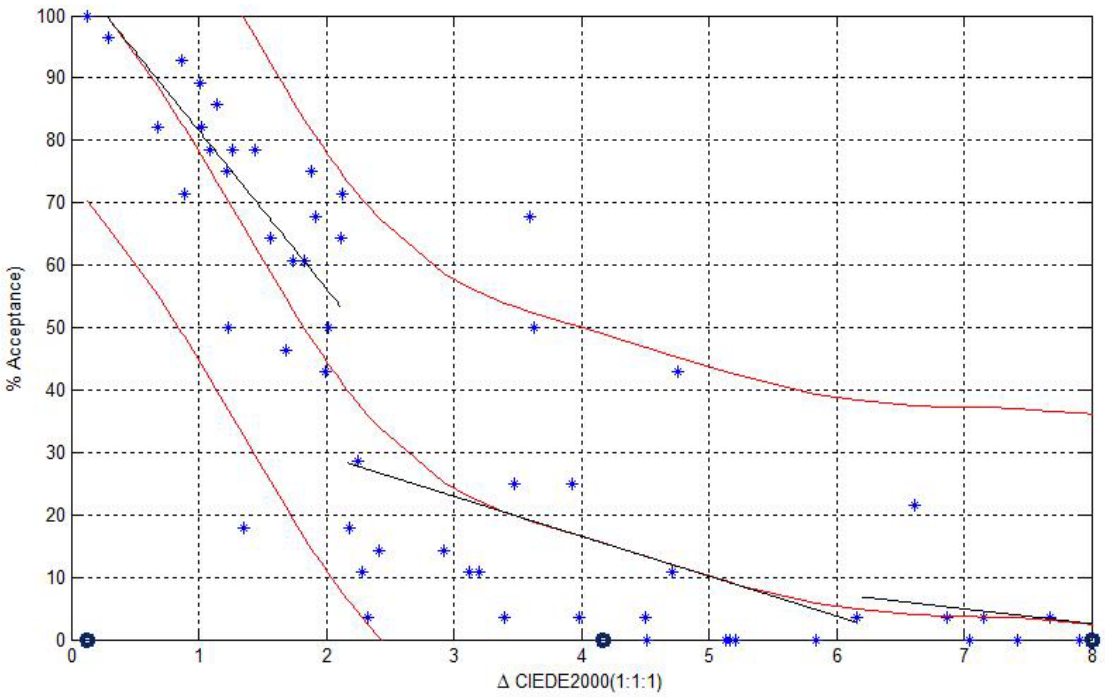

Figure 5.4: %Acceptance vs CIEDE(1:1:1) color difference values for each sample pair with corresponding TaSe Fuzzy Approximation fitting curves, 95% Confidence Intervals, the rule centers and the linear models of the respective rule consequents in the area covered by each rule.

The real shape of the curve representing the relationship between the instrumental color differences and the response of the human-visual system is unknown. It has been proven in previous chapters of this PhD Thesis, that the TSK Fuzzy models enable soft and accurate approximations, without limiting the expected shape of the objective function.

The use of an adequate color difference formula is important to obtain a better correlation of acceptability to instrumental color difference values. Improved correlation might provide a more accurate clinical interpretation of color differences which can result in research targeted at improving the color replication process in dentistry. Nevertheless, it seems appropriate to study the CIEDE2000 weighting functions (S_L, S_C, and S_H), which may result in an even better fit with the visual judgments. The use of an efficient research design to determine the optimum adjustment functions for color of human teeth is also beneficial. Using a valid and applicable formula will improve the modeling of tooth colored esthetic materials and, ultimately, patient satisfaction.

The PF/3 index may be used to compare the results provided by two different color-difference formulas, the visual assessments for a given set of color pairs by two different procedures, the results found by two different observers (inter-observer variability), the results found for the same observer in different experimental sessions (intra-observer variability) and, finally, the instrumentally measured color differences (ΔE) and the visual color differences (ΔV). There is no upper limit for PF/3 values or any of its components. Lower values of γ, V_{AB}, CV and PF/3 are translated into a better performance.

In Table 5.2 are presented the values obtained for the three indices involved in the definition of PF/3 as well as the values obtained for the performance factor PF/3 and for the STRESS parameter both for CIEDE2000(1:1:1) and CIEDE2000(2:1:1) total color difference formulas. In our study, we obtained lower values for CIEDE2000(2:1:1) when compared to CIEDE2000(1:1:1), for all parameters involved in the PF/3 calculation, indicating, in a first approach, the better agreement between the CIEDE2000(2:1:1) color difference formula and the visual results.

ΔE_{00}	PF/3				STRESS
	γ	V_{AB}	CV	PF/3	
CIEDE(1:1:1)	4.08	1.79	102.57	196.43	0.85
CIEDE(2:1:1)	3.99	1.74	97.44	190.33	0.83

Table 5.2: Values of the performance parameters for CIEDE2000(1:1:1) and CIEDE2000(2:1:1) total color difference formulas.

The Standard Residual Sum of Squares (STRESS) parameter is often addressed as a measure of the relationship between the two data sets to compare. Just like in the case of the PF/3 parameter, the usual goal is to achieve values close to zero, but there are several differences between the two parameters. The PF/3 factor is not symmetrical, due to the normalization to average ΔE when computing CV, but this flaw is corrected by the STRESS parameter. Another important difference is that, since for the PF/3 there is no value limit, STRESS values are always between 0 and 1 (also can be given as percentages) allowing a more easy and effective interpretation and comparison of the results.

As it can be seen in Table 5.2, we obtained slightly lower values for the CIEDE2000(2:1:1) formula when compared with the CIEDE2000(1:1:1), but it has to be mentioned that the values obtained in both cases are very high values, often considered as a poor configuration (Kruskal, 1964; Coxon, 1982) formula. Therefore, the second hypothesis of this study was also rejected, since the CIEDE2000(2:1:1) total color difference formula outperformed the CIEDE2000(1:1:1) total color difference formula in terms of fitting the visual data, as indicated by the values of the PF/3 and STRESS performance parameters.

In summary, the use of K_L=2 instead of K_L=1 in the computation of the CIEDE2000 color difference formula result in a better fitting of the computed color difference with the visual judgments, suggesting a review of the parametric factors, so that the CIEDE2000 color difference formula can be properly used for applications involving samples of the dental color space.

CHAPTER 6

PREDICTIVE ALGORITHMS

APPLICATION TO EXPERIMENTAL DENTAL RESIN COMPOSITES

6.1 STATE OF THE ART

Composite restorative materials represent one of the many successes of modern biomaterials research, since they replace biological tissue in both appearance and function (Cramer et al., 2011). In a recent review of treatment considerations for esthetic restorations, it has been pointed out that, at least half of the posterior direct restoration placement, now rely on composite materials (Sadowsky, 2006). The development and implementation of composite dental restorative materials implies a comprehensive understanding of each component of the composite and consideration of methods for changing and/or improving each one of them.

Currently, methacrylate resin formulations dominate both the commercial market and research studies. The resin phase is composed primarily of dimethacrylate monomers (typically selected from Bis-GMA, BisEMA, and/or UDMA or a mixture of them) and, due to their high viscosity, low-viscosity reactive diluents (most commonly TEGDMA) are incorporated. The monomer interactions, polymerization kinetics, and polymer properties resulting from these materials are complex. These base monomers result in restorative materials with excellent mechanical properties, rapid polymerization, and low shrinkage. On the other hand, they are reported to generally result in low methacrylate conversion, which leads to significant amounts of unreacted monomer that may be leached from the restoration over time, resulting in concerns regarding long-term biocompatibility (Cramer et al., 2011).

There are several research studies that implement the use of experimental dental composites, as a continuous effort to understand the interrelationships among composition, resin viscosity, degree of conversion, shrinkage, flexural strength, fracture toughness, water sorption and solubility, etc. Atai and collaborators studied de physical and mechanical properties of an experimental dental composite based on new methacrylate monomer (BTDA) through comparisons with a commonly used Bis-GMA monomer (Atai et al., 2004). For the formulation of the latter one, they handmixed 29% by weight of a mixture of Bis-GMA/TEGDMA (50/50 wt%), 70% of silanated quartz filler, 0.5% initiator (CQ) and 0.5% accelerator (DMAEMA). The same group, in order to study the effects of ceramic and porous fillers on the mechanical

properties of experimental dental composites, used mixtures of 70/30% wt% of Bis-GMA and TEGDMA as resin matrix (approximately 28% of total weight), different types of glass and glass-ceramic fillers (approximately 71% of total weight) and 0.5% CQ and 0.5% DMAEMA for chemical formulations of their samples (Zandinejad et al., 2006).

Calheiros and collaborators also formulated experimental dental resin composite systems to study the influence of irradiant energy on the degree of conversion, polymerization rate and shrinkage stress (Calheiros et al., 2008). The chemical formulation they used included a mixture of 50/50% BiS-GMA/TEGDMA as resin matrix, silane treated glass paricles, 0.5% of CQ, 0.5% DMAEMA. They also incorporated 0.5% of butylated hydroxytoluene (BHT) as inhibitor. Schneider and collaborators also included the BHT as inhibitor, although in a smaller amount (0.05% wt%), within the chemical formulation of the experimental dental resin composites used for studying the effect of co-initiator ratio on the polymer properties (Schneider et al., 2009) and the curing efficiency of dental resin composites (Schneider et al., 2012). Furthermore, Park and collaborators, in their study on the influence of the fluorescent whitening agent on the fluorescent emission of resin composites, incorporated the fluorescent agent to the experimental dental resin formulation. For chemical formulation, they used 50 wt% silane coated filler, 50 wt% mixture of 1/1/1 Bis-GMA//UDMA TEGDMA as resin matrix, 0.7% CQ, 0.35% DMAEMA, 0.05% BHT and fluorescent agent (FWA) in increasing concentration from 0.01 to 0.1 % of the resin composite (Park et al., 2007).

A common ultimate goal of color measurement or shade specification in dentistry is the reproduction by prosthetic materials of most of the appearance characteristic of natural oral structures. It would be ideal to achieve a restoration that has identical colors as the tooth structure under various illumination conditions, within at least acceptable limits, but more preferably within limits of perceived color difference (Johnston, 2009). Although the importance of the pigments on the final color and appearance of the dental resin composite is well known, to the best of our knowledge, there is still no research study that made use of them when formulating the experimental dental resin composites. Therefore, in our study, we incorporate the use of pigments to the chemical formulation of the resin composites.

Color prediction in dentistry is a research area that has barely been explored. Results from our research group showed that the polymerization dependent color changes in resin composites can be successfully predicted using multivariable linear models of statistical inference (Ghinea et al., 2010). Also, Herrera and collaborators were able to predict the color change after tooth bleaching using a novel fuzzy logic model (Herrera et al., 2010). They proposed a Fuzzy Logic based approach in order to model a set of pre-bleaching and post-bleaching tooth colorimetric values by using a set of rules whose antecedents correspond to the chromatic coordinate values of a Vita shade guide. Wee and collaborators were able to predict the final color of 25 opaque feldspathic dental ceramic specimens fabricated by mixing six different pure shades in different concentrations. The color differences they found between measured and predicted L*, a* and b* values were below the threshold of human perceptibility (Wee et al., 2005).

The spectral data (usually the Reflectance Factors) are used to predict the pigment and their concentration in different applications. Koirala and collaborators used a least-square pseudo-inverse calculation to predict the amount of pigment concentrations in opaque samples made of pigments dispersed in filling materials (Koirala et al., 2008), Solovchenko used reflectance data to predict the pigment content in apple fruits (Solovchenko, 2010) while Sims and Gamon used it for prediction of pigment content of leaf (Sims and Gamon, 2002).

The main objectives of this Chapter are, on one hand, the development of prediction models of color and reflectance spectrum of experimental dental resin composites from quantities and types of pigments used in its chemical formulation and, on the other hand, the development of models which enable the determination of the quantity and type of pigments used in the formulation of the experimental dental resin composites based on their final chromaticity coordinates and spectral reflectance values.

6.2 MATERIALS AND METHODS

For the development of this study, 49 different types of experimental dental resin composites (samples) were formulated as a mixture of organic matrix, inorganic filler, photo activator and other components in minor quantities: accelerator, inhibitor, fluorescent agent and four types of Pigments (in various mixtures) in order to generate composites with different colors. All samples underwent an artificial chromatic aging, and their reflectance spectrum was analyzed both before and after the aging procedure was applied. A Multiple Nonlinear Regression Model was used to predict the final color of the samples, in terms of L*a*b* chromatic coordinates and to predict the reflectance spectrum (380nm-780nm) of the experimental resin composites, and also to predict the relative quantities (% percentages) of the four types of pigments within the formulation, starting from the L*a*b* chromatic coordinates of the samples before and after aging. A Partial Least Squares Regression model was used to predict the relative quantities (% percentages) of the four types of pigments within the formulation, starting from the Reflectance Factor values of the experimental resin composites before and after aging at 2nm steps in the 380nm-780nm interval.

The experimental techniques used as well as all the procedures followed are outlined below.

6.2.1 EXPERIMENTAL DENTAL RESIN COMPOSITES

*All the manufacturing steps of the specimens, including chemical formulation, mold packing and photo-polymerization were performed at the **Laboratory of Inorganic Chemistry of the University of Granada Spain**.*

The experimental dental resin composites used in this study were formulated as a mixture of organic matrix, inorganic filler, photo activator and other components in minor quantities: accelerator, inhibitor, fluorescent agent and four types of Pigments (in various mixtures), according to available standards and literature, and following standard manufacturing procedures.

In Table 6.1 are listed the chemical names of the components used to formulate the experimental resin composite as well as their corresponding manufacturers.

Component		Chemical Name		CAS	Lot #	Manufacturer
Organic Matrix	**BisGMA**	Bisphenol A glycerolate dimethacrylate		1565-94-2	MKBJ3076V	SIGMA – ALDRICH Quimica S.L. Madrid, Spain
	TEGDMA	Triethylene glycol dimethacrylate		109-16-0	STBC5193V	
	UDMA	Diurethane Dimethacrylate		72869-86-4	MKBH6234V	
Inorganic Filler		SiO_2 Glass Spheres [Φ: 9-13μm]		65997-17-3	MKBC8823V	
Coupling Agent		3-(Trimethoxysilyl)propyl methacrylate		2530-85-0	SLBC0787V	
Photo Activator		Camphorquinone		10373-78-1	S12442V	
Accelerator		2-(Dimethylamino)ethyl methacrylate		2867-47-2	BCBF8391V	
Inhibitor		Butylated hydroxytoluene		128-37-0	MKBH3026V	
Fluorescent Agent		1.4-Bis(2-benzoxazolyl)naphthalene		5089-22-5	XGVZG-CI	CYMIT Quimica S.L. Barcelona, Spain
Pigment		Pigment 1 (P1)	FeO·OH			Inorganic Chemistry Lab UGR, Spain
		Pigment 2 (P2)	FeO			
		Pigment 3 (P3)	TiO_2	13463-67-7	SZB90340V	SIGMA – ALDRICH Quimica S.L. Madrid, Spain
		Pigment 4 (P4)	Fe_2O_3	1309-37-1	10012LEV	

Table 6.1: Chemical components and their corresponding manufacturers used to formulate the experimental dental resin composites used in this study.

Component		% w/t (from total)
Organic Matrix	45% w/t BisGMA 45% w/t TEGDMA 10% w/t UDMA	68.8% (Average)
Inorganic Filler		30%
Photo Activator		0.7%
Accelerator		0.35%
Inhibitor		0.05%
Fluorescent Agent		0.04%
Pigment		0.06% (Average)

Table 6.2: Chemical components as well as the relative percentages within the total mixture (by weight w/t) used to formulate the resin composites used in this study.

The chemical components used to formulate the experimental dental resin composites were mixed following the details specified in Table 6.2, and previously described in literature (Park et al., 2007).

A total of 49 different mixtures of pigments were generated by varying the relative amount of each of the four pigments, according to proportions specified in Table 6.3.

All chemical components were weighted using a high precision digital scale (BL 60 S, Sartorius AG, Goettingen, Germany) and carefully hand-mixed until a homogeneous mixture was obtained. All the procedures were carried out by the same experienced experimenter, in order to reduce variability. Until final preparation, the mixture was stored in a completely dark recipient inside a low temperature chamber, in order to avoid both photo-chemical and/or thermal polymerization. The components used for the chemical formulation of the experimental dental resin composites are presented in Figure 6.1.

Figure 6.1: Image of the chemical components used for the formulation of the experimental dental resin composites (left) and Inorganic Chemistry Laboratory of the University of Granada (right).

Organic Matrix [45% BisGMA + 45% TEGDMA + 10% UDMA by w/t]	Inorganic Filler [SiO_2 Glass Spheres 9-13µm)	CQ	Acc	Inh	FWA	Pigment (mixtures of P1, P2, P3 and P4)
68.8% (Average)	30%	0.7%	0.35%	0.05%	0.04%	0.06% (Average)

Sample		% Pigments				Sample		% Pigments			
		% P1	% P2	% P3	% P4			% P1	% P2	% P3	% P4
1	Organic Matrix + Inorganic Filler + CQ + Acc + Inh + FWA	0	0	0	0	26	Organic Matrix + Inorganic Filler + CQ + Acc + Inh + FWA	0.076464	0	0.040417	0.008739
2		0.059745	0	0	0	27		0.034117	0	0.018034	0.003899
3		0.102534	0	0	0	28		0.022101	0	0.011682	0.002526
4		0.039849	0	0	0	29		0	0.088254	0.033561	0
5		0	0.092783	0	0	30		0	0.021502	0.008177	0
6		0	0.049776	0	0	31		0	0.066872	0.025430	0
7		0	0.036612	0	0	32		0	0.043134	0.016403	0
8		0	0.023220	0	0	33		0	0.035042	0.018420	0.002696
9		0	0	0.099870	0	34		0	0.063877	0.033577	0.004914
10		0	0	0.032925	0	35		0	0.099051	0.052065	0.007619
11		0.023083	0	0	0	36		0	0.018493	0.009720	0.001423
12		0	0.052466	0.056502	0	37		0.006442	0.055443	0	0.000792
13		0	0.086047	0.092666	0	38		0.002377	0.020462	0	0.000292
14		0	0.022245	0.023956	0	39		0.009170	0.078918	0	0.001127
15		0	0.014304	0.015405	0	40		0.018325	0.157716	0	0.002253
16		0	0	0	0.072749	41		0.022348	0.010760	0.045800	0
17		0	0	0	0.023056	42		0.038512	0.018543	0.078927	0
18		0	0	0	0.013156	43		0.007477	0.003600	0.015324	0
19		0	0.014745	0.014745	0.007012	44		0.015831	0.007622	0.032444	0
20		0	0.009302	0.009302	0.004423	45		0.022426	0.018937	0.012210	0.002741
21		0	0.026643	0.026643	0.012670	46		0.035597	0.030060	0.019381	0.004351
22		0.038063	0	0.038063	0	47		0.046098	0.038927	0.025098	0.005634
23		0.059424	0	0.059424	0	48		0.011854	0.010010	0.006454	0.001449
24		0.021422	0	0.021422	0	49		0.005259	0.004441	0.002863	0.000643
25		0.058210	0	0.030768	0.006653						

Table 6.3: Detailed formulations of each of the 49 types of experimental dental resin composites.

To perform the present study, a total of 147 specimens (49 types x 3 specimen each) of experimental dental resin composites were manufactured. All specimens were cylinder shaped with a diameter of Φ=20mm and 1.5mm thickness (Figure 6.2).

Each of the 147 specimens was carefully packed in a custom built silicon mold in a glass plate sandwich with a mylar strip on both sides. The specimens were light cured during 60 seconds on each side using a light curing unit (BluePhase, Ivoclar Vivadent AG, Schaan, Liechtenstein). According to the manufacturer, the total irradiance of the Bluephase curing unit is 1100mW/cm^2± 10%, and taking into account the diameter and thickness of our samples, a 60 seconds on each side of the sample ensured proper polymerization (in terms of full monomer conversion) of the samples. The light cured specimens were stored in sealed recipients until color measurements were performed.

In order to mimic a clinical situation and before storage, all samples were polished using a one-step diamond micro-polishing system (PoGo, Dentsply, USA), by applying light intermittent pressure at moderate speed during 40s. The Pogo System uses a “one-step” technique to create a high glass-like lustre finish and, according to the manufacturer recommendations, it can be used to polish all types of composites: microfills, flowables and micro-hybrids. This type of polishing systems are frequently used in dental studies to analyze the color stability (Ergucu et al., 2008) or the influence of the polishing procedure on the surface roughness (Gonulol and Yilmaz, 2012) of different types of dental resin composites.

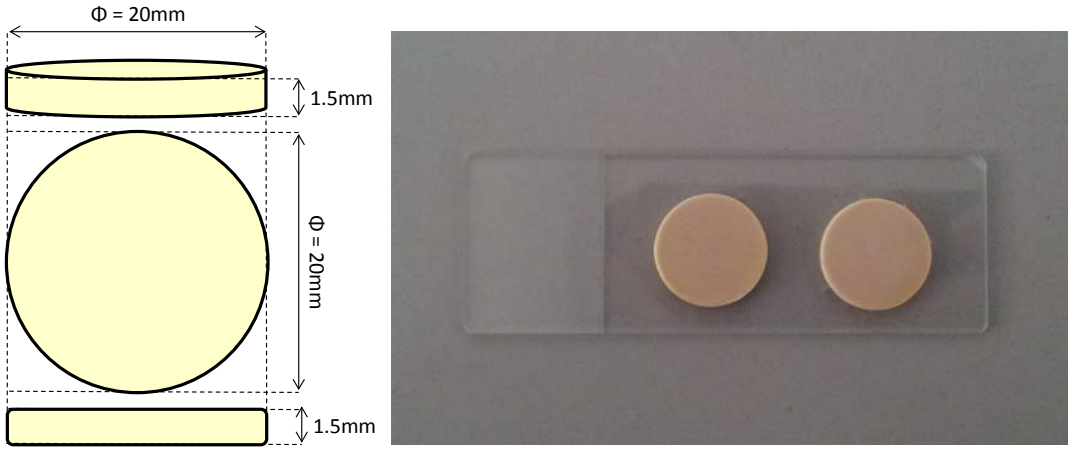

Figure 6.2: Schematic representation of the experimental dental resin composites (left) and picture of two of the manufactured specimens (right).

6.2.2 REFLECTANCE MEASUREMENTS AND COLOR CALCULATIONS

All the reflectance measurements were performed at the ***Houston Center for Biomaterials and Biomimetic (HCBB) of the School of Dentistry at University of Texas – Health Science Center at Houston.***

The reflectance spectrum of all specimens was measured inside a completely dark room using a spectroradiometer (PR 670, PhotoResearch, USA) and a spectrally calibrated reflectance standard (SRS-3, PhotoResearch, USA) (Figure 6.3).

The PR670 SpectraScan spectroradiometer is equipped with a 256 detector photodiode array and a Pritchard Optical System, which is widely accepted as the most accurate and versatile in use today. The Pritchard system allows the user to see a bright and magnified image of the sample with a black aperture which accurately and unambiguously defines the measuring field within the field of view. According to the manufacturer, it has a spectral accuracy of ±1nm, a luminance accuracy of ±2% and a color accuracy of ±0.0015 in CIE xy, and it has been recently the objective color measurement instrument chosen to perform numerous studies in dental research (Lim et al., 2010; Son et al., 2010; An et al., 2013).

For reflectance measurements, all specimens were placed on a custom built sample holder, 40cm away from the spectroradiometer and illuminated using a Xe-Arc Light Source (Oriel Research, Newport Corporation, USA).

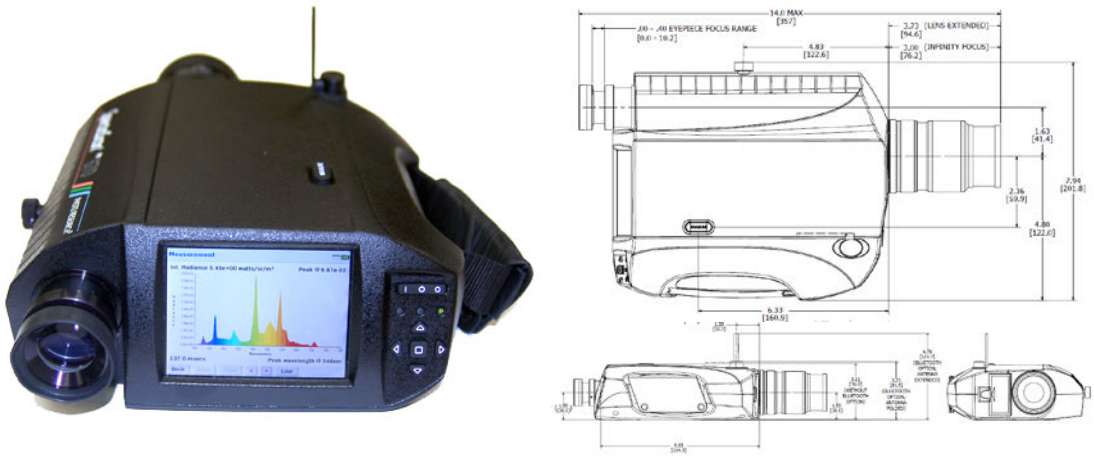

Figure 6.3: Photoresearch PR670 Spectroradiometer used for reflectance measurements.

The illuminating/measuring geometry used corresponded to CIE 45°/0°. The aperture of the spectroradiometer was set to 1°, which allowed the measurement of a central spot (measuring field) of the specimen of approximately 0.7cm. The experimental set-up used for reflection measurements is schematically presented in Figure 6.4.

Three repeated measurements were performed for each specimen and the results for each specimen were averaged. The reflectance spectrum for each type of experimental resin composite (sample) was the mean value between the three specimens corresponding to the type. Color calculations were subsequently performed in base of the CIE D65 Standard Illuminant and the CIE Colorimetric 2° Standard Observer assumptions.

Reflectance measurements were performed both before and after the chromatic artificial aging procedure was applied.

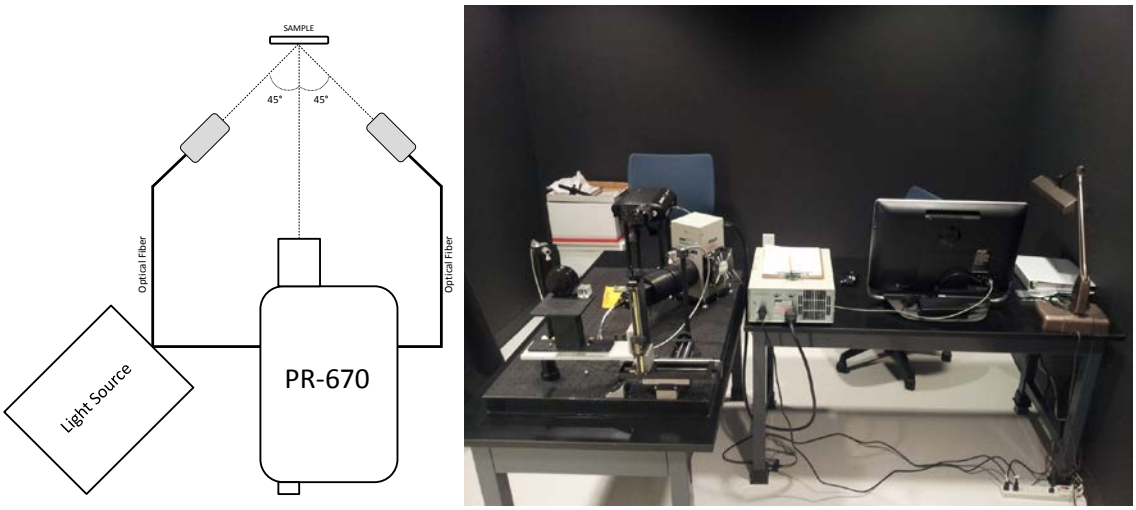

Figure 6.4: Schematic representation of the experimental set-up used for reflectance measurements (left) and image of the assembly at the HCBB (right).

6.2.3 ARTIFICIAL CHROMATIC AGING

All the aging procedures were performed at the ***Houston Center for Biomaterials and Biomimetic (HCBB) of the School of Dentistry at University of Texas – Health Science Center at Houston****.*

After the measurement of the reflectance spectrum before aging was performed, all the studied specimens were placed inside an artificial aging chamber (Suntest XXL, ATLAS, USA) and subjected to artificial aging according to ISO 4892-2 A1 and ISO 7491 Standards (Figure 6.5).

The Atlas Suntest XXL is equipped with 3x1700W air-cooled Xenon Lamps with daylight filter, and a 3000cm^2 exposure test chamber, ideal for simultaneous testing of a high number of samples. It is pre-programmed with international standard test methods but also allows the user to program its own artificial aging cycle. For the development of this study, we used the 2 hours test cycle specified in ISO 4892-2 A1, which consists of 102 minutes of light exposure and 50% relative humidity at 38°C and 18 minutes of water spraying, with a black panel temperature of 65°C and irradiance control in the 300nm-400nm interval of 60W/m^2. The test cycles were repeated until the switch off criteria of 450.0 KJ/m^2 total dosage level was achieved.

Figure 6.5: ATLAS Suntest XXL artificial aging device at HCBB (left) and placement of the sample inside the artificial aging chamber (right).

6.2.4 DESIGN OF THE PREDICTIVE MODELS

*The design of the predictive models was carried out at the **Laboratory of Biomaterials Optics of the Department of Optics of the University of Granada Spain**.*

Before starting the design of the predictive models, the samples were divided into a Training (Active) Group, which contained 44 samples (sample 1 to 44) from the total of 49 samples available, and a Testing (Validation) Group, which contained 5 samples from the total of 49 samples available (Sample 45 to 49). As shown in Table 6.3, Samples 45-49 are the only ones that present a combination of the 4 pigments, this criterion being the one by which these samples were selected as test samples. The reflectance factors and chromatic coordinates for each sample represented the average values over the three specimens correspond to the sample. In all cases, the Active (Training) Group was used to build the predictive model while the Validation Group was used exclusively for testing the appropriate functioning of the built model as well as its accuracy.

For this study, two different types of Predictive models were used: Multiple Nonlinear Regression (MNLR) and Partial Least Squares Regression (PLSR). The study is structured into four blocks, and for each block a different predictive model was used. The four different analysis blocks and their corresponding models are described in Table 6.4.

	Study	Predictive Model
1	Prediction of L*a*b* colorimetric coordinates values before and after aging from % Pigment (%P1, %P2, %P3 and %P4) within the formulation.	**Multiple Nonlinear Regression (MNLR)**
2	Prediction of Reflectance Factors in the 380nm-780nm interval from % Pigment (%P1, %P2, %P3 and %P4) within the formulation.	
3	Prediction of % Pigment (%P1, %P2, %P3 and %P4) within the formulation from L*a*b* colorimetric coordinates before and after aging.	
4	Prediction of % Pigment (%P1, %P2, %P3 and %P4) within the formulation from Reflectance Factors at 2nm step in the 380nm-780nm interval	**Partial Least Squares Regression (PLSR)**

Table 6.4: The four types of analysis blocks and the their corresponding predictive models.

*6.2.4.1 Prediction of L*a*b* colorimetric coordinates values before and after aging from % Pigment (%P1, %P2, %P3 and %P4) within the formulation*

A Multiple Nonlinear Regression Model (MNLR) was used to predict the values of the L*a*b* colorimetric coordinates values before and after aging from % Pigment (%P1, %P2, %P3 and %P4) within the formulation.

The equation describing the model is a 4th Order Polynomial, as described by:

$$Y = pr1 + pr2 \cdot X_1 + pr3 \cdot X_2 + pr4 \cdot X_3 + pr5 \cdot X_4 + pr6 \cdot X_1^2 + pr7 \cdot X_2^2 + pr8 \cdot X_3^2 + pr9 \cdot X_4^2 + \\ + pr10 \cdot X_1^3 + pr11 \cdot X_2^3 + pr12 \cdot X_3^3 + pr13 \cdot X_4^3 + pr14 \cdot X_1^4 + pr15 \cdot X_2^4 + pr16 \cdot X_3^4 + pr17 \cdot X_4^4$$

where:

- Y is the predicted variable: the chromatic coordinates L*a*b* before and after aging;
- X_i are the input variables: %P1, %P2, %P3 and %P4;
- pr1, …, pr17 are the parameters of the model.

The models were built using the Training Group and tested using the Validation Group. The model was considered to be accurate after 200 iterations were performed and/or a convergence of 0.00001 was achieved.

A total of 6 models (one for each colorimetric coordinate before and after aging) were designed. All the Multiple Nonlinear Regression (MNLR) predictive models were designed using the XLSTAT-Pro commercial software (XLSTAT, Addinsoft, USA).

6.2.4.2 Prediction of Reflectance Factors in the 380nm-780nm interval from % Pigment (%P1, %P2, %P3 and %P4) within the formulation

A Multiple Nonlinear Regression Model (MNLR) was used to predict the values of the Reflectance Factors values in the visible range (380nm-780nm) before and after aging from % Pigment (%P1, %P2, %P3 and %P4) within the formulation.

The equation describing the model is a 4th Order Polynomial, as described by:

$$Y = pr1 + pr2 \cdot X_1 + pr3 \cdot X_2 + pr4 \cdot X_3 + pr5 \cdot X_4 + pr6 \cdot X_1^2 + pr7 \cdot X_2^2 + pr8 \cdot X_3^2 + pr9 \cdot X_4^2 + \\ + pr10 \cdot X_1^3 + pr11 \cdot X_2^3 + pr12 \cdot X_3^3 + pr13 \cdot X_4^3 + pr14 \cdot X_1^4 + pr15 \cdot X_2^4 + pr16 \cdot X_3^4 + pr17 \cdot X_4^4$$

where:

- Y is the predicted variable: Reflectance Factors values in the visible range (380nm-780nm) at 2nm step the before and after aging;
- X_i are the input variables: %P1, %P2, %P3 and %P4;
- pr1, …, pr17 are the parameters of the model.

The models were built using the Training Group and tested using the Validation Group. The model was considered to be accurate after 200 iterations were performed and/or a convergence of 0.00001 was achieved.

A total of 402 models (one for each Reflectance Factor before and after aging) were designed. All the Multiple Nonlinear Regression (MNLR) predictive models were designed using the XLSTAT-Pro commercial software (XLSTAT, Addinsoft, USA).

*6.2.4.3 Prediction of % Pigment (%P1, %P2, %P3 and %P4) within the formulation from L*a*b* colorimetric coordinates before and after aging*

A Multiple Nonlinear Regression Model (MNLR) was used to predict the values of the % Pigment (%P1, %P2, %P3 and %P4) within the formulation from L*a*b* colorimetric coordinates before and after aging.

The equation describing the model is a 4th Order Polynomial, as described by:

$$Y = pr1 + pr2 \cdot X_1 + pr3 \cdot X_2 + pr4 \cdot X_3 + pr5 \cdot X_1^2 + pr6 \cdot X_2^2 + pr7 \cdot X_3^2 + \\ + pr8 \cdot X_1^3 + pr9 \cdot X_2^3 + pr10 \cdot X_3^3 + pr11 \cdot X_1^4 + pr12 \cdot X_2^4 + pr13 \cdot X_3^4$$

Where:

- Y is the predicted variable: %P1, %P2, %P3 and %P4;
- X_i are the input variables: the chromatic coordinates L*a*b* before and after aging;
- pr1, …, pr13 are the parameters of the model.

The models were built using the Training Group and tested using the Validation Group. The model was considered to be accurate after 200 iterations were performed and/or a convergence of 0.00001 was achieved.

A total of 8 models (one for each relative percentage of Pigment - %P1, %P2, %P3 and %P4 - within the formulation starting from the L*a*b* chromatic coordinates before and after aging) were designed. All the Multiple Nonlinear Regression (MNLR) predictive models were designed using the XLSTAT-Pro commercial software (XLSTAT, Addinsoft, USA).

6.2.4.4 Prediction of % Pigment (%P1, %P2, %P3 and %P4) within the formulation from Reflectance Factors at 2nm step in the 380nm-780nm interval

A Partial Least Squares Regression Model (PLSR) was used to predict the values of the % Pigment (%P1, %P2, %P3 and %P4) within the formulation from Reflectance Factors at 2nm step in the 380nm-780nm interval.

The equation describing the model is:

$$Y = \alpha + \beta_1 \cdot X_1 + \beta_2 \cdot X_2 + \beta_3 \cdot X_3 + \beta_4 \cdot X_4 + \ldots + \beta_{201} \cdot X_{201}$$

where:

- Y is the predicted variable: %P1, %P2, %P3 and %P4;
- α is the Intercept;
- X_i are the input variables: the Reflectance Factors at 2nm steps in the 380nm-780nm range before and after aging;
- β_1, … , β_{201} are the parameters of the model.

The models were built using the Training Group and tested using the Validation Group. The model was considered to be accurate when a Qi^2 improvement at a level of 0.05 was achieved. Confidence intervals at a level of 95% were calculated for all predictive models.

A total of 8 models (one for each relative percentage of Pigment within the formulation - %P1, %P2, %P3 and %P4 - starting from the Reflectance Factors at 2nm steps in the 380nm-780nm range before and after aging) were designed. All the Partial Least Squares Regression (PLSR) predictive models were designed using the XLSTAT-Pro commercial software (XLSTAT, Addinsoft, USA).

6.2.5 COLOR DIFFERENCES

The total color differences between the predicted and the measured (real) values of the L*a*b* chromatic coordinates were calculated according to ΔE^*_{ab} and ΔE_{00} total color difference formulas:

$$\Delta E^*_{ab} = \sqrt{\left(\Delta L^*\right)^2 + \left(\Delta a^*\right)^2 + \left(\Delta b^*\right)^2}$$

$$\Delta E_{00} = \sqrt{\left(\frac{\Delta L'}{K_L S_L}\right)^2 + \left(\frac{\Delta C'}{K_C S_C}\right)^2 + \left(\frac{\Delta H'}{K_H S_S}\right)^2 + R_T\left(\frac{\Delta C'}{K_C S_C}\right)\left(\frac{\Delta H'}{K_H S_H}\right)}$$

6.3 RESULTS AND DISCUSSION

6.3.1 PREDICTION OF L*a*b* COLORIMETRIC COORDINATES VALUES BEFORE AND AFTER AGING FROM % PIGMENT (%P1, %P2, %P3 AND %P4) WITHIN THE FORMULATION.

The values of the chromatic coordinates L*a*b* of the 49 samples (average values over the three specimens fabricated for each sample) as calculated from the reflectance measurements and according to the CIE 2° Standard Observer and CIE D65 standard illuminant, are presented in Table 6.5.

As a prior step to the design of the predictive model, the correlation between the input variables (percentage of each type of Pigment used - %P1, %P2, %P3 and %P4) and the values of the L*a*b* colorimetric coordinates before and after the artificial aging, was studied. The correlation matrix, showing the values obtained for the Pearson Correlation Coefficient, is shown in Table 6.6.

It is generally accepted that a PCC value between 0-0.2 represent a very weak to negligible correlation, a value between 0.2-0.4 is addressed as a weak correlation, a value between 0.4-0.7 is considered as a moderate correlation, a value between 0.7-0.9 is a strong correlation while values higher than 0.9 represent a very strong correlation between the studied variables. In our case, we found a strong direct correlation (p=0.699 before aging and p=0.713 after aging) between the percentage of the second pigment (% P2) and the CIE b* value, implying that a higher quantity of this pigment will result in a higher value of b* (a more yellowish material).

Variables	Pearson correlation coefficient					
	Before Aging			After Aging		
	L*	a*	b*	L*	a*	b*
% P1	-0.117	-0.144	0.322	-0.116	-0.140	0.288
% P2	-0.222	0.113	0.699	-0.243	0.132	0.713
% P3	0.194	-0.218	0.105	0.162	-0.217	0.093
% P4	-0.763	0.827	-0.122	-0.761	0.832	-0.122

Table 6.6: Correlation Matrix between %Pigment and L*a*b* values before and after aging.

On the other hand, the quantity of the fourth pigment (% P4) is inversely correlated (p=-0.763 before aging and p=-0.761 after aging) with the lightness of the sample (L* value), suggesting that higher levels of this pigment will decrease the lightness value of the experimental resin composite. The percentage of this pigment is also highly directly correlated (p=0.827 before aging and p=0.832 after aging) with the values of the red-green (a*) axis. Therefore, higher quantities of this type of pigment will generate a reddish effect on the overall final color of the experimental dental resin composite. This result is not surprising, since the Iron(III) oxide, or ferric oxide, used as the fourth pigment in this study (P4), has a dark red color. The analysis of the correlation matrix between all studied variables showed no other relationship between them.

Sample	Before Aging			After Aging		
	L*	a*	b*	L*	a*	b*
1	89.73	1.31	-0.72	88.73	0.67	1.41
2	83.63	1.50	10.04	82.75	1.28	10.48
3	82.61	2.59	13.03	81.65	2.24	13.53
4	85.32	1.58	5.07	84.44	1.12	6.31
5	83.70	3.25	13.19	82.69	2.82	14.66
6	85.35	2.28	8.92	84.25	1.95	10.14
7	86.46	2.15	7.67	85.26	1.76	9.17
8	87.16	1.68	4.10	86.34	1.11	6.02
9	88.03	1.32	-0.85	87.12	0.69	1.09
10	87.62	1.09	0.37	86.81	0.63	1.62
11	85.57	1.74	5.44	84.74	1.21	6.65
12	85.83	2.22	8.97	84.21	1.89	10.31
13	84.53	3.10	12.56	83.30	2.75	13.13
14	87.60	1.77	4.68	86.52	1.21	6.48
15	87.77	1.51	4.03	86.50	1.08	5.46
16	70.29	15.64	5.19	69.36	14.90	6.62
17	76.90	11.78	2.74	76.32	10.82	4.58
18	78.59	10.33	2.25	78.01	9.34	4.36
19	82.95	6.71	3.31	81.47	5.97	5.47
20	84.82	5.45	2.84	83.51	4.77	4.75
21	80.59	8.77	5.56	79.24	8.00	7.23
22	85.73	1.72	8.16	84.51	1.18	9.23
23	84.75	1.92	9.99	82.66	1.42	11.47
24	86.49	1.44	4.83	85.17	0.76	6.66
25	79.71	5.02	7.38	78.75	4.34	8.27
26	79.39	5.89	9.17	78.43	5.18	10.02
27	83.66	4.28	5.12	82.78	3.49	6.68
28	85.38	3.75	4.29	84.44	2.99	5.81
29	84.03	3.01	12.52	82.41	2.70	13.21
30	86.97	1.64	5.28	85.65	1.09	7.10
31	83.21	2.56	10.67	81.86	2.02	11.98
32	84.91	1.98	6.96	83.77	1.39	8.66
33	84.68	3.80	5.82	83.37	3.17	7.62
34	81.59	5.30	9.83	80.50	4.68	10.89
35	80.67	6.77	12.04	79.12	6.19	12.84
36	85.29	3.05	4.14	84.18	2.38	6.04
37	81.95	4.84	9.04	81.63	4.11	9.87
38	84.98	3.04	4.89	84.06	2.47	6.09
39	80.43	5.47	10.42	79.73	4.85	11.21
40	77.14	7.92	14.81	75.99	7.31	15.37
41	85.81	1.81	6.35	84.75	1.21	7.58
42	84.94	2.23	9.42	83.88	1.61	10.29
43	87.63	1.44	1.93	86.31	0.73	3.77
44	86.93	1.68	4.68	85.64	1.01	6.40
45	83.84	3.77	7.39	82.78	3.10	8.74
46	81.70	5.12	10.72	81.18	4.26	11.70
47	81.27	5.86	12.18	79.66	5.11	12.91
48	85.76	2.88	4.84	84.52	2.11	6.58
49	86.61	2.47	2.41	84.92	1.61	4.74

Table 6.5: Average L*a*b* values of the 49 samples of experimental dental resin composites used in this study.

*6.3.1.1 Multiple Nonlinear Regression of chromatic coordinate L**

The statistical parameters describing the goodness of fit for the L* variable are presented in Table 6.7. When building a prediction model, the evaluation of the accuracy of the outcome by comparing the measured (real) and the predicted values in a quantitative way is required. Two of the most extensively used parameters for these purposes are the Coefficient of Determination (R^2) and the Root Mean Square Error (RMSE) (Willmott et al., 1985). The Coefficient of Determination describes the proportion of the total variance explained by the predictive model, and varies between 0 (no correlation) and 1 (perfect correlation). Although R^2 is usually accepted as one of the most reliable measures of a model's ability to estimate the output, not always it is consistently related to the accuracy of the prediction, and, although a high value of R^2 was achieved, there still can be statistically significant differences between the expected output (real measured values) and the values provided by the predictive model. Therefore, the use of complementary parameters of goodness of fit are required, such as the RMSE or a plot of the residual values. The average error produced by a model is well represented by a difference measure, such as the root square of the mean squared error (RMSE). The RMSE has the same unit as the observed and predicted variables (input and output, respectively) but, unlike the Determination Coefficient, it does not have a fixed scale, being dependent on the values of the variables. Schunn and Wallach (Schunn and Wallach, 2005), when evaluating the goodness-of fit in comparison of models to data, pointed out that there is still no reliable criterion for how high R^2 should be in order to consider a fit as "good", and for the RMSE the situation is even less clear, since its values depends on the measure of the studied variable. Even so, it is generally accepted that a lower value of the RMSE it is translated into a better fit of the predictive model.

L*	Before Aging	After Aging
Observations	44	44
DF	27	27
R^2	0.963	0.965
SSE	20.906	19.149
MSE	0.774	0.709
RMSE	0.880	0.842

Table 6.7: Goodness of fit statistics of variable L* before and after aging.

The Multiple Nonlinear Regression Model designed for variable L* shows a R^2=0.963 before aging and a R^2=0.965 after aging while for the Root Mean Square Error (RMSE) the values displayed by the regression model are 0.880 before aging and 0.842 after aging. The high values of the Coefficient of Determination are guarantees of the reliability and accuracy of the built model, as well as the low values (when compared with the magnitude of the variable) of the RMSE (0.880 and 0.842 compared to average L* values of 82 units).

The Nonlinear regression model designed for predicting the final color of the experimental dental composites as a function of the relative quantities of pigment inside the chemical formulation is described by seventeen parameters (pr1 -> pr17). The values of the parameters of the nonlinear regression model built for the variable L* both before and after the artificial aging procedure was applied , together with their corresponding Standard Errors, are presented in Table 6.8.

Model Parameter	Before Aging		After Aging	
	Value	Standard Error	Value	Standard Error
pr1	87.950	0.491	86.947	0.470
pr2	-161.836	71.066	-125.584	68.013
pr3	-9.376	51.446	-14.720	49.236
pr4	31.034	65.448	-8.153	62.636
pr5	-598.568	207.944	-546.114	199.011
pr6	3604.241	4007.607	2192.156	3835.448
pr7	-2957.821	1822.083	-2606.702	1743.809
pr8	-454.960	3605.949	1012.439	3451.044
pr9	-7886.196	33517.180	-12650.005	32077.343
pr10	-47847.659	70588.515	-29204.417	67556.161
pr11	41929.868	21607.477	36966.485	20679.259
pr12	10212.467	64056.659	-14517.276	61304.901
pr13	739575.828	1412683.258	922913.555	1351996.953
pr14	226656.063	373960.635	146048.212	357895.966
pr15	-156461.049	76758.709	-138631.298	73461.294
pr16	-85354.291	352674.034	56526.902	337523.799
pr17	-7751980.481	13672481.081	-9505416.621	13085136.151

Table 6.8: Model parameters of variable L* before and after aging.

The predicted values of the L* chromatic coordinate as well as the measured values and corresponding residuals are shown in Table 6.9. For lightness values before aging, the lowest residual value was found for Sample 49 (Residual = -0.183), while the highest value was found for Sample 47 (Residual = 2.399). For L* values after aging, the lowest difference between the predicted value and the real (measured) lightness value was 0.006. Again, the highest value of lightness registered was in the case of the Sample 47, although it is slightly smaller than before aging (Residual = 1.806).

Four of the five samples included in the Validation Group presented a value of the Residual (the difference between the predicted and the measured value) lower than 0.9 before aging. These values are lower than the lightness perceptibility threshold (ΔL*=1.0) established by Lindsey and Wee in a study on the perceptibility and acceptability of tooth color differences using computer-generated pairs of teeth with simulated gingival displayed on a calibrated monitor (Lindsey and Wee, 2007). After aging, only three of the studied samples presented values below the perceptibility threshold for lightness.

It is worth mentioning that, for this model, the residual values depend inversely on the variable value. We found the biggest positive residual values for samples with low lightness, and a progressive decrease of the residual was registered with increase of lightness, reaching negative values for the sample with the highest L* value (Sample 49). This behavior appears both for samples before and after aging.

Figure 6.6 shows the absolute values of the lightness differences between the predicted and the measured values, as well as the levels of perceptibility and acceptability thresholds.

Sample	Before Aging			After Aging		
	L*	Pred(L*)	Residuals	L*	Pred(L*)	Residuals
45	83.836	83.320	0.516	82.784	82.413	0.370
46	81.704	80.816	0.889	81.185	79.846	1.338
47	81.272	78.873	2.399	79.663	77.857	1.806
48	85.759	85.415	0.344	84.525	84.519	0.006
49	86.609	86.793	-0.183	84.916	85.858	-0.942

Table 6.9: Predictions and residuals of variable L* before and after aging.

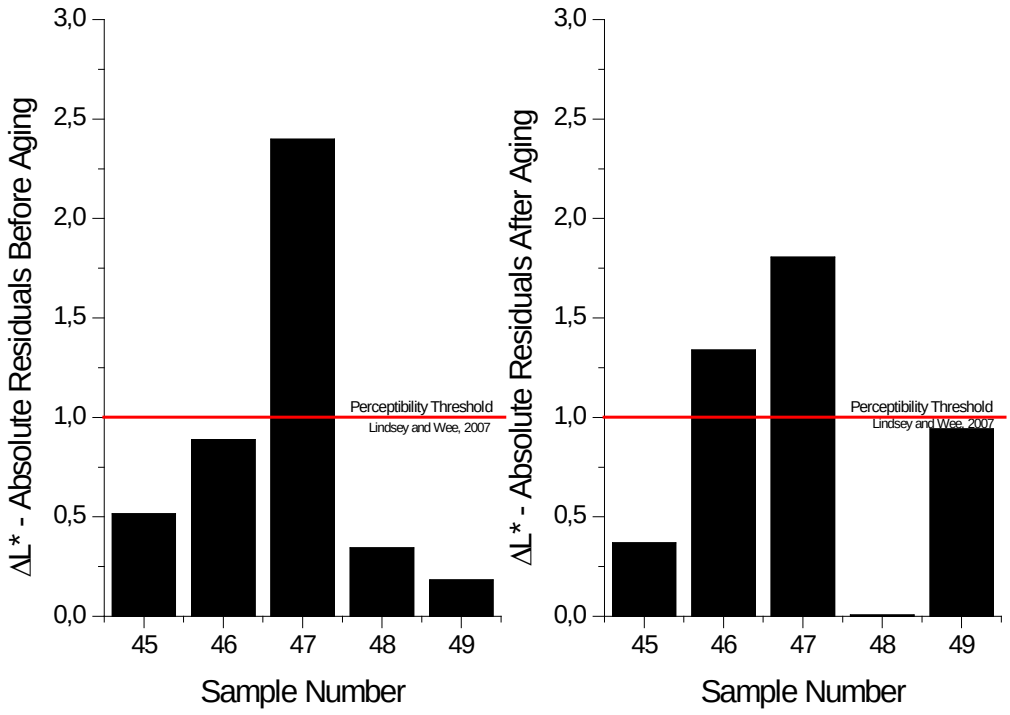

Figure 6.6: ΔL* - Absolute Residual Values of variable L* before and after aging.

In Figure 6.7 are plotted the predicted values against the measured values of the L* colorimetric coordinate before and after aging, both for the Training Group (Active) and the Validation Group. As it can be seen, the results obtained with the predictive model are good, the ratio between the predicted and real values being in all cases very close to 1. For the five samples included in the Validation Group, both before and after aging, the model is constantly underestimating the values of L*, except for highest values, where the relationship is inverse. Constant over or under estimations of a model compared to the expected values is a frequent problem when building predictive models, and are usually related with the variance in data (Roberts and Pashler, 2000). Hence, manufacturing experimental dental composites (samples) which cover wider areas of the dental color space, as well as reducing the variability of the experimental measuring procedures, it is expected to provide better outcomes in terms of the predictive capability of the models.

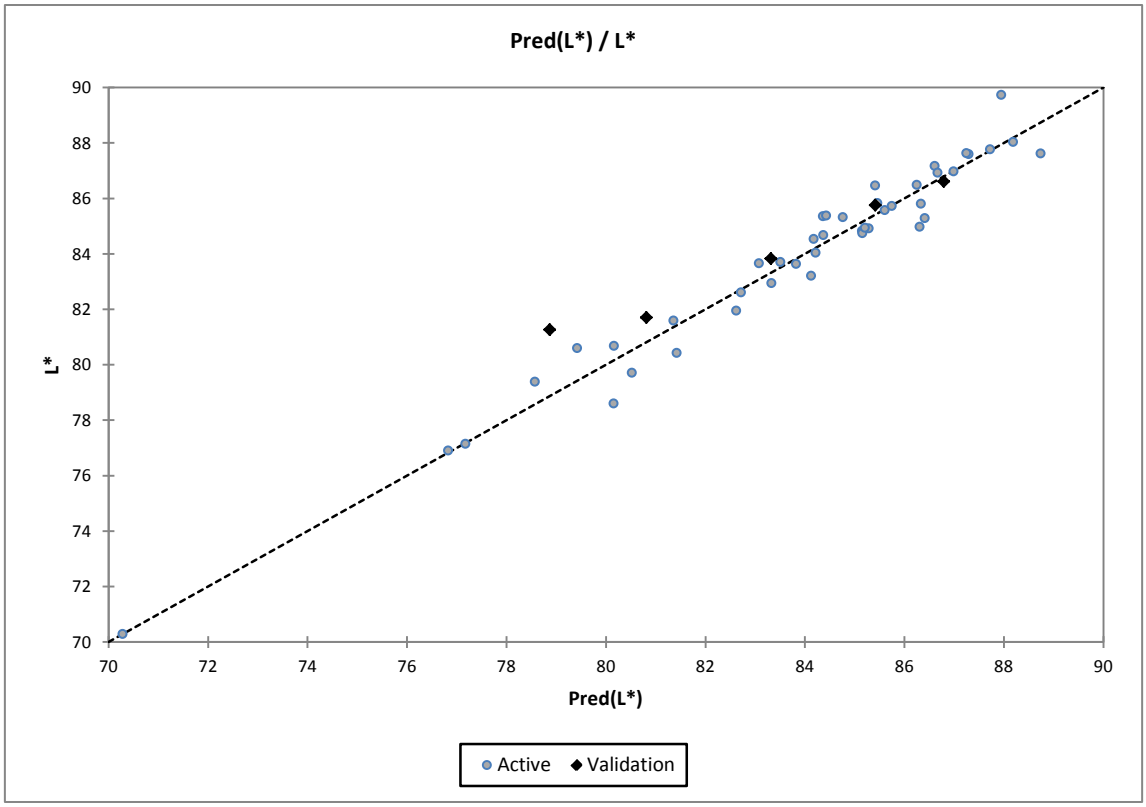

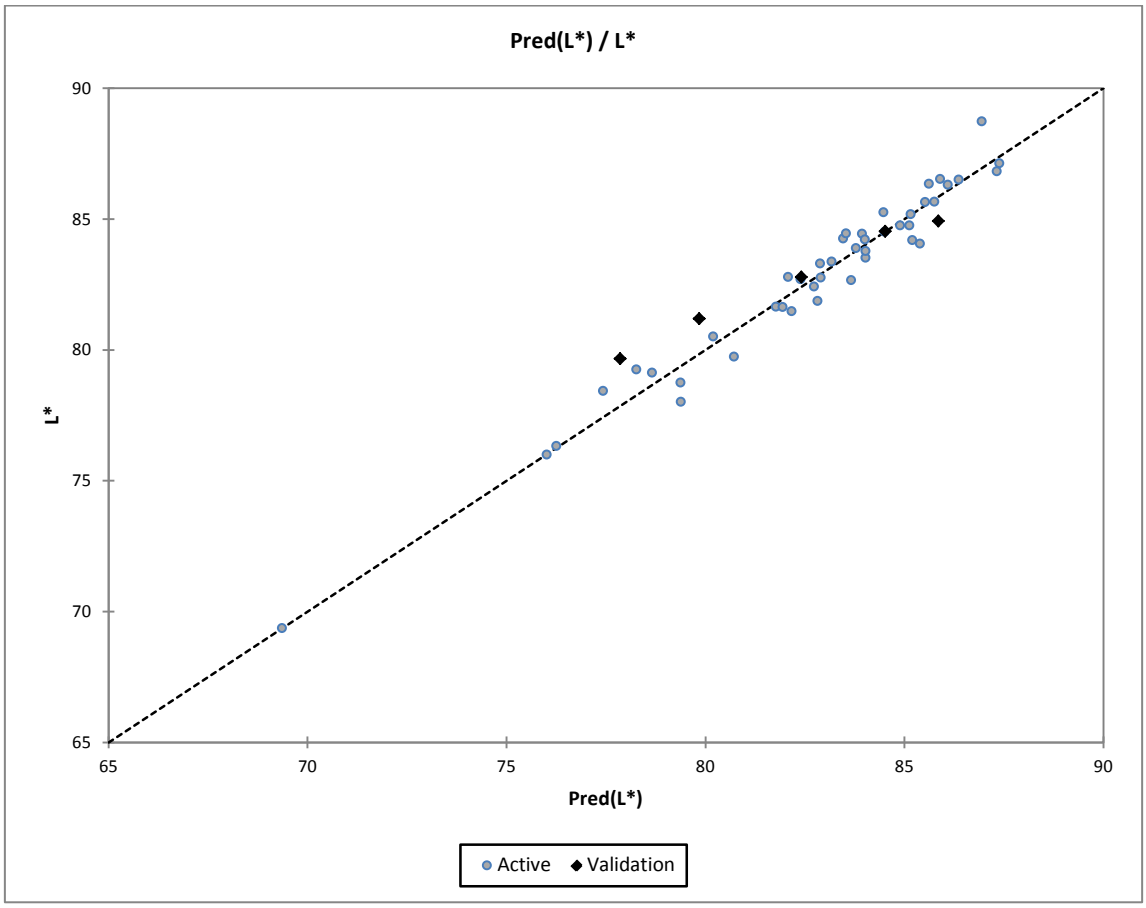

Figure 6.7: Predicted against measured values for the variable L* before aging (top) and after aging (bottom).

*6.3.1.2 Multiple Nonlinear Regression of chromatic coordinate a**

The statistical parameters describing the goodness of fit for a* variable are presented in Table 6.10. In terms of accuracy of the model, for this variable, both before and after the artificial aging procedure was carried out, we obtained a R^2 value of 0.981 while for the RMSE parameter we registered a value of 0.548 before aging and 0.527 after aging, both confirming a good agreement between the predicted values and the measured values for this variable.

The values of the parameters of the nonlinear regression models built for the variable a* (before and after aging), together with their respective Standard Errors, are presented in Table 6.11.

Table 6.12 shows both the measured and the predicted values for the variable a* before and after artificial aging, as well as the corresponding differences between them (Residuals) for the five samples included in the Validation Group.

Among all the three studied variables, the a* chromatic coordinate presented the lowest residual values (absolute residual value <0.53 for all five studied samples of the Validation Group). For all five samples included in our Validation group both before and after aging, the difference between the predicted and the measured a* values were lower than the 50:50% perceptibility threshold for dental samples (Δa*=1.0) (Lindsey and Wee, 2007), which will make it impossible to observe with the naked eye.

Figure 6.8 shows the absolute values of the differences between the predicted and the measured values (Δa* - Absolute Residual Value), as well as the level of perceptibility threshold for this chromatic coordinate.

a*	Before Aging	After Aging
Observations	44	44
DF	27	27
R^2	0.981	0.981
SSE	8.095	7.508
MSE	0.300	0.278
RMSE	0.548	0.527

Table 6.10: Goodness of fit statistics of variable a* before and after aging.

Model Parameter	Before Aging		After Aging	
	Value	Standard error	Value	Standard error
pr1	1.833	0.305	1.300	0.294
pr2	86.893	44.222	61.157	42.586
pr3	-4.510	32.013	-1.331	30.829
pr4	-21.894	40.726	-29.332	39.220
pr5	757.812	129.396	704.454	124.611
pr6	-3560.507	2493.787	-2285.212	2401.570
pr7	1168.478	1133.815	1093.272	1091.888
pr8	-1041.124	2243.850	-600.918	2160.876
pr9	-10935.278	20856.513	-8234.903	20085.270
pr10	42967.686	43924.646	24424.719	42300.378
pr11	-16048.511	13445.541	-14978.393	12948.345
pr12	35261.536	39860.112	27586.822	38386.144
pr13	-214899.883	879061.025	-278807.686	846554.645
pr14	-154765.079	232701.999	-69708.279	224097.023
pr15	62005.125	47764.132	57724.971	45997.885
pr16	-232676.936	219456.128	-192951.940	211340.964
pr17	3544913.333	8507883.963	4044325.849	8193274.964

Table 6.11: Model parameters of variable a* before and after aging.

Sample	Before Aging			After Aging		
	a*	Pred(a*)	Residuals	a*	Pred(a*)	Residuals
45	3.771	4.296	-0.526	3.101	3.515	-0.414
46	5.118	5.121	-0.004	4.261	4.427	-0.165
47	5.858	5.721	0.137	5.108	5.102	0.006
48	2.883	3.386	-0.504	2.109	2.621	-0.512
49	2.471	2.611	-0.140	1.610	1.938	-0.328

Table 6.12: Predictions and residuals of variable a* before and after aging.

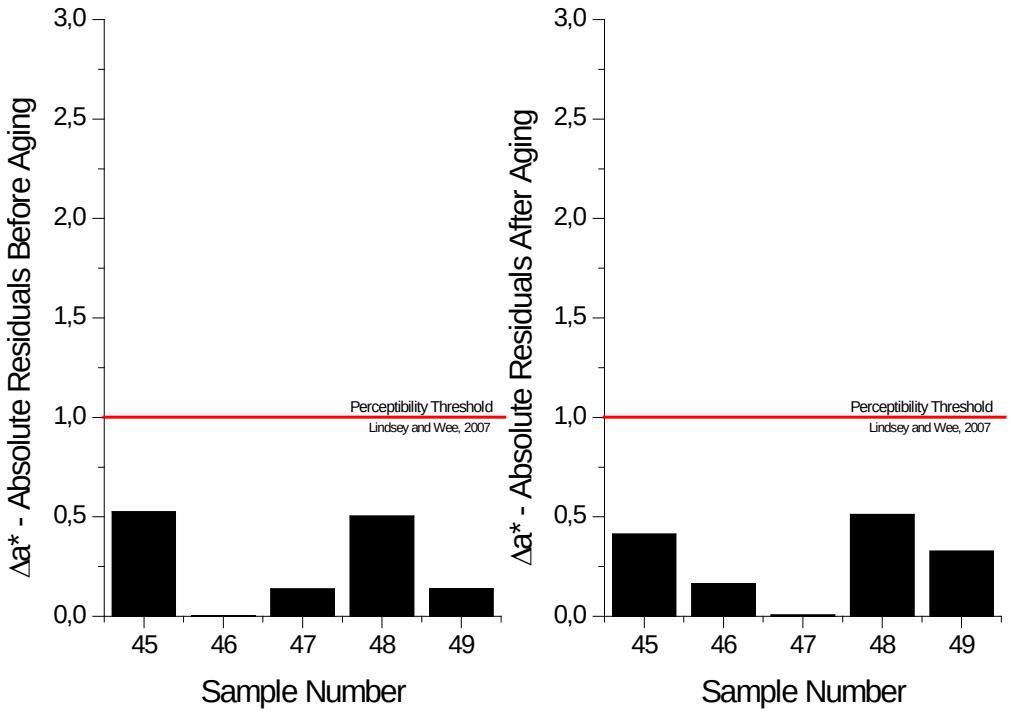

Figure 6.8: Δa* - Absolute Residual values of variable a* before aging and after aging.

Figure 6.9 show the predicted values against the measured values for the a* colorimetric coordinate before and after the artificial aging procedure was applied, both for the Training Group (Active) and the Validation Group. Contrary to what occurs in the case of the L* coordinate, both before and after the aging, the multiple nonlinear regression model tended to overestimate the values of the variable for the five samples included in the Testing Group. Also, it seems that there is an inverse correlation between the value of the residual and the value of the variable. Again, for higher values of a* the relationship between the predicted and the measured value approaches 1, and, only for the highest a* value, the predicted value is smaller than the measured one.

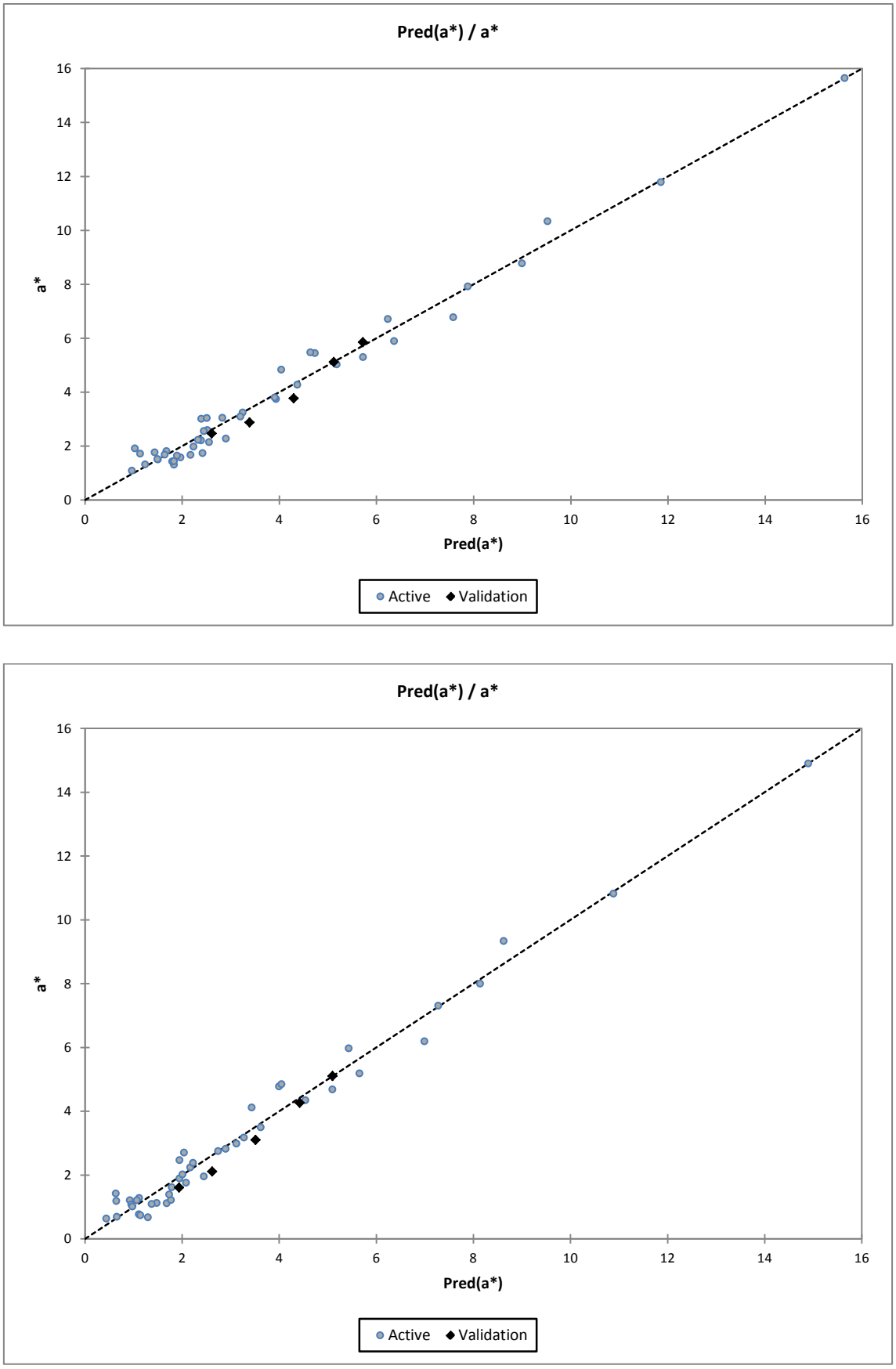

Figure 6.9: Predicted against measured values for the variable a* before aging (top) and after aging (bottom)

*6.3.1.3 Multiple Nonlinear Regression of chromatic coordinate b**

Table 6.13 shows the values of the statistical parameters describing the goodness of fit for the b* variable. The Coefficient of Determination (R^2) presented very high values both before and after aging (0.961 and 0.951 respectively), although slightly lower than the values found for the L* and a* chromatic coordinates. In the case of the RMSE parameter, we registered a value of 0.950 before aging and 0.970 after aging. One of the main advantages when using R^2 is that it provides a measure of how well relative trend magnitudes are captured and it provides a direct interpretation of the variance accounted for. In our case, the predictive model is able to explain more than 95% of the variance within the data, which is an excellent indicator for the adequacy of the built model to predict the values within the data set.

The parameters, together with their corresponding Standard Errors, describing the two models designed to predict b* values both before and after aging, are schematically presented in Table 6.14.

Table 6.15 shows both measured and predicted values for the variable b* before and after artificial aging, as well as the corresponding Residuals. In the case of the variable b*, the Residuals obtained where within the 0.207 – 1.039 range for samples before aging and within the 0.172 – 1.142 for samples after aging. These results can be easily analyzed by comparing these values with the 50:50% threshold level established by Lindsey and Wee for the b* coordinate, which has a value of Δb*=2.6 units (Lindsey and Wee, 2007). In our case, for all studied samples, the values of the residuals are considerably lower than the threshold value, and this, together with the good values of R^2 and RMSE, are encouraging us to state that the model presents good accuracy.

b*	Before Aging	After Aging
Observations	44	44
DF	27	27
R^2	0.961	0.951
SSE	24.344	25.418
MSE	0.902	0.941
RMSE	0.950	0.970

Table 6.13: Goodness of fit statistics of variable b* before and after aging.

Model Parameter	Before Aging		After Aging	
	Value	Standard error	Value	Standard error
pr1	0.967	0.530	2.872	0.541
pr2	60.386	76.686	34.418	78.360
pr3	186.244	55.515	177.096	56.726
pr4	66.861	70.624	88.696	72.165
pr5	-493.516	224.390	-487.099	229.287
pr6	5685.161	4324.551	5935.811	4418.932
pr7	-1011.330	1966.183	-1152.106	2009.094
pr8	-3584.263	3891.128	-4770.929	3976.049
pr9	67965.190	36167.908	69217.455	36957.254
pr10	-108241.773	76171.054	-110084.473	77833.449
pr11	6533.791	23316.319	8270.455	23825.186
pr12	65171.282	69122.622	84748.936	70631.188
pr13	-2355487.161	1524406.238	-2451163.539	1557675.629
pr14	567951.124	403535.556	573558.717	412342.514
pr15	-28501.234	82829.222	-33065.224	84636.927
pr16	-375245.625	380565.491	-476181.900	388871.139
pr17	20968810.789	14753778.201	22013752.406	15075771.901

Table 6.14: Model parameters of variable b* before and after aging.

Sample	Before Aging			After Aging		
	b*	Pred(b*)	Residuals	b*	Pred(b*)	Residuals
45	7.389	6.811	0.578	8.737	8.176	0.561
46	10.720	10.513	0.207	11.700	11.528	0.172
47	12.177	13.109	-0.932	12.907	13.847	-0.940
48	4.840	3.801	1.039	6.577	5.435	1.142
49	2.413	2.108	0.305	4.741	3.898	0.843

Table 6.15: Predictions and residuals of variable a* before and after aging.

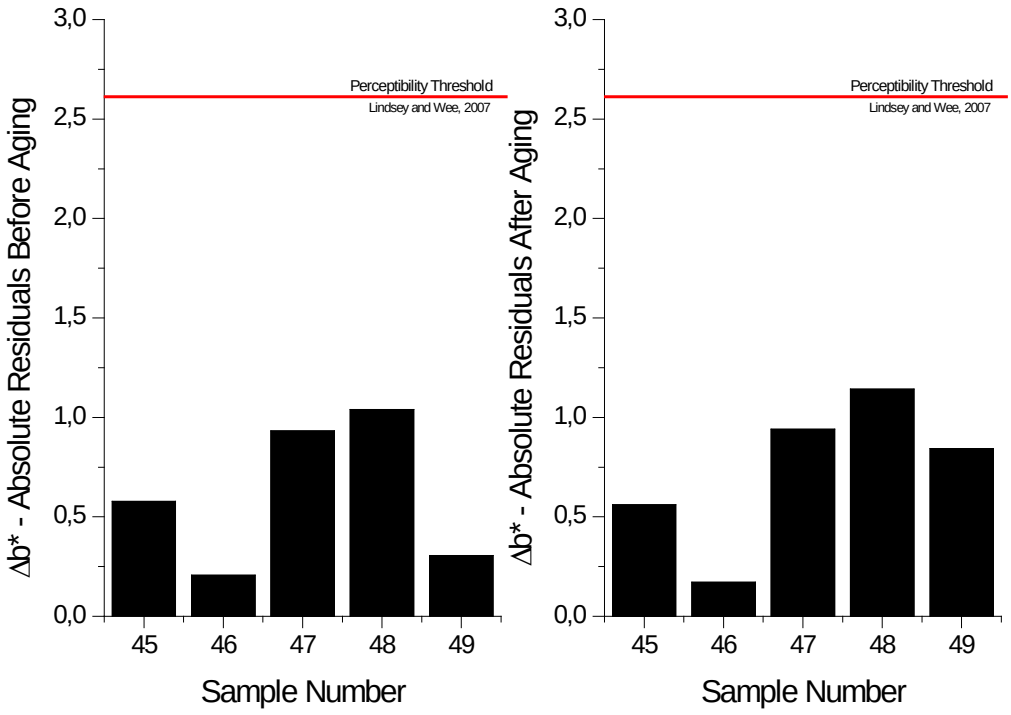

Figure 6.10.: Δb* - Absolute Residual Values of variable b* before and after aging.

Figure 6.10 shows the absolute values of the differences between the predicted and the measured values (Δb* - Absolute Residual Value), as well as the level of perceptibility threshold for this chromatic coordinate.

In Figure 6.11 are plotted the predicted values against the measured values of the b* colorimetric coordinate before and after aging, both for the Training Group (Active) and the Validation Group. The ratio between the predicted and real values is in all cases very close to unit. As the case of lightness, for the five samples included in the Validation Group, both before and after aging, for lower values of b*, the model is constantly underestimating the variable, while for higher values of b* it seems that an inflection occurs in the trend of the model, providing higher predicted values (overestimating).

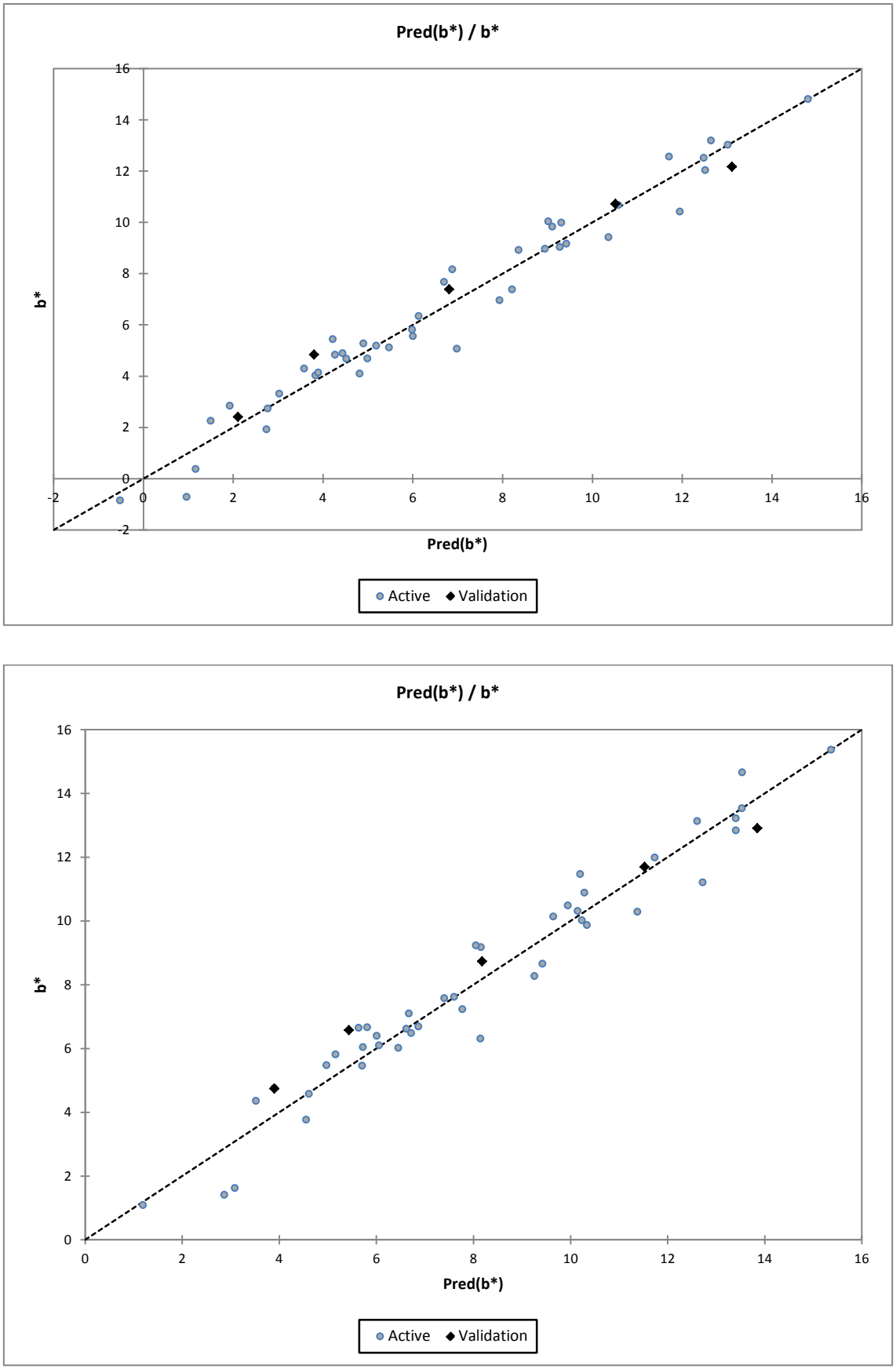

Figure 6.11: Predicted against measured values for the variable b* before aging (top) and after aging (bottom).

6.3.1.4 Total Color Differences between the predicted and the measured values

In order to broaden the perspective on the proper functioning of the developed predictive models, the total color differences (in terms of ΔE_{00} and ΔE^*_{ab}) between the predicted and the measured values (both before and after aging) for the 5 samples included in the Validation Group, were calculated. The results are plotted in Figure 6.12 (before aging) and in Figure 6.13 (after aging).

According to previous results obtained in our laboratory and discussed in Chapter 3 of this PhD Thesis (Ghinea et al., 2010), the perceptibility threshold level for dental ceramics were established as ΔE_{00}=1.25 and ΔE^*_{ab}=1.74 units, while the acceptability levels were set as ΔE_{00}=2.23 and ΔE^*_{ab}=3.48 units.

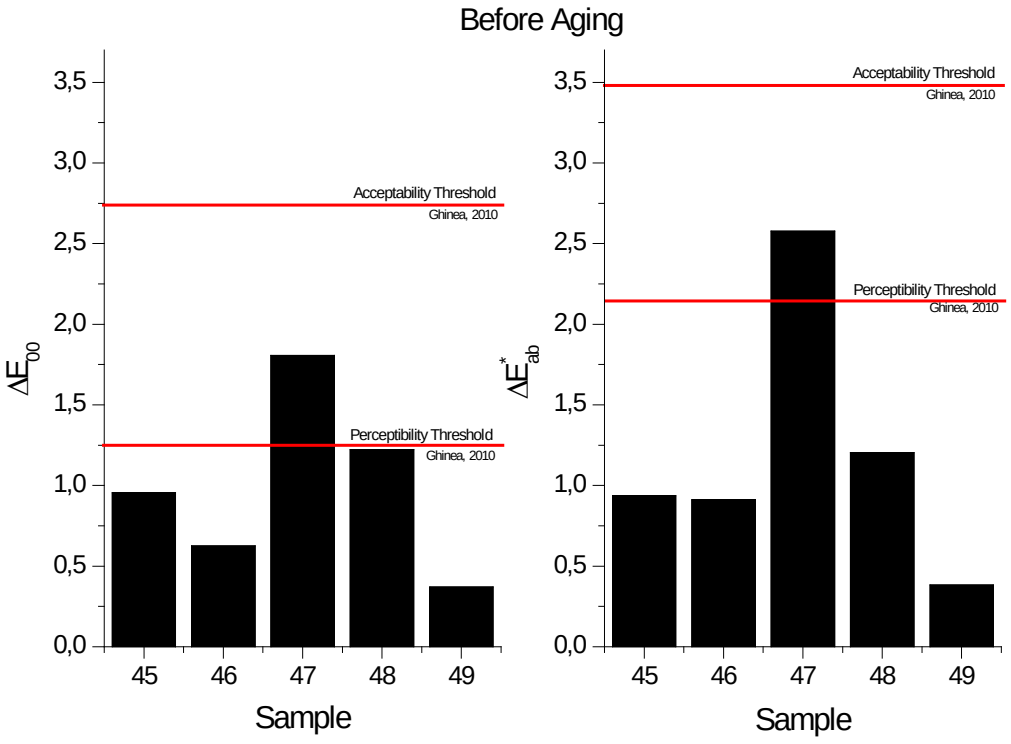

Figure 6.12: Total color differences in terms of ΔE_{00} (left) and ΔE_{ab} (right) between the predicted and measured values for samples in the Validation Group before aging.

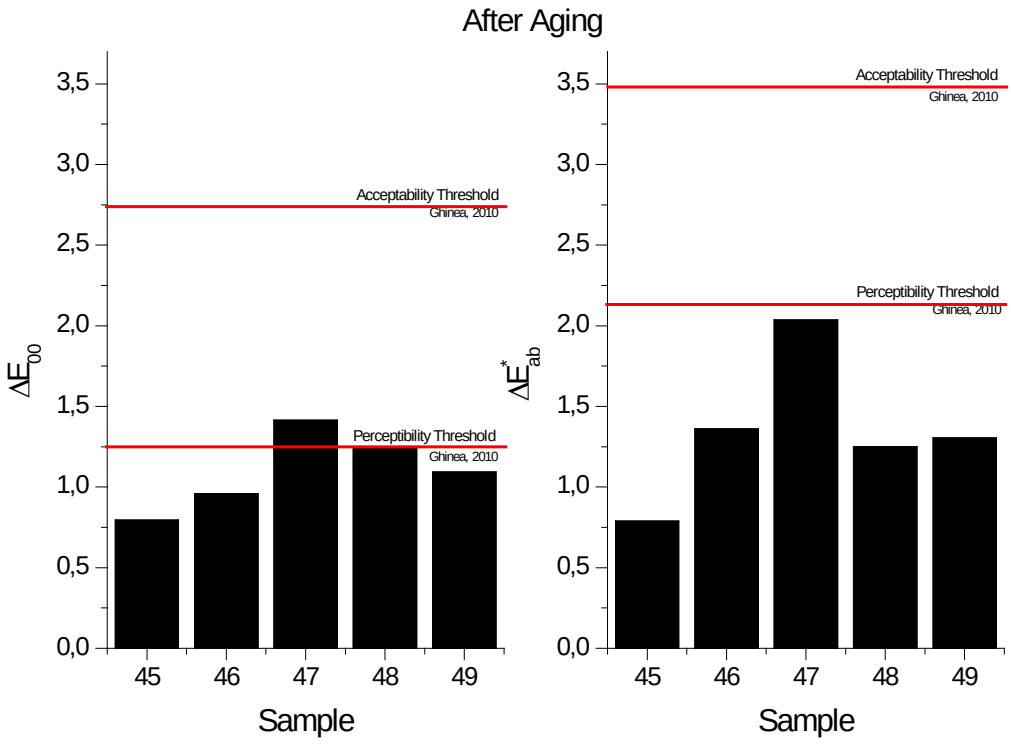

Figure 6.13: Total color differences in terms of ΔE_{00} (left) and ΔE_{ab} (right) between the predicted and measured values for samples in the Validation Group after aging.

When we studied the sample before aging, the differences between the predicted and real values were lower than the acceptability threshold, and in 80% of the cases, were even lower than the perceptibility threshold, independently of the color difference formula used to perform the comparisons. For samples after aging, the developed model worked properly, since in 100% of the cases, the color differences between the predicted and real values were below the acceptability threshold, independently of the color difference formula used. Moreover, in the case of the ΔE^*_{ab}, all differences were found to be smaller than the perceptibility threshold while when the ΔE_{00} formula is employed, 80% of the samples included in the validation group exhibited color differences which cannot be perceived by the human eye in a clinical situation.

The absolute values of the differences in lightness (ΔL'), chroma (ΔC') and hue (ΔH') between the predicted and the measured values for the five samples included in the validation group (both before and after aging) are presented in Figure 6.14.

In Chapter 4 of this Phd Thesis, the visual 50:50% acceptability thresholds for lightness, chroma and hue were determined using dental ceramics, a 30-observer panel evaluating three subsets of ceramic samples and the TSK Fuzzy Approximation as fitting procedure (Perez et al., 2011). According to our results, the levels of acceptability thresholds for dentistry were established as ΔL'=2.92, ΔC'=2.52 and ΔH'=1.90 units. The differences we found between the predicted and the measured values are smaller than the acceptability thresholds for all the studied colorimetric dimensions (lightness, chroma and hue), independently if the samples are analyzed before or after the aging procedure was applied.

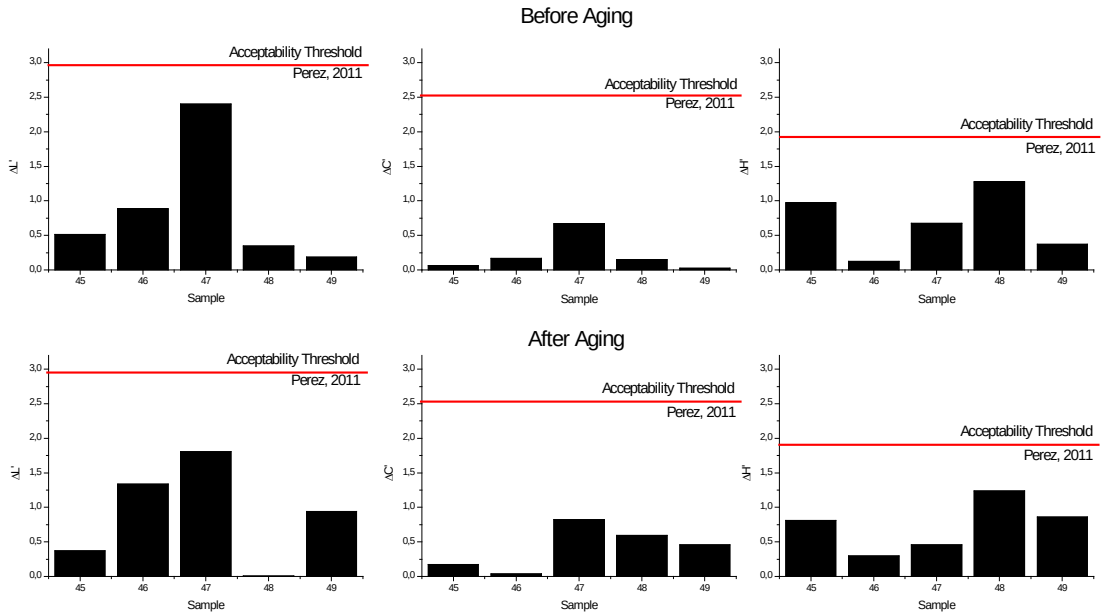

Figure 6.14: Absolute values of the differences in lightness (ΔL'), chroma (ΔC') and hue (ΔH') between predicted and measured values for the Validation Group before aging (top) and after aging (bottom).

6.3.2 PREDICTION OF REFLECTANCE FACTORS IN THE 380nm-780nm INTERVAL FROM % PIGMENT WITHIN THE FORMULATION

The reflectance spectra of all 49 samples was measured between 380nm and 780nm at 2nm steps, as described in the Materials and Methods section. Similar to the previous sections, the samples were divided into a Training Group containing 44 samples and a Validation Group, containing 5 samples.

As performed in the case of modeling the colorimetric coordinates L*a*b*, as a prior step to the built of the predictive model, a study of the correlation between the input variables (percentage of each type of Pigment used - %P1, %P2, %P3 and %P4) and the values of the output variables (each reflectance factor between 380nm-780nm at 2nm step, both before and after artificial aging) was carried out. The obtained results are graphically represented in Figure 6.15 and Figure 6.16, for samples prior to artificial aging and after the artificial aging procedure was applied, respectively.

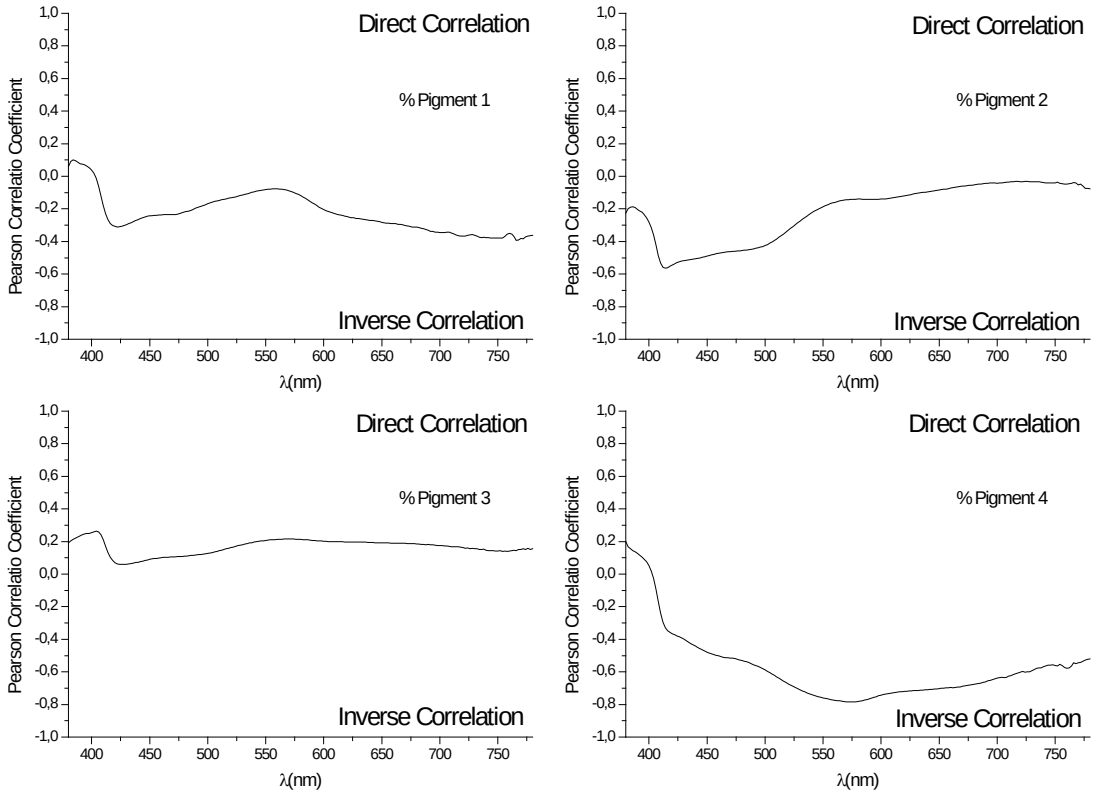

Figure 6.15: Pearson Correlation Coefficients between % Pigment and 380nm-780nm Reflectance Factors before aging.

The correlation between variables, when biomaterials are studied, is considered to be strongly direct if the value of the Pearson Coefficient exceeds 0.7 and is considered to be strongly inverse if the value of the Pearson Coefficient is lower than -0.7. As it can be observed in Figure 6.15, for the 5 samples included in the testing group (validation group) before aging, there is a strong inverse correlation between the quantity of the fourth Pigment (%P4) and reflectance factors of wavelengths between 525nm-650nm. This implies that higher quantities of Pigment 4 within the mixture of the experimental resin composite will decrease the values of the reflectance factors between the specified interval, affecting the lightness value of the sample and generating an orange-reddish color shift. These results are supported by the findings of the previous study of correlation between quantities of Pigment in the mixture and colorimetric coordinates L*a*b*, where it was established that the %P4 is strongly inversely correlated with the value of L* and directly correlated with the value of a*.

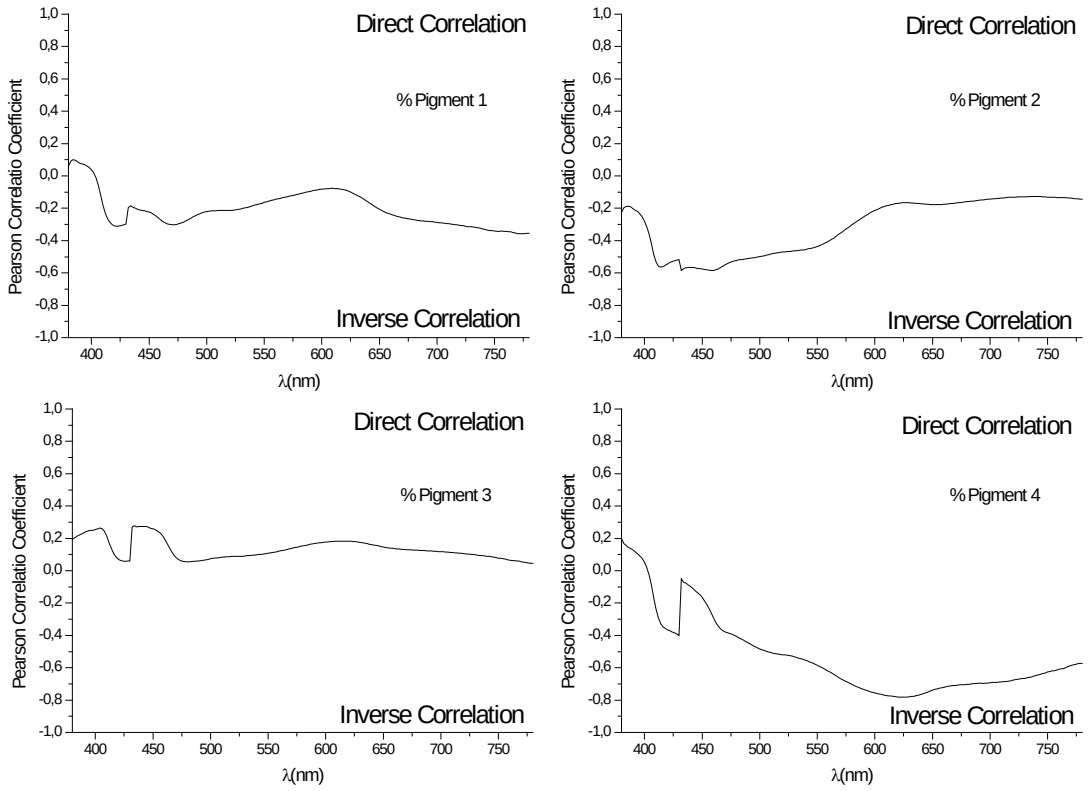

Figure 6.16: Pearson Correlation Coefficients between % Pigment and 380nm-780nm Reflectance Factors after aging.

For samples after aging (Figure 6.16) the only strong correlation observed is between the percentage of Pigment 4 and the values of the reflectance factors for wavelengths between 575nm-725nm. Again, as previously described, this correlation is supposed to lower the lightness value of the sample as well as generate more pronounced reddish effect on the overall appearance of the experimental resin composite. This behavior was already pointed out when, in the previous chapter, the correlation matrix between the quantities of Pigments within the mixture and the L*a*b* values of the samples after aging, was studied.

The goodness of fit, in terms of R^2 and the Root Mean Square Error (RMSE) for the predictive models of the Reflectance Factors for wavelengths between 380nm-780nm, both before and after the artificial aging procedure was carried out, is displayed on Figure 6.17.

Numerical measures of goodness of fit are divided into two type measures: measures of deviation from the real (measured) values and measures of how well the trend relative magnitudes are predicted. If only one type of these measurements is used, only one of these two types of information is being captured, and that it is why several researchers recommend the use of a combination of R^2 for trend relative magnitude and RMSE for deviation from exact data location (Schunn, 2005). We found high values (>0.7) of the Coefficient of Determination for the predictive models of the Reflectance Factors for wavelengths higher than 425nm, both before and after aging. However, it seems that the predictive model works best for wavelengths between 425nm and 600nm, since in this interval the R^2 values are higher than 0.9.

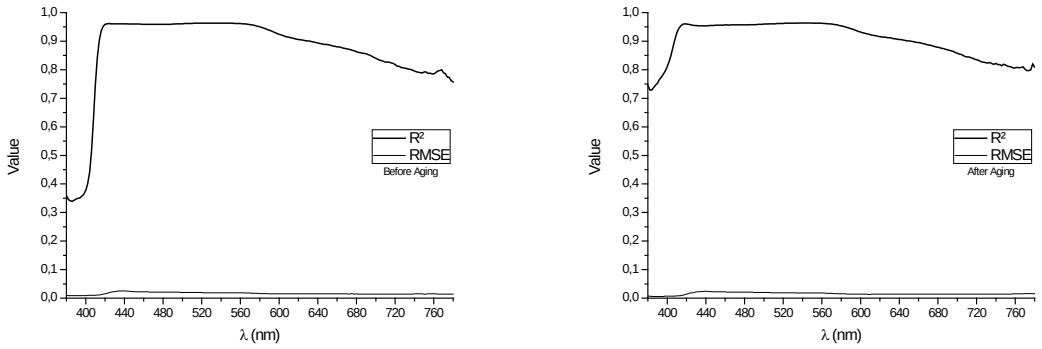

Figure 6.17: Goodness of fit (in terms of R^2 and RMSE) for the Reflectance Factors (380nm-780nm) for samples before aging (left) and after aging (right).

This mean that future works should be focused on improving the MNLR models in order to obtain better performance for large wavelengths. It should be noted that, if we assess the quality of the predictive model on the exclusive basis of the value of R^2, the model performs better for aged samples, since the values obtained for the Coefficient of Determination are slightly higher. Both before and after aging, the RMSE values are very low, in accordance to the interval of the studied variable (in this case, the Reflectance Factors between 380nm-780nm). All these results support the quality of the Multiple Nonlinear Regression Predictive model designed and, together with the spectral and colorimetric results presented hereafter, serve to ensure the proper development of the method.

One of the best methods for assessing the accuracy of point predictions is to use overlay scatter plots and overlay line graphs. In these graphical forms, the model and data are overlaid on the same graph, allowing a direct comparison of the real (measured) data and the predicted values. The reflectance spectrum of the five samples included in the Validation Group, as measured with the PR-670 Spectrorradiometer and as predicted with the Multiple Nonlinear Regression model, both before and after aging, are presented in Figure 6.18 – 6.22.

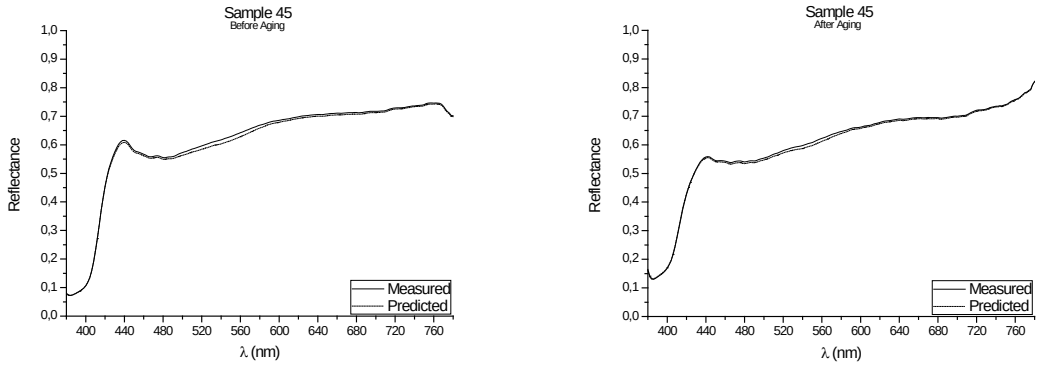

Figure 6.18: Real (measured) and Predicted spectral reflectance of Sample 45 between 380nm-780nm before aging (left) and after aging (right).

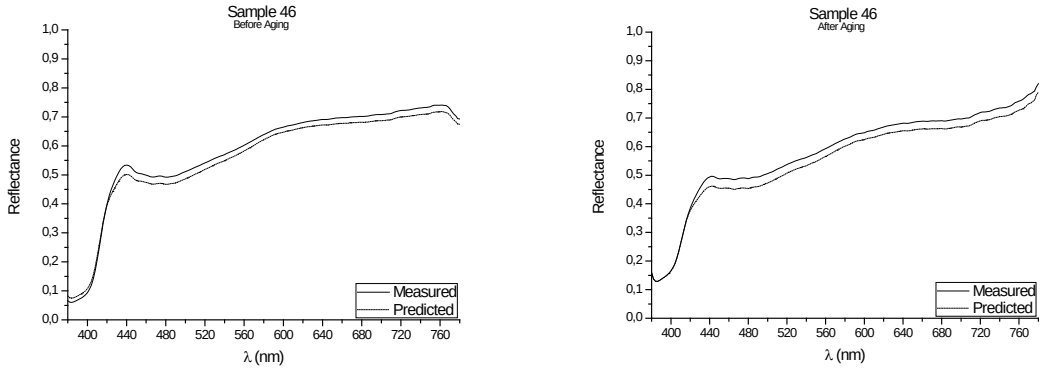

Figure 6.19: Real (measured) and Predicted spectral reflectance of Sample 46 between 380nm-780nm before aging (left) and after aging (right).

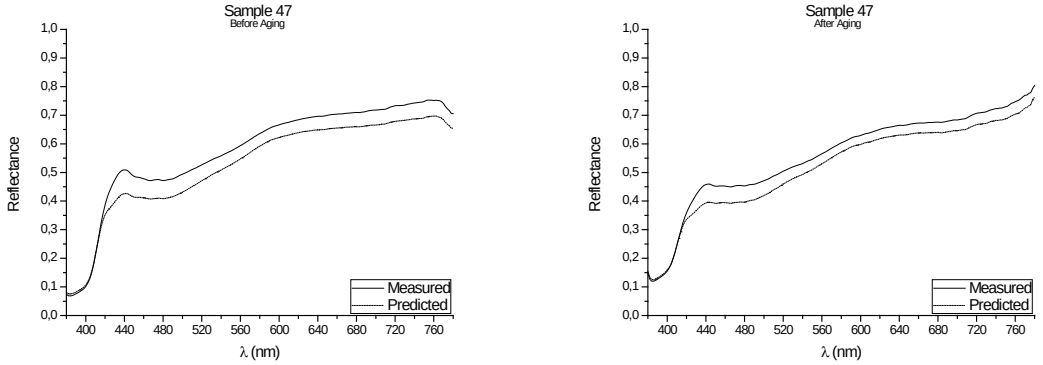

Figure 6.20: Real (measured) and Predicted spectral reflectance of Sample 47 between 380nm-780nm before aging (left) and after aging (right).

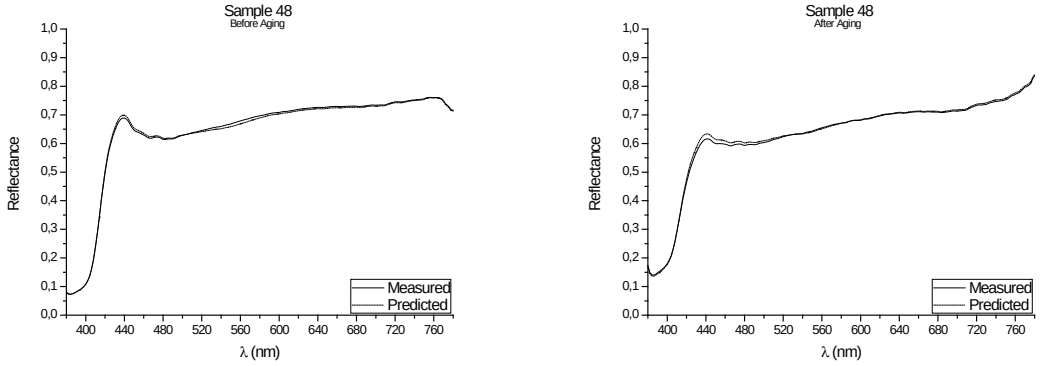

Figure 6.21: Real (measured) and Predicted spectral reflectance of Sample 48 between 380nm-780nm before aging (left) and after aging (right).

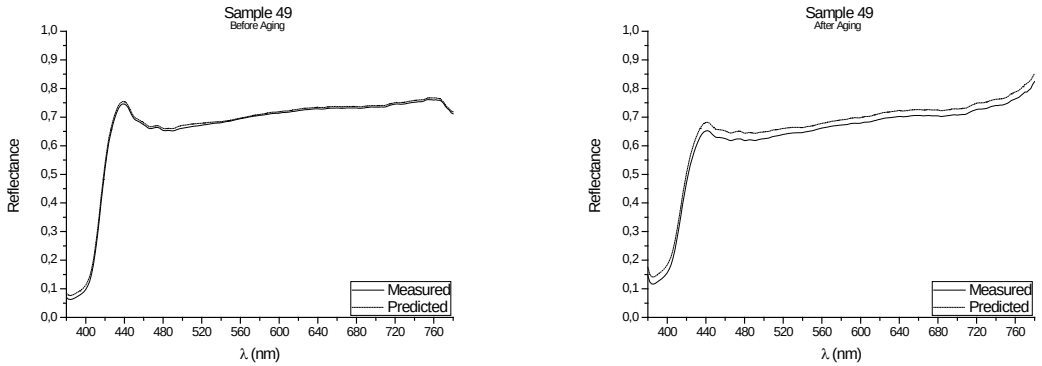

Figure 6.22.: Real (measured) and Predicted spectral reflectance of Sample 49 between 380nm-780nm a.) Before aging and b.) After aging.

Visual displays of goodness of fit are useful for a rough estimate of the degree of fit and for indicating where the fits are most problematic. Visual displays are also useful for diagnosing a variety of types of problems (e.g., systematic biases in model predictions). Noteworthy, the human visual system is not particularly accurate in assessing small to moderate differences in the fits of model to data. Our visual system is also subject to many visual complications that can produce systematic distortions in the visual estimates of the quality of a fit (Schunn, 2005). However, as it can be observed in Figures 6.18-6.22, the quality of the fit is excellent for almost the entire spectrum, providing accurate estimates of the Reflectance Factors for all wavelengths.

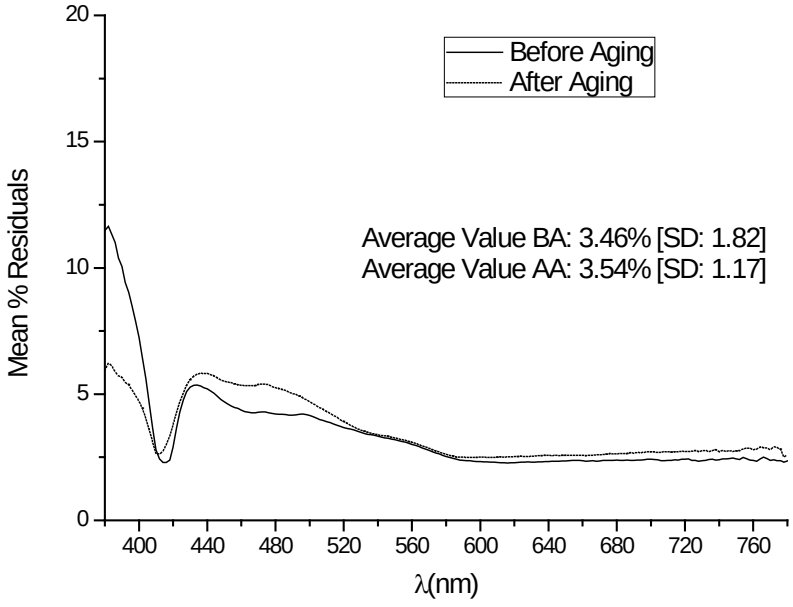

Figure 6.23: Mean %Residuals of all samples of the Validation Group, before and after aging, in the 380nm-780nm interval.

In order to assess the overall quality of the prediction capacity of the proposed models, the mean value over the 5 samples (relative to the value of the variable – Reflectance Factor) along the 380nm-780nm interval was calculated. The results for samples before and after the aging procedure was applied are schematically shown in Figure 6.23. For samples before aging, the average value of the prediction error of the model was 3.46% (SD: 1.82), showing higher values for shorter wavelengths and considerably lower values for longer wavelengths In the case of the samples after aging, the average value of the prediction error was 3.54% (SD:1.17), exhibiting, as the case of samples before aging, lower error for longer wavelengths. The high errors obtained for short wavelengths are probably caused by the instability of the measuring system (the spectrorradiometer) which presents variability in the measured data for wavelengths lower than 400nm. This variability is expected to affect the quality of the predictive model, since no clear pattern in the input data can be established, so the provided output variables are distant from the measured ones.

6.3.2.1. Colorimetric coordinates as calculated from the Reflectance Factors

L*a*b* colorimetric coordinates were calculated according to the CIE D65 standard illuminant and CIE 2° Standard Colorimetric Observer, from the measured and predicted reflectance spectra.

The measured (real values) as well as the predicted values with their corresponding residuals for all three studied chromatic coordinates (L*, a* and b*) are displayed in Table 6.16, for samples before aging, and in Table 6.17 for samples after aging.

In the case of the samples before aging, for the L* chromatic coordinate the differences between the measured and the predicted values ranged between -0.232 and 2.811 before aging and between -0.024 and 2.212 for samples after aging, with the smallest difference found for the samples which exhibited the highest lightness (samples 45, 48 and 49). In this case, the Multiple Nonlinear Regression model tends to underestimate the value of the variable, similar to the behavior registered when the chromatic coordinates were directly predicted.

Sample	Before Aging								
	L*			a*			b*		
	Meas	Pred	Residual	Meas	Pred	Residual	Meas	Pred	Residual
45	83.836	83.282	0.554	3.771	4.362	-0.591	7.389	6.990	0.399
46	81.704	80.593	1.111	5.118	5.367	-0.249	10.720	11.490	-0.770
47	81.272	78.461	2.811	5.858	6.120	-0.262	12.177	15.074	-2.897
48	85.759	85.460	0.299	2.883	3.343	-0.460	4.840	3.751	1.089
49	86.609	86.841	-0.232	2.471	2.541	-0.070	2.413	2.086	0.327

Table 6.16: L* a* b* values as calculated from reflectance spectrum for real (measured) and predicted values and corresponding residuals for samples before aging.

Sample	After Aging								
	L*			a*			b*		
	Meas	Pred	Residual	Meas	Pred	Residual	Meas	Pred	Residual
45	82.784	82.373	0.411	3.101	3.561	-0.460	8.737	8.418	0.319
46	81.185	79.633	1.552	4.261	4.639	-0.378	11.700	12.492	-0.792
47	79.663	77.451	2.212	5.108	5.477	-0.369	12.907	15.694	-2.787
48	84.525	84.549	-0.024	2.109	2.580	-0.471	6.577	5.444	1.133
49	84.916	85.891	-0.975	1.610	1.881	-0.271	4.741	3.890	0.851

Table 6.17: L* a* b* values as calculated from reflectance spectrum for real (measured) and predicted values and corresponding residuals for samples after aging.

Among the three chromatic coordinates studied, for all the five samples included in the Validation Group, the a* variable showed the smallest residuals, with absolute residual values smaller than 0.6 in all cases. Although this outcome may be very promising, the magnitude of the studied variable it must be taken into account, since the a* chromatic coordinates vary within a scale of 2-6 units, while the b* coordinate can reach double superior values and the L* coordinate values are within the 80-85 units range. Therefore, obtaining very low values of residuals for this particular variable it is not so surprising, and the differences between the predicted and the measured values must be evaluated from a more objective point of view, such as comparisons with the chromatic perceptibility thresholds in dentistry. In the case of the yellow-blue axis of the color space (b*), the predicted values matched very closely the measured ones. The smallest residual registered was in the case of the Sample 45 (0.319) while the biggest one was registered in the case of the Sample 47 (-2.787).

In Figure 6.24 are plotted the absolute values of the Residuals for the L* variable for samples both before and after aging. Similarly, the absolute values of the Residuals for the a* variable for samples both before and after aging are shown in Figure 6.25, while the absolute values of the Residuals for the b* variable for samples both before and after aging are presented in Figure 6.26.

As pointed out in the previous section, in a study on the perceptibility and acceptability of tooth color differences using computer-generated pairs of teeth with simulated gingival displayed on a calibrated monitor, Lindsey and Wee (Lindsey and Wee, 2007) established that $\Delta L^*=1.0$, $\Delta a^*=1.0$ and $\Delta b^*=2.6$ units are considered as 50:50% perceptibility threshold for the human eye. In our study, the differences between the predicted and the measured values of the chromatic coordinates exceeded the lightness threshold for 40% of the studied samples (both before and after aging). For the b* chromatic coordinate, 80% of the samples presented differences which were unable to be perceived by a human observer with normal color vision, while for the red-green axis (a* coordinate) all the studied samples exhibited differences bellow the perceptibility threshold for this coordinate, independently if the sample were analyzed before or after the aging procedure was applied.

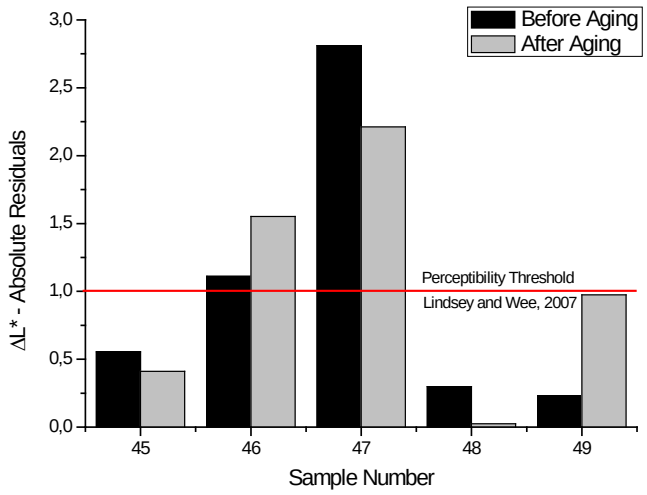

Figure 6.24: ΔL* - Absolute Residual Values of variable L* before and after aging.

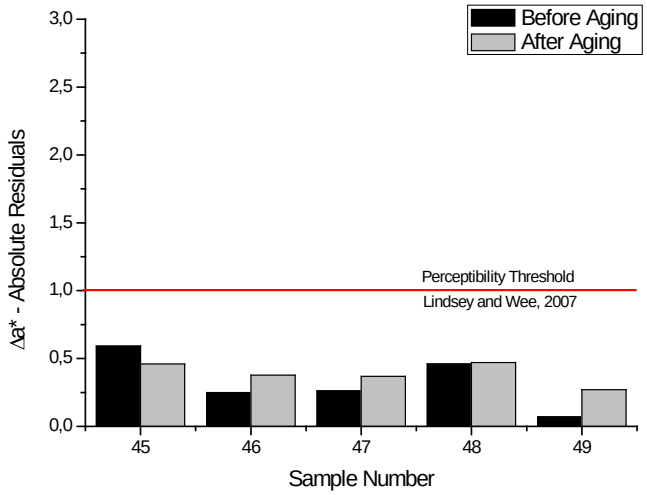

Figure 6.25: Δa* - Absolute Residual Values of variable a* before and after aging.

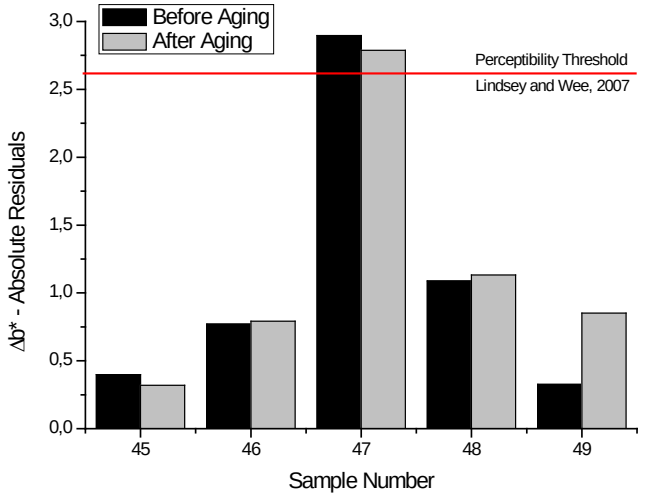

Figure 6.26: Δb* - Absolute Residual Values of variable b* before and after aging.

6.3.2.2 Total Color Differences between the predicted and the measured values

The study on the accuracy of the MNLR predictive models can be extended, apart from the calculation of the chromatic coordinates, with the calculation of the total color differences (in terms of ΔE_{00} and ΔE^*_{ab}), between the predicted and measured values of the chromatic coordinates, and consequently evaluate them through comparisons with the perceptibility and acceptability thresholds presented and discussed in Chapter 3 of this Thesis.

The values of the total color differences (in terms of ΔE_{00} and ΔE^*_{ab}) between the predicted and the measured values for the 5 samples included in the Validation Group are plotted in Figure 6.27 (before aging) and in Figure 6.28 (after aging).

In the case of the sample before aging, for four of the five experimental dental resin composites studied, the differences between the measured and predicted values were lower than both the acceptability and the perceptibility threshold, independently of the color difference formula used to compute it.

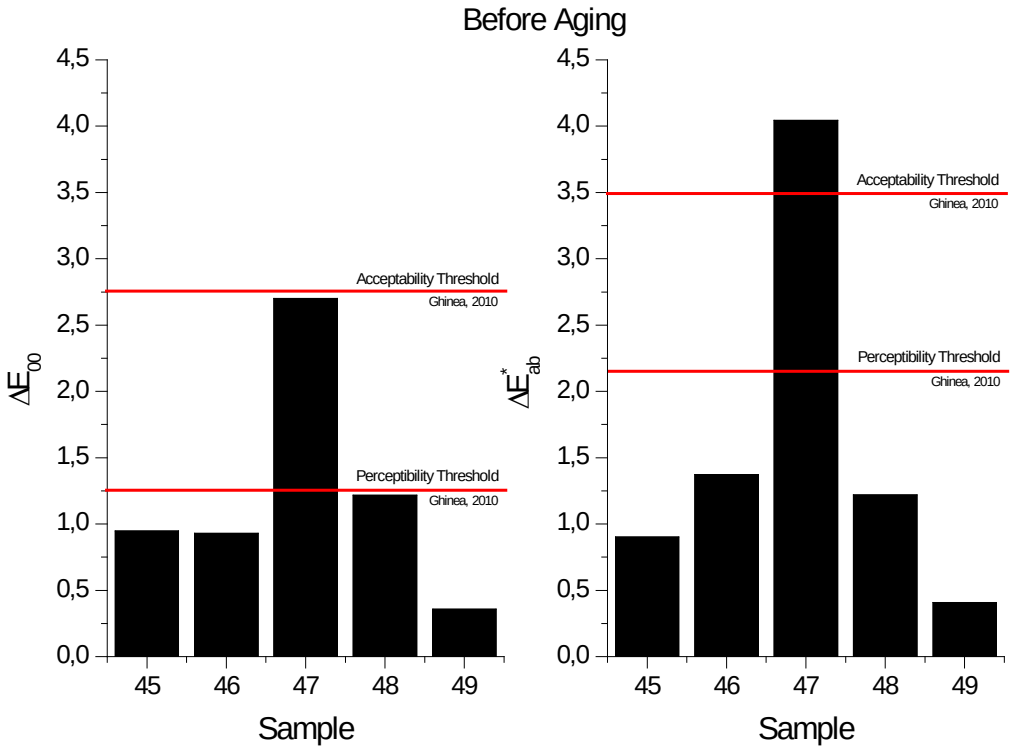

Figure 6.27: Total color differences in terms of ΔE_{00} (left) and ΔE_{ab} (right) between the predicted and measured values for samples in the Validation Group before aging.

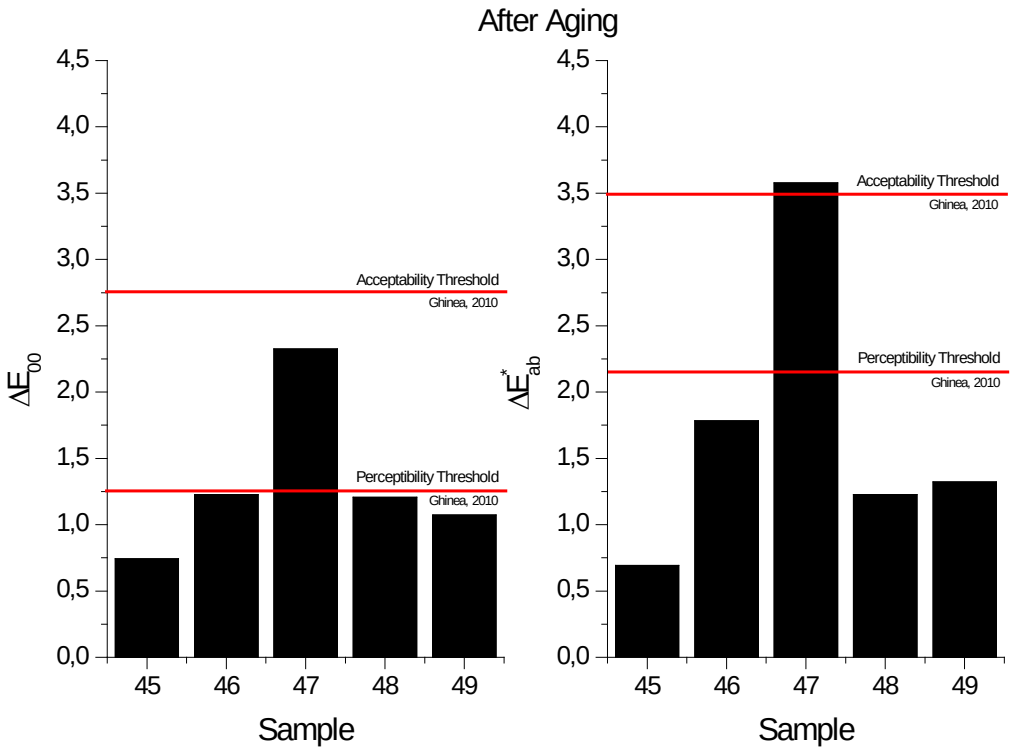

Figure 6.28: Total color differences in terms of ΔE_{00} (left) and ΔE_{ab} (right) between the predicted and measured values for samples in the Validation Group after aging

In the case of Sample 47, the differences found were higher than both thresholds, probably due to the high discrepancies between the predicted and measured value of lightness (L*). After the artificial aging procedure was applied, if the differences between the predicted and measured values are computed with the newest ΔE_{00} formula, all values fall within the acceptability threshold, and in 75% of the studied cases, the differences are even smaller than the perceptibility threshold. If, instead, the CIE1976 total color difference formula is used (ΔE^*_{ab}), for Sample 47, similar to what happens before aging, the value of the difference is higher than both thresholds, while for the other 4 samples included in the Validation Group, the calculated total color differences are smaller than both perceptibility and acceptability thresholds.

The absolute values of the differences in lightness (ΔL'), chroma (ΔC') and hue (ΔH') between the predicted and the measured values for the five samples included in the validation group (both before and after aging) are presented in Figure 6.29.

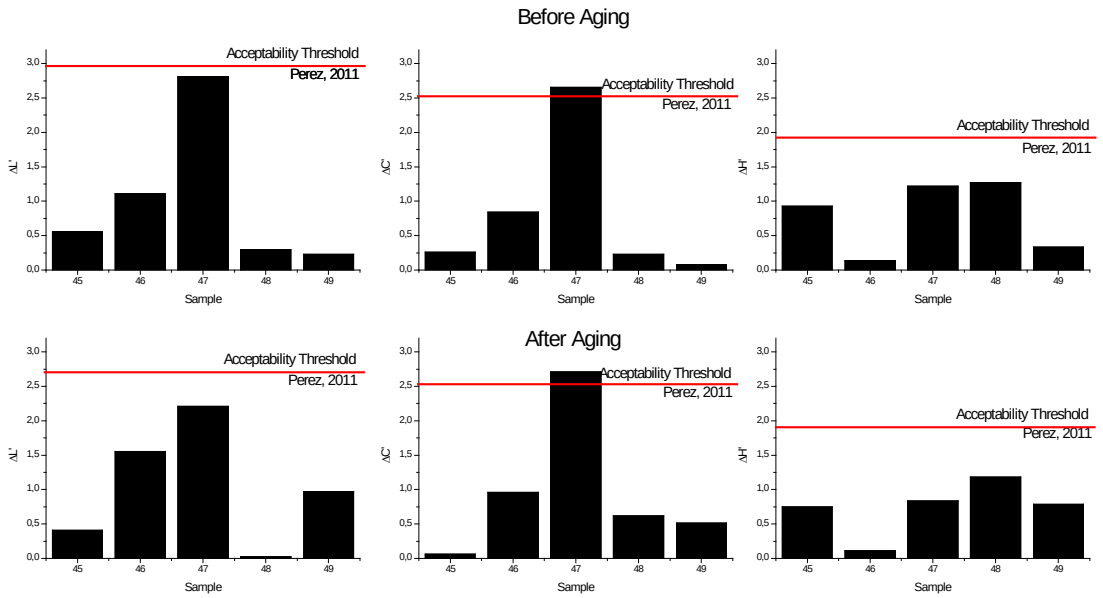

Figure 6.29: Absolute values of the differences in lightness (ΔL'), chroma (ΔC') and hue (ΔH') between predicted and measured values for the Validation Group before aging (top) and after aging (bottom).

As pointed out in Chapter 4, the visual 50:50% acceptability thresholds for lightness, chroma and hue in dentistry were established as ΔL'=2.92, ΔC'=2.52 and ΔH'=1.90 units (Perez et al., 2011), The differences we found between the predicted and the measured values are smaller than the acceptability thresholds for lightness and hue, independently if the samples are analyzed before or after the aging procedure was applied. In the case of chroma differences (ΔC'), for one of the samples included in the Validation Group, the computed difference exceeded the acceptability threshold, while all the other four samples exhibited values considerably lower than the threshold.

At this point, If we make a comparative analysis of the performance of the two proposed prediction models, based exclusively on the values of the residuals, it may be concluded that using a nonlinear regression model to predict directly the L*a*b* values provides better and more reliable results, with smaller prediction errors (the estimated values are closer to the real measured values). However, one should not underestimate the importance of the exact knowledge of the reflectance spectrum of the samples to be analyzed, since by knowing the reflectance factor values for any wavelength within the visible spectrum (380n-780nm) we are able to calculate the values of the chromaticity coordinates under any illuminant (not only the daylight simulator – CIE D65) and for any CIE Colorimetric Standard Observer. This can provide

priceless additional information, and before deciding which model should be used, the researcher must clearly establish the objective of the study. If interested exclusively in simulating typical experimental set-up for dental applications (daylight illumination and small samples) it can go directly to design the direct predictive model for the L*a*b* values, since it provides the best adjustment in terms of measures of goodness of fit. However, if the study is intended to cover a more widely range of colorimetric coordinates under different Standard Illuminants and with different Standard Observers, it is advisable to design predictive models for reflectance factors at each wavelength, which will allow to make various calculations based on the equations provided by the International Commission on Illumination (CIE).

Several Multiple Nonlinear Regression predictive models have been developed, which achieved to accurately predict both the final color (in terms of the chromatic coordinates L*a*b*) and the reflectance spectrum of the manufactured experimental dental resin composites. These models are very helpful when, in a laboratory situation, the chromatic behavior of the samples needs to be controlled. In this study, we considered the pigments as the main responsible (not exclusive) of the final color of the composites, and therefore we centered the study on the influence of the four types of pigments on the final color of the experimental dental resin composites. The range of application of the proposed predictive models is narrow, since they are designed to work exclusively with the experimental dental resins developed in this study. It is necessary to expand the present work with further studies on multiple areas, such as varying the materials used for the formulation, varying amounts of both the organic matrix and the inorganic filler as well as the quantities of the other components used in the chemical formulation.

It would also be interesting to study more carefully the behavior of the different pigments, through a wider range of combinations between them and, on the other hand, other pigments can be used for colorimetric formulations. Another development path for future studies is an improved experimental design, in terms of better coverage of the dental color space with the manufactured samples. A proper distribution of the samples within the area of interest of the color space will allow the use of newer, more accurate and reliable predictive methods, such as Fuzzy Logic.

*6.3.3 PREDICTION OF % PIGMENT (%P1, %P2, %P3 AND %P4) WITHIN THE FORMULATION FROM L*a*b* COLORIMETRIC COORDINATES BEFORE AND AFTER AGING*

Although the predictive models designed in the previous sections present a great scientific interest, from a practical-clinical point of view, in dentistry, would be useful to have reliable algorithms that can accurately predict the exact chemical formulation of a dental resin composite in order for it to match the color or the reflectance spectrum of a dental structure.

In the first case, if we can reproduce the chromatic coordinates L*a*b* of a sample (calculated for an average human observer - 2° CIE Standard Observer - with normal color vision under typical daylight illumination – CIE D65 Illuminant) we will provide a metameric match for that sample (Fairchild, 2005). In the second case, if we are able to reproduce the complete reflectance spectrum (in terms of reflectance factors in the 380nm-780nm range) of sample, we will provide an isomeric (or identical) match for that sample. The isomeric color match holds for any observer and under any viewing conditions. It will be impossible to perceive a difference between them as long as they are viewed together under the same physical conditions. It is easy to understand that such a situation is of great interest in dentistry, since the color match is the starting point for any successful restoration. The final color of a restorative material is a function of its spectral reflectance, and matching the reflectance spectra of a restorative material with the reflectance spectra of the surrounding tooth structure will lead to highly desirable “perfect” tooth-restorative isomeric match, both illuminant and observer independent

In order to predict the relative quantities of the four types of pigments (%P1, %P2, %P3 and %P4) within the formulation from L*a*b* colorimetric coordinates (calculated according to the CIE D65 standard illuminant and CIE 2° Standard Colorimetric Observer) before and after aging, the samples were divided into a Training Group and Validation Group

As a prior step to the design of the predictive model, the correlation between the input variables of the model (the values of the L*a*b* colorimetric coordinates before

and after the artificial aging procedure) and the output variables of the model (percentage of each type of Pigment used - %P1, %P2, %P3 and %P4), was studied. The correlation matrix, showing the values obtained for the Pearson Correlation Coefficient is shown in Table 6.18.

We found a strong direct correlation (p=0.699 before aging and p=0.713 after aging) between the value of the b* chromatic coordinate and the percentage of the second pigment (% P2), which is translated into a more yellowish sample with higher quantities of this. Also, the lightness of the samples is inversely correlated with the quantity of the fourth pigment (% P4) (p=-0.763 before aging and p=-0.761 after aging), while the value of the CIE a* chromatic coordinate (p=0.827 before aging and p=0.832 after aging) is directly correlated with the quantity of this pigment (% P4). This implies that higher quantities of this type of pigment will generate a reddish effect on the overall final color of the experimental dental resin composite. The analysis of the correlation matrix between all studied variables showed no other relationship between the studied variables.

Table 6.19 shows the parameters describing the goodness of fit for the variables %P1, %P2, %P3 and %P4 as predicted from the values of L*a*b* before and after aging. For the relative quantity of the first pigment within the formulation (%P1), for samples before aging, only 49.5% of the total variance can be explained with the predictive model, while for the samples after aging the percentage of variance which can be explained by the model slightly increases up to 52.1%. These values registered for the Coefficient of Determination (R^2) are signaling an overall moderate performance of the Multiple Nonlinear Regression model. Also, the high values of the RMSE compared with the magnitude of the variable, are strengthening this idea. Still, a final assessment of the performance of the predictive model should not be done prior to comparing the differences between the predicted and the measured values with the real value of the variable. It has to be taken into account, that, in this situation, the space of the input variables is three-dimensional (L*, a*, b*) while the space of the output variables is four-dimensional, and this could affect the quality of the model.

Variables		Pearson correlation coefficient			
		%P1	%P2	%P3	%P4
L*	Before Aging	-0.117	-0.222	0.194	-0.763
	After Aging	-0.116	-0.243	0.162	-0.761
a*	Before Aging	-0.144	0.113	-0.218	0.827
	After Aging	-0.140	0.132	-0.217	0.832
b*	Before Aging	0.322	0.699	0.105	-0.122
	After Aging	0.288	0.713	0.093	-0.122

Table 6.18: Correlation Matrix between L*a*b* values before and after aging and %Pigment.

In the case of the second pigment, for the model built using the color coordinates of the samples before the artificial chromatic aging procedure, a value of R^2 of 0.757 was obtained, while for the model built using the color coordinates of the samples after they underwent the artificial aging, the value registered for the Coefficient of Determination was 0.788. However, for the Root Mean Square Error, the values found were comparable with the mean value of the studied variable (%P1), suggesting that the accuracy of the model is not at an optimal level.

The models built to predict the relative quantity of Pigment 3 within the formulation, presented the lowest quality of fit (in terms of R^2 and RMSE) among the four studied pigments. For samples before aging, only 44.8% of total variance could be explained by the predictive model, while for samples after aging, the value of the variance that could be explained by the model drops to 40.9%. The Root Mean Square Error has a value of 0.022 and 0.023 for sample before and after they underwent the artificial aging, respectively. Although they are within the range of the output variable, the RMSE values exceeded in almost l cases the values of %P3.

For Pigment 4, we registered the highest value of R^2 (0.991 for samples before aging and 0.992 for samples after aging) as well as the lowest values of the Root Mean Square Error (0.001 in both cases). These good values of the two parameters are pointing towards a good performance of the predictive model, and, as a first approach, indicate that this variable is the one that we can better control with the predictive models. It has to be recalled that precisely for this variable we found a strong inverse correlation with the lightness of the samples as well as a strong direct correlation with the value of the chromatic coordinate a*, both these correlation favoring a good performance of the predictive models.

	%P1		%P2		%P3		%P4	
	Before Aging	After Aging	Before Aging	After Aging	Before Aging	After Aging	Before Aging	After Aging
Observations	44	44	44	44	44	44	44	44
DF	31	31	31	31	31	31	31	31
R^2	0.495	0.521	0.757	0.788	0.448	0.409	0.991	0.992
SSE	0.013	0.012	0.014	0.012	0.016	0.017	0.000	0.000
MSE	0.000	0.000	0.000	0.000	0.001	0.001	0.000	0.000
RMSE	0.020	0.020	0.021	0.020	0.022	0.023	0.001	0.001

Table 6.19: Goodness of fit statistics of variables %P1, %P2, %P3, and %P4 for the predictive models designed for samples before and after aging.

The predicted values of percentage of Pigment 1, Pigment 2, Pigment 3 and Pigment 4 within the chemical formulation of the experimental dental resin composites, as well as the measured values and corresponding residuals are shown in Tables 4.20-23, respectively.

In the case of %P1, for the models built from samples before aging, the predicted values were smaller than the real (measured) value for all five samples included in the Validation Group. The lowest difference between the predicted and the measured value was found for Sample 49, while the highest residual value was registered for Sample 47. For the predictive models designed with the chromatic coordinates after aging as input variables, the smallest residual was found for Sample 48, while the highest value was found, again, in the case of the Sample 47.

For Pigment 2, when the model was designed using as input variables the chromatic coordinates of the samples before aging, for all five samples included in the Validation Group, the predicted values were higher than the real quantities. In terms of differences between the predicted and the measured values, the biggest difference was found for the Sample 47, while the smallest difference was found for Sample 49, but it has to be considered that the value of %P1 for Sample 49 is also the smallest among the five samples included in the Testing Group. In the other case, when the Multiple Nonlinear Regression model was designed using as input variables the L*a*b values of the sample after the aging procedure was applied, the smallest residual was found for Sample 48, while the highest was registered, again, in the case of the Sample 47.

Sample	Before Aging			After Aging		
	%P1	Pred(%P1)	Residuals	%P1	Pred(%P1)	Residuals
45	0.022	0.015	0.007	0.022	0.016	0.006
46	0.036	0.019	0.017	0.036	0.012	0.024
47	0.046	0.012	0.034	0.046	0.019	0.027
48	0.012	0.005	0.007	0.012	0.013	-0.001
49	0.005	0.002	0.003	0.005	0.023	-0.018

Table 6.20: Predictions and residuals of variable %P1 for models designed for samples before and after aging.

Sample	Before Aging			After Aging		
	%P2	Pred(%P2)	Residuals	%P2	Pred(%P2)	Residuals
45	0.019	0.027	-0.008	0.019	0.025	-0.006
46	0.030	0.057	-0.027	0.030	0.061	-0.031
47	0.039	0.082	-0.043	0.039	0.077	-0.038
48	0.010	0.019	-0.009	0.010	0.013	-0.003
49	0.004	0.006	-0.002	0.004	-0.007	0.011

Table 6.21: Predictions and residuals of variable %P2 for models designed for samples before and after aging.

When the models were calculated using the colorimetric coordinates of the samples before aging as input variables, the differences between the measured and the predicted values of the relative quantity of Pigment 3 within the chemical formulation of the experimental dental resin composites varied within the 0.008 – 0.0015 range, with the lowest value found for Sample 47 and the highest value found for Samples 46 and 49. When the input variables of the predictive model were the L*a*b* values of the samples after they underwent the artificial aging procedure, the residuals were within the 0.004 – 0.020 range, with the highest difference found for Sample 46 and the lowest for Sample 48.

In the case of the fourth pigment, the differences between the predicted and real values were very small, ranging from 0 to 0.001 for models built from chromatic coordinates of samples before and after aging. It has to be taken into account that the values of this variable are also the smallest ones, so these results are not so surprising.

Sample	Before Aging			After Aging		
	%P3	Pred(%P3)	Residuals	%P3	Pred(%P3)	Residuals
45	0.012	0.022	-0.009	0.012	0.020	-0.008
46	0.019	0.035	-0.015	0.019	0.039	-0.020
47	0.025	0.034	-0.008	0.025	0.036	-0.011
48	0.006	0.015	-0.009	0.006	0.010	-0.004
49	0.003	0.018	-0.015	0.003	0.010	-0.007

Table 6.22: Predictions and residuals of variable %P3 for models designed for samples before and after aging.

Sample	Before Aging			After Aging		
	%P4	Pred(%P4)	Residuals	%P4	Pred(%P4)	Residuals
45	0.003	0.002	0.000	0.003	0.002	0.000
46	0.004	0.004	0.000	0.004	0.004	0.001
47	0.006	0.005	0.001	0.006	0.005	0.001
48	0.001	0.001	0.001	0.001	0.001	0.001
49	0.001	0.000	0.001	0.001	0.000	0.001

Table 6.23: Predictions and residuals of variable %P4 for models designed for samples before and after aging.

If we analyze the relative value of the residual compared with the real value of the variable %P1, we can observe that, for all samples before aging, the residual do not exceed 75% of the value of the measured variable, with an average of 54.25% (SD=15.72) among the five samples included in the Validation Group. For samples after aging, the absolute value of the difference between the predicted and the measured quantities of %P1, do not exceeded 70% for four of the studied samples, while for Sample 49 was higher than 350%. Due to the high value obtained in the case of Sample 49, the average value for this group was 104.19% with a standard deviation of 144.93 (Figure 6.30).

It should be emphasized that, if we exclude the high value obtained for Sample 49 after aging, the two predictive models perform adequately, with an error of approximately 55%±15%. Although this number may seem high, it should be noted that it is very difficult to predict the relative quantities of pigment within the chemical formulation of the experimental dental resin composites, since they are found in a very small range of values, with limited variability. Moreover, as we noted at the beginning, moving from a three-dimensional space to a four-dimensional space involves loss of precision and some inaccuracies in the predictions are expected to be caused.

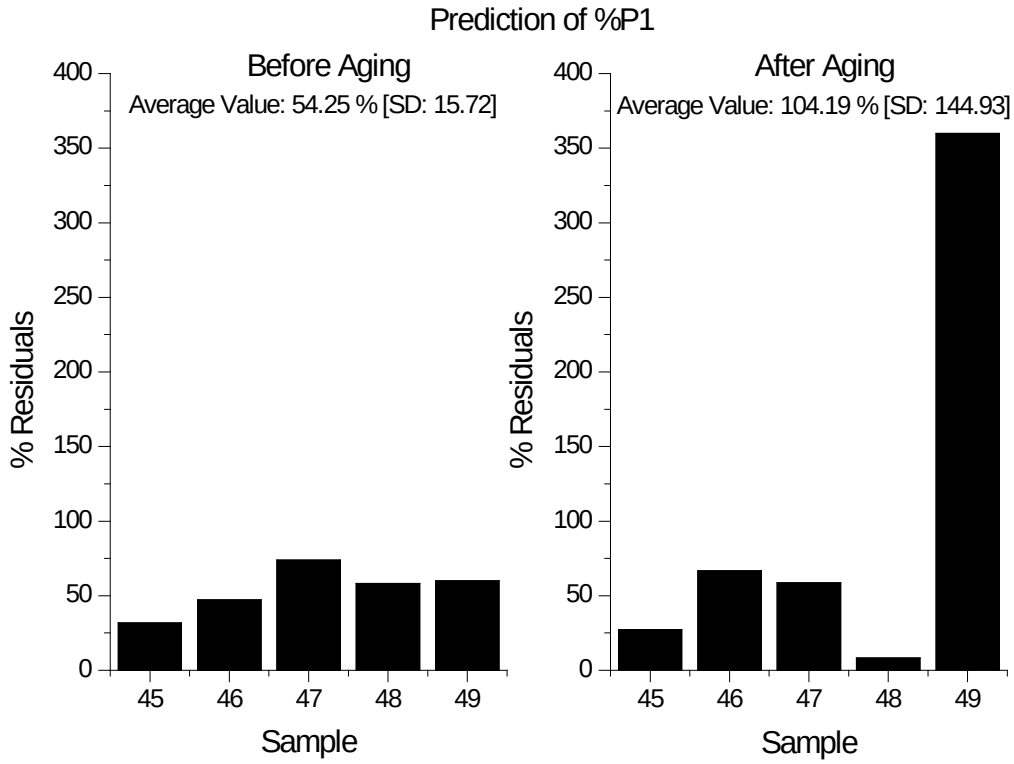

Figure 6.30: Absolute Residual Values of variable %P1 for models designed for samples before and after aging.

For samples before aging, the difference between the predicted and the real quantity of Pigment 2 within the mixture, did not exceeded 110% in any of the five studied cases, with an average value of 76.47% (SD=29.10) (Figure 6.31). In the case of samples after aging, for four of the five samples included in the validation group, the differences between the predicted and the real values were lower than 105%, while for Sample 49 the proportion between the residual value and the real value of %P2 was 275%. The average value registered for this group was 107.46%, with a Standard Deviation of 99.93%. It is worth mentioning that one must be very cautious when reporting this kind of results, since, as you can see, our predictive model, for samples after aging, presents the highest error for Sample 49, sample for which the value of the difference between the predicted and the real quantity of Pigment 2 in the formulation it is not the biggest one.

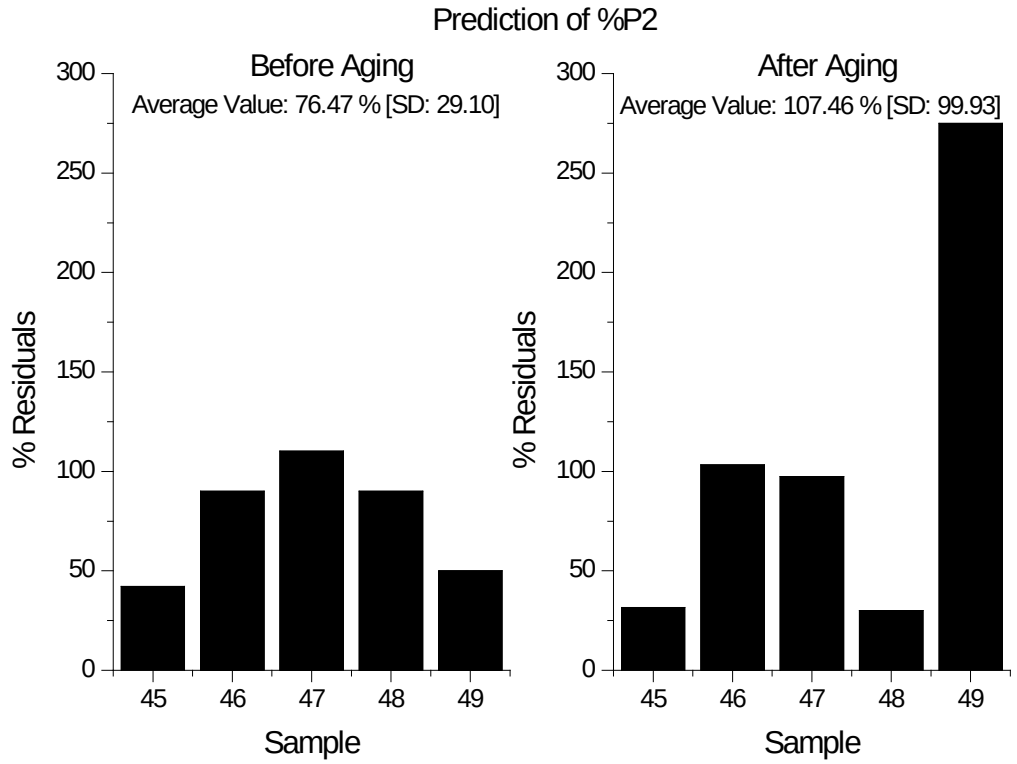

Figure 6.31: Absolute Residual Values of variable %P2 for models designed for samples before and after aging.

If we compare the value of the residual with the magnitude of the variable (in this case %P3), it can be observed that, for samples before aging, in four of the five samples studied, the difference between the predicted and measured values is lower than 150%, while for one sample (Sample 49), the relative value of the residual with respect to the real value of the variable was 500% (Figure 6.32). In this case, the highest residual found correspond to the highest relative value. The average value for the five samples included in the Validation Group was 167.18% with a Standard Deviation of ±190.80. For sample after aging, the relative value of the residual with respect to the real value of %P3 are lower, in none of the five studied cases exceeding 235%, with an average value of 103.18% (SD=76.01). As the case of samples before aging, the highest relative value was registered in the case of Sample 49.

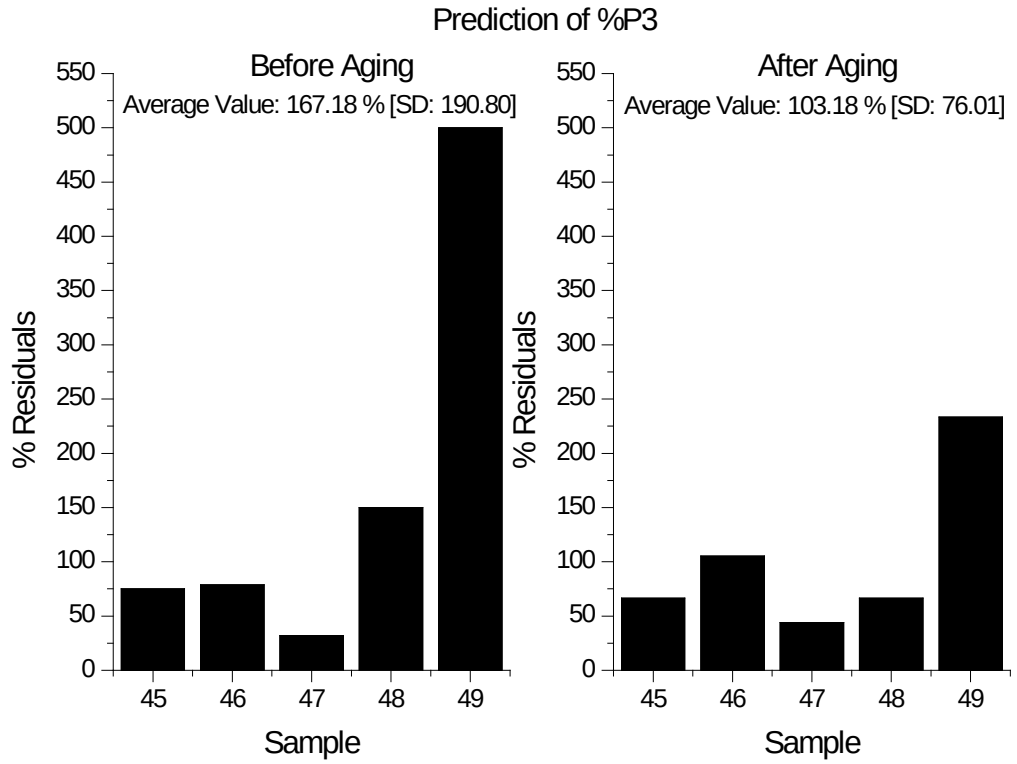

Figure 6.32: Absolute Residual Values of variable %P3 for models designed for samples before and after aging.

If we analyze the relative size of the differences between the predicted and measured values compared with the real value of %P4 (Figure 6.33), both for models built for samples before and after the aging procedure was applied, the residuals do not exceed 100% of the expected value. Moreover, for the five samples included in the Validation Group, we found 2 perfect matches in the cases of samples before aging (Sample 45 and 46) and one perfect match for samples after aging (Sample 45). The average values registered were 43.33%±52.17 for models designed for samples before aging and 48.33%±48.01 for models designed for samples after they underwent the artificial chromatic aging procedure. These are by far the lowest values found among the four studied variables, and, if we take into account the good values of the goodness of fit, we can state that the relative quantity of Pigment 4 within the chemical formulation of the experimental dental composites is the one which most accurately can be predicted.

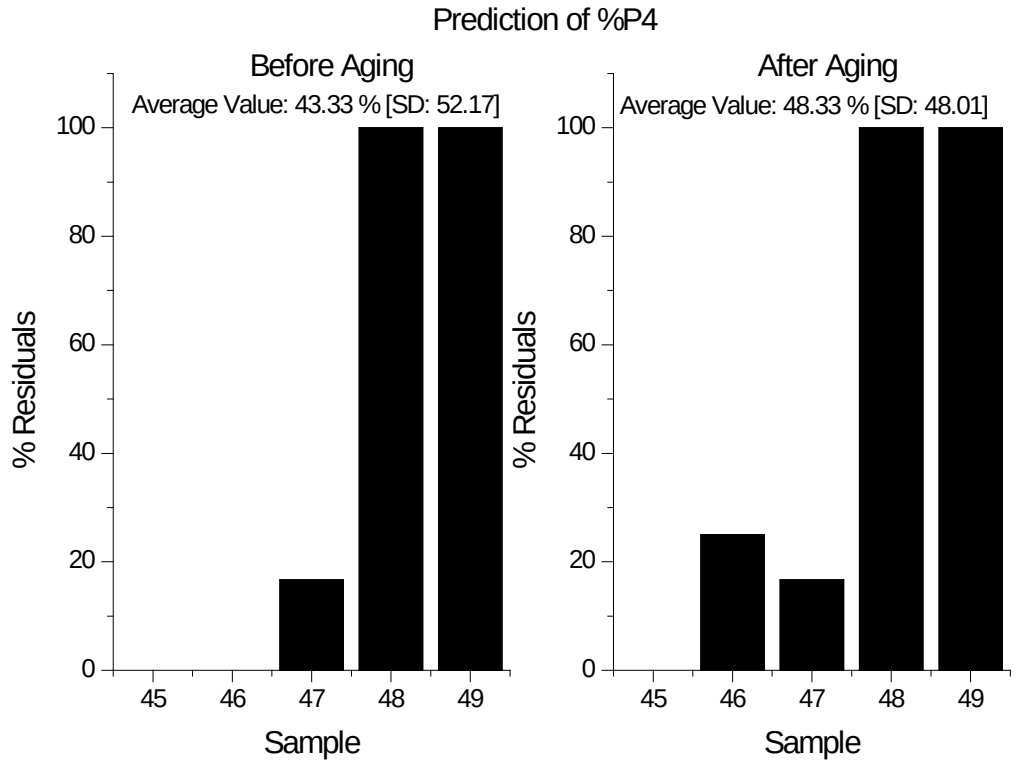

Figure 6.33: Absolute Residual Values of variable %P4 for models designed for samples before and after aging.

In Figure 6.34 are plotted the predicted values against the measured values of the variable %P1 for models designed for samples before and after aging, both for the Training Group (Active) and the Validation Group. As it can be seen, although there is a variation between the predicted and the measured values, the ratio between the two values is close to unity for the two types of models (before and after aging).

Figure 6.35 show the predicted values against the measured values of the variable %P2 for models designed for samples before and after aging, both for the Training Group (Active) and the Validation Group. For the five samples included in the Validation Group before aging, the predictive model tends to over-estimate the value of the variable, since the ratio between the predicted and the real %P2 falls constantly under the line which defines the perfect agreement (ratio =1). The same behavior it can be observed for the models which use the chromatic coordinates of the samples after aging as input variables to predict the %P2 in the formulation, since 4 of the samples presented a ratio below 1. As pointed out in previous section, Roberts and Pashler (Roberts and Pashler, 2000) found a relationship between the high variance in data and constant over or under estimations of a model compared to the expected

values. A wider study, including a greater number of samples with more variability in the relative quantities of Pigments used, it is highly likely to, in a first instance, avoid the over-estimation of the predictive model, and finally to improve its overall predictive capability. Further studies should be performed in order to solve this issue.

In Figure 6.36 are plotted the predicted values against the measured values of the variable %P3 for models designed for samples before and after aging, both for the Training Group (Active) and the Validation Group. For the five samples included in the Validation Group, our Multiple Nonlinear Regression predictive models, both for samples before and after the artificial chromatic aging was applied, constantly over-estimates the value of the quantity of Pigment 3 in the formulation, providing higher values than the expected ones.

The ratio between the predicted and the measured values of %P4, for the sample included in the Active and the Validation group, both before and after the aging procedure was applied, are shown in Figure 6.37. It can be seen that for all samples, not only for the five samples included in the Validation Group, the ratio is very close to unity, which indicates a perfect agreement between the predicted and the real values of this variable. This observation reinforces the conclusion that this variable provides the best results in terms of prediction quality of the Multiple Nonlinear Regression models.

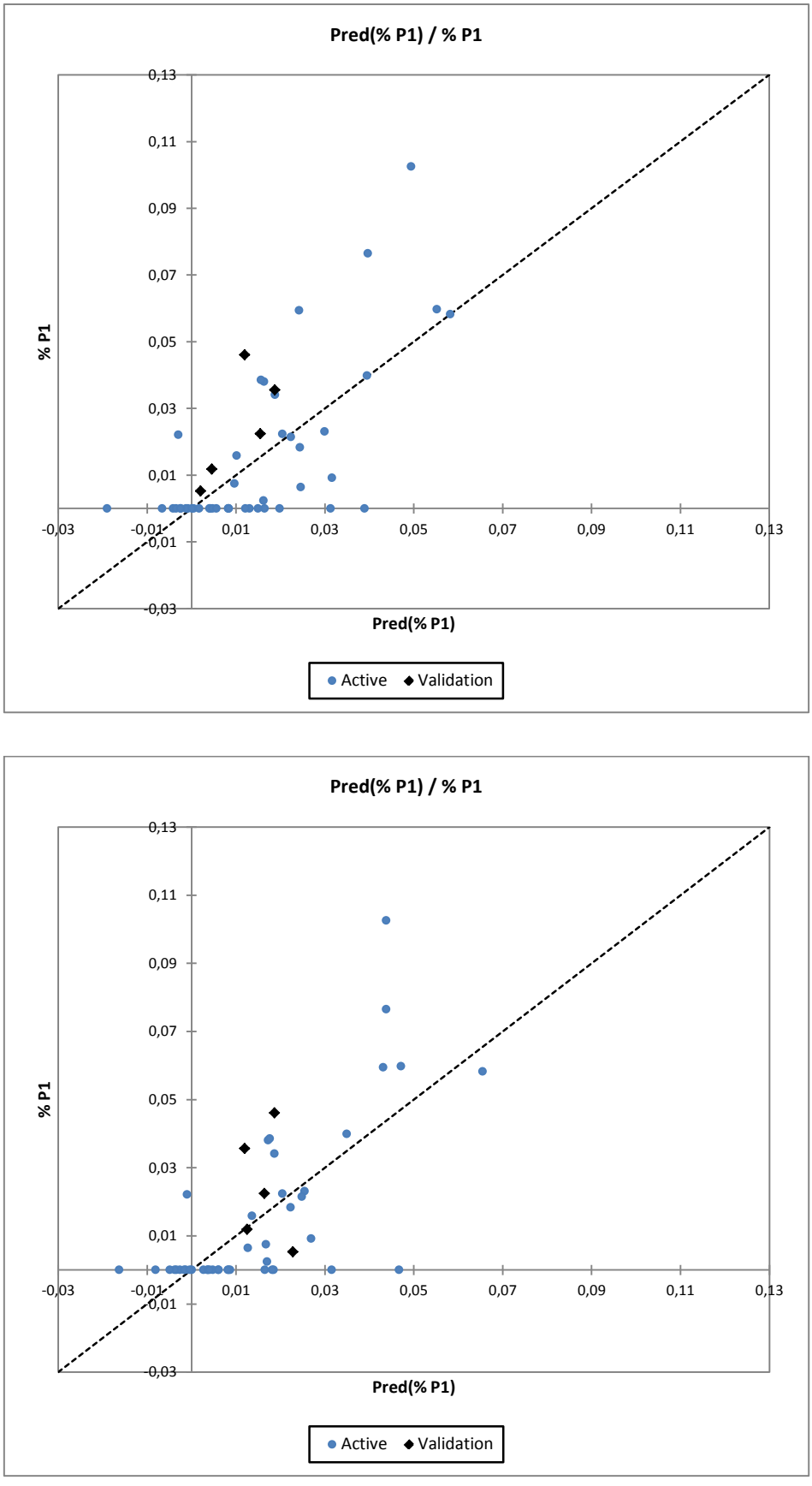

Figure 6.34: Predicted against measured values for the variable %P1 for models designed for samples before aging (top) and after aging (bottom).

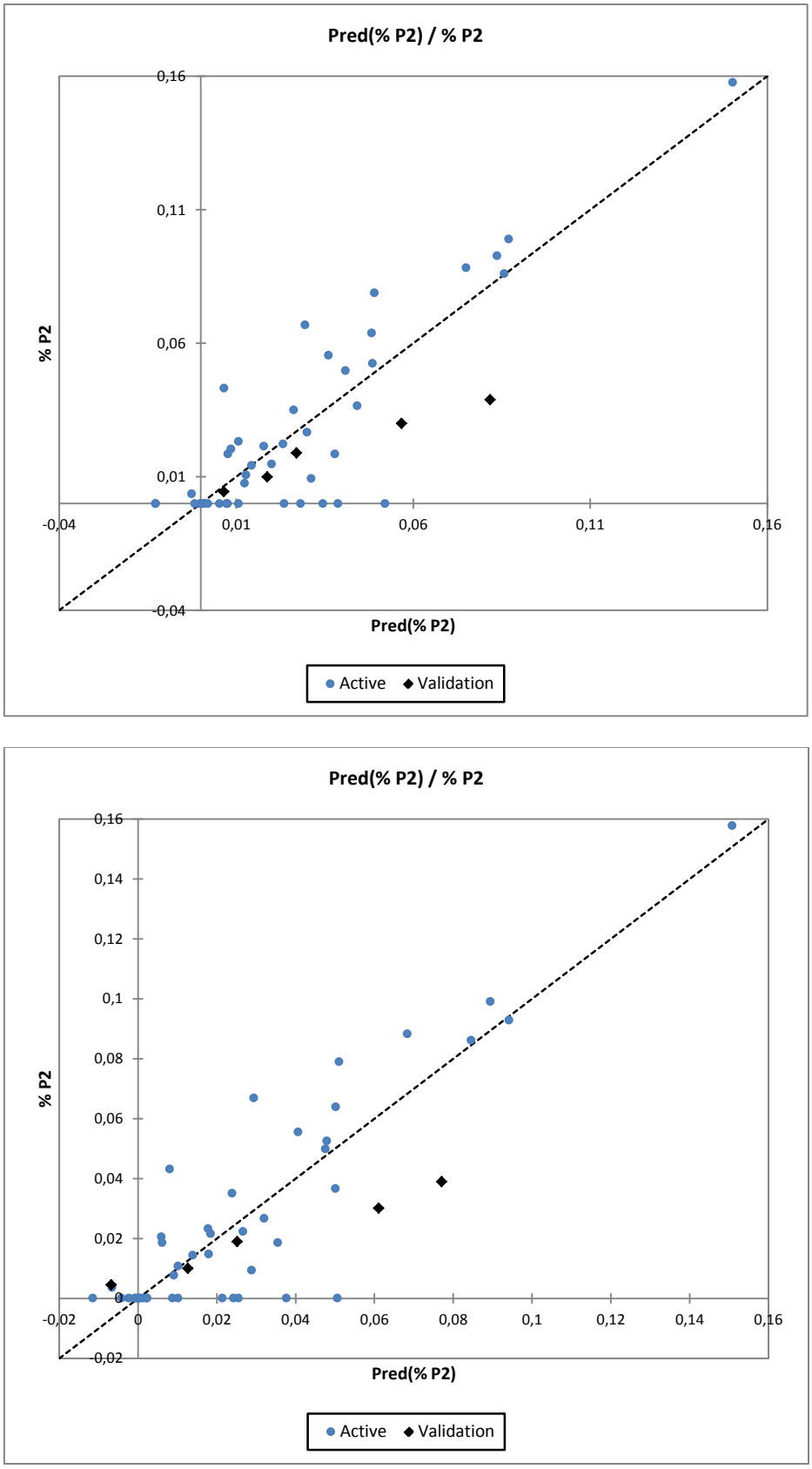

Figure 6.35: Predicted against measured values for the variable %P2 for models designed for samples before aging (top) and after aging (bottom).

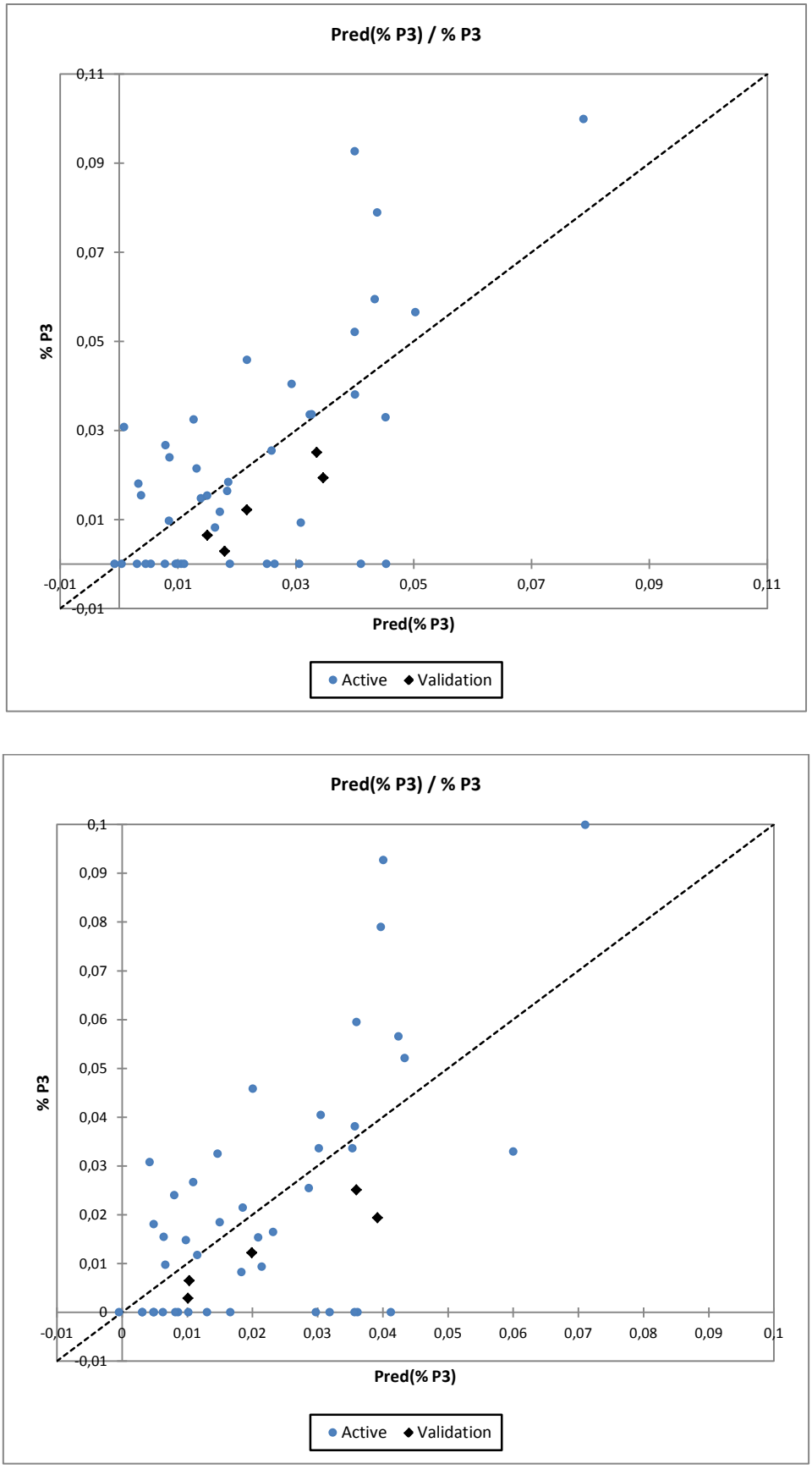

Figure 6.36: Predicted against measured values for the variable %P3 for models designed for samples before aging (top) and after aging (bottom).

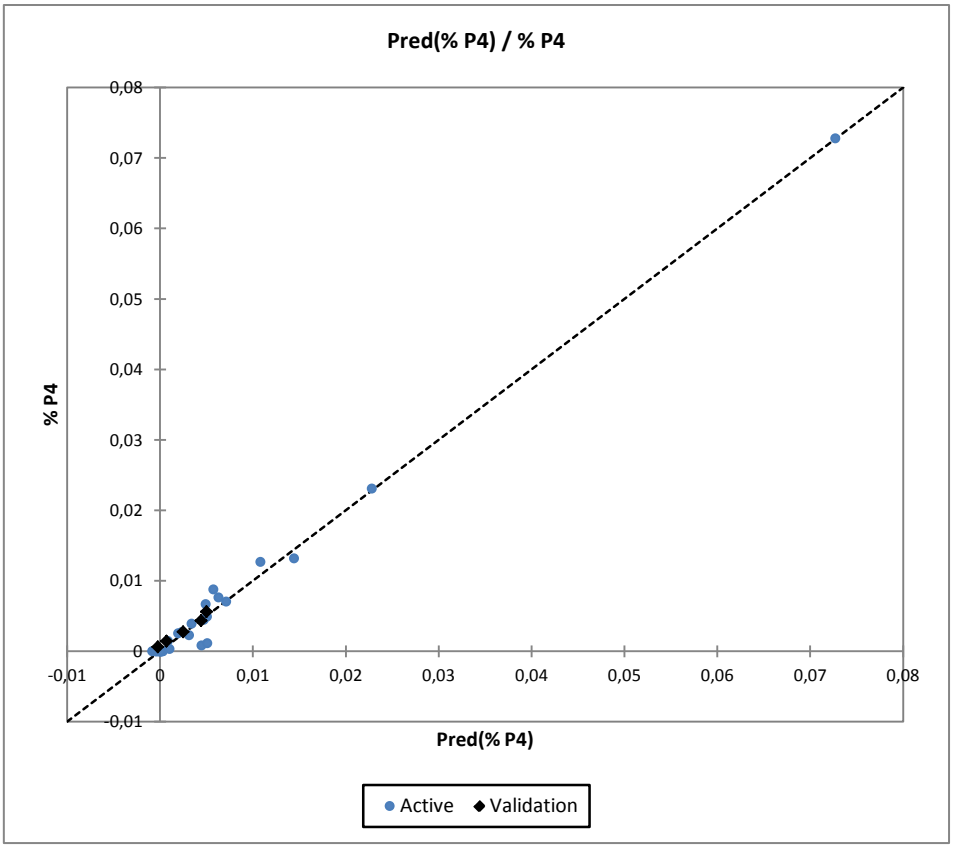

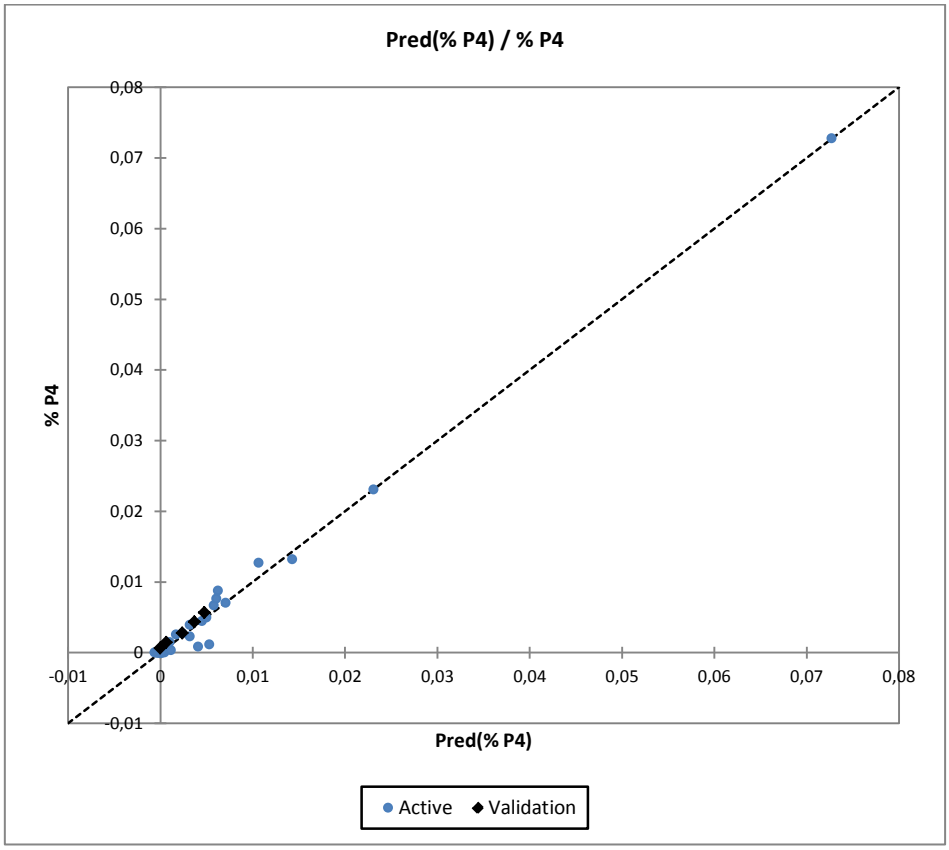

Figure 6.37: Predicted against measured values for the variable %P4 for models designed for samples before aging (top) and after aging (bottom).

6.3.4 PREDICTION OF % PIGMENT (%P1, %P2, %P3 AND %P4) WITHIN THE FORMULATION FROM REFLECTANCE FACTORS AT 2nm STEP IN THE 380nm-780nm INTERVAL

The research in science and biomedical applications often involves using controllable and/or easy to measure variables (input factors) to explain, regulate or predict the behavior of other variables (output factors or dependent variables). When we are dealing with a reduced number of input factors which are not significantly redundant and have a strong relationship with the output variables, the Multiple Nonlinear Regression (MNLR) is one of the best options to take into account for modeling the data. However, if any of the three conditions mentioned above are not fulfilled, MNLR can be inefficient or inappropriate. These so-called soft science applications involve a large number of variables with not so clear relationships among them, and the objective of such a study is to build a good predictive model which explains as much of the dependent variables as possible.

Reflectance spectra of samples are often used to estimate the amount of different compounds in a chemical formulation (Koirala et al., 2008; Solovchenko, 2010). In this case, the input data are the Reflectance Factors that comprise the spectrum while the output data (predicted variables) are component amounts that the researcher wants to predict in future samples. In such cases, when we are dealing with a high number of factors which are highly collinear, the Partial Least Square (PLS) can be a useful tool. The emphasis of the PLS method is on predicting the responses and not necessarily on trying to understand the underlying relationship between the variables, and it is not usually appropriate for screening out factors that have a negligible effect on the output data.

The Partial Least Squares method was developed in 1966 by Herman Wold as an econometric technique (Wold, 1966) and further improved for multivariate linear modeling (Wold, 1995). In addition to spectrometric calibration, has been applied to monitoring and controlling industrial processes with very large numbers of input and/or output variables.

The Multiple Nonlinear Regression can be used in studies with large numbers of input variables (or at least larger than the number of input data), but it is very likely to obtain a predictive model that fits well the input data but it is unable to predict new data. This phenomenon is called over-fitting, and occurs when, although there are many manifest input factors, only a few underlying or latent factors account for most of the variation in the output data. The PLS method try to extract these latent factors accounting for as much of the manifest factor variation as possible while modeling the output variables. However, Dijkstra pointed out that the Partial Least Squares regression does not yield consistent estimates of what are called latent variables in formal structural equation modeling (Dijkstra, 1983).

In the previous section of this Chapter, the relative quantities of the four types of pigments (%P1, %P2, %P3 and %P4) within the formulation were predicted using a Multiple Nonlinear Regression Model using as input variables the L*a*b* colorimetric coordinates (calculated according to the CIE D65 standard illuminant and CIE 2° Standard Colorimetric Observer) before and after aging. In this section the relative quantities of the four types of pigments (%P1, %P2, %P3 and %P4) within the formulation were predicted using as input variables the Reflectance Factors at 2nm steps in the 380nm-780nm interval.

In the development process of a predictive model, the correlation between the input variables of the model (in this case, the Reflectance Factors at 2nm steps in the 380nm-780nm interval before and after the artificial aging) and the output variables of the model (in this case, the percentage of each type of Pigment used - %P1, %P2, %P3 and %P4), is usually carried out as an initial step. The results obtained for the Pearson Correlation coefficient are graphically presented Figure 6.38.

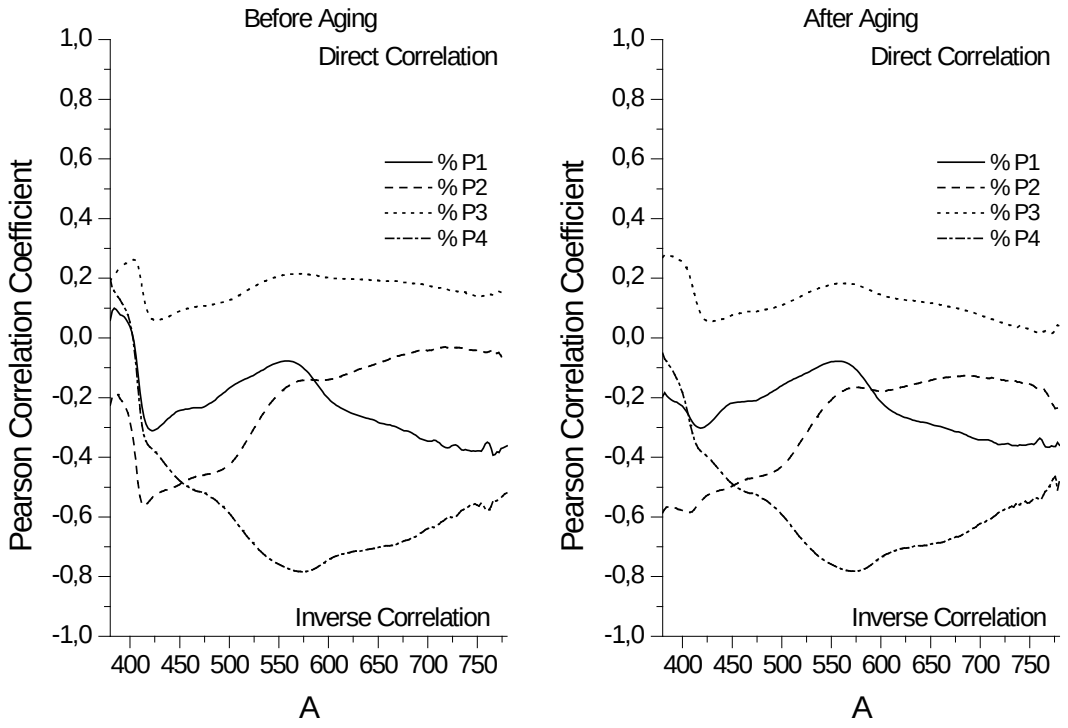

Figure 6.38: Pearson Correlation Coefficients between 380nm-780nm Reflectance Factors before and after aging and % Pigment.

These correlations were also studied when the reverse models were designed (prediction of Reflectance Factors from the relative quantity of Pigment within the chemical formulation). It can be observed that for the models built for samples before aging there is a strong inverse correlation between the relative quantity of Pigment 4 and the Reflectance Factors for wavelengths between 525nm-650nm. For the predictive models using the Reflectance factors of the samples after aging as input variables, there was no strong correlation (neither direct nor inverse) between the input and output variables. As observed for anterior models, a strong correlation usually is associated with increased performance of the predictive model, but no conclusion should be drawn before analyzing the other parameters of the quality of fit, such as goodness of fit or relative residuals.

	%P1		%P2		%P3		%P4	
	Before Aging	After Aging	Before Aging	After Aging	Before Aging	After Aging	Before Aging	After Aging
Observations	44	44	44	44	44	44	44	44
DF	39.000	37.000	39.000	37.000	39.000	37.000	39.000	37.000
R^2	0.488	0.810	0.650	0.805	0.133	0.326	0.749	0.850
SSE	0.018	0.011	0.022	0.017	0.025	0.023	0.006	0.005
MSE	0.000	0.000	0.000	0.000	0.001	0.000	0.000	0.000
RMSE	0.017	0.010	0.021	0.016	0.024	0.021	0.006	0.004

Table 6.24: Goodness of fit statistics of variables %P1, %P2, %P3 and %P4 for the PLS predictive models designed for samples before and after aging.

In Table 6.24 are presented the parameters which describe the goodness of fit of the Partial Least Squares predictive models built to predict the variables %P1, %P2, %P3 and %P4 from Reflectance Factors at 2nm steps in the 380nm-780nm interval, for samples both before and after aging.

For %P1, in the case of samples before aging, the predictive model can explain only 48.8% of the variance within data, as shown by the value of the Coefficient of Determination. Also, the value of the RMSE is considerably high (0.0017) compared to the magnitude of the variable. However, in the case of the samples after aging, the R^2 exhibits a value of 0.810, while the Root Mean Square Error remains in an acceptable 0.010 value. According to these results, it is expected that the PLS predictive model built for samples after aging to perform considerably better than the model designed for samples before aging.

In the case of Pigment 2, in terms of the Coefficient of Determination, the model designed from Reflectance Factors of samples before aging presented a value of 0.650, while in the case of the model designed from Reflectance Factors of samples after aging, the variance of data which can be explained by the Partial Least Squares predictive model is 80.5%. The RMSE values registered were 0.021 for samples before aging and 0.016 for samples after aging. If we analyze the two parameters describing the goodness of fit (R^2 and RMSE), it can be concluded that the predictive model it is expected to perform above average, providing a good output for this variable.

Among the four studied variables (%P1, %P2, %P3 and %P4), for %P3 we obtained the lowest values of the Coefficient of Determination (R^2=0.133 before aging

and R^2=0.326 after aging) as well as the highest value of the Root Mean Square Error (RMSE=0.024 before aging and RMSE=0.021 after aging). The combination of these two parameters clearly point out to a below average predictive capability of the PLS model, but before evaluating how the model performs, the analysis should be completed with the assessment of the value of the Residuals.

In terms of accuracy of the model, for variable %P4, both before and after the chromatic artificial aging procedure was carried out, we obtained the highest value of R^2 (0.749 and 0.850, respectively). Also, for the Root Mean Square Error we obtained the lowest value among the four studied variables. These small values of RMSE could be explained by the fact that the magnitude of the RMSE is related with the size of the studied variable, and the relative quantity of Pigment 4 (%P4) was the lowest among the four type of Pigments used. Still, the good result in term of goodness of fit opens the door for some good expectations for the performance of the Partial Least Squares predictive model for this variable.

The real values of the relative quantity of Pigment 1 within the chemical formulation of the experimental dental resin composites (%P1) as well as the predicted values using the Partial Least Squares predictive model (Pred(%P1)), together with their corresponding Residuals, for the five samples included in the Validation Group both before and after the artificial chromatic aging procedure was applied, are presented in Table 6.25. In the case of the samples before aging, the differences found between the predicted and the real values of this variable ranged from a minimal value of 0.015 (in the case of Sample 48) to a maximum value of 0.059 (in the case of Sample 47) while for the samples after aging, the Residual were included in the interval ranging from 0.002 (Sample 49) up to 0.020 (Sample 47).

Table 6.26 show the real values of the relative quantity of Pigment 2 (%P2) within the chemical formulation of the experimental dental composites, the predicted values according to the PLS model (Pred(%P2)) ant the corresponding difference between the predicted and measured values, for models built from Reflectance Factors of samples before and after they underwent the artificial chromatic aging procedure for the five samples included in the Validation Group.

Sample	Before Aging			After Aging		
	%P1	Pred(%P1)	Residuals	%P1	Pred(%P1)	Residuals
45	0.022	0.006	0.017	0.022	0.020	0.003
46	0.036	-0.007	0.042	0.036	0.028	0.008
47	0.046	-0.012	0.059	0.046	0.027	0.020
48	0.012	-0.003	0.015	0.012	0.018	-0.007
49	0.005	-0.013	0.018	0.005	0.003	0.002

Table 6.25: Predictions and residuals of variable %P1 for PLS models designed for samples before and after aging.

Sample	Before Aging			After Aging		
	%P2	Pred(%P2)	Residuals	%P2	Pred(%P2)	Residuals
45	0.019	0.046	-0.027	0.019	0.035	-0.016
46	0.030	0.087	-0.057	0.030	0.050	-0.020
47	0.039	0.100	-0.061	0.039	0.068	-0.029
48	0.010	0.033	-0.023	0.010	0.013	-0.003
49	0.004	0.027	-0.022	0.004	0.038	-0.033

Table 6.26: Predictions and residuals of variable %P2 for PLS models designed for samples before and after aging.

It is important to point out that, independently if the input variables were the Reflectance Factors of samples before or after aging, all the predicted values were higher than the real values of %P2. The range of the Residuals was 0.022 – 0.061 for samples before aging, and 0.003 – 0.033 for samples after aging.

In Table 6.27 are listed the values of the real and predicted %P3 for the five samples included in the Validation Group, for models built from Reflectance Factors of samples before and after the artificial aging procedure was carried out. Surprisingly, although the parameters describing the goodness of fit did not present very good values, in terms of the differences between the predicted and real values of %P3, the PLS models performed acceptably. The lowest residual for samples before aging was registered for Sample 45 and Sample 49, with a value of only 0.004, while the highest absolute residual value was found for Sample 47, with a value of 0.0015. In the case of samples after aging, the residuals were included in the 0.002 (for Sample 45) and 0.030 (for Sample 47) range.

Table 6.28 shows both the measured as well as the predicted values for the variable %P4 before and after artificial aging, as well as the corresponding differences between them (Residuals) for the five samples included in the Validation Group.

Sample	Before Aging			After Aging		
	%P3	Pred(%P3)	Residuals	%P3	Pred(%P3)	Residuals
45	0.012	0.017	-0.004	0.012	0.010	0.002
46	0.019	0.006	0.013	0.019	0.007	0.012
47	0.025	0.010	0.015	0.025	-0.005	0.030
48	0.006	0.016	-0.010	0.006	0.019	-0.013
49	0.003	0.007	-0.004	0.003	-0.023	0.026

Table 6.27: Predictions and residuals of variable %P3 for PLS models designed for samples before and after aging.

Sample	Before Aging			After Aging		
	%P4	Pred(%P4)	Residuals	%P4	Pred(%P4)	Residuals
45	0.003	0.002	0.001	0.003	-0.001	0.004
46	0.004	0.001	0.003	0.004	0.002	0.002
47	0.006	0.003	0.003	0.006	0.005	0.001
48	0.001	-0.001	0.002	0.001	0.000	0.001
49	0.001	-0.003	0.004	0.001	-0.006	0.007

Table 6.28: Predictions and residuals of variable %P4 for PLS models designed for samples before and after aging.

In all cases, the differences between the real and predicted values of the relative quantity of Pigment 4 within the chemical formulation of the experimental dental composite are positive, which means that all the predicted values were lower than the real values. Among the four studied variables, %P4 presented the lowest absolute residual values (residual values < 0.005 for samples before aging and residual values <0.008 for samples after aging).

Sample 47 exhibits the highest absolute difference between the predicted and the real values of %P1, but since it also has the highest relative value of Pigment 1 in the formulation, the relative value of the residual compared with the magnitude of the variable it is not the highest (Figure 6.39). For the models built from samples before aging, Sample 49 displayed a relative value of the Residual compared with the real value of %P1 higher than 350%, although the average value between the five samples included in the Validation Group was 161.44%, with a Standard Deviation of 112.85. For samples after aging, the relative size of the Residuals compared with the magnitude of the variable is considerably lower, with the highest value of approximately 60% registered for Sample 48. The average value among the five samples included in the Validation Group was 35.53% (SD=17.74), the lowest from all

the models designed for predicting the percentage of Pigment within the formulation from the Reflectance Factors.

If we analyze the relative size of the differences between the predicted and real values with respect to the real values of %P2 (Figure 6.40), it can be observed that for samples before aging the residuals are considerably high, for all of the five samples included in the Validation Group exceeding 100%. The Average Value of the error of this model is 253.70%, with a Standard Deviation of 169.06%. In the case of the model built with the Reflectance Factors of samples after aging as input variables, the relative size of the Residuals is considerably lower, with four of the five samples included in the Validation Group exhibiting values lower than 100%. However, in the case of Sample 49, the difference between the predicted and real value of %P2 is higher than 800%, which increase the average error of the model for this group up to 216.04% (SD=341.03).

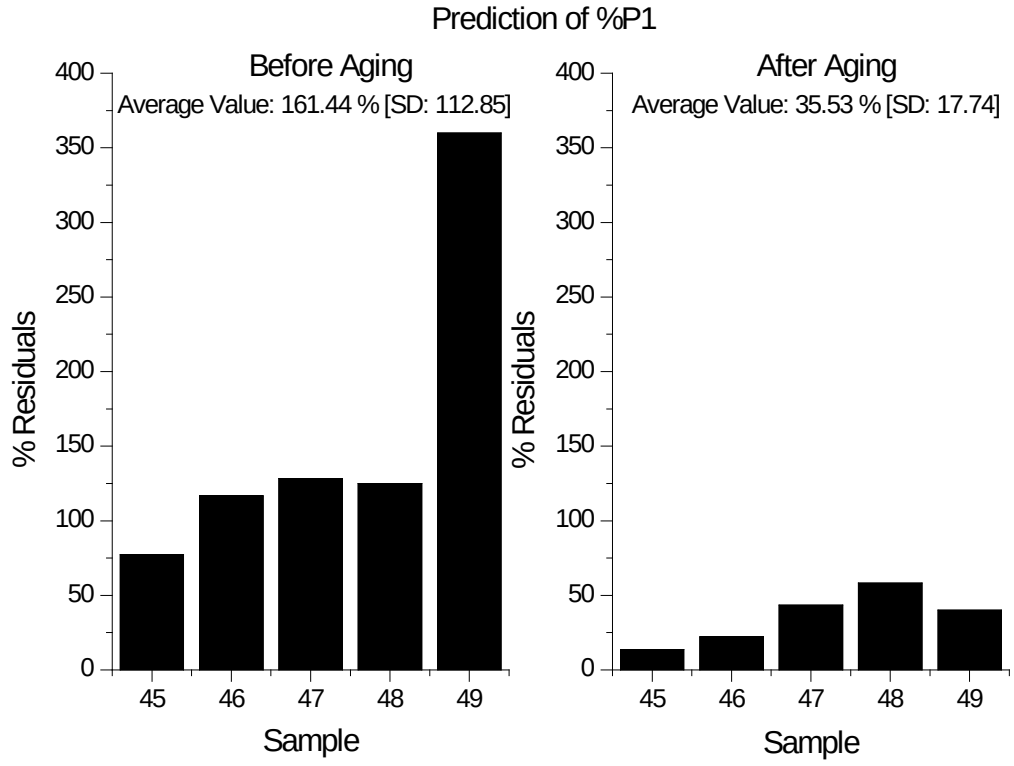

Figure 6.39: Absolute Residual Values of variable %P1 for PLS models designed for samples before and after aging.

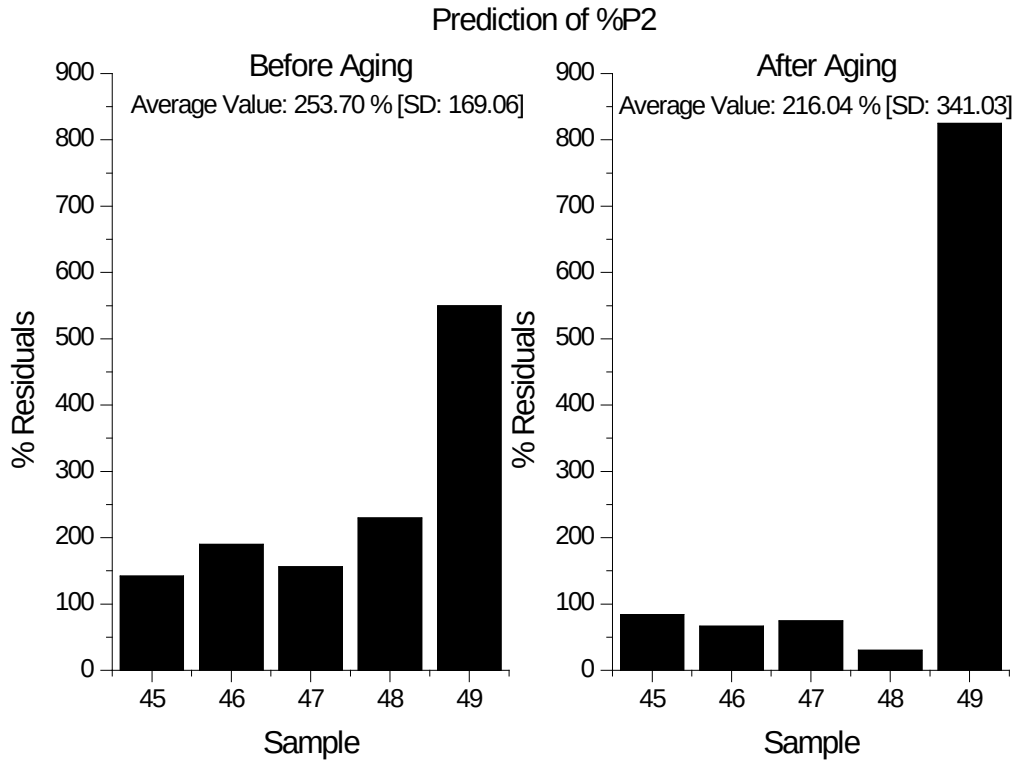

Figure 6.40: Absolute Residual Values of variable %P2 for PLS models designed for samples before and after aging.

The relative size of the differences between the predicted and real values (% Residuals) of the variable %P3 with respect to the real value of %P3 for PLS models designed for samples both before and after aging for the five samples included in the Testing Group are presented in Figure 6.41. In the first case, the model showed an average value of 92.35% (SD=55.46) and for three of the five studied samples the Residual was lower than 100%. In the case of samples after aging, the average error of the model was high, with a value of 256.63% and an associated Standard Error of 349.07, especially due to the value found for Sample 49, which exceeded 850%. Again, it is surprising that, despite the very low value of Coefficient of Determination (R^2=0.133), for the models built from Reflectance Factors of samples before aging, the average value of the differences between the predicted and real values of %P3 among the five samples of the Validation Group was considerably lower than for the models built from Reflectance Factors of samples after aging.

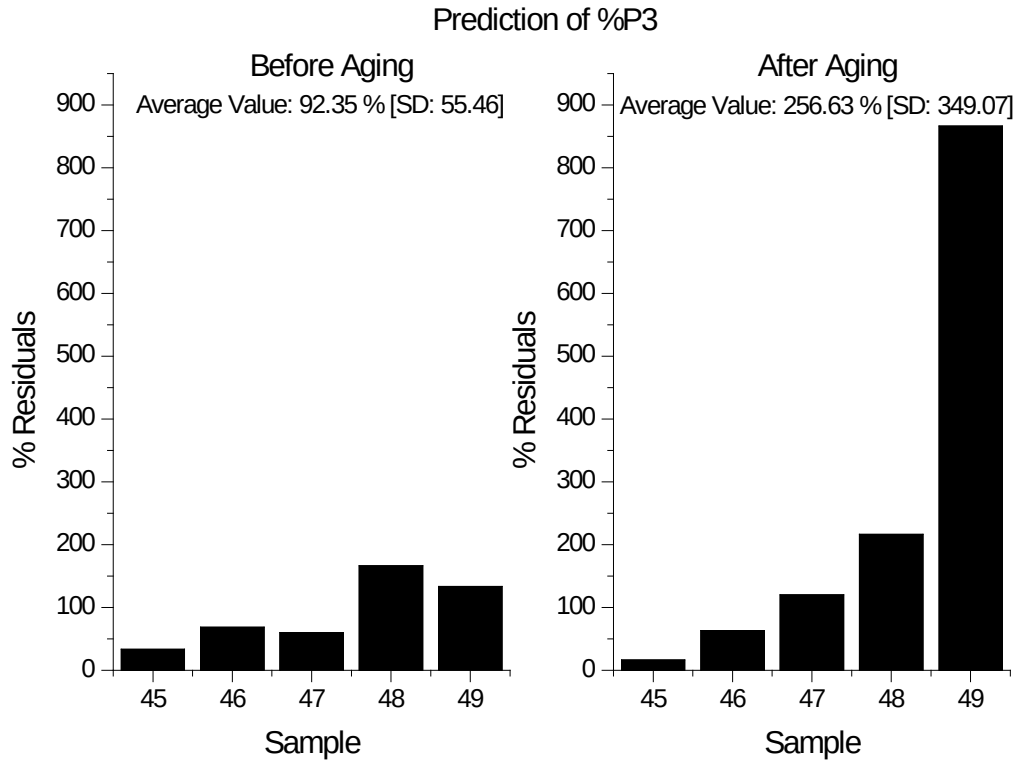

Figure 6.41: Absolute Residual Values of variable %P3 for PLS models designed for samples before and after aging.

If the relative size of the residuals compared with the real value of the variable %P4 (%Residuals) is analyzed for the five samples of the Validation Group (Figure 6.42) it can be observed that for three of the five samples before aging the %Residual is higher than 100%, with an average value of 151.66% and a Standard Error of 153.47, while for the samples after aging the average value of the discrepancy between the predicted and real values of the variable reaches 200% (SD=283.08), especially due to extremely high value (700%) found for the Sample 49. Taking into account these results, despite the encouraging values of the goodness of fit parameters, the PLS predictive model built for this variable seems to perform below average.

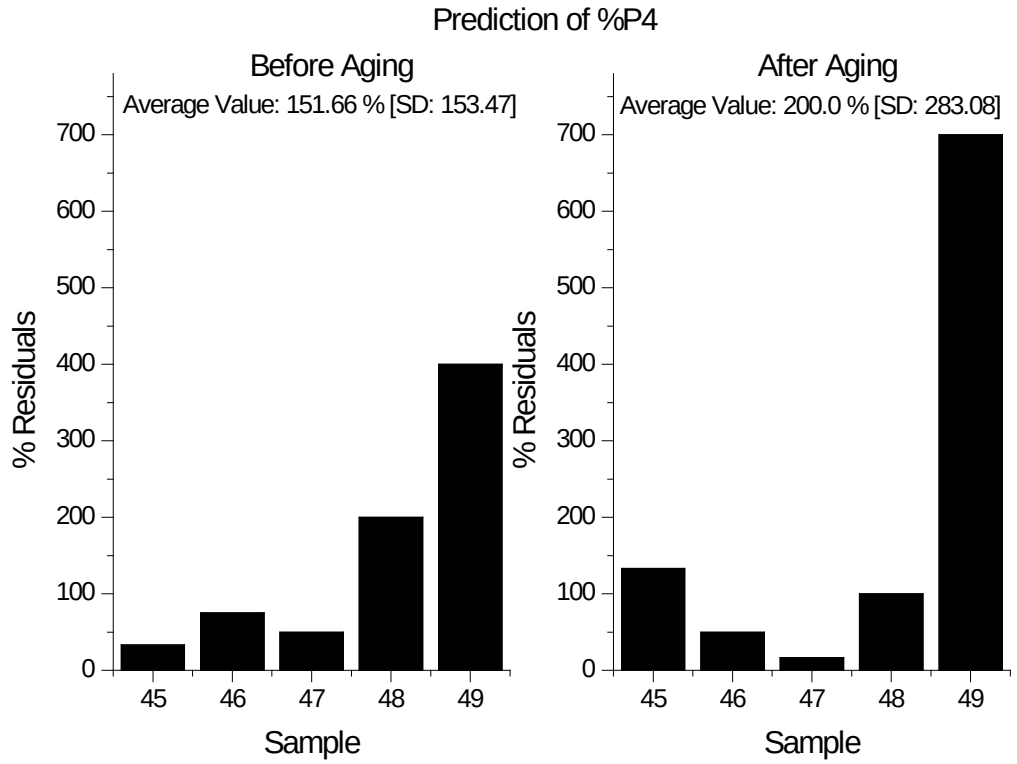

Figure 6.42: Absolute Residual Values of variable %P4 for PLS models designed for samples before and after aging.

Figure 6.43 shows the predicted against the real values of the variable %P1 for the models designed from Reflectance Factors before and after aging and for the samples included in both the Training and the Validation Group, as well as their 95% confidence intervals. For samples before aging, the predictive models underestimates the values of %P1 for all five samples included in the Validation Group, while for the samples after aging, the same tendency is found for four of the five samples of the Validation Group. As stated before, an improved experimental design, with less variability in the input data is expected to solve constant tendency of the predictive models to over or under estimate the measured variables.

In Figure 6.44 are plotted the real and predicted values of the relative quantity of Pigment 2 (%P2) within the chemical formulation of the resin composite together with the 95% confidence curves, for the samples of the Training (Active) and Validation Groups and for models built from Reflectance Factor of sample both before and after aging. As pointed out earlier, the Partial Least Squares predictive models tend to overestimate the value of the variable (%P2) in all cases.

In Figure 6.45 are displayed the predicted against the real values of the variable %P3 as well as their 95% confidence intervals, for the models designed from Reflectance Factors before and after aging and for the samples included in both the Training and the Validation Group. For this specific variable there is no established trend of over or under estimation of the variable by the PLS predictive models.

Figure 6.46 shows the predicted values against the measured values of the %P4 variable before and after artificial aging, both for the Training Group (Active) and the Validation Group, as well as the corresponding 95% upper and lower confidence limits. As pointed out before, both predictive models (for samples before and after aging) are underestimating the value of the variable for the five samples in the Validation Group, providing lower values than the real relative quantity of Pigment 4 within the chemical formulation of the experimental dental resin composites.

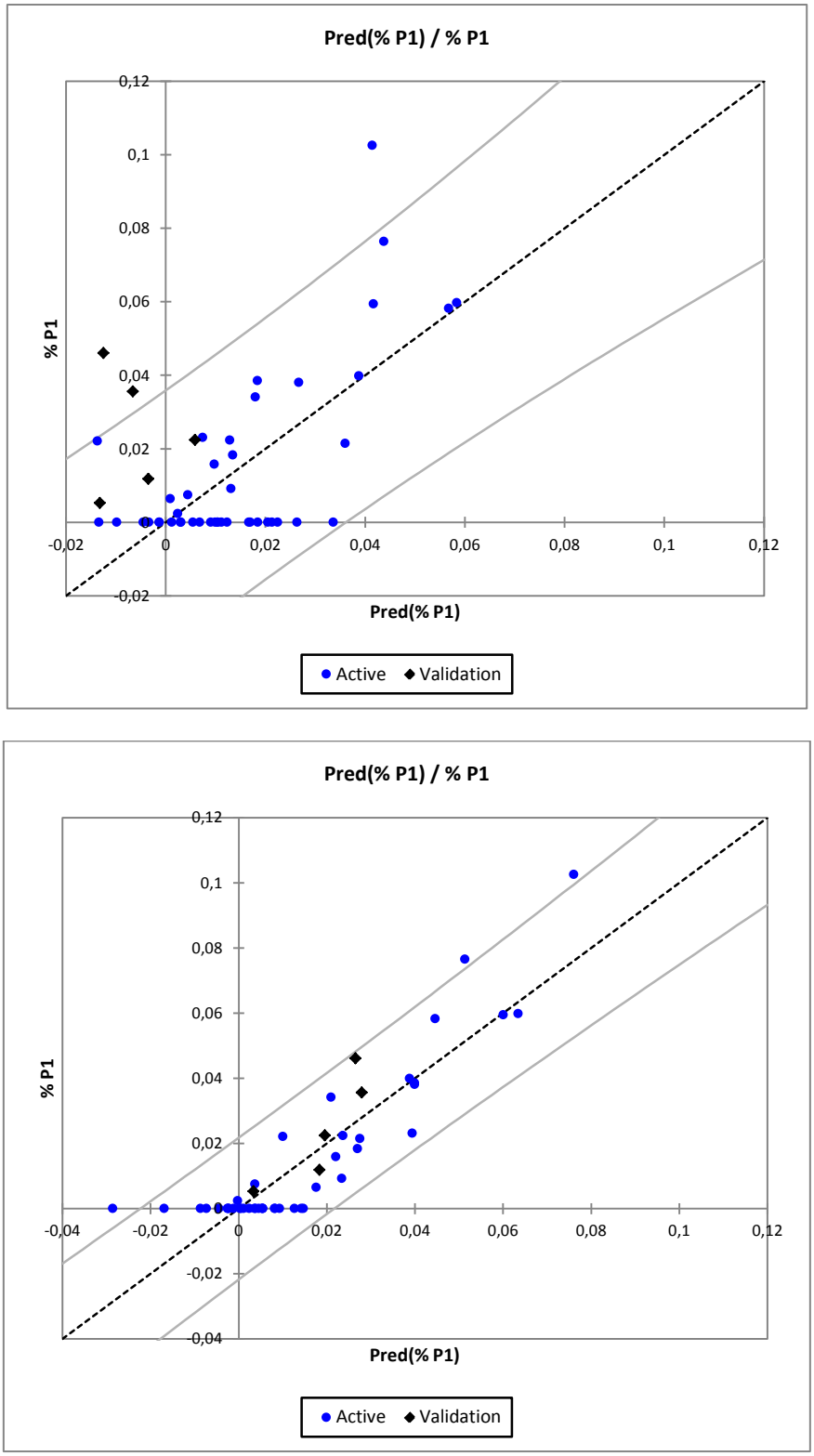

Figure 6.43: Predicted against measured values and 95% confidence curves for the variable %P1 for PLS models designed for samples before aging (top) and after aging (bottom).

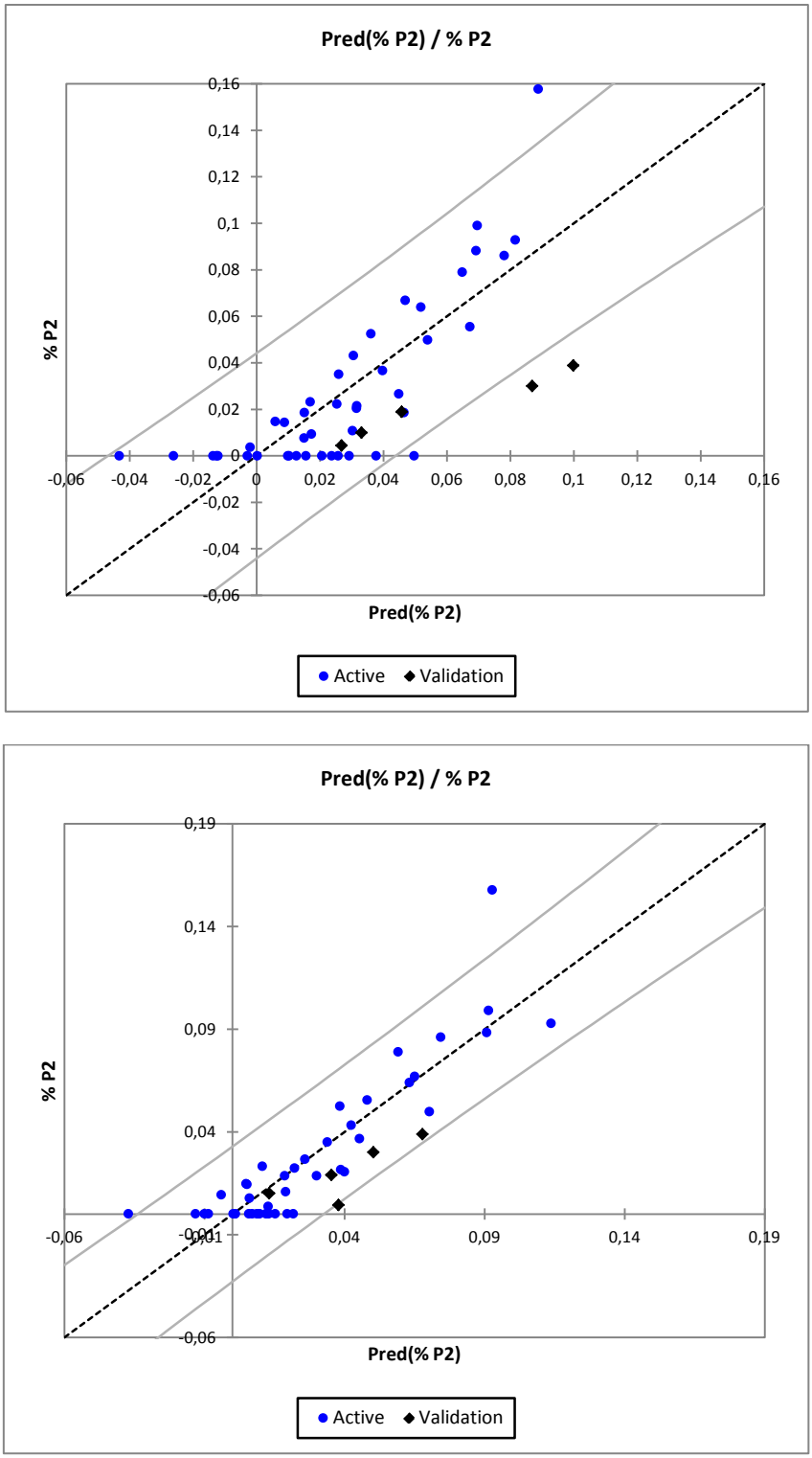

Figure 6.44: Predicted against measured values and 95% confidence curves for the variable %P2 for PLS models designed for samples before aging (top) and after aging (bottom).

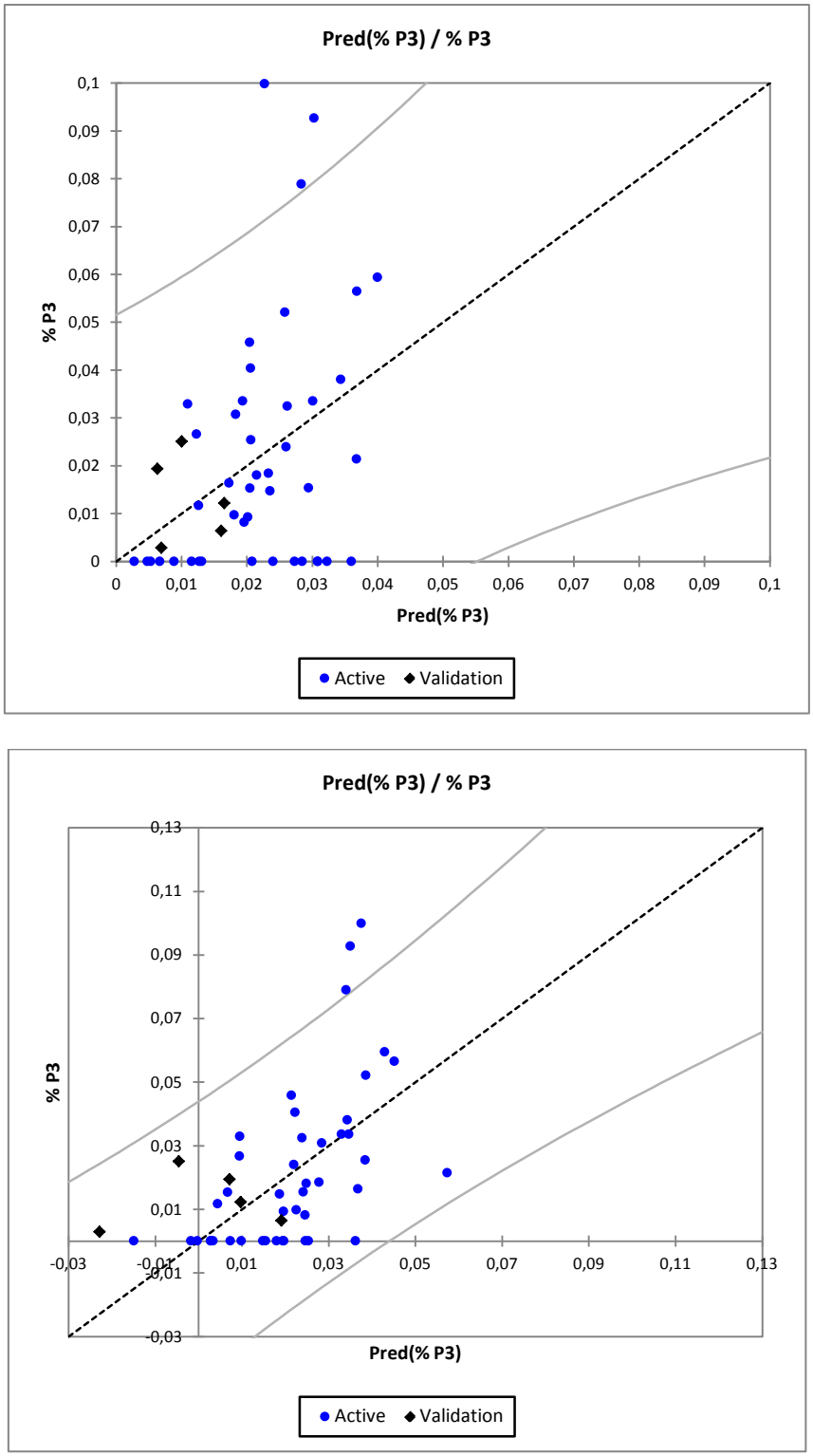

Figure 6.45: Predicted against measured values and 95% confidence curves for the variable %P3 for PLS models designed for samples before aging (top) and after aging (bottom).

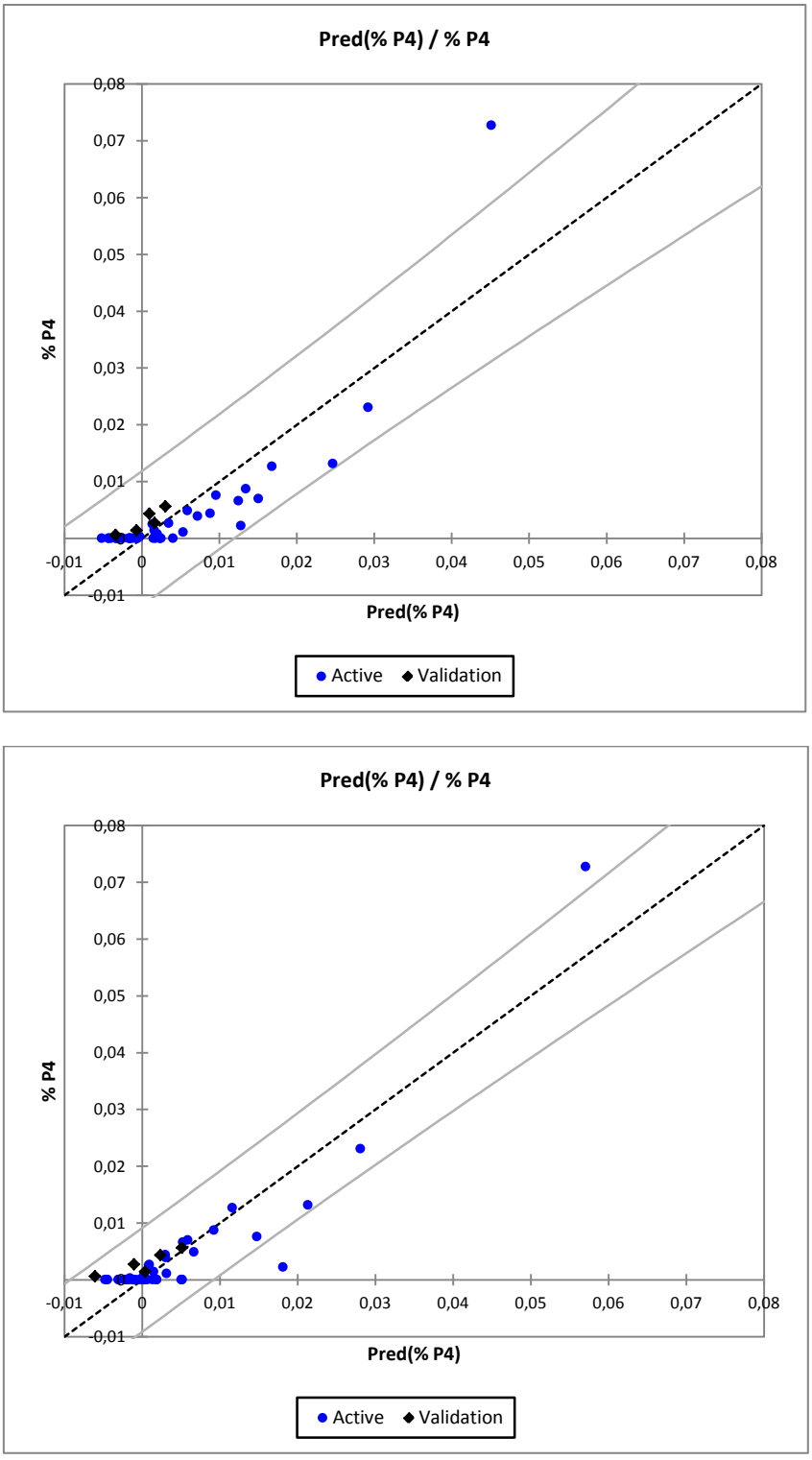

Figure 6.46: Predicted against measured values and 95% confidence curves for the variable %P4 for PLS models designed for samples before aging (top) and after aging (bottom).

Soft science applications involve so many variables that it is not practical to seek a model which explicitly relates them all. The Partial Least Squares Regression is one of the possible solutions and although it is continuously evolving as a statistical modeling technique, there are other fields which can provide also good results, such as principal components regression, maximum redundancy analysis, methods which handle the collinearity in regression, such as the ridge regression proposed by Banerjee and Carr (Banerjee and Carr, 1971), or newer methods such as the neural networks (Golden, 1997). The neural networks are probably the strongest competitors for PLS in terms of flexibility and robustness of the predictive models, but they do not explicitly incorporate a linear extraction of latent factors – that is dimension reduction (Frank and Friedman, 1993).

In future studies on this topic it is important to modify and refine the predictive models in order to avoid significant errors, such as obtaining values of the relative quantity of the Pigments within the chemical formulation of the experimental dental composites below zero, which are physically impossible.

This study is intended as a pilot study, which opens the door to future research in this area, since in the field of esthetic dentistry, the ability to emulate (mimic) with high accuracy the tooth structure intended to replace or repair is gaining immense importance. Therefore, being able to manufacture restorative materials which perfectly match the color of a dental structure under certain illuminant (metameric match) or, even better, the reflectance spectrum of a dental structure in the visible range (isomeric match), will give the dental clinician the ability to perform and provide outstanding restoration which will lead to full patient satisfaction.

CHAPTER 7

CONCLUSIONS

CONCLUSIONES

1. The TSK Fuzzy Approximation proposed in this PhD Thesis is an adequate procedure for calculations of the color difference thresholds compared with traditional fitting methods. The CIEDE2000 color difference formula is better correlated with the visual perception, recommending its use in dental research and for in vivo dental color measurements. The values 1.25 CIEDE2000 units and 2.23 CIEDE2000 units found for perceptibility and acceptability thresholds, respectively, can be used as reference in future research, for the design of new dental materials or clinical evaluation of dental restorations.

2. There are significant differences in visual sensitivity for variations in lightness, chroma and hue ($\Delta L'$=2.92, $\Delta C'$=2.52, $\Delta H'$=1.90) for samples of the dental chromatic space. Therefore, for a proper use of the CIEDE2000 total color difference formula in visual and instrumental clinical assessment in dentistry, it is necessary to revise the parametric factors K_L, K_C y K_H of the formula. The values obtained for the CIEDE2000 differences in lightness (ΔE_L=2.86), chroma (ΔE_C=1.34) and hue (ΔE_H=1.65) indicate that the use of the parametric factor K_L=2 (CIEDE2000(2:1:1)) might be recommended for the evaluation of color difference between samples of the dental color space. Moreover, the directional acceptability thresholds estimated in this PhD Thesis can result of great utility in future research in dentistry as well as in industrial applications, such as dental whitening procedures, dental aging, design of new dental materials, and a proper use of these materials in the clinical practice.

3. The Fuzzy Approximation of the percentage of acceptance curves, using a TSK TaSe model, developed in this Thesis, enables the calculations of the values of the acceptability thresholds in the dental color space. The CIEDE2000(2:1:1) color difference formula displays a better performance against visual judgments compared to the CIEDE2000(1:1:1) formula, as shown by the values of the statistical factors PF/3 and STRESS (PF/3: 190.33 compared to 196.43; STRESS: 0.83 compared to 0.85). Therefore, the use of the parametric factor K_L=2 instead of K_L=1 should be implemented in the computation of the CIEDE2000(K_L:K_C:K_H) color difference formula for an improvement in the color difference calculations in the dental field.

Nevertheless, the high value obtained for the statistical factor PF/3 for this formula indicates the need for continued progress in the study of the adequacy of color difference formulas that correlate with clinical visual assessment.

4. The nonlinear predictive models developed in this PhD Thesis on a group of 49 samples of experimental dental resin composites designed in our laboratory, allow the prediction, with a high degree of accuracy, of both the final color – in terms of CIE L*a*b* chromatic coordinates (R^2 >0.950 in all cases) – and the reflectance spectrum of the experimental dental resin composites (average error <3.54% across all wavelengths of the visible spectrum). In general, the differences found between the predicted and measured values of the chromatic coordinates are smaller than the acceptability threshold established for this type of materials and, for some of the models, are even below the perceptibility threshold. These results open the way for custom design of dental resin composites, with multiple direct and immediate clinical applications, such as the manufacture of dental shade guides, development of new dental materials, and finally, performing dental restorations that perfectly match the color of their surrounding dental structures. However, before bringing these materials to the clinic, the present work has to be complemented with studies on other physical and chemical properties of the material, such as polymerization shrinkage, hardness, wear resistance, degree of polymerization, temporal and thermo chromatic stability, etc.

5. Within the framework of this pilot study, the predictive models proposed in this PhD Thesis allow the quantification of the amount and type of pigments used in the chemical formulation of the experimental dental composites based on the values of the CIEL*a*b* chromatic coordinates (R^2 >0.409) and the reflectance spectrum of the samples in the visible range (R^2 >0.133). Nevertheless, due to the low values of the quality indexes describing the goodness of fit, future work in this research area must implement the use of other type of predictive algorithms, such as the principal component analysis (PCA) or the more recent Fuzzy Logic which, since it does not incorporate a dimensional reduction, may be able to provide more flexibility and robustness to the predictive models. However, the research studies in the field of

esthetic dentistry have become very important, since being capable of accurately emulate, from a colorimetric point of view, the tooth structure which will be replaced, will provide the clinician the capacity of performing high esthetic dental restorations which will lead to full satisfaction of the dental patient.

1. La aproximación TSK Fuzzy propuesta en esta tesis doctoral es un adecuado procedimiento de cálculo de los umbrales de color frente a los métodos tradicionales de ajuste. La fórmula de diferencia de color CIEDE2000 está mejor correlacionada con la percepción visual que la formula CIELAB, recomendando su uso en investigación en odontología así como para medida de color dental *in vivo.* Los valores 1.25 unidades CIEDE2000 y 2.23 unidades CIEDE2000 encontrados para los umbrales de perceptibilidad y aceptabilidad, respectivamente, pueden ser empleados como referencia en futuros trabajos de investigación, para el diseño de nuevos materiales dentales y para la evaluación clínica de restauraciones dentales.

2. Existen diferencias significativas en sensibilidad visual para cambios en luminosidad, croma y tono ($\Delta \mathrm{L}'$=2.92, $\Delta C'$=2.52, $\Delta \mathrm{H}'$=1.90) para muestras del espacio cromático dental. Por ello, para un uso adecuado de la formula CIEDE2000 en la evaluación clínica visual e instrumental en odontología, es necesario revisar los factores paramétricos K_L, K_C y K_H de esta fórmula. Los valores obtenidos para las diferencias CIEDE2000 en luminosidad (ΔE_L=2.86), croma (ΔE_C=1.34) y tono (ΔE_H=1.65) indican que el uso del factor paramétrico K_L=2 (CIEDE2000(2:1:1)) podría ser recomendable para la evaluación de diferencia de color de muestras pertenecientes al espacio cromático dental. Por otra parte, los umbrales de aceptabilidad direccionales estimados en esta Tesis Doctoral pueden ser de gran utilidad en futuros trabajos de investigación y aplicaciones industriales, tales como procesos de blanqueamiento dental, envejecimiento dental, diseño de nuevos materiales dentales, así como para un adecuado uso en clínica de éstos.

3. La aproximación Fuzzy de las curvas de porcentaje de aceptabilidad desarrollada en esta tesis doctoral, utilizando un modelo TSK TaSe, permite calcular los valores de los umbrales de aceptabilidad en el espacio dental. La fórmula de diferencia de color CIEDE2000(2:1:1) presenta un mejor rendimiento frente a los juicios visuales en comparación con la formula CIEDE2000(1:1:1), tal y como muestran los valores de los factores estadísticos PF/3 y STRESS (PF/3: 190.33 frente a 196.43; STRESS: 0.83 frente a 0.85). Es decir, el factor paramétrico K_L=2 en lugar de K_L=1 en la

fórmula de diferencia de color CIEDE2000(K_L:K_C:K_H) debería ser empleado para una mejora en el cálculo de las diferencias de color en el ámbito odontológico. No obstante, el alto valor del factor estadístico PF/3 para esta fórmula nos indica la necesidad de seguir avanzando en el estudio de la adecuación de fórmulas de diferencia de color que se correlacionen con la apreciación visual del clínico dental.

4. Los modelos predictivos de regresión múltiple nolineal desarrollados en esta tesis doctoral sobre un grupo de 49 muestras de resinas de composite experimentales diseñadas en nuestro laboratorio, permiten predecir, con un alto grado de precisión, tanto el color final - en términos de las coordenadas CIE L*a*b* (R^2 >0.950 en todos los casos) - como el espectro de reflectancia de las resinas de composite experimentales (error medio <3.54% a lo largo de todas las longitudes de onda del espectro visible). En general, las diferencias encontradas entre los valores de las coordenadas de cromaticidad predichas y las medidas son menores que el umbral de aceptabilidad establecido para este tipo de materiales e incluso, para algunos de los modelos, menores que el umbral de perceptibilidad. Estos resultados abren el camino para el diseño personalizado de resinas de composite dentales, con múltiples aplicaciones clínicas directas e inmediatas, como la fabricación de guías dentales, desarrollo de nuevos materiales y, por último, la realización de restauraciones dentales que igualan perfectamente en color a las estructuras dentales que las rodean. No obstante, antes de llevar estos materiales a la clínica hay que complementar este trabajo con estudios sobre otras propiedades físico-químicas del material, como pueden ser la contracción de polimerización, dureza, resistencia al desgaste, grado de polimerización, estabilidad cromática temporal y térmica, etc.

5. Dentro del marco de este estudio piloto, los modelos predictivos que se han propuesto en esta tesis doctoral permiten determinar la cantidad y tipo de pigmentos utilizados en la formulación química de las resinas de composite experimentales a partir de los valores de las coordenadas cromáticas CIE L*a*b*(R^2>0.409) y el espectro de reflectancia de las muestras en el rango visible (R^2>0.133). Sin embargo, debido a los bajos valores de los índices de calidad de los ajustes, trabajos futuros en esta línea de investigación tienen que implementar el uso de otros algoritmos predictivos, tales

como análisis de componentes principales o los recién incorporados modelos de lógica difusa (Fuzzy Logic) que, por no incorporar una reducción dimensional, pueden proporcionar más flexibilidad y robustez a los modelos predictivos. Sin embargo, los trabajos en el campo de la odontología estética han cobrado gran importancia, ya que ser capaz de emular con precisión, desde un punto de vista colorimétrico, la estructura dental que se va a reemplazar proporcionará al clínico dental la capacidad de realizar restauraciones de alta calidad estética que conducirán a la plena satisfacción del paciente.

CHAPTER 8

REFERENCES

An, J. S., et al. (2013). "The influence of a continuous increase in thickness of opaque-shade composite resin on masking ability and translucency." Acta Odontologica Scandinavica71(1): 120-129.

Anusavice, K. J., et al. (2013). Phillips' science of dental materials. St. Louis, Mo., Elsevier/Saunders.

Atai, M., et al. (2004). "Physical and mechanical properties of an experimental dental composite based on a new monomer." Dental Materials20(7): 663-668.

Baltzer, A. K.-J., V. (2004). "The determination of tooth colors." Quintessenz Zahntech 30(7): 726-740.

Banerjee, K. S. and R. N. Carr (1971). "Ridge Regression - Biased Estimation for Non-Orthogonal Problems." Technometrics 13(4): 895-&.

Bayindir, F., et al. (2007). "Coverage error of three conceptually different shade guide systems to vital unrestored dentition." Journal of Prosthetic Dentistry 98(3): 175-185.

Berns, R. S. (1996). "Deriving instrumental tolerances from pass-fail and colorimetric data." Color Research and Application 21(6): 459-472.

Berns, R. S. (2000). Billmeyer and Saltzman's - Principles of color technology. New York, USA, John Wiley & Sons, Inc.

Berns, R. S., et al. (1991). "Visual Determination of Suprathreshold Color-Difference Tolerances Using Probit Analysis." Color Research and Application 16(5): 297-316.

Bikdash, M. (1999). "A highly interpretable form of Sugeno inference systems." IEEE Transactions on Fuzzy Systems 7(6): 686-696.

Braden, M. C., RL; Nicholson, J; Parker, S; Braden, M (1997). Polymeric Dental Materials (Macromolecular Systems - Materials Approach) USA, Springer.

Bryant, R. W. and K. L. Hodge (1994). "A clinical evaluation of posterior composite resin restorations." Australian Dental Journal 39(2): 77-81.

Buckley, J. J. (1992). "Universal Fuzzy Controllers." Automatica 28(6): 1245-1248.

Calheiros, F. C., et al. (2008). "Influence of irradiant energy on degree of conversion, polymerization rate and shrinkage stress in an experimental resin composite system." Dental Materials24(9): 1164-1168.

Castro, J. L. (1995). "Fuzzy-Logic Controllers Are Universal Approximators." IEEE Transactions on Systems Man and Cybernetics 25(4): 629-635.

Choo, S. and Y. Kim (2003). "Effect of color on fashion fabric image." Color Research and Application 28(3): 221-226+166.

Chou, W., et al. (2001). "Performance of lightness difference formulae." Coloration Technology 117(1): 19-29.

Chu, S. J., et al. (2010). "Dental color matching instruments and systems. Review of clinical and research aspects." Journal of Dentistry 38(SUPPL. 2): e2-e16.

CIE (1964). CIE Publication 11 A. Official recommendations, Committee E-1.3.1 - Colorimetry. Vienna, Austria. A: 35.

CIE (1967). CIE Publication 14: Proceedings of the CIE Washington Session: Recommendations on standard illuminants for colorimetry. A: 95-97.

CIE (1995). Technical Report: Industrial color-difference evaluation. Vienna, Austria, International Commission on Illumination.

CIE (2001). Technical Report: Improvement to industrial color difference equation, International Commission on Illumination.

CIE (2004). Technical Report : Colorimetry. Vienna, Austria, International Comission on Illumination.

Clarke, F. J. J., et al. (1984). "Modification to the Jpc79 Color-Difference Formula." Journal of the Society of Dyers and Colourists 100(4): 128-132.

Cordon, O. H., F; Hoffmann, F; Magdalena, L (2001). Genetic fuzzy systems: evolutionary tuning and learning of fuzzy knowledge bases. O. Cordon, World Scientific. Volume 19 of Advances in Fuzzy Systems.

Coxon, A. P. M. (1982). The User's Guide to Multidimensional Scaling.

Craig, R. G. and J. M. Powers (2002). Restorative dental materials. St. Louis, Mosby.

Cramer, N. B., et al. (2011). "Recent advances and developments in composite dental restorative materials." Journal of Dental Research 90(4): 402-416.

Del Mar Pérez, M., et al. (2007). "Study of the variation between CIELAB ΔE* and CIEDE2000 color-differences of resin composites." Dental Materials Journal 26(1): 21-28.

Del Mar Pérez, M., et al. (2009). "Light polymerization-dependent changes in color and t ranslucency of resin composites." American Journal of Dentistry 22(2): 97-101.

Dijkstra, T. (1983). "Some Comments on Maximum-Likelihood and Partial Least-Squares Methods." Journal of Econometrics 22(1-2): 67-90.

Dionysopoulos, P. and D. C. Watts (1990). "Sensitivity to ambient light of visible light-cured composites." Journal of Oral Rehabilitation 17(1): 9-13.

Douglas, R. D. and J. D. Brewer (1998). "Acceptability of shade differences in metal ceramic crowns." The Journal of prosthetic dentistry 79(3): 254-260.

Douglas, R. D., et al. (2007). "Intraoral determination of the tolerance of dentists for perceptibility and acceptability of shade mismatch." Journal of Prosthetic Dentistry 97(4): 200-208.

Driankov, D. H., H; Reinfrank, M (1996). An introduction to fuzzy control. Second Edition, Springer.

Ergucu, Z., et al. (2008). "Color stability of nanocomposites polished with one-step systems." Operative Dentistry 33(4): 413-420.

Fairchild, M. D. (2005). Color Appearance Models - Second Edition. England, John Wiley & Sons Ltd.

Fairchild, M. D. (2010). "Color appearance models and complex visual stimuli." Journal of Dentistry 38 Suppl 2: e25-33.

Frank, I. E. and J. H. Friedman (1993). "A Statistical View of Some Chemometrics Regression Tools." Technometrics 35(2): 109-135.

García, P. A., et al. (2007). "Measurement of the relationship between perceived and computed color differences." Journal of the Optical Society of America A: Optics and Image Science, and Vision 24(7): 1823-1829.

Gebelein, C. G., et al. (1981). Biomedical and dental applications of polymers. New York, Plenum Press.

Ghinea, R. H., LJ; Ugarte, L; Ionescu, AM; Cardona, JC; Perez, MM (2010). Development of a linear model to predict polymerization dependent color changes. SCAD, Newport Beach, USA.

Ghinea, R., et al. (2010). "Color difference thresholds in dental ceramics." Journal of Dentistry 38(SUPPL. 2): e57-e64.

Golden, R. M. (1997). "Neural networks: A comprehensive foundation - Haykin,S." Journal of Mathematical Psychology 41(3): 287-292.

Golub, G. V. L., F (2012). Matrix computations. Fourth Edition, JHU Press.

Gonulol, N. and F. Yilmaz (2012). "The effects of finishing and polishing techniques on surface roughness and color stability of nanocomposites." Journal of Dentistry 40: E64-E70.

Goodkind, R. J. and W. B. Schwabacher (1987). "Use of a fiber-optic colorimeter for in vivo color measurements of 2830 anterior teeth." The Journal of prosthetic dentistry 58(5): 535-542.

Gozalo-Diaz, D. J., et al. (2007). "Measurement of color for craniofacial structures using a 45/0-degree optical configuration." Journal of Prosthetic Dentistry 97(1): 45-53.

Griffin, L. D. and A. Sepehri (2002). "Performance of CIE94 for nonreference conditions." Color Research and Application 27(2): 108-115.

Gruber, H. F. (1992). "Photoinitiators for Free-Radical Polymerization." Progress in Polymer Science17(6): 953-1044.

Guan, S. S. and M. R. Luo (1999). "Investigation of parametric effects using small colour differences." Color Research and Application 24(5): 331-343.

Guild, J. (1931). "The colorimetric properties of the spectrum." Philosophical Transactions of the Royal Society of London A. 230: 149-187.

Hasegawa, A., et al. (2000). "Color and translucency of in vivo natural central incisors." Journal of Prosthetic Dentistry 83(4): 418-423.

Hasegawa, A., et al. (2000). "Color of Natural Tooth Crown in Japanese People." Color Research and Application 25(1): 43-48.

Haykin, S. (2009). Neural networks and learning machines. Third Edition, Prentice Hall.

Herrera, L. J., et al. (2005). "TaSe, a Taylor series-based fuzzy system model that combines interpretability and accuracy." Fuzzy Sets and Systems 153(3): 403-427.

Herrera, L. J., et al. (2010). "Prediction of color change after tooth bleaching using fuzzy logic for Vita Classical shades identification." Applied Optics 49(3): 422-429.

Herrera, L. J., et al. (2011). "The TaSe-NF model for function approximation problems: Approaching local and global modelling." Fuzzy Sets and Systems 171(1): 1-21.

Huertas, R. (2004). Diferencias de color en muestras con textura simulada. Optics. Granada, Spain, University of Granada. PhD.

Huertas, R., et al. (2006). "Influence of random-dot textures on perception of suprathreshold color differences." Journal of the Optical Society of America A: Optics and Image Science, and Vision 23(9): 2067-2076.

Johnston, W. M. (2009). "Color measurement in dentistry." Journal of Dentistry 37(SUPPL. 1): e2-e6.

Johnston, W. M. and E. C. Kao (1989). "Assessment of appearance match by visual observation and clinical colorimetry." Journal of Dental Research 68(5): 819-822.

Johnston, W. M., et al. (1995). "Translucency parameter of colorants for maxillofacial prostheses." The International journal of prosthodontics 8(1): 79-86.

Joiner, A. (2004). "Tooth colour: a review of the literature." Journal of Dentistry 32 Suppl 1: 3-12.

Judd, D. B., et al. (1964). "Spectral Distribution of Typical Daylight as Function of Correlated Color Temperature." Journal of the Optical Society of America 54(8): 1031-1040.

Kim, S. H., et al. (2005). "Influence of porcine liver esterase on the color of dental resin composites by CIEDE2000 system." Journal of Biomedical Materials Research - Part B Applied Biomaterials 72(2): 276-283.

Koirala, P., et al. (2008). "Color Mixing and Color Separation of Pigments with Concentration Prediction." Color Research and Application 33(6): 461-469.

Kruskal, J. B. (1964). "Multidimensional scaling by optimizing goodness of fit to a nonmetric hypothesis." Psychometrika 29(1): 1-27.

Kuehni, R. G. (1976). "Color-tolerance data and the tentative CIE 1976 L a b formula." Journal of the Optical Society of America 66(5): 497-500.

Kuehni, R. G. and R. T. Marcus (1979). "Experiment in Visual Scaling of Small Color Differences." Color Research and Application 4(2): 83-91.

Lee, Y. K. (2005). "Comparison of CIELAB Δe* and CIEDE2000 color-differences after polymerization and thermocycling of resin composites." Dental Materials 21(7): 678-682.

Lee, Y. K. (2007). "Influence of scattering/absorption characteristics on the color of resin composites." Dental Materials 23(1): 124-131.

Lim, H. N., et al. (2010). "Spectroradiometric and Spectrophotometric Translucency of Ceramic Materials." Journal of Prosthetic Dentistry 104(4): 239-246.

Lindsey, D. T. and A. G. Wee (2007). "Perceptibility and acceptability of CIELAB color differences in computer-simulated teeth." Journal of Dentistry 35(7): 593-599.

Luo, M. R. and B. Rigg (1987). "Bfd (1-C) Color-Difference Formula .1. Development of the Formula." Journal of the Society of Dyers and Colourists 103(2): 86-94.

Luo, M. R., et al. (2001). "The development of the CIE 2000 colour-difference formula: CIEDE2000." Color Research and Application 26(5): 340-350.

Luo, W., et al. (2009). "Development of a whiteness index for dentistry." Journal of Dentistry 37(SUPPL. 1): e21-e26.

Lutz, F. and R. W. Phillips (1983). "A Classification and Evaluation of Composite Resin Systems." Journal of Prosthetic Dentistry 50(4): 480-488.

MacAdam, D. L. (1942). "Visual sensitivities to color differences in daylight." Journal of the Optical Society of America 32(5): 247-274.

Mahfouf, M., et al. (2001). "A survey of fuzzy logic monitoring and control utilisation in medicine." Artificial Intelligence in Medicine 21(1-3): 27-42.

Mangine, H., et al. (2005). "A preliminary comparison of CIE color differences to textile color acceptability using average observers." Color Research and Application 30(4): 288-294.

Martínez, J. A., et al. (2001). "Note. Visual and instrumental color evaluation in red wines." Food Science and Technology International 7(5): 439-444.

Mclaren, K. (1980). "Cielab Hue-Angle Anomalies at Low Tristimulus Ratios." Color Research and Application 5(3): 139-143.

Melgosa, M. (1999). "Testing CIELAB-Based Color-Difference Formulas." Color Research and Application 25(1): 49-55.

Melgosa, M., et al. (1995). "Sensitivity differences in chroma, hue, and lightness from several classical threshold datasets." Color Research and Application 20: 220-225.

Melgosa, M., et al. (2004). "Relative significance of the terms in the CIEDE2000 and CIE94 color-difference formulas." Journal of the Optical Society of America A: Optics and Image Science, and Vision 21(12): 2269-2275.

Montag, E. D. and R. S. Berns (2000). "Lightness dependencies and the effect of texture on suprathreshold lightness tolerances." Color Research and Application 25(4): 241-249.

Nayatani, Y. (2005). "Differences in attributes between color difference and color appearance (chroma and hue) for near-neutral colors." Color Research and Application 30(1): 42-52.

Nicholson, J. (2002). The chemistry of medical and dental materials. Cambridge, UK, The Royal Society of Chemistry.

O'Brien, W. J., et al. (1991). "Coverage errors of two shade guides." The International journal of prosthodontics 4(1): 45-50.

O'Brien, W. J., et al. (1997). "Color distribution of three regions of extracted human teeth." Dental materials : official publication of the Academy of Dental Materials 13(3): 179-185.

Odioso, L. L., et al. (2000). "Impact of demographic, behavioral, and dental care utilization parameters on tooth color and personal satisfaction." Compendium of continuing education in dentistry. (Jamesburg, N.J. : 1995). Supplement(29): S35-41.

Okubo, S. R., et al. (1998). "Evaluation of visual and instrument shade matching." The Journal of prosthetic dentistry 80(6): 642-648.

Paravina, R. D., et al. (2005). "Evaluation of polymerization-dependent changes in color and translucency of resin composites using two formulae." Odontology 93(1): 46-51.

Park, M. Y., et al. (2007). "Influence of fluorescent whitening agent on the fluorescent emission of resin composites." Dental Materials 23(6): 731-735.

Perez, M. D. M., et al. (2011). "Dental ceramics: A CIEDE2000 acceptability thresholds for lightness, chroma and hue differences." Journal of Dentistry 39(SUPPL. 3): e37-e44.

Pomares, H. (2004). "Online global learning in direct fuzzy controllers." IEEE Transactions on Fuzzy Systems 12(2): 218-229.

Pomares, H. R., I; Gonzalez, J; Prieto, A. (2002). "Structure identification in complete rule-based fuzzy systems." IEEE Transactions on Fuzzy Systems 10(3): 349-359.

Ragain Jr, J. C. and W. M. Johnston (2000). "Color acceptance of direct dental restorative materials by human observers." Color Research and Application 25(4): 278-285.

Roberts, S. and H. Pashler (2000). "How persuasive is a good fit? A comment on theory testing." Psychological Review 107(2): 358-367.

Rojas, I., et al. (2000). "Self-organized fuzzy system generation from training examples." IEEE Transactions on Fuzzy Systems 8(1): 23-36.

Rosenstiel, S. F., et al. (1989). "Colour measurements of all ceramic crown systems." Journal of Oral Rehabilitation 16(5): 491-501.

Rosenstiel, S. F., et al. (1989). "Comparison of glazed and polished dental porcelain." The International journal of prosthodontics 2(6): 524-529.

Rubino, M., et al. (1994). "Colour measurement of human teeth and evaluation of a colour guide." Color Research and Application 19(1): 19-22.

Ruyter, I. E., et al. (1987). "Color stability of dental composite resin materials for crown and bridge veneers." Dental Materials 3(5): 246-251.

Sadowsky, S. J. (2006). "An overview of treatment considerations for esthetic restorations: a review of the literature." Journal of Prosthetic Dentistry 96(6): 433-442.

Schanda, J. (2007). Colorimetry. Understanding the CIE System. . USA, John Wiley & Sons, Inc. .

Schneider, L. F. J., et al. (2009). "Effect of co-initiator ratio on the polymer properties of experimental resin composites formulated with camphorquinone and phenyl-propanedione." Dental Materials 25(3): 369-375.

Schneider, L. F. J., et al. (2012). "Curing efficiency of dental resin composites formulated with camphorquinone or trimethylbenzoyl-diphenyl-phosphine oxide." Dental Materials 28(4): 392-397.

Schunn C, W. D. (2005). Evaluating goodness-of fit in comparison of models to data in Psychologie der Kognition: Reden and Vorträge anlässlich der Emeritierung von Werner Tack, University of Saarland Press, Saarbrücken, Germany.

Schwabacher, W. B., et al. (1994). "Interdependence of the hue, value, and chroma in the middle site of anterior human teeth." Journal of Prosthodontics 3(4): 188-192.

Seghi, R. R., et al. (1989). "Performance assessment of colorimetric devices on dental porcelains." Journal of Dental Research 68(12): 1755-1759.

Seghi, R. R., et al. (1989). "Visual and instrumental colorimetric assessments of small color differences on translucent dental porcelain." Journal of Dental Research 68(12): 1760-1764.

Sharma, G., et al. (2005). "The CIEDE2000 color-difference formula: Implementation notes, supplementary test data, and mathematical observations." Color Research and Application 30(1): 21-30.

Sim, C. P. C., et al. (2001). "Color perception among different dental personnel." Operative Dentistry 26(5): 435-439.

Sims, D. A. and J. A. Gamon (2002). "Relationships between leaf pigment content and spectral reflectance across a wide range of species, leaf structures and developmental stages." Remote Sensing of Environment 81(2-3): 337-354.

Soderholm, K. J. (1981). "Degradation of Glass Filler in Experimental Composites." Journal of Dental Research 60(11): 1867-1875.

Solovchenko, A. C., OB; Gitelson AA; Merzlyak, MN (2010). "Non-destructive estimation pogment content, ripening, quality and damage in apple fruit with spectral reflectance in the visible range " Fresh Produce 4(Specil Issue 1): 91-102.

Son, H. J., et al. (2010). "Influence of dentin porcelain thickness on layered all-ceramic restoration color." Journal of Dentistry 38: e71-e77.

Speranskaya, N. (1959). "Determination of spectral color co-ordinates for twenty-seven normal observers." Optics Spectroscopy 7: 424-428.

Steen, D. and D. Dupont (2002). "Defining a practical method of ascertaining textile color acceptability." Color Research and Application 27(6): 391-398.

Stiles, W. S. B., JM. (1959). "N.P.L. color-matching investigation: Final report (1958)." Optica Acta 6: 1-26.

Strocka, D., et al. (1983). "influence of experimental parameters on the evaluation of color-difference ellipsoids." Color Research and Application 8(3): 169-175.

Sustercic, D., et al. (1997). "Determination of curing time in visible-light-cured composite resins of different thickness by electron paramagnetic resonance." Journal of Materials Science: Materials in Medicine 8(8): 507-510.

Takagi, T. and M. Sugeno (1985). "Fuzzy identification of systems and its applications to modeling and control." IEEE Transactions on Systems, Man and Cybernetics 15(1): 116-132.

ten Bosch, J. J. and J. C. Coops (1995). "Tooth color and reflectance as related to light scattering and enamel hardness." Journal of Dental Research 74(1): 374-380.

Ten Bosch, J. J. and J. R. Zijp (1987). "Optical properties of dentin." Dentine and Dentine Reactions in the Oral Cavity: 59-65.

Terry, D. A., et al. (2002). "Anatomical form defines color: function, form, and aesthetics." Practical procedures & aesthetic dentistry : PPAD 14(1): [d]59-67; quiz 68.

van der Burgt, T. P., et al. (1990). "A comparison of new and conventional methods for quantification of tooth color." The Journal of prosthetic dentistry 63(2): 155-162.

Watts, D. C., et al. (1984). "Characteristics of visible-light-activated composite systems." British Dental Journal 156(6): 209-215.

Wee, A. G., et al. (2005). "Color formulation and reproduction of opaque dental ceramic." Dental Materials 21(7): 665-670.

Wee, A. G., et al. (2006). "Color accuracy of commercial digital cameras for use in dentistry." Dental Materials 22(6): 553-559.

Wee, A. G., et al. (2007). "Use of a porcelain color discrimination test to evaluate color difference formulas." Journal of Prosthetic Dentistry 98(2): 101-109.

Wichmann, F. A. and N. J. Hill (2001). "The psychometric function: I. Fitting, sampling, and goodness of fit." Perception & Psychophysics 63(8): 1293-1313.

Willmott, C. J., et al. (1985). "Statistics for the Evaluation and Comparison of Models." Journal of Geophysical Research-Oceans 90(Nc5): 8995-9005.

Wold, H. (1966). Estimation of principal components and related models by iterative least squares. Multivariate Analysis. P. R. Krishnaiah. USA, New York: Academic Press: 391-420.

Wold, S. (1995). PLS for Multivariate Linear Modelling. Chemometric Methods in Molecular Design. Methods and Principles in Medicinal Chemistry. . H. van de Waterbeemd. Weinheim, New York, Basel, Cambridge, Tokyo, VCH Publishers. 2: 195-218.

Wright, W. (1929). "A re-determination of the trichromatic coefficients of the spectral colours." Transactions of the Optical Society of London 30: 141-164.

Wright, W. (1930). "A re-determination of the mixture curves of the spectrum." Transactions of the Optical Society of London 31: 201-218.

Wyszecki, G. and W. S. Stiles (1982). Color Science: Concepts and Methods, Quantitative Data and Formulae.

Xin, J. H., et al. (2005). "Investigation of texture effect on visual colour difference evaluation." Color Research and Application 30(5): 341-347.

Zadeh, L. A. (1965). "Fuzzy Sets." Information and Control 8(3): 338-&.

Zandinejad, A. A., et al. (2006). "The effect of ceramic and porous fillers on the mechanical properties of experimental dental composites." Dental Materials22(4): 382-387.

Zhao, Y. and J. Zhu (1998). "In vivo color measurement of 410 maxillary anterior teeth." The Chinese journal of dental research : the official journal of the Scientific Section of the Chinese Stomatological Association (CSA) 1(3): 49-51.

Zijp, J. and J. ten Bosch (1993). "Theoretical model for the scattering of light by dentin and comparison with measurements." Applied Optics 32(4): 411-415.

CHAPTER 9

SCIENTIFIC PRODUCTION

JOURNAL ARTICLES

R Ghinea, MM Perez, LJ Herrera, MJ Rivas, A Yebra, RD Paravina, Color difference thresholds in dental ceramics. JOURNAL OF DENTISTRY 2010; 38(s):e57-e64;

Pérez MM, **Ghinea R**, Herrera LJ, Ionescu AM, Pomares H, Pulgar R, Paravina RD. Dental Ceramics: A CIEDE2000 acceptability thresholds for lightness, croma and hue differences. JOURNAL OF DENTISTRY 2011;39(3):e37-e44;

Toledano M, **Ghinea R**, Cardona JC, Cabello I, Yamauti M, Perez MM, Osorio R. Digital image analysis method to assess the performance of conventional and self-limiting concepts in dentine caries removal. JOURNAL OF DENTISTRY 2013 Mar 15. doi:pii: S0300-5712(13)00075-4. 10.1016/j.jdent.2013.03.003. [Epub ahead of print] PMID: 23507398

Pecho O.E., **Ghinea R**., Ionescu A.M., Cardona J.C., Paravina R.D., Perez M.M. Colour and translucency of zirconia ceramics, human dentine and bovine dentine. JOURNAL OF DENTISTRY 2012; 40(s2):e34-e40;

MM Perez, **R Ghinea**, LI Ugarte-Alvan, R Pulgar, RD Paravina. Color and translucency in silorane-based resin composite compared to universal and nanofilled composites. JOURNAL OF DENTISTRY 2010; 38(s):e110-e116;

R Ghinea, L Ugarte-Alvan, A Yebra, OE Pecho, RD Paravina, MM Perez. Influence of surface roughness on the color of dental-resin composites. JOURNAL OF THE ZHEJIANG UNIVERSITY: SCIENCE B 2011, 2(7):552-562;

CONFERENCE PAPERS

Ghinea R, Cardona, JC, Ionescu, AM, Pérez, MM, Herrera, LJ. Using Takagi Sugeno-Kang approximation fuzzy logic for evaluating the performance of color difference formulas in dentistry. Proceedings of the IEEE Intelligent Systems Design and Applications 2011;247-2521.

Fernández-Oliveras, A., Carrasco, I.M., **Ghinea, R**., Pérez, M.M., Rubiño, M. Comparison between experimental and computational methods for scattering anisotropy coefficient determination in dental-resin composites. Progress in Biomedical Optics and Imaging - Proceedings of SPIE 8427, 2012. art. no. 84272B.

Pérez Gómez, MM, **Ghinea R**, Ionescu, AM, Cardona Pérez, JC. Changes in scattering and absorption during curing of dental resin composites: silorane and nanocomposite. Proceedings of SPIE 2011;8001:8001321-8001326.

LJ Herrera, H Pomares, I Rojas, J Santana, R Pulgar, **R Ghinea**, MM Perez. Sistema neuro-difuso para el modelado de la evolución del color. Modelado de un proceso de blanqueamiento dental. Proceedings of ESTYLF 2010, 447-452.

R Ghinea, L Ugarte-Alvan, AM Ionescu, JC Cardona, A Yebra, MM Perez. Influence of the size and distribution of filler particles on the colour of resin composites. Proceedings of CGIV 2008, 296-299.

CONFERENCE PROCEEDINGS

M Yamauti, JC Cardona, **R Ghinea**, I Cabello, MM Perez, R Osorio, M Toledano. Minimal invasiveness caries removal using polymer burs: a digital image evaluation. Histology and Histopatology 2011, 26(1):305-306.

LJ Herrera, **R Ghinea**, AB Cara, RD Paravina, MM Perez. On color threshold calculations in oral tissues and dental materials. Histology and Histopatology 2011, 26(1):306-307.

L Ugarte-Alvan, **R Ghinea**, RD Paravina, MM Perez. Optical characterization of nanocomposites compared to universal dental composites. Journal of Dental Research 2010, 89(b) 802-802.

MM Perez, L Ugarte-Alvan, **R Ghinea**, OE Pecho, RD Paravina. Organic matrix influence on color and translucency of dental composites. Journal of Dental Research 2010, 89(b) 4103-4103.

Pecho, OE, **Ghinea R**, Ionescu, AM, González-López S, Pérez MM. Optical characterization in different bovine dentin zones. Histology and Histopathology 2011;26(1): 306

Ghinea R, Ugarte-Alvan L, Ionescu AM, Cardona JC, Perez MM. Optical Characterization of Dental- Resin Composites Based on Image Analysis. Journal of Dental Research 2010; 89(B): 803-803

Pecho OE, **Ghinea R,** Ionescu AM, González-López S, Perez MM. Optical Properties in Bovine Dentin. Journal of Dental Research 2010; 89(B) 4099-4099.

Ghinea R, Perez MM, Ionescu A.M., Paravina R.D. Assessment of a digital shade-matching technique. Comparison with conventional method. 4th Annual Conference of the Society for Color and Appearance in Dentistry (SCAD). 2012. Chicago, USA

Ghinea R, Pecho, OE, Cardona, JC, Ionescu, AM, Perez, MM. Color evaluation of colored zirconia structures compared to human dentin. 3rd Annual Conference of the Society for Color and Appearance in Dentistry (SCAD) 2011. Chicago, USA.

Ghinea R, Herrera Maldonado, LJ, Ugarte-Alván, L, Ionescu, AM, Cardona Pérez, JC, Pérez Gómez, MM. Development of a linear model to predict polymerization-dependent color changes. 2nd Annual Conference of the Society for Color and Appearance in Dentistry (SCAD).2010. Newport, USA.

Pérez, MM, Ugarte-Alván, L, **Ghinea R**, Yebra, A, Ionescu, AM, Cardona, JC, Asselman, A. *Comunicación oral:* Comparison between optical properties of nanocomposites and

classical resin composites. Optique & Traitement de l'information, 17-18 Abril 2008, Mohammedia, Morroco

MM Perez, **R Ghinea**, LJ Herrera, A Garcia-Salas, MJ Rivas, RD Paravina. Using CIELAB or CIEDE2000 color-difference formulas in dental research? 2nd Annual Conference of the Society for Color and Appearance in Dentistry (SCAD) 2010, Newport USA.

R Pulgar, L Ugarte-Alvan, **R Ghinea**, JC Cardona. Comparacion de las propiedades ópticas de diferentes colores de un nanocomposite. XVI SEOC y VI SEMO 2008.

ORGANIZATION OF MEETINGS AND SPECIAL SESSIONS

***Co-Chair**: Special Session on Soft-Computing for biomedical engineering and application.. ISDA 2011.*

***Organizer:** Symposium on physical methods and techniques for the evaluation and quality control of biomaterials and artificial tissues. TERMIS EU-2011.*

PhD SCHOLARSHIP

***Training of Teaching and Research Faculty (4 years)** – Ministry of Economy, Innovation, Science and Employment – Government of Andalucía.*

RESEARCH STAGES

*University of Texas - School of Dentistry: Houston Center for Biomaterials and Biomimetics. USA. – **3 months**.*

AWARDS

***Best poster presentation**: **Ghinea R**, Pecho OE, Cardona JC, Ionescu AM, Perez MM. "Color evaluation of colored zirconia structures compared to human dentin" SCAD 2011 Society for Color and Appearance in Dentistry, Chicago, IL, Sep 23-24, 2011.*

***Best poster presentation**:* MM Perez, **R Ghinea**, LJ Herrera, A Garcia-Salas, MJ Rivas, RD Paravina. Using CIELAB or CIEDE2000 color-difference formulas in dental research? 2nd Annual Conference of the Society for Color and Appearance in Dentistry (SCAD) 2010, Newport USA.